Studies in early transition metal organometallic chemistry

Kingsley, Andrew James

Studies in Early Transition Metal Organometallic Chemistry

A thesis submitted in part fulfilment of the degree of Doctor of Philosophy

Andrew James Kingsley

Grey College, University of Durham

February 1998

Statement of Copyright

Declaration

The work described in this thesis was carried out at the University of Durham, Department of Chemistry, between October 1994 and September 1997.

All the work is my own unless stated otherwise, and it has not been submitted previously for a degree at this or any other university.

Publications

1) Titanium and Zirconium Neopentyl Chloro Complexes, MNp_xCl_{4-x} (x = 1–4); A.K. Hughes and A.J. Kingsley, *J. Organomet. Chem.*, 1997, **539**, 109.

2) Novel Synthesis of Linked Cyclopentadienyl-Amide Complexes; A.K. Hughes and A.J. Kingsley, *J. Chem. Soc., Dalton Trans.*, 1997, 4139.

3) Unexpected Co-Crystallisation of Monomeric and Dimeric Molybdenum Bis Imido Complexes; A. Bastanov, J.A.K. Howard, A.K. Hughes, A.J. Kingsley, J.M. Rawson and D.F. Wass, *Polyhedron*, submitted 1997.

Acknowledgements

First and foremost, I would like to thank my supervisor Dr. Andrew Hughes for his continued support and encouragement throughout the last three years, without which this thesis would not have been possible.

I'd like to thank all the occupants of lab 108, who have made the last three years that much more enjoyable; Brian Bridgewater, Patrick Gemmell, Andrew Johnson, Sarah Marsh, Mark Roden and Melanie Thompson. All the inorganic groups deserve a special thankyou for making it such a hip and happening section.

On the technical side, thanks must also go to Gordon Haswell and Ray Hart for their glassblowing, Julia Say and Alan Kenwright for their NMR services, Mike Jones and Lara Turner for mass spectroscopic analysis, Jaraka Dostal for elemental analysis, Brian Hall for standardising many a bottle of ^{n}BuLi, and Judith Howard, Angus Mackinnon, Christian Lehmann, Janet Moloney and Roy Copley for X-ray crystallography.

I would like to give special thanks to Andrew Johnson for his enthusiasm and gathering of odds and ends for this thesis. Finally, I thank my Mum, Dad and Michael for continuous support throughout.

Abstract

The work in this thesis is separated into two sections:
Chapters 1 to 6 are concerned with the synthesis and characterisation of amide functionalised cyclopentadienyl complexes of Group 4, 5, 6 and 8 transition metals. Chapters 7 to 9 involve a study into complexes containing potential α-agostic interactions.

Chapter 1 provides an introduction to functionalised cyclopentadienyl complexes and also to the ligand $C_5H_5(CH_2)_3N(H)Me$.

Chapter 2 describes the synthesis of the Group 6 complexes of tungsten and molybdenum, $M[\eta^5:\eta^1\text{-}C_5H_4(CH_2)_3NMe](NR)_2$ by different routes, their chemistry, and subsequent reactions.

Chapter 3 covers the preparation of the Group 4 complexes of zirconium and titanium, $M[\eta^5:\eta^1\text{-}C_5H_4(CH_2)_3NMe](C_5H_5)Cl$, their subsequent reactions, and potential as olefin polymerisation catalysts.

Chapter 4 contains the synthesis of the Group 5 complexes of niobium and tantalum, $M[\eta^5:\eta^1\text{-}C_5H_4(CH_2)_3NMe](N^tBu)(NH^tBu)$.

Chapter 5 deals with the preparation of the Group 5 and 6 vanadium and chromium chloride complexes $M[\eta^5:\eta^1\text{-}C_5H_4(CH_2)_3NMe]Cl$, their reactions, and potential as olefin polymerisation catalysts.

Chapter 6 descibes the preparation of some iron complexes. The synthesis of the ferrocene, $Fe[\eta^5\text{-}C_5H_4(CH_2)_3N(H)Me]_2$, and the bridged carbonyl complex, $\{Fe[\eta^5:\eta^1\text{-}C_5H_4(CH_2)_3N(H)Me](CO)(\mu\text{-}CO)\}_2$, are described.

Chapter 7 provides an introduction to α-agostic interactions, the use of the Isotopic Perturbation of Resonance (IPR) technique as a means of characterisation, and the preparation of deuterated starting materials to perform such investigations.

Chapter 8 investigates the complexes $MeTiCl_3L$ (L = dme, tmeda, diphos), $W(N^tBu)_2Me_2$, and $Mo(N\text{-}2,6\text{-}^iPr_2C_6H_3)_2Me_2$ for α-agostic interactions, using the IPR technique

Chapter 9 describes the synthesis of and investigation for α-agostic bonds in zirconium and titanium neopentyl chloro complexes MNp_xCl_{4-x} (x = 1 – 4).

The Appendices outline the preparative and analytical methods used, and X-ray crystallographic data.

Abbreviations

^{n}Bu	^{n}Butyl group, C_4H_9
^{t}Bu	^{t}Butyl group, $C(CH_3)_3$
^{i}Pr	Isopropyl group, $CH(CH_3)_2$
Ph	Phenyl group, C_6H_5
Me	Methyl group, CH_3
Np	Neopentyl group, $CH_2C(CH_3)_3$
Ts	Tosylate group, $3\text{-}CH_3C_6H_4SO_2$
Ar"	$2,6\text{-}[(CH_3)_2CH]_2C_6H_3$
Ar^f	$3\text{-}CF_3C_6H_4$
dmpe	Dimethylphosphinoethane, $CH_3PCH_2CH_2PCH_3$
dme	1,2-dimethoxyethane, $CH_3OCH_2CH_2OCH_3$
tmeda	N,N,N',N'-tetramethylethylenediamine, $(CH_3)_2NCH_2CH_2N(CH_3)_2$
diphos	1,2-bis(diphenylphosphino)ethane, $Ph_2PCH_2CH_2PPh_2$
THF	Tetrahydrofuran, C_4H_8O
TMS	Trimethylsilyl, $(CH_3)_3Si$
DMSO	Dimethyl Sulphoxide, $(CH_3)_2SO$
HMPA	Hexamethylphosphoramide
L	General two electron ligand
X	General one electron ligand
Z	Carbon or silicon bridge
R	Any hydrocarbon group
CpH	Cyclopentadiene, C_6H_5
CpNMe	$C_5H_4(CH_2)_3NMe$
FAL	Tris Fluoro Alkyl Aluminoxane
MAO	Methyl Aluminoxane, $[AlOMe]_n$
IR	Infra-Red
NMR	Nuclear Magnetic Resonance
COSY	COrrelation SpectroscopY
HETCOR	HETeronuclear CORrelation
NOE	Nuclear Overhauser Effect

MO	Molecular Orbital
HOMO	Highest Occupied Molecular Orbital
IPR	Isotopic Perturbation of Resonance

Abbreviations for IR and NMR spectra

s	singlet
d	doublet
t	triplet
q	quartet
quin	quintet
sept	septet
m	multiplet
br	broad
$\Delta\delta$	$\Delta[\delta(CH_3) - \delta(CH_2D)]$
S	solvent
*	impurity

Contents

Appendices

Chapter 1

Introduction to Amide Functionalised Cyclopentadienyl Complexes

1.1 Metal-Cyclopentadienyl Chemistry

Two major lines of research currently dominate metal-cyclopentadienyl chemistry. The first concerns linked bis-cyclopentadienes (or substituted cyclopentadienes) which when coordinated to a metal form *ansa*-metallocenes. The second concerns cyclopentadienyl ligands linked to a functionalised side-chain, containing a donor atom such as oxygen or, more commonly, a nitrogen atom. This project is concerned with the second area and Chapter 1 begins with an introduction to this type of work followed by the system used in the project and its synthesis.

1.1.1 Metallocenes

Organometallic chemistry leaped forward in the early 1950's when the structure of ferrocene, $Fe(\eta^5\text{-}C_5H_5)_2$ was elucidated.[1] Prior to that, ideas regarding metal-ligand interactions included only the coordinate covalent bond (e.g. M-CO) and the covalent bond (e.g. M-CH_3). It was revolutionary in bonding theory to propose a metal-ligand bond between a metal and the π orbitals of $[C_5H_5]^-$. Depending on the electron counting method adopted, the cyclopentadienyl ligand may be viewed as either a five-electron donor (neutral atom) or a six-electron donor (oxidation state). Ferrocene was the first of many complexes that came to be known as metallocenes, a name that arose because they participated in reactions similar to those of aromatic molecules. Cyclopentadienyl derivatives are now known for every main group and transition metal of the periodic table and for most of the f-block metals.[2]

The introduction of Group 3 and 4 metallocenes in the early 1980's has revolutionised the area of Ziegler-Natta catalysis.[3] The industrially important Ziegler-Natta catalyst, which is heterogeneous, is made by treating titanium tetrachloride with triethylaluminium to form a fibrous material that is partially alkylated (Et_2AlCl is used as a cocatalyst). Third generation catalysts (introduced ca. 1980) use a $MgCl_2$ support for $TiCl_4$. The titanium does not have a filled coordination sphere and acts as a Lewis acid, accepting ethylene and propylene as another ligand.

A range of homogeneous catalysts based on cyclopentadienyl titanium complexes has been extensively explored since 1980. The introduction of a cyclopentadienyl ligand is known to act predominantly as an inert supporting ligand for a reactive transition metal centre by not actively participating in a given substrate transformation. For the first time in the history of this industrially important process, critical polymerisation parameters such as activity, molecular weight, polydispersity and microstructure of the resulting polyolefins can be controlled by structurally well-defined metal complexes, modifiable on the molecular level. Moreover the use of metallocenes as homogeneous polymerisation catalysts has dramatically improved the understanding of mechanistic features such as the nature of the active sites and the influence of ligand structure on the regio- and stereo-selectivity.[4]

However one of the advantages generally associated with the bis(cyclopentadienyl) ligand systems occasionally turns into a disadvantage; the characteristic and highly consistent electronic and steric situation within the bent metallocene unit has long been recognised to cause substantial steric blocking of the metal-centred reaction site.[5] This reduction in activity has led to the study of new catalytic systems.

1.1.2 Bis cyclopentadienyl complexes (*ansa*-metallocenes)

Enhancement of catalytic activity is observed when the two cyclopentadienyl rings are "tied back" using an alkyl or silyl bridge thereby alleviating some steric constraint, and also allowing rigid definition of stereochemistry. For example an ethylene bridge has been used in many Brintzinger type *ansa*-metallocene complexes (figure 1.1).

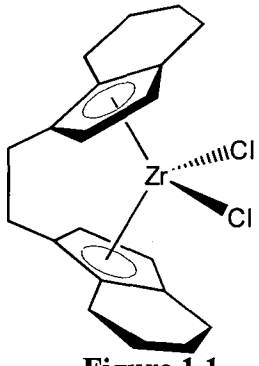

Figure 1.1

Even in such cases the "wedge" of the metallocene moiety still turns out to be too congested to allow, for instance, the efficient polymerisation of α-olefins other than ethene and propene.[6] Each cyclopentadienyl group occupies three coordination sites thereby causing steric congestion. This has led to a search for new ligand systems.

1.1.3 Functionalised cyclopentadienyl complexes

In order to alleviate the steric constraint of metallocenes one could utilise, in place of two cyclopentadienyl ligands, one cyclopentadienyl ligand that contains an additional coordinating site (X or L) tethered to the periphery of the five-membered ring via a bridge (Z). Such bidentate ligands form chelate complexes in which the cyclopentadienyl group and the additional donor group X or L are both interacting with one metal centre (figure 1.2).

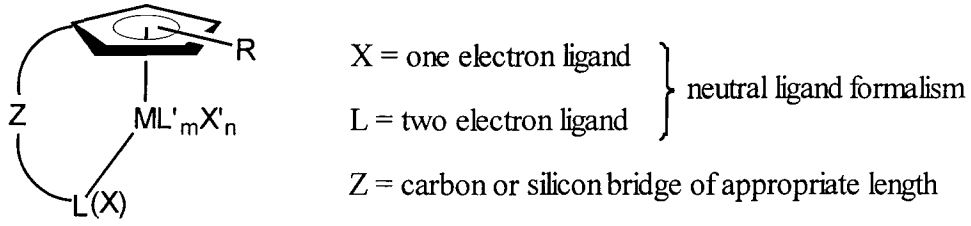

Figure 1.2

Another advantage of this system is that under certain conditions, the cyclopentadienyl ligand may be involved in irreversible chemical reactions or may even dissociate from the metal. If a second donor, preferably a multiply bonding ligand, is tethered to the cyclopentadienyl ligand and is bound as firmly as a cyclopentadienyl ligand, it will add to the stability of the entire ligand framework and prevent exchange or decomposition reactions.

There are many possibilities for such bifunctional ligands in which one cyclopentadienyl ligand of an *ansa* metallocene may be replaced, for example with hard donors (e.g. nitrogen or oxygen), or soft donors (e.g. phosphorus, sulphur or even arsenic). To date,

only nitrogen and oxygen cyclopentadienyl ligands have been reported, primarily due to such groups being ubiquitous in organometallic chemistry and to early transition metals being hard acids. These ligands can be placed into the following categories:

LX_2 Type - Imido (Z-N=)

An imido group (Z)N= is a ligand isolobal to the cyclopentadienyl ligand (replacing 5 electron 1σ, 2π $C_5H_5^-$ by 4 electron 1σ, 2π RN^{2-}) and therefore can be expected to function as a second donor site, but so far only one example of such a bidendate ligand has been reported (discussed in Chapter 4 section 4.1.3).

L Type - Amino ($Z\text{-}NR'_2$) and Ether (Z-OR')

Numerous half-sandwich compounds containing the neutral donor functions (L) have been prepared using amine functions (NR'_2) or ether (OR') groups at the tether (Z) (some of which are discussed in later chapters).[7] These neutral donors are labile, and so can be pendant or attached to the metal centre.

LX Type - Amido (Z-NR') and Oxo (Z-O)

The replacement of one cyclopentadienyl moiety in a bridged bis(cyclopentadienyl) ligand by an amido NR' ligand, or close analogue, the oxo OR' ligand, connected via a bridge Z, **A**, results in ligand systems that form complexes differing from both *ansa*-metallocenes, **B**, and the simple unlinked half-sandwich complexes without the link Z, **C**, (figure 1.3). The amido group is a three electron ligand of the LX-type (including π-donation from the sp^2-hybridised nitrogen atom), in contrast to the five-electron L_2X-type cyclopentadienyl ligand. The oxo ligand can however act as either a 3 or 5 electron ligand.

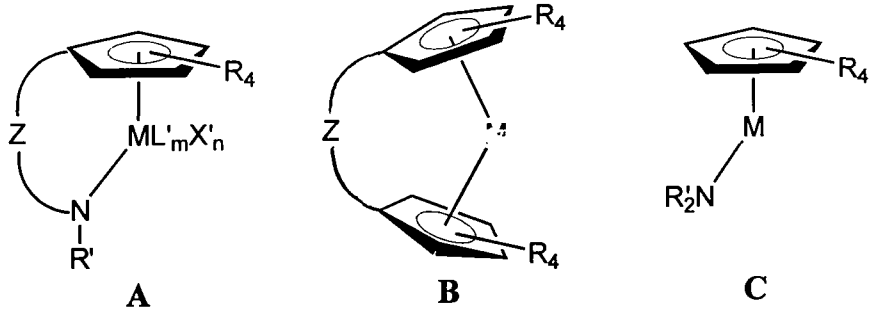

Figure 1.3

Like the cyclopentadienyl ligand, an LX type ligand can bind strongly to the metal centre, therefore adding stability to the entire ligand framework, but unlike the L_2X type there is a degree of flexibility, allowing the possibility of it being labile. Therefore it is the LX type ligand that is of most interest. By independently modifying the nature of the fragments C_5R_4, X, L, and Z in the bifunctional cyclopentadienyl systems, a great potential emerges for imparting novel properties to the chelate complexes and for controlling the metal reactivity.

The chemistry of linked amido and alkoxo-cyclopentadienyl ligands and their applications to Group 4 (and some Group 3) metal complexes is discussed below. Previous work relevant to the following chapters is discussed in those chapters, for example related Group 5 complexes are discussed in Chapter 4 whereas Group 6 complexes are discussed in Chapters 2 and 5.

1.2 LX Functionalised Cyclopentadienyl Systems

1.2.1 Complexes with amide functionalised cyclopentadienyl ligands

In the late 1980's Bercaw and Shapiro introduced the first complexes of bridged amido-cyclopentadienyl ligands in the context of developing structurally well-characterised single-component olefin polymerisation catalysts.[8] Electronically more unsaturated and sterically more accessible analogues of *ansa*-scandocene complexes of the type $Sc(\eta^5:\eta^1\text{-}C_5Me_4SiMe_2N^tBu)X$ (X = H, alkyl) were synthesised and shown to exhibit much higher reactivity towards α-olefins.[9] In order to explore sterically demanding derivatives of this dianionic ligand, the synthesis of iron and titanium complexes followed shortly after, and led to a flurry of independent development in the research laboratories of Dow Chemical and Exxon Chemicals.[10] This has led to a deluge of patents and therefore much of the data on this subject resides in the patent literature. For the complexation of the linked amido-cyclopentadienyl ligand several different synthetic procedures have been developed and these are described.

Metathesis Reactions

The metathetical reaction of the doubly metallated ligand precursor $(C_5R_4ZNR')^{2-}$ with appropriate metal halides appears to be the most common route to such complexes. The first amide functionalised titanium complex was $Ti[\eta^5:\eta^1\text{-}(C_5H_3{}^tBu)SiMe_2N^tBu]Cl_2$, obtained from the reaction of $TiCl_4(THF)_2$ with $[(C_5H_3{}^tBu)SiMe_2N^tBu]Li_2$.[11] The accompanying facile reduction of $TiCl_4(THF)_2$ led to the use of $TiCl_3(THF)_3$ followed by oxidation, giving higher yields.[12] Lead dichloride, introduced by Teuben and coworkers, was found to be the best reagent for the chlorination/oxidation of the Ti^{3+} intermediates,[13] which led to the formation of many amide functionalised cyclopentadienyl titanium dichloride complexes (figure 1.4).[14,15,16,17]

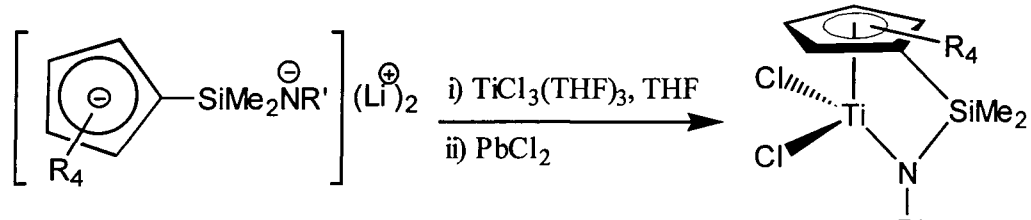

$C_5R_4 = C_5Me_4, C_5H_3{}^tBu, C_9H_6$

$R' = {}^iPr, {}^tBu, CH_2Ph, CHMePh, C_6H_{11}$

Figure 1.4

Occasionally, low yields of product are encountered, with reduction of the metal centre being a synthetic obstacle whenever strongly reducing (i.e., more ionic) cyclopentadienyl anions are employed, especially the unsubstituted cyclopentadienyl ring.[18] In certain cases the preferred formation of bis(ligand) complexes of the type $Ti(\eta^5:\eta^1\text{-}C_5R_4ZNR')_2$ may account for the low yield. For example, irrespective of molar ratio, the reaction between $(C_5H_4SiMe_2N^tBu)Li_2$ and $ZrCl_4$ leads exclusively to the formation of the bis(ligand) complex, **A**, whereas the reaction of $(C_5Me_4SiMe_2N^tBu)Li_2$ with $ZrCl_4$ or $ZrCl_4(THF)_2$ gives the desired mono(ligand) complex, **B** (figure 1.5).

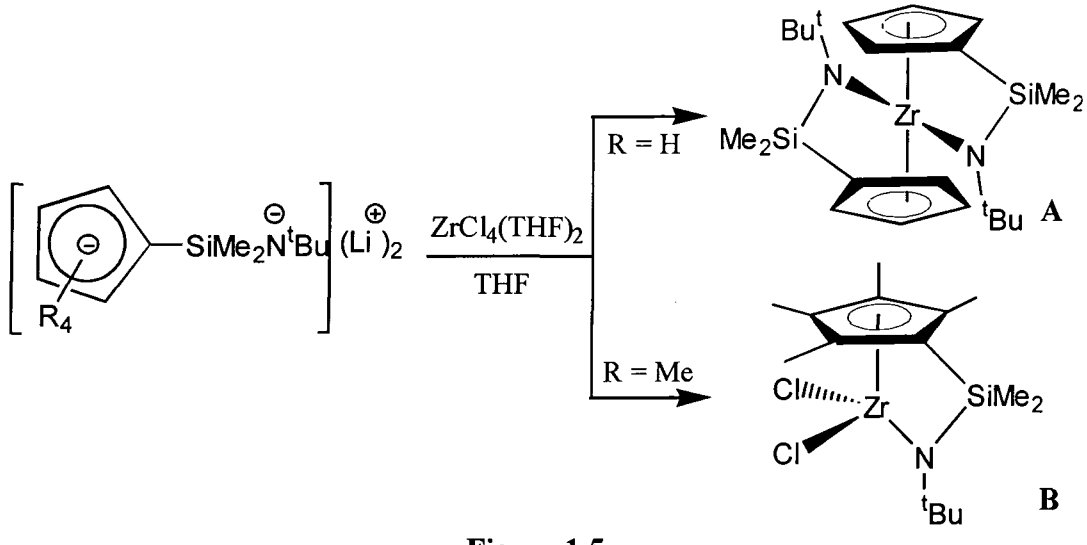

Figure 1.5

The expected higher Lewis acidity of linked amido-cyclopentadienyl complexes often results in the formation of solvent adducts which may then interfere with subsequent alkylation reactions or with activation procedures during olefin polymerisation. For example the scandium and zirconium complexes, $Sc(\eta^5:\eta^1\text{-}C_5Me_4SiMe_2N^tBu)$-$Cl.LiCl(THF)_x$ and $Zr(\eta^5:\eta^1\text{-}C_{13}H_8SiMe_2N^tBu)Cl_2(L)$ (L = THF, Et_2O) are formed as

solvent adducts, although the solvent can be irreversibly lost upon heating.[9,19] By changing the size of the bridging group Z from a $SiMe_2$ group to a CH_2SiMe_2 group in the zirconium complex, the solvent-free fluorenyl complexes, $M(\eta^5:\eta^1\text{-}C_{13}H_8CH_2SiMe_2N^tBu)Cl_2$ (M = Ti, Zr, Hf) can be obtained.[20]

Homoleptic amide reactions

In order to avoid some of the problems associated with the metathesis method, the reaction of homoleptic amides $M(NR''_2)_n$ with functionalised cyclopentadienes, and subsequent amine elimination has been widely studied. This method, introduced by Lappert in 1968 for the synthesis of complexes of the type $M(C_5R_5)_x(NR'')_y$,[21] was recently expanded to the stereoselective synthesis of Brintzinger-type ansa-metallocenes.[22] It was first applied to the synthesis of complexes containing linked amide ligands with a dimethylene or trimethylene bridge, $C_5H_5(CH_2)_nNR'$ (n = 2, 3; R'= Me, ^{i}Pr, ^{t}Bu).[23,24,25] The reaction of the free ligand with $M(NMe_2)_4$ (M = Ti, Zr, Hf) produces the bis amide complexes, as distillable oils (figure 1.6) (discussed further in section 1.4.5).

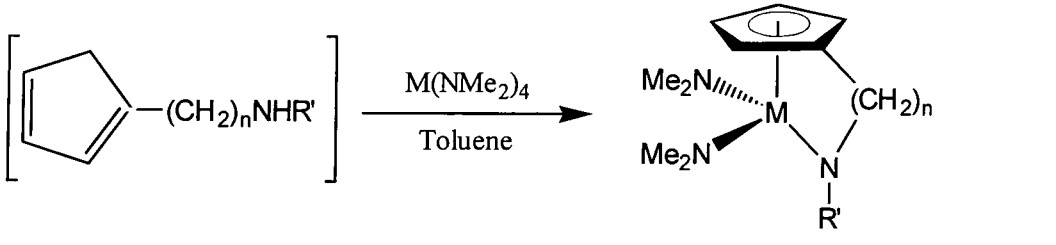

n = 2: R' = Me, ^{t}Bu; n = 3: R' = Me, ^{t}Bu

M= Zr, Ti

Figure 1.6

The reaction also works for indenyl systems, yielding $M[\eta^5:\eta^1\text{-}C_9H_6(CH_2)_nNR'](NMe_2)_2$ (M = Zr, Hf; n = 2: R'= Me, ^{t}Bu; n = 3: R' = Me). Analogous reactions of $C_5H_5SiMe_2NHR'$ (R' = ^{t}Bu, Ph) with $Ti(NR'')_4$, $Zr(NR'')_4$ (R''= Me, Et) and $Hf(NMe_2)_4$ give corresponding complexes of the general type $M(\eta^5:\eta^1\text{-}C_5H_4SiMe_2NR')(NR'')_2$.[18] Similarly the yttrium complex $Y(\eta^5:\eta^1\text{-}C_5Me_4SiMe_2N^tBu)N(SiMe_3)_2$ has been synthesised from $Y[N(SiMe_3)_2]_3$. The zirconium dichloro complex, $Zr[\eta^5:\eta^1\text{-}C_5H_4(CH_2)_2N^tBu]Cl_2$, is

found to be accessible by reacting $Zr(NMe_2)_2Cl_2(THF)_2$ and the ligand $C_5H_5(CH_2)_2N(H)^tBu$.

Part of the driving force for these reaction is the generation of volatile amines $NHMe_2$ and $NHEt_2$ (b.pt. = 7 and 55°C respectively) with the products forming in nearly quantitative yields. The reactions have been found to be accelerated with more acidic ligands and less sterically demanding cyclic systems. However the products are often oils, and compared to the metathesis reactions, the amide ligands in the products are not as versatile as chloride ligands (discussed further in section 1.4.5).

Amide linkage from preformed half sandwich complexes

An alternative approach to amido-bridged cyclopentadienyl complexes consists of introducing the amido linkage within the preformed half-sandwich complex.[26] The ligand, $C_5H_4(SiMe_2Cl)SiMe_3$, reacts with $TiCl_4$ forming $Ti(\eta^5\text{-}C_5H_4SiMe_2Cl)Cl_3$ (figure 1.7). Reacting this with lithium amides LiNHR' (R'= ^{t}Bu,[26] ^{i}Pr,[17] CH_2Ph,[17]) in the presence of a base, gives the desired linked titanium systems in good yields (figure 1.7).

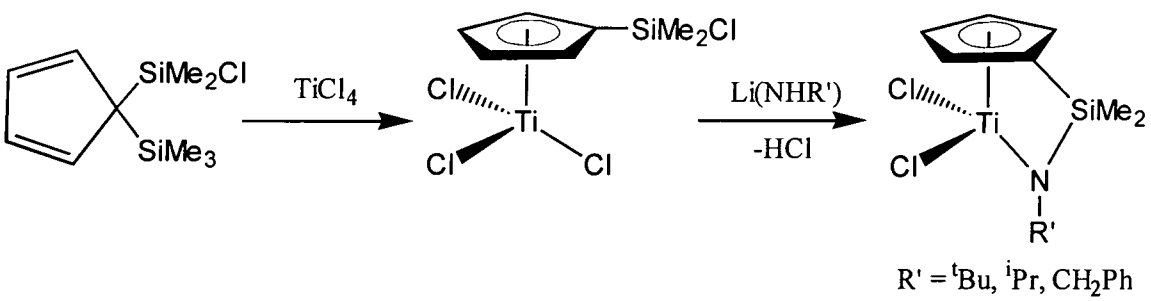

Figure 1.7

However this method has only been found to work with the unsubstituted cyclopentadienyl system, C_5H_4, so far and does not apply to metal systems other than titanium.

1.2.2 Alkyl and hydrido complexes

The synthesis of alkyl complexes from chloro and amido derivatives is frequently studied in view of their importance as precusors for α-olefin polymerisation catalysts. Organolithium or Grignard alkylating reagents without β-hydrogens are generally employed, including methyl, benzyl, trimethylsilylmethyl, neophyl and neopentyl, and bulkier alkyl groups are found to provide more thermally and photochemically stable complexes.

A fairly extensive range of Group 4 dialkyl complexes has been reported. For example the reaction of dichloro complexes with two equivalents of organolithium or Grignard reagents give a number of silyl bridged alkyl complexes, $M(\eta^5:\eta^1\text{-}C_5Me_4SiMe_2N^tBu)R''_2$ (figure 1.8).[17,26,27,28,29] In the case of zirconium complexes with carbon links, the amine adduct $Zr[\eta^5:\eta^1\text{-}C_5H_4(CH_2)_3NMe]Cl_2(NHMe_2)$ is converted directly into the dialkyl (discussed in detail in section 1.4.5).[23]

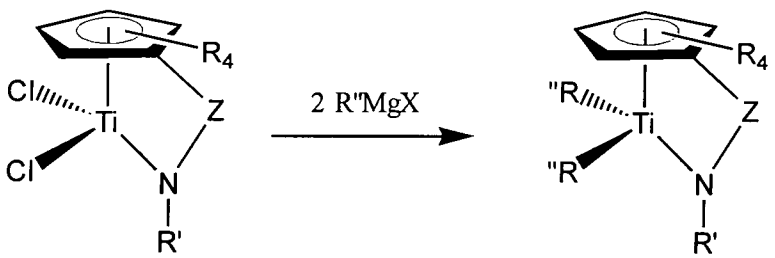

Figure 1.8

It appears that the retention of solvent molecules depends on the steric bulk of the alkyl groups. Whereas the zirconium dimethyl derivatives $Zr[\eta^5:\eta^1\text{-}C_{13}H_8(SiMe_2N^tBu]Me_2(THF)$,[19] or $Zr[\eta^5:\eta^1\text{-}C_5H_4(CH_2)_3NMe]Me_2(Et_2O)_{0.5}$,[23] tend to retain solvents, the complexes with larger alkyls are isolated without any coordinated solvent. This is also found to be the case with $Cr(\eta^5:\eta^1\text{-}C_5H_4SiMe_2N^tBu)R''$ where THF is coordinated when R" = Me but not when R" = $SiMe_2$ (discussed in detail in Chapter 5).

Since the dichloro complexes $M(\eta^5:\eta^1\text{-}C_5R_4ZNR')Cl_2$ (M = Ti, Zr, Hf) are suitable precursors for alkylations, conversion of the bis amido complexes, $M(\eta^5:\eta^1\text{-}C_5R_4ZNR')(NMe_2)_2$, obtained from the amine elimination reactions, to the dichloro derivatives is therefore useful. Complete conversion, in good yields, is obtained from the reaction of the titanium complexes $Ti(\eta^5:\eta^1\text{-}C_5R_4ZNR')(NMe_2)_2$ with an excess of chlorotrimethylsilane or phosphorus pentachloride.[18] The reaction of the zirconium analogue, $Zr(\eta^5:\eta^1\text{-}C_5H_4SiMe_2N^tBu)(NMe_2)_2$, with two equivalents of chlorotrimethylsilane gives the dimeric $[Zr(\eta^5:\eta^1\text{-}C_5H_4SiMe_2N^tBu)Cl(\mu\text{-}Cl)]_2$.[23]

The reaction of two equivalents of protic reagents such as HCl or $(NHEt_3)Cl$ with $Ti(\eta^5:\eta^1\text{-}C_5H_4SiMe_2N^tBu)(NMe_2)_2$ results in inseparable mixtures of $Ti(\eta^5:\eta^1\text{-}C_5H_4SiMe_2N^tBu)Cl_2$ and $Ti(\eta^5:\eta^1\text{-}C_5H_4SiMe_2Cl)Cl_2(NMe_2)(NMe_2H)$. In contrast the reaction with the corresponding zirconium complexes provides only one product, $Zr(\eta^5:\eta^1\text{-}C_5H_4SiMe_2N^tBu)Cl_2(NMe_2H)$.[27] Similarly, the reaction of $NHMe_2$:HCl or $NHMe_2$:HI with $M[\eta^5:\eta^1\text{-}C_5H_4(CH_2)_3NMe](NMe_2)_2$ (M = Zr, Hf) gives $M[\eta^5:\eta^1\text{-}C_5H_4(CH_2)_3NMe]X_2(NHMe_2)$ (X = Cl, I) in good yields (discussed in further detail in section 1.4.5).[23] These results illustrate the tendency of four-coordinate zirconium complexes to complex additional L-type ligands (figure 1.9).

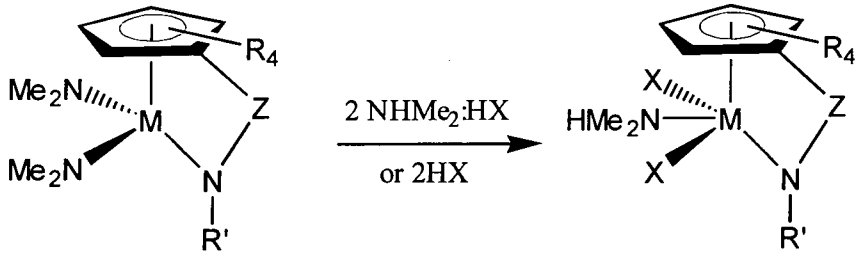

Z = $SiMe_2$; M = Zr; R' = ^{t}Bu; X = Cl

Z = $(CH_2)_3$; M = Zr, Hf; R' = Me; X = Cl, I

Figure 1.9

1.2.3 Structure

Single crystal structure analysis of numerous dichloro complexes of the type $M(\eta^5:\eta^1\text{-}C_5R_4ZNR')Cl_2$ have been performed in the context of explaining the specific polymerisation properties of Group 4 complexes containing the linked amido-cyclopentadienyl ligand. Figure 1.10 shows the molecular structure of $Ti(\eta^5:\eta^1\text{-}C_5H_4SiMe_2N^iPr)Cl_2$ as a representative example.[17]

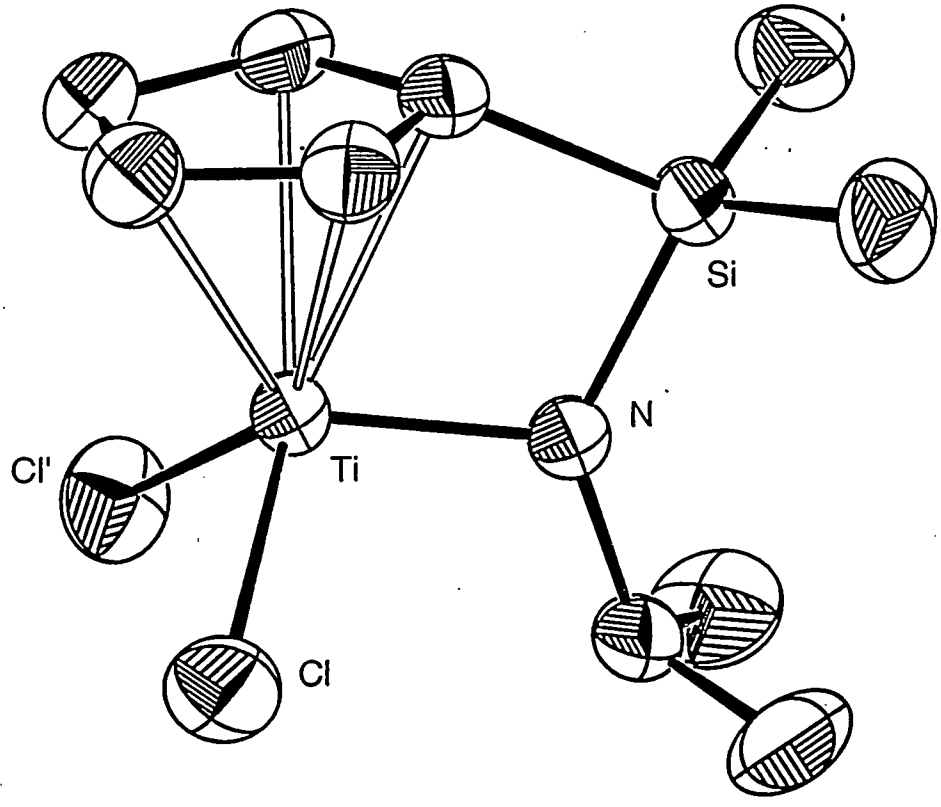

Figure 1.10

These complexes basically adopt a three-legged piano stool or pseudo-tetrahedral geometry with the bifunctional amido-cyclopentadienyl ligand C_5R_4ZNR' in addition to two terminal ligands, X. The cyclopentadienyl ligand C_5R_4 is bonded in the usual η^5 fashion and the metal-ligand bond lengths are in the expected range. As a result of the constraint of the chelating ligand, the metal centre is often unsymmetrically bound to the cyclopentadienyl ring.

The distances between the metal and the amido-nitrogen are fairly sensitive to the nature of the metal fragment and are shorter than those observed for single bonds. For dichloro titanium(IV) complexes, $Ti(\eta^5:\eta^1\text{-}C_5R_4ZNR')Cl_2$, Ti-N distances shorter than 1.91Å are usually observed, whereas Ti-N single bonds vary between 1.96 and 1.97Å.[30] On the other hand these bond lengths are slightly larger than those found in non-bridged monocyclopentadienyl amido complexes. Thus the Ti-N distances in $Ti(\eta^5\text{-}C_5R_5)(N^iPr)Cl_2$ are 1.865(2)Å (R = H)[31] and 1.865(5)Å (R = Me)[31] compared to 1.901(3)Å (R = H)[18] and 1.908Å (R = Me)[32] in $Ti(\eta^5:\eta^1\text{-}C_5R_4SiMe_2N^tBu)Cl_2$. An optimal overlap of the amido nitrogen p_π orbital with the titanium d_π orbital seems to be disturbed by the chelation. The sum of the bond angles around the appended amido-nitrogen is usually 360°. This is clearly due to the sp^2 hybridisation caused by the d_π-p_π bond between the amido-nitrogen and the metal centre.

The Cp-M-N angles in complexes $M(\eta^5:\eta^1\text{-}C_5R_4ZNR')X_2$ usually range between 95-110°[18,24,32] and are 25-35° smaller than typical Cp-M-Cp angles in the corresponding 16 electron metallocene complexes, $M(\eta^5\text{-}C_5R_5)_2X_2$, where angles vary between 125-135°.[5] Strain within the ligand system and an openness of the coordination sphere can be deduced from this finding. While there is a clear trend of increasing Cp-M-N angle with increasing length of the bridge Z, a correlation of this geometric parameter with reactivity should not be overly emphasised.[24,32] Chelation also results in the slight reduction of the M-Cp distance, as shown by the comparison of $Ti(\eta^5:\eta^1\text{-}C_5H_4SiMe_2N^tBu)Cl_2$ (Ti-Cp: 2.019Å)[18] and $Ti(\eta^5\text{-}C_5H_5)(NH^tBu)Cl_2$ (Ti-Cp: 2.032Å).[33]

The shifts to lower frequency for the C_{ipso} of the cyclopentadienyl group in the $^{13}C\{^1H\}$ NMR spectra of complexes of the type $Ti(\eta^5:\eta^1\text{-}C_5R_4ZR')Cl_2$ have been found to be characteristic for the presence of a chelating amido group. For example in $Ti(\eta^5\text{-}C_5H_4SiMe_2Cl)Cl_3$ the ^{13}C chemical shift for the ipso carbon was found to be 135.1ppm[17] compared to 110.0ppm in $Ti(\eta^5:\eta^1\text{-}C_5H_4SiMe_2N^tBu)Cl_2$.[26]

1.2.4 Complexes with alkoxo functionalised cyclopentadienyl ligands

Compared to the amido-bridged half sandwich derivatives discussed earlier, complexes containing a cyclopentadienyl with an alkoxo-functionalised side chain (X = O in figure 1.2) are relatively scarce. The first example $Ti[\eta^5:\eta^1\text{-}C_5Me_4(CH_2)_3O]Cl_2$, is formed by the thermolysis of the titanium ylide $Ti[\eta^5:\eta^1\text{-}C_5Me_4(CH_2)_3OMe](CHPPh_3)Cl_2$ at 150°C (figure 1.11).[34]

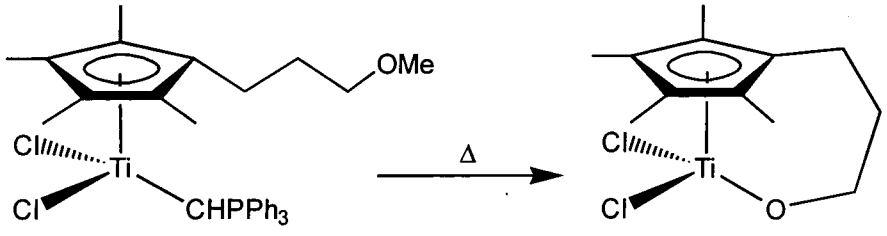

Figure 1.11

More rationally, the complexes $Ti[\eta^5:\eta^1\text{-}C_5H_4(CH_2)_nO]Cl_2$ are prepared in quantitative yields by reacting the ligands as trimethylsilylethers, $C_5H_4(SiMe_3)(CH_2)_nOSiMe_3$, with $TiCl_4$ (figure 1.12).[35]

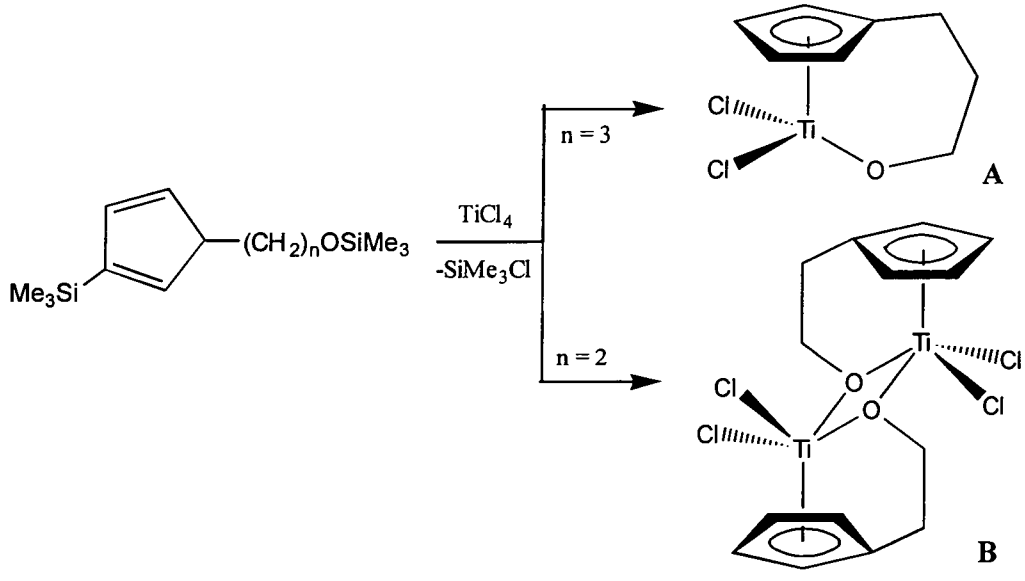

Figure 1.12

The length of the bridge, Z, is found to influence the molecular structure dramatically. The trimethylene chain, $(CH_2)_3$, gives rise to the monomeric complex, **A**,[35] whereas the shorter dimethylene chain, $(CH_2)_2$, affords the centrosymmetric dimer, **B**, in which the alkoxo-functions bridge the two titanium centres.[36]

The reaction of acetophenone with the monomeric titanium fulvene complex $Ti(\eta^5\text{-}C_5Me_5)[\eta^7\text{-}C_5Me_4(CH_2)_2]$, generated by thermolysis of $Ti(\eta^5\text{-}C_5Me_5)_2R$ (R = Me, Et, ^iPr), gives an alkoxo bridging titanium complex (figure 1.13).[37] Likewise $Ti(C_5H_4Me)(Ph)(\eta^6\text{-}C_5H_4CH_2)$ undergoes insertion with various aldehydes and ketones.[38]

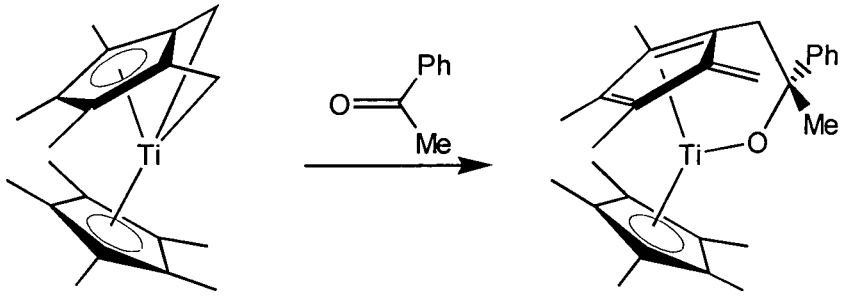

Figure 1.13

The formation of a chelate complex is observed during thermolysis of a titanium complex containing a tetramethylcyclopentadienyl ligand with a 2,6-dimethoxyphenyl group (figure 1.14).

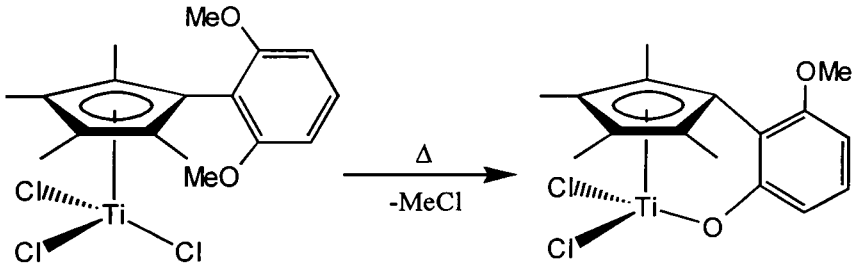

Figure 1.14

Similarly, $Ti(\eta^5\text{-}C_5H_4CEt_2C_6H_4OMe)(\eta^5\text{-}C_5H_5)Cl_2$ in the presence of LiBr, is converted into a benzyloxo bridged complex $Ti(\eta^5\text{:}\eta^1\text{-}C_5H_4CEt_2C_6H_4OMe)(\eta^5\text{-}C_5H_5)Cl_2$, following cleavage of the methoxy group.[39]

1.2.5 Complexes with polydentate amide functionalised cyclopentadienyl ligands

In order to attenuate the Lewis acidity of early transition metal centres, new ligands with a side chain incorporating an additional weak neutral donor site within the chelating amido-cyclopentadienyl ligand framework have been introduced. Donor groups such as OMe or NMe_2 attached to the amido functionality offer new possibilities in tailoring the coordination sphere around a reactive transition metal centre. The synthesis of such tridentate ligands has been achieved by following synthetic methodologies analogous to those for simpler substituents. Using the metathetical pathway, tetramethyl cyclopentadienyl titanium, zirconium and hafnium complexes $Ti(\eta^5:\eta^1\text{-}C_5Me_4SiMe_2NCH_2X)Cl_2$ (M = Ti, Zr, Hf; X = $CH{=}CH_2$, CH_2OMe, CH_2NMe_2) were prepared (figure 1.15).[40,41,42]

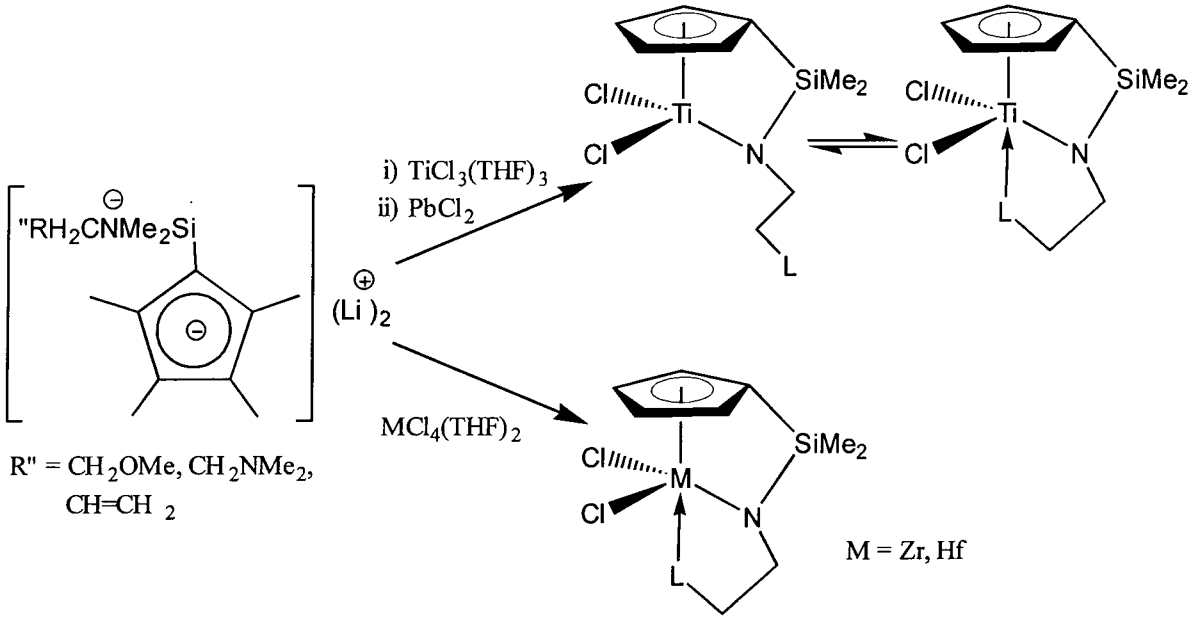

Figure 1.15

The question of whether the additional donor is rigidly bonded or in a fluxional manner cannot be decided by ^1H and ^{13}C NMR spectroscopy, including variable-temperature NMR spectroscopy. The use of X-ray crystallography and the use of NOE measurements on the corresponding dimethyl complexes have been used to study the coordination mode.

1.3 Applications of Amide Functionalised Cyclopentadienyl Complexes in Catalysis

1.3.1 Ziegler-Natta catalysis

One of the great discoveries of organometallic chemistry was the catalysed polymerisation of alkenes at atmospheric pressure and ambient temperature.[43] Vast quantities of polyethylene and polypropylene are made by Ziegler-Natta catalysis. The Zeigler-Natta catalyst, which is heterogeneous, is made by treating titanium tetrachloride with triethylaluminium to form a fibrous material that is partially alkylated (Et_2AlCl is used as a cocatalyst). Third generation catalysts (introduced about 1980) use a $MgCl_2$ support for the $TiCl_4$. The titanium does not have a filled coordination sphere and acts as a Lewis acid, accepting ethylene or propylene as another ligand.

1.3.2 Polymerisation of ethylene and α-olefins

As mentioned earlier, the great interest in linked amido-cyclopentadienyl complexes of group 4 metals, sometimes referred to as " constrained geometry catalysts", stems from their great potential as a new generation of olefin polymerisation catalysts. The possibility of producing polyolefins with new rheological properties and good processibility at temperatures as high as 160°C, has stimulated great activity in synthesising and testing such complexes. This has also led to the interest of similar Group 3 and 5 complexes.

Titanium complexes of the type $Ti(\eta^5:\eta^1\text{-}C_5H_4ZNR')Cl_2$ with methylaluminoxane are close to being commercially utilised catalysts for olefin polymerisation. Preliminary activity-structure relationships show that these catalysts form, depending on the nature of the ligand framework, high molecular weight polyethylene with long-chain branching, resulting from the incorporation of olygoethylene chains formed by β-hydride elimination.[32] Also, superior properties such as copolymerisation have been recognised, allowing efficient and uniform incorporation of higher α-olefins such as 1-octene to give low-density polyethylene with thermoelastic properties. This pronounced ability to incorporate higher olefins is ascribed to the more open coordination sphere, compared to

conventional systems.[32,44] Zirconium systems seem to be less active than titanium systems.[32,45] An open coordination site can sometimes turn into a disadvantage with significant regioirregularity and low selectivity sometimes observed.

The nature of the ligand substituents R in the C_5R_4 ring, R' of the amido substituent in NR', and the length bridge Z, are found to influence the catalytic activity. Since cataslyst precursors with the shorter bridge Z, are found to give the best polymerisation characteristics, the bite angle of the chelating ligand (angle Cp-Ti-N) is proposed to be an important geometrical criteria for a catalyst to perform well.[24] The electronic properties imparted by R, R' and Z are important as well, with a peralkylated cyclopentadienyl ring and t-butyl group as the amido substituent appearing to be more preferable.[32]

In contrast to the 14-electron Group 4 bis cyclopentadienyl polymerisation catalysts , **A**, but in analogy to the scandium catalyst, **B**, the 12-electron alkyl cation is thought to be the active species in Group 4 amide functionalised cyclopentadienyl complexes, **C** (figure 1.16).[46]

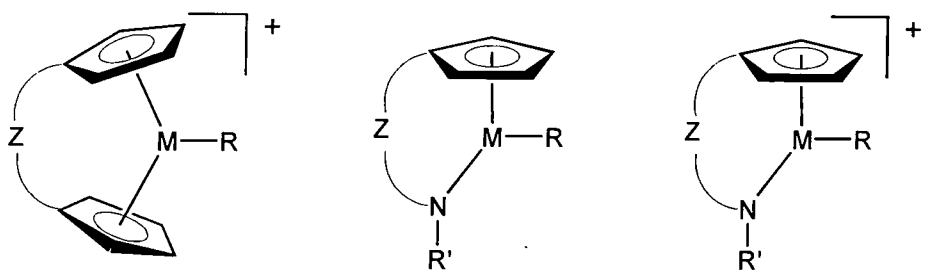

Group 4, **A** Group 3, **B** Group 4, **C**

Figure 1.16

The catalytic species can either be generated by the reaction of the pro-catalyst with methylaluminoxane, or by reacting a dialkyl pro-catalyst with a Lewis acid such as $B(C_6F_5)_3$. Structurally characterised cationic complexes include $[Zr(\eta^5:\eta^1\text{-}C_5Me_4SiMe_2N^tBu)Me]^+[FAL(C_{12}F_{10})_3]$.[45] Variable temperature NMR studies have revealed an activation barrier of 19.3 kcal/mol for the ion pair reorganisation and symmetrization, caused by the back-skip of the alkyl group in $[Zr(\eta^5:\eta^1\text{-}C_5Me_4SiMe_2N^tBu)Me]^+[MeB(C_6F_5)_3]^-$.[45]

The efficient copolymerisation of ethylene and styrene became possible only with the use of metallocene catalysts, since conventional Ziegler-Natta catalysts normally induce homopolymerisation of each of the monomers. Metallocene catalysts allow poly(ethene-co-styrene) to be formed, but still suffer low incorporation of styrene. One of the best copolymerisation catalysts consists of the titanium complex $Ti(\eta^5:\eta^1\text{-}C_5Me_4SiMe_2N^tBu)Cl_2$, which has high activity and results in the production of ethylene-styrene co-polymer with up to 30mol% of styrene. By studying the influence of substituents R and R' in $Ti(\eta^5\eta^1\text{-}C_5Me_4SiMe_2NR')Cl_2$, it was shown that both activity and the incorporation of styrene is sensitive to the nature of R and R'.[47]

The dimeric scandium hydride complex $[Sc(\eta^5:\eta^1\text{-}C_5Me_4SiMe_2N^tBu)(PMe_3)]_2(\mu\text{-}H)_2$ is capable of catalysing the aspecific oligomerisation of the α-olefins, propylene, 1-butene, and 1-pentene.[9] Although this presents an advantage over the scandocenes, the polymerisation occurs slowly with the formation of relatively low molecular weights [M_n = 3000 for poly(1-pentene)], and the addition of PMe_3 results in slower olefin polymerisation rates.

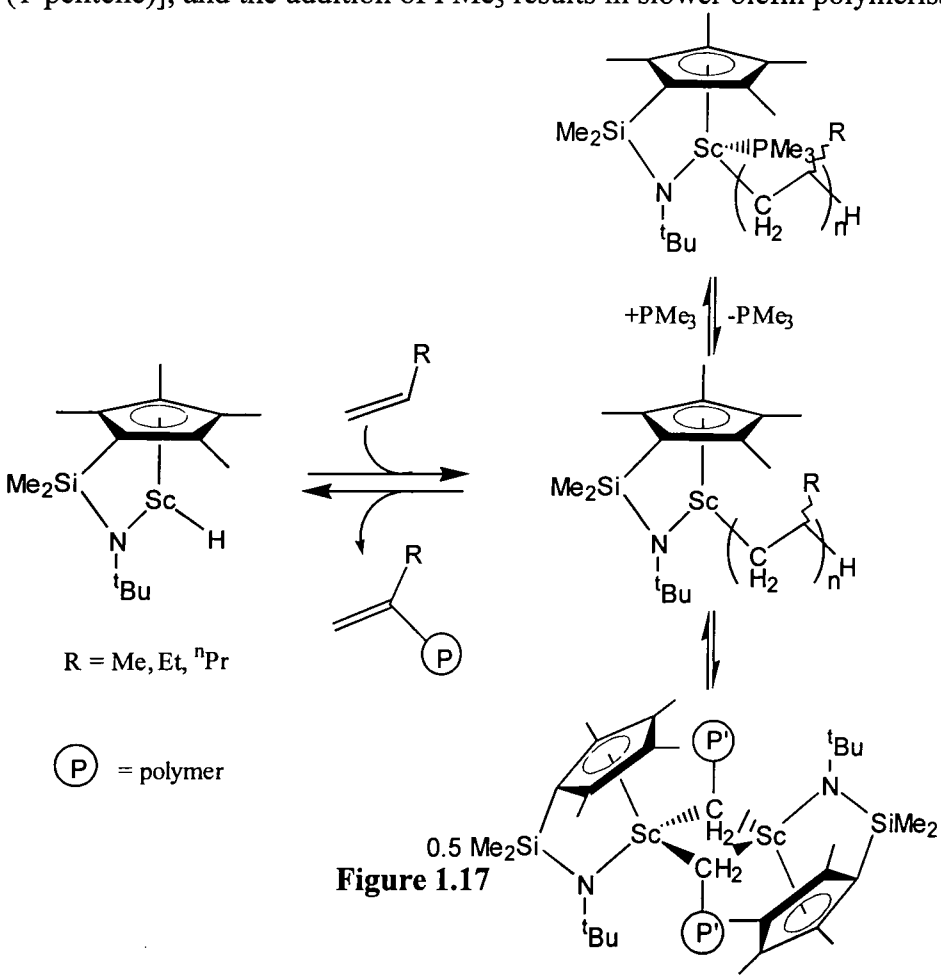

Figure 1.17

The dimeric Lewis-base-free n-alkyl complexes $[Sc(\eta^5:\eta^1\text{-}C_5Me_4SiMe_2N^tBu)]_2(\mu\text{-}CH_2CH_2R)_2$ (R = Me, Et) were shown to be more active catalyst precursors than the hydrido complex, and polymers with higher molecular weights are obtained (M_n = 6000 for poly(1-pentene). Low temperature ^{13}C NMR spectroscopic studies of the model complexes $[Sc(\eta^5:\eta^1\text{-}C_5Me_4SiMe_2N^tBu)(PMe_3)(CH_2CHMeCH_2CH_2Me)]$ and $[Sc(\eta^5:\eta^1\text{-}C_5Me_4SiMe_2N^tBu)(PMe_3)[^{13}CH_2CH(^{13}CH_3)_2]$ indicate that one PMe_3-adduct is in equilibrium with only one PMe_3-free species. By its symmetry it is concluded to be the monomeric 12-electron alkyl complex $Sc(\eta^5:\eta^1\text{-}C_5Me_4SiMe_2N^tBu)R$" (figure 1.17).

1.3.3 Hydrogenation and hydroboration

The overwhelming interest in utilising linked amido-cyclopentadienyl complexes in olefin polymerisations has meant that only two other applications of this class of catalyst have so far been reported in the literature, hydrogenation and hydroboration.

The enantioselective catalytic hydrogenation of substituted olefins, and in particular of imines have been successfully achieved using reductively activated chiral Brintzinger-type titanocene derivatives.[48] When optically active titanium complexes of the type $Ti(\eta^5:\eta^1\text{-}C_5R_4SiMe_2NR')Cl_2$ (R = H, Me; R' = CHMePh) are treated with ^{n}BuLi, similarly active hydrogenation catalysts for imines are generated, although with low enantioselectivity (figure 1.18).[16] As with the titanocene system, the catalytically active species is presumed to be a titanium(III) hydrido species, possibly of the type $Ti(\eta^5:\eta^1\text{-}C_5R_4SiMe_2NR')H$.

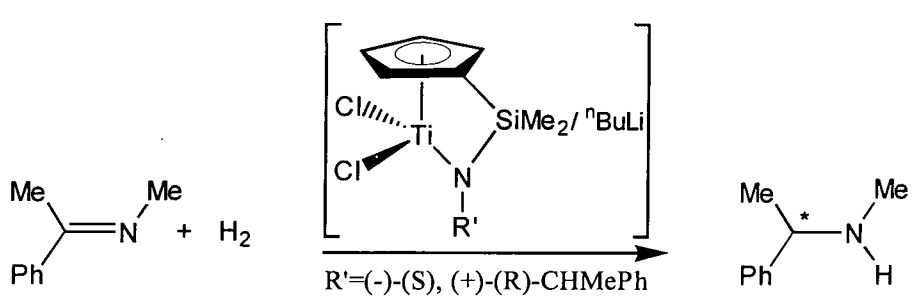

Figure 1.18

Hydroboration of alkenes with catecholborane is known to be catalysed by metallocenes of group 3 metals.[48] The complexes $Ti[\eta^5:\eta^1(CH_2)_3NMe]Me_2$ and $Zr[\eta^5:\eta^1(CH_2)_3NMe]X_2$ ($X = BH_4$, CH_2Ph) are moderately active as catalysts for the hydroboration of 1-hexane using catecholborane (figure 1.19).[49]

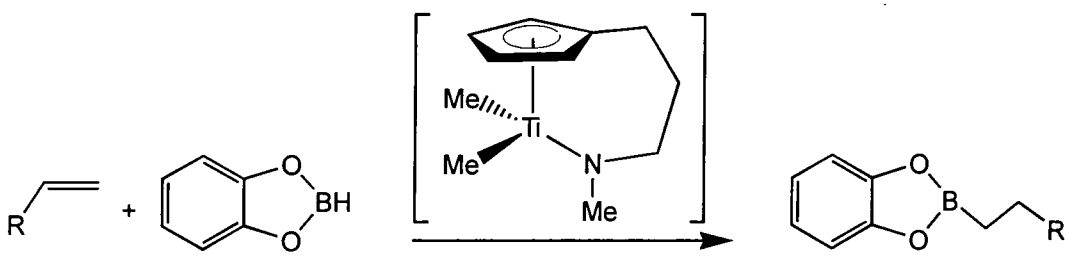

Figure 1.19

1.4 Preparation of Amide Functionalised Cyclopentadienyl Complexes

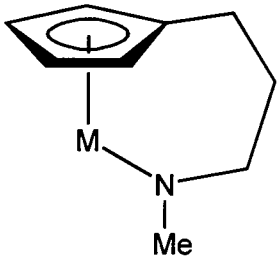

A cyclopentadienyl ring linked by a trimethylene chain to a secondary amide system.

In an attempt to synthesise novel functionalised cyclopentadienyl complexes the above ligand system, $C_5H_5(CH_2)_3N(H)Me$, was prepared and used for the following reasons:

Z = A Trimethylene Backbone

A short bridging group (Z = SiR_2, CR_2, C_2R_4 R = H or Me) has the effect of opening up one side of the complex, producing a highly open and reactive site. This does not allow for much steric control of the polymerisation reaction, and homopoly α-olefins are generally atactic. A trimethylene backbone would allow for more steric control and would produce less strained complexes when coordinated intramolecularly. The reactivity and possible cleavage of Si-N bonds led to the use of a carbon rather than silicon backbone.

L = Nitrogen: A Secondary Amine

A secondary amine is an LX ligand and when coordinated to a metal forming an amide it has the ability of stabilising the metal electronically. It is more versatile than an imido ligand, being able to donate one or three electrons to the metal, and form stronger bonds than the labile amino complexes.

X = Methyl: Methylamine

Although t-butyl groups have been found to enhance catalytic activity, previous work with $C_5H_5(CH_2)_3N(H)^tBu$ gave complexes that were mainly oils.[25] Using a methyl group is therefore thought to be able to give complexes of a more crystalline nature.

1.4.1 Synthesis of amine functionalised cyclopentadienyl ligands

Following the traditional route to metallocene complexes, amido-bridged half-sandwich complexes are most commonly synthesised by first assembling the ligand $(C_5H_4H)Z(NHR')$ and then coordinating it to the metal centre. Dimethylsilyl, $SiMe_2$, is commonly used as a bridging function Z and the ligand is usually synthesised by the reaction of $Li(C_5R_4H)$ with $SiMe_2Cl_2$ to give $(C_5R_4H)SiMe_2Cl$ (R = H or Me). This is then reacted with a variety of lithium amides Li(NHR'), to give the ligand precursor $(C_5R_4H)SiMe_2NHR'$. For di- and tri-methylene linked ligands the reaction of $[Br(CH_2)_nN^+H_2R'']Br^-$ (N = 2, 3; R = Me, ^{i}Pr, ^{t}Bu) with an excess of $Na(C_5H_5)$ forms $C_5H_5(CH_2)_nNHR'$ as several bond isomers. A slightly modified and improved synthesis was used for the synthesis of the ligand $C_5H_5(CH_2)_3N(H)Me$, **1.1**, previously prepared by Teuben and co-workers.[23]

1.4.2 Synthesis of $C_5H_5(CH_2)_3N(H)Me$ 1.1

$EtO_2C(CH_2)_2N(H)Me$

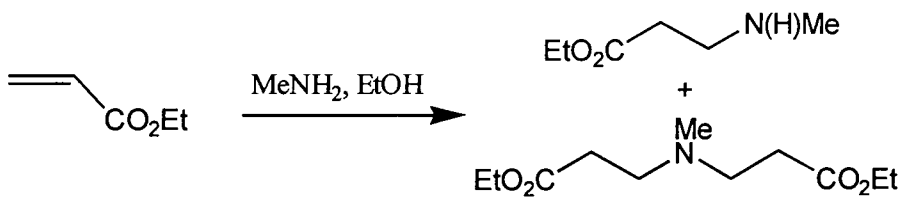

Figure 1.20

Initially, $EtO_2C(CH_2)_2N(H)Me$ was synthesised via the conjugate addition of methylamine to ethyl acrylate in ethanol.[50] Distillation produces the mono-substituted ester in a moderate, 35%, yield. Unfortunately a similar quantity of the di-substituted product is also produced (figure 1.20). Bulkier amines are known to give higher yields of the desired mono-substituted product, e.g. t-butylamine gives the mono-substituted complex $EtO_2C(CH_2)_2N(H)^tBu$ in >95% yield.[51]

$HO(CH_2)_3N(H)Me$

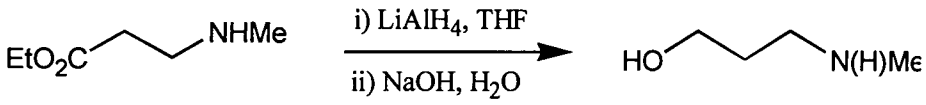

Figure 1.21

The reduction of the ester to the corresponding alcohol, $HO(CH_2)_3N(H)Me$, was accomplished using $LiAlH_4$ followed by aqueous work-up, yielding the alcohol in 74% yield (figure 1.21). The original researchers achieved only moderate yields of 38%[52] and 48%,[53] and initially similar yields were achieved. By adding a solution of the ester, diluted with twice the volume of THF, to the $LiAlH_4$, slowly over 3 hours at 0°C, followed by the slow addition of water that was diluted with five times the volume of THF gave improved yields. The main reason for low yields is thought to be due to the heat produced at the point of contact of the ester (or water for the aqueous work-up) and reducing agent being sufficient to evaporate some ester or alcohol.

It was also discovered that a large percentage of the product formed was being absorbed onto the solid $Al_2O_3:nH_2O$ produced during the aqueous work-up, and that ether extraction was removing only small quantities of the alcohol. To overcome this problem, the work-up was carried out using a saturated aqueous NaOH solution, rather than water, the high pH causing most of the hydrolysis products to dissolve in the aqueous layer. Extraction of the aqueous layer with several portions of THF produced the desired alcohol as a colourless oil that was pure by NMR spectroscopy.

$Cl(CH_2)_3N(H)Me.HCl$

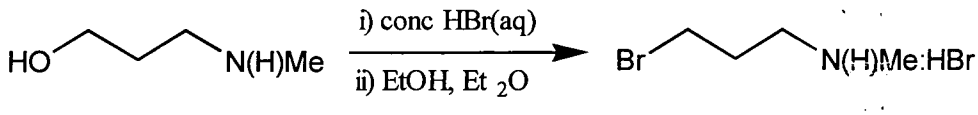

Figure 1.22

In previous work, the alcohol, $HO(CH_2)_3N(H)Me$, was converted into the bromide salt, $Br(CH_2)_3N(H)Me{:}HBr$, using an experimental procedure based on that described by Cortese (figure 1.22).[54] The alcohol was added to an aqueous solution of HBr, followed by reflux, then distillation and extraction of the product into ethanol. The addition of diethylether to the solution and cooling gave hydrobromide salt in a moderate 58% yield. However studies carried out on an analogous product, $HO(CH_2)_3N(H)^tBu$, found that the aqueous reaction conditions and the mildly hygroscopic nature of the compound made it difficult to obtain a sample which was completely dry, thereby causing problems with the synthesis of the cyclopentadiene in the next step.[51]

Conversion of the alcohol, $HO(CH_2)_3N(H)Me$, into the hydrochloride salt, $Cl(CH_2)_3N(H)Me.HCl$, using thionyl chloride is the preferred method, and is based upon the literature synthesis of N-dimethyl-2-chloroethylamine hydrochloride (figure 1.24).

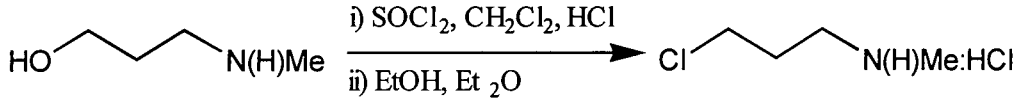

Figure 1.24

Previous related studies found that the addition of thionyl chloride to pure undiluted alcohol, $HO(CH_2)_3N(H)^tBu$, gave an exothermic reaction causing the HCl formed to escape the mixture as a gas and, therefore, not available to protonate the amine.[51] This allowed ring-closure to occur forming a large quantity of N-^{t}butylazetidine and a smaller yield of the hydrochloride salt, <30% (figure 1.25).

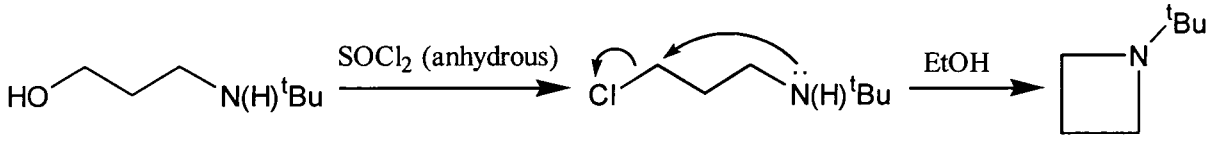

Figure 1.25

To prevent formation of this side product, CH_2Cl_2 is used as the solvent, and a few drops of concentrated HCl are added to ensure protonation of the amine occurs. Refluxing the suspension with ethanol was carried out to destroy the excess $SOCl_2$. Removal of the

solvents followed drying under reduced pressure gives $Cl(CH_2)_3N(H)Me.HCl$ as an off white solid, pure by ^1H NMR spectroscopy. Recrystallisation from hot acetonitrile can be carried out but reduces the yield significantly.

$C_5H_5(CH_2)_3N(H)Me$ **1.1**

The desired functionalised cyclopentadiene, $C_5H_5(CH_2)_3N(H)Me$, **1.1**, was synthesised from the reaction of the hydrochloride salt, $Cl(CH_2)_3N(H)Me.HCl$, with two equivalents of sodium cyclopentadiene in THF (figure 1.26).

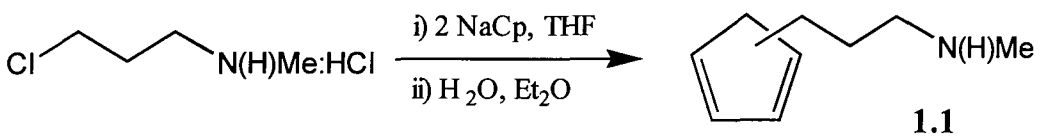

Figure 1.26

Two equivalents of NaCp are required since one equivalent is used to convert the amine hydrochloride to the analogous free amine while the second nucleophilic $C_5H_5^-$ couples with the chloride. However, when following a previous synthesis using 3 rather than 2 equivalents of NaCp, the yield of mono-substituted product was significantly lower (<25%).[23] A second product distilled at a slightly higher temperature. NMR and mass spectroscopic analysis found it to be the disubstituted product (figure 1.27).

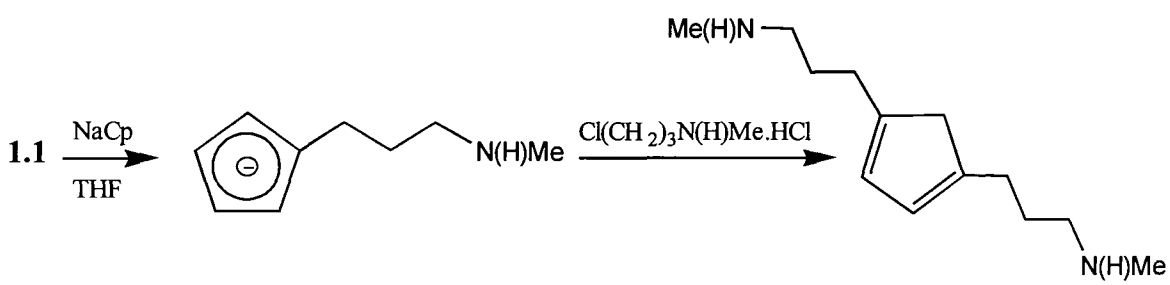

Figure 1.27

Upon work-up, NMR spectroscopy showed a 5:1 mixture of **1.1** and dicyclopentadiene which distillation failed to separate. The mixture was purified by taking advantage of the basic amine and extracting the product with dilute HCl followed by immediate addition to

a basic solution. Distillation gave $C_5H_5(CH_2)_3N(H)Me$, **1.1** as a colourless oil, in 42% yield. At room temperature the product slowly dimerises, rapidly turning yellow then brown, and therefore the oil was stored at -40°C where it is stable for many months.

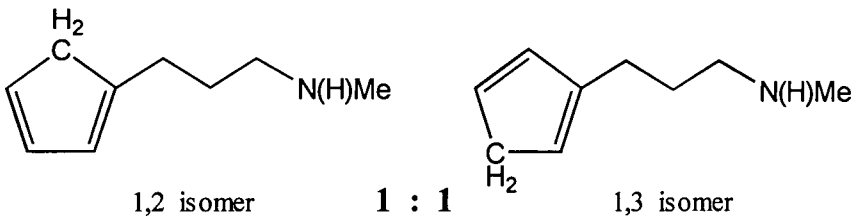

Figure 1.28

Both ^1H and ^{13}C NMR spectroscopy show that $C_5H_5(CH_2)_3N(H)Me$ exists as a mixture of two of the three possible isomers (figure 1.28), in a ratio very close to 1:1. The ^{13}C NMR spectrum is the more informative, showing two quarternary resonances at 149.1 and 146.5ppm, and a total of six olefinic CH resonances between 125 and 135ppm. It has not proved possible to totally assign the C_5H_5 resonances in the ^1H NMR spectrum on account of heavy overlap, although the two sets for each of the CH_2N and $CH_2C\underline{H_2}CH_2$ group are clearly resolved.

1.4.3 Synthesis of lithium salts

For the complexation of the linked amido-cyclopentadienyl ligand the metathetical reaction of the doubly metallated ligand ligand precursor $(C_5R_4ZNR')^{2-}$ with appropriate metal halides appears to be the most common employed reaction. In general an amine substituted cyclopentadiene undergoes mono- and di- deprotonation reactions (dependant on the stoichiometry of the reaction and solvent employed) with strong bases such as n-butyl lithium or potassium hydride. The use of Grignard reagents to prepare magnesium derivatives for use as less reducing ligand transfer reagents has also been reported.[55] The salts are most commonly used in situ without isolation, although occasionally isolation is possible; e.g. $(C_5Me_4SiMe_2N^tBu)Li_2$ is obtained as a tan powder. Based on what is known about both cyclopentadienyl and amido lithium complexes in solution, complicated structures can be assumed for such dianions. Temperature dependent NMR spectra of

$[(C_{13}H_8)SiMe_2N^tBu)]Li_2$ indicate an unsymmetrical structure devoid of a mirror plane.[19] Lithium salts of Lewis-base substituted cyclopentadienides, in particular, have found extensive applications, reported in the literature, for the preparation of transition metal complexes and substituted ferrocenes. These are discussed in detail in Chapters 2 to 6.

To be able to carry out reactions with metal chloride complexes, alkali metal salts, particularly lithium salts, formed by the deprotonation of $C_5H_5(CH_2)_3N(H)Me$ were prepared.

1.4.3a) Mono-lithiated salt - $[C_5H_4(CH_2)_3N(H)Me]^-Li^+$ 1.2

Studies have shown that amine functionalised cyclopentadienes undergo selective deprotonation at the ring first and not the amine nitrogen, in certain solvents. This is to be expected, since cyclopentadienes are more acidic than amines (C_5H_6 in MeOH pKa = 14-15,[56] RNH_2, R_2NH pK_a = ~35,[57]), and therefore a more thermodynamically favourable reaction.

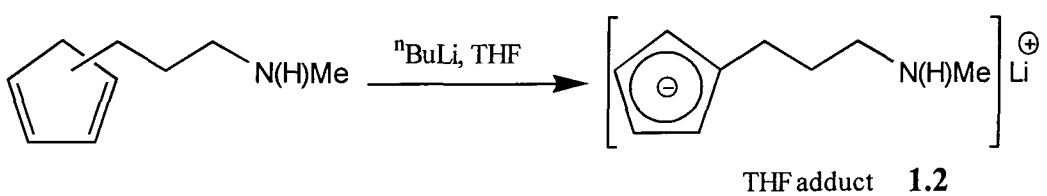

THF adduct **1.2**

Figure 1.29

The neutral ligand, $C_5H_5(CH_2)_3N(H)Me$, **1.1**, reacts cleanly and rapidly with one stoichiometric equivalent of n-butyl lithium in hexane at room temperature, yielding $[C_5H_4(CH_2)_3N(H)Me]Li$, **1.2**, as a white solid (figure 1.29). This precipitates from solution, thus preventing any di-lithium salt from forming by further reaction with the unreacted n-butyl lithium. Due to the highly air sensitive and insoluble nature of the salt in accessible NMR solvents ($CDCl_3$, C_6D_6, etc.) the product was not isolated or characterised, but reacted in situ assuming >95% completion. Such reactions are discussed in Chapter 6.

1.4.3b) Di-lithiated salt - $[C_5H_4(CH_2)_3NMe]^{2-}Li_2^+$, 1.3

The ligand $C_5H_5(CH_2)_3N(H)Me$ reacts with two equivalents of n-butyl lithium in THF, at 0°C. During the addition $[C_5H_4(CH_2)_3NMe]Li_2$, **1.3**, forms as a white insoluble precipitate (figure 1.30). The reaction was performed at 0°C to prevent n-butyl lithium from ring-opening the tetrahydrofuran, a reaction that occurs slowly at room temperature.

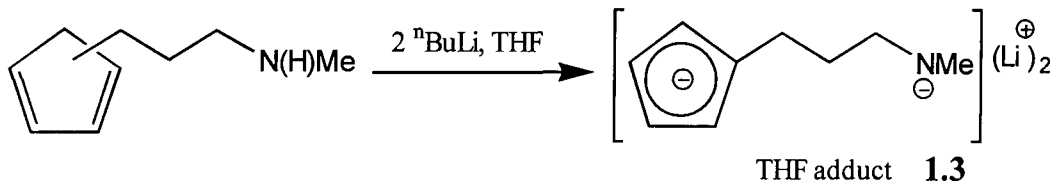

Figure 1.30

Once again, due to the sensitive and insoluble nature of the product it was not isolated and characterised but used in situ assuming >95% completion. Isolation of the product would prove difficult, requiring the removal of coordinated tetrahydrofuran using hexane washings, or quantifying the amount of THF present.

1.4.4 Synthesis of $[C_5H_4(CH_2)_3NMe](SiMe_3)_2$, 1.4

In cases where reactions with the dianion, **1.3**, are unsuccessful a milder reagent may be required and therefore the bis-trimethylsilyl complex, **1.4**, was used. Two equivalents of Me_3SiCl were added to a suspension of the dianion, **1.3**, in THF (figure 1.31). Extraction of the product into toluene gave $[C_5H_4(CH_2)_3NMe](SiMe_3)_2$, **1.4**, as a pale yellow oil, in 85% yield.

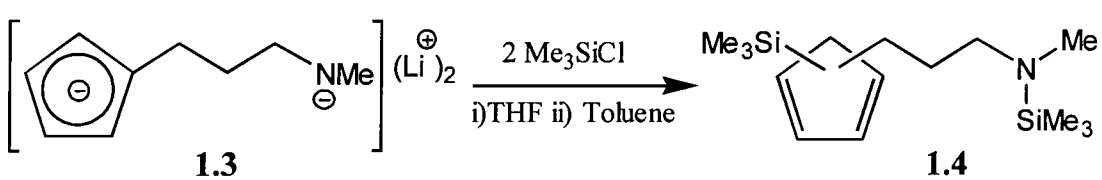

Figure 1.31

The ^{1}H NMR spectrum in C_6D_6 shows two singlets each integrating to 9 protons each, at 0.10 and –0.06 ppm for the $C_5H_4SiMe_3$ and $NSiMe_3$ groups, respectively. The C_5H_4 fragment is seen as an AA'BB' spin system with two triplets at 6.45 and 6.14ppm. The NCH_3 resonance is only slightly shifted compared to **1.1** with a singlet appearing at 2.39ppm, and the trimethylene backbone observed as a series of multiplets.

1.4.5 Previous work with $C_5H_5(CH_2)_3N(H)Me$, 1.1

To date, previous work in preparing ring closed complexes with $C_5H_5(CH_2)_3N(H)Me$, **1.1**, has been with the Group 4 homoleptic amides $M(NMe_2)_4$.[23] Reaction of the neutral ligand, **1.1**, with stoichiometric amounts of $Zr(NMe_2)_4$ and $Hf(NMe_2)_4$ gave the bis amide zirconium and hafnium complexes, **A** and **B** in high yield (figure 1.32).

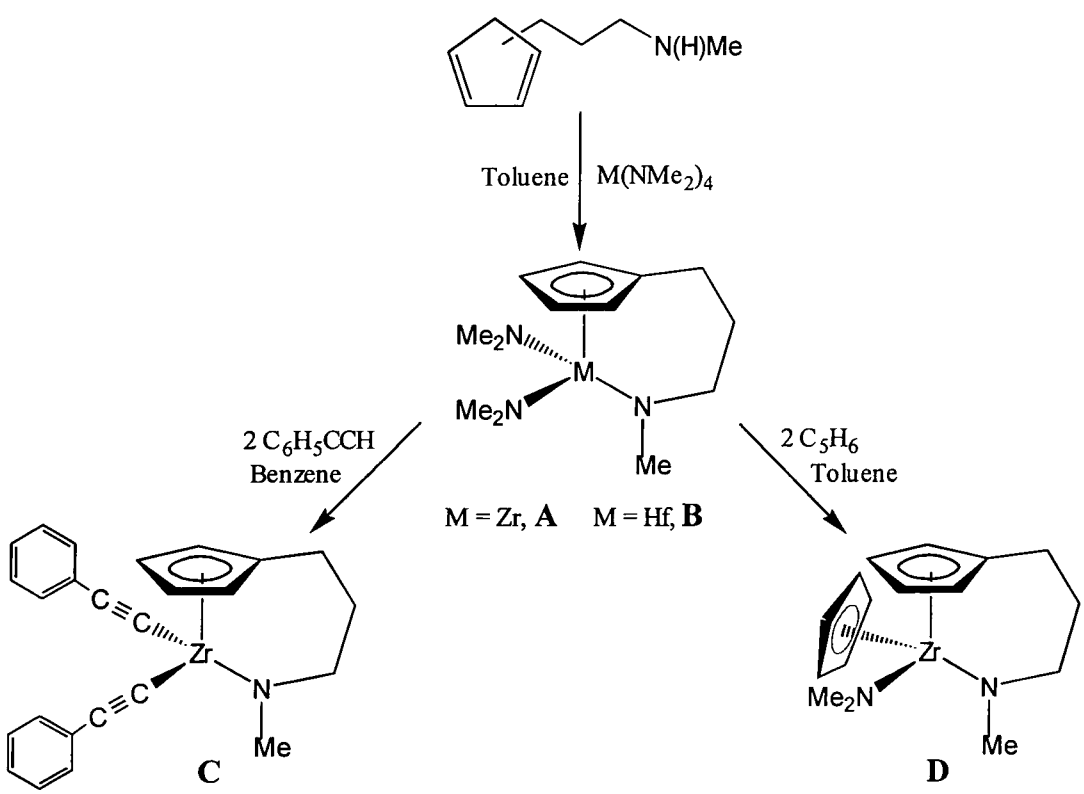

Figure 1.32

Although the reaction of metal-halide complexes with alkylating reagents is the most widely used method for the synthesis of metal-carbon bonds, the aminolysis reaction of the metal amides in **A** and a suitably acidic hydrocarbon (pK_a <35) also gave metal "alkyl" complexes. The reaction of **A**, with 2 equivalents of phenylacetylene gave the corresponding bis alkyl complex, **C**, whereas the reaction with an excess of cyclopentadiene gave the chiral mono-substituted complex, **D**.

The advantages of the aminolysis route for the metallation of cyclopentadienes are that it is a simple, one step procedure and that the elimination product (dimethylamine) is gaseous and easily removed from the reaction, thus making purification of the final product easier. The aminolysis reaction is fairly versatile and can be used to synthesise Group 4 complexes of a variety of ligands. The pK_a of secondary amines is in the range 35-40, and thus transition metal amides, M-NR_2, will react with a wide range of "acids". However cyclopentadienyl metal amides appear to be less versatile and useful as starting materials than cyclopentadienyl metal chlorides. Metal chlorides can be used to prepare a variety of interesting complexes, particularly metal alkyls. Therefore the dimethylamide complexes were converted to halides by dimethylammonium halides which act as a source of HX which can be weighed and used stoichiometrically. From the chloride further reactions were carried out.

Aminolysis by the addition of 2 equivalents of acid (HCl or HI), in the form of dimethylamine hydrohalide, to **A** and **B** provides a facile route to the dihalide complexes **E**, **F**, and **G** (figure 1.33). The dichloride, **E**, was found to be an excellent precursor to various alkyl complexes. The reaction with 2 equivalents of the alkylating agents MeMgCl or Me_3SiCH_2Li gave the corresponding bis alkyl complexes, **H** and **I**, and the reaction of one equivalent of $C_6H_5CH_2MgCl$ gave the dimer, **J**. Instead of distorting the benzyl ligands, the electron defficiency is relieved by forming bridging chloro ligands. The crystal structure exhibits two different Zr-Cl distances due to the trans influence of the benzyl ligand. The reaction of **E** with excess $LiBH_4$ gave the colourless bis-tetrahydroborate, **K**, which contains rapidly exchanging terminal and bridging hydrido ligands.

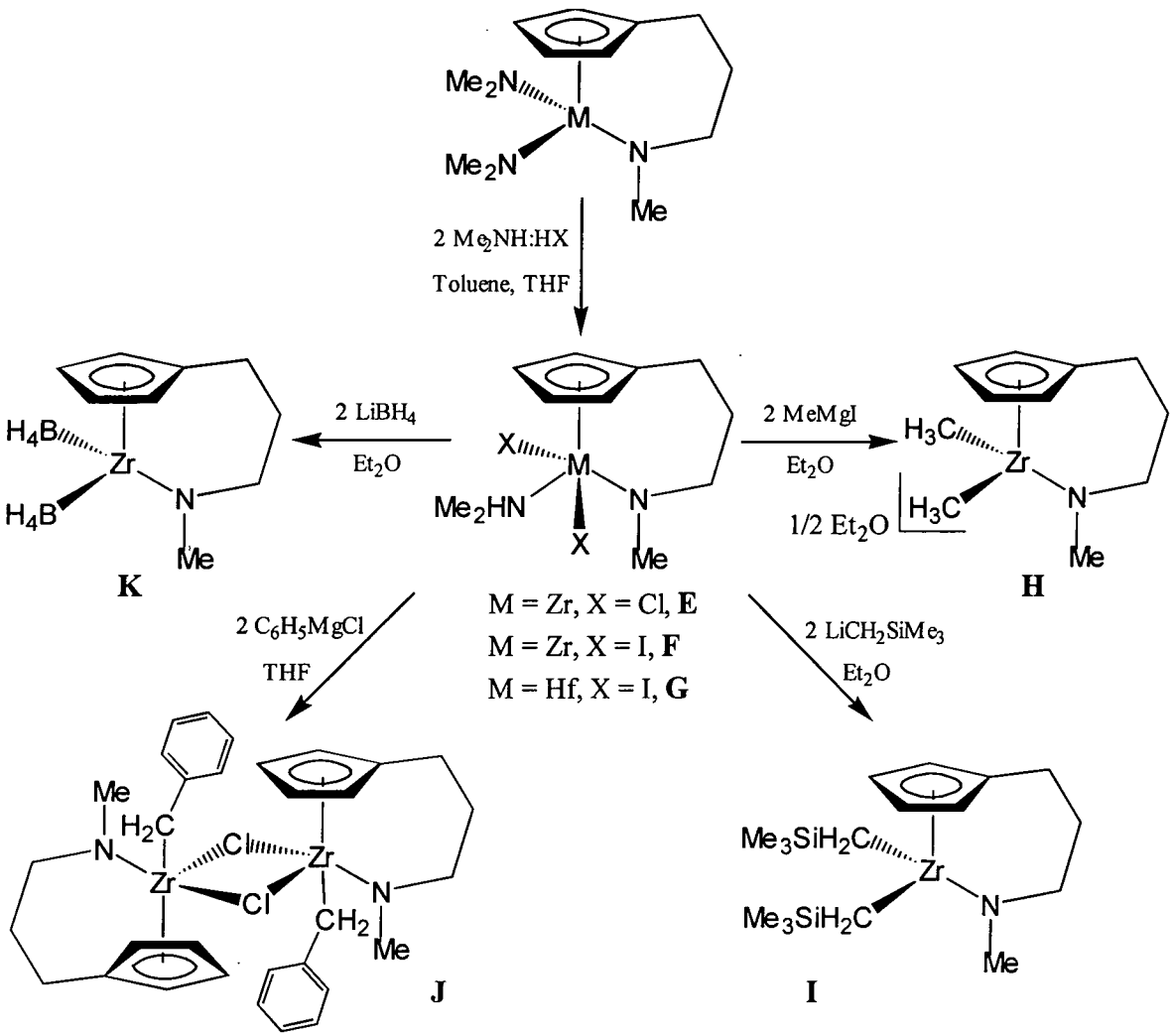

Figure 1.33

Attempts to prepare the group 4 amine substituted metal chlorides by the direct route have always been unsuccessful. Both the dilithiated or disilylated derivatives of $C_5H_5(CH_2)_3N(H)R$ (R = Me or ^tBu) gave unidentifiable products on work-up following the reaction with $TiCl_4$, $TiCl_3(THF)_3$, and $TiCl_4(THF)_2$. The reactions gave highly insoluble products, possibly indicating a polymeric structure.[23,51]

1.5 Aims

The introduction of the linked amido-functionalised ligand as a replacement for the bridged bis(cyclopentadienyl) ligand in ansa-metallocenes has led to a class of outstanding olefin polymerisation catalysts. However, many coordination chemical aspects have not been fully explored yet and it remains to be seen whether this ligand framework provides a metal template as versatile as the metallocene unit $M(\eta^5\text{-}C_5R_5)_2$. The linked amido-cyclopentadienyl complexes may be considered as a hybrid between ansa-metallocenes and complexes containing bis amide ligands. The latter type has also emerged as homogeneous olefin catalysts.

In order to explore further the potential of amide-functionalised cyclopentadienyl complexes, the ligand $C_5H_5(CH_2)_3N(H)Me$, **1.1**, was used to prepare and investigate such species. Since previous work with this ligand system involves reactions of the neutral ligand with the Group 4 homoleptic amides (section **1.4.5**), one of our main interests was to investigate reactions of the dianion $[C_5H_4(CH_2)_3NMe]^{2-}$ with metal chloride complexes.

Recently many cyclopentadienyl and amide complexes of the Group 5 and 6 transition metals have shown catalytic activity, particularly in olefin polymerisation. With very few amide functionalised cyclopentadienyl complexes of these groups synthesised previously, our other main interest was to synthesise such complexes, as well as those of the more common Group 4 transition metals.

1.6 Experimental

1.6.1 Preparation of $C_5H_5(CH_2)_3N(H)Me$, 1.1

$EtO_2C(CH_2)_2N(H)Me$

An aqueous solution of methylamine (200ml of a 40% solution, 2.3mol) was added dropwise with vigourous stirring to NaOH (100g, 2.5mol) placed under a static vacuum, and the methylamine produced was collected in ethanol (300ml) at -78°C (dry ice/acetone). Ethyl acrylate (220g, 2.2mol) was added dropwise to the solution of $MeNH_2$ at 0°C. After stirring at room temperature for 24hr the solvents were removed on a rotary evaporator. Distillation (27°C, 10^{-3}mmHg) yielded $EtO_2C(CH_2)_2N(H)Me$ as a colourless oil (101g, 0.77mol, 35% yield with respect to ethyl acrylate).

^1H NMR δ/ppm $CDCl_3$; 4.16 (q, 2H, $C\underline{H}_2CH_3$), 2.83 (t, 2H, CH_2N), 2.48 (t, 2H, CH_2CO_2), 2.42 (s, 3H, CH_3N), 1.48 (br s, 1H, NH), 1.24 (t, 3H, $CH_2C\underline{H}_3$)

$HO(CH_2)_3N(H)Me$

Caution: This reduction requires $LiAlH_4$ to be used in THF, rather than Et_2O. This is hazardous as $LiAlH_4$ has been known to detonate in THF, so vigorous stirring and efficient cooling are required.

A suspension of $LiAlH_4$ (31.0g, 0.81mol) in THF (2L) was stirred in a 3L two-necked flask fitted with condenser open to the nitrogen bubbler until the evolution of gas had ceased, and then cooled to 0°C. A solution of $EtO_2C(CH_2)_2N(H)Me$ (101g, 0.77mol) in THF (200ml) was added dropwise over 3hr, the suspension then stirred at room temperature for 24hr followed by reflux for 3hr. The mixture was cooled to 0°C and the excess $LiAlH_4$ destroyed by adding cautiously a solution of water (30ml) in THF (150ml), followed by NaOH (0.8g, 0.25mol) in water (30ml). The viscous white suspension was filtered in air, washed with isopropanol (2 x 200ml) and the combined filtrates dried over anhydrous $MgSO_4$. The solvents were removed on a rotary evaporator to yield $HO(CH_2)_3N(H)Me$ as a colourless viscous oil (50.7g, 0.57mol, pure by NMR, 74% yield).

^{1}H NMR δ/ppm $CDCl_3$; 3.78 (t, 2H, CH_2O), 3.16 (br s, 1-2H, NH, OH), 2.82 (t, 2H, CH_2N), 2.41 (s, 3H, CH_3N), 1.67 (quin, 2H, $CH_2C\underline{H_2}CH_2$)

$Cl(CH_2)_3N(H)Me.HCl$

Caution: $Cl(CH_2)_3N(H)Me.HCl$ is a potential nitrogen mustard and was therefore handled in a fume hood wearing protective clothing.

In air, a slurry of $HO(CH_2)_3N(H)Me$ (50.7g, 0.57mol) in dichloromethane (150ml) was cooled to 0°C and HCl (6ml of a 10M solution, 6mmol) added dropwise. Thionyl chloride (52ml, 0.6mol) was added dropwise over 30min giving off white fumes, and the mixture stirred at room temperature for 24hr. Warm ethanol (10ml at 50°C) was added slowly, and the mixture stirred for 2hr to remove any unreacted thionyl chloride. The solvents were then removed under reduced pressure leaving crude $Cl(CH_2)_3N(H)Me.HCl$ (80g, 0.55mol, 97% yield) as a hygroscopic off white solid.

Purification could be carried out by recrystallisation from the minimum amount of hot ethanol, producing pure $Cl(CH_2)_3N(H)Me.HCl$ as a white crystalline solid. However this reduces the yield dramatically and therefore the crude product was used directly in the next stage of the reaction.

^{1}H NMR δ/ppm D_2O; 3.71 (t, 2H, CH_2Cl), 3.22 (t, 2H, CH_2N), 2.74 (s, 3H, CH_3N), 2.16 (quin, 2H, $CH_2C\underline{H_2}CH_2$).

$C_5H_5(CH_2)_3N(H)Me$, 1.1

A 3L two-necked flask fitted with a condenser, was charged with $Cl(CH_2)_3NHMe.HCl$ (80g, 0.55mol), and THF (500ml, Na dried). The solution was degassed and cooled to 0°C, under nitrogen. A solution of NaC_5H_5 (ca. 1.3mol, from 130ml, 1.30mol C_5H_6, and 31.5g, 1.33mol Na in 1.5L THF) was added dropwise over 15min and the dark red mixture stirred at room temperature for 24hr, followed by reflux for 3hr. In air, the suspension was cooled to 0°C and treated with water (600ml). The organic layer was separated and the aqueous layer washed with diethyl ether (2 x 300ml). The combined organic layers were washed with water (100ml) and the volatiles removed on a rotary evaporator, leaving a 5:1 mixture of $C_5H_5(CH_2)_3N(H)Me$ and dicyclopentadiene, as a light brown oil. Distillation failed to separate the product from dicyclopentadiene, and therefore the mixture was purified taking advantage of the basic amine function.

Petroleum ether (400ml, b.pt. 40-60°C) was added to the oil and extracted with three portions of dilute HCl (total 800ml 0.75M solution, 0.6mol), the aqueous extracts being added directly to a solution of NaOH (30g, 0.75mol) in water (400ml) and diethyl ether (600ml). The ether layer was separated from the basic aqueous layer, which was further extracted with diethyl ether (2 x 200ml) followed by petroleum ether (200ml, b.pt. 40-60°C). The combined organic extracts were dried over anhydrous $MgSO_4$ and the solvent removed on a rotary evaporator leaving a light brown oil. Distillation (30°C, 10^{-3}mmHg) yielded pure $C_5H_5(CH_2)_3N(H)Me$, **1.1**, (31.2g, 0.23mol, 41.4% yield) as colourless oil, in an approximate 1:1 mixture of the 1,2 and 1,3 isomers. The product was stored at -40°C where it was stable for many months.

^1H NMR δ/ppm $CDCl_3$; 6.43 (overlapped m, 3H, 2xCH of C_5H_5 of isomer 1, 1xCH of isomer 2), 6.25 (m, 1H, CH of C_5H_5 isomer 2), 6.16 (hept, 1H, CH of C_5H_5 isomer 2), 6.02 (hept, 1H, CH of C_5H_5 isomer 1), 2.95 (sext, 2H, CH_2 of C_5H_5 isomer 1), 2.88, quart, 2H, CH_2 of C_5H_5 isomer 2), 2.60 (t, 2H, CH_2N), 2.59 (t, 2H, CH_2N), 2.43 (s, 6H, $2xNMe_2$), 2.43 (m, 4H, $2xC\underline{H}_2C_5H_5$), 1.75 (pent, 2H, $CH_2C\underline{H}_2CH_2$), 1.74 (pent, 2H, $CH_2C\underline{H}_2CH_2$), 1.26 (br s, 2H, 2xNH).

1.6.2 Preparation of $[C_5H_4(CH_2)_3N(H)Me]Li$, 1.2

A solution of **1.1** (0.82g, 6mmol) in THF (30ml) was cooled to 0°C. ^nBuLi (3.75ml of a 1.6M solution in hexane, 6mmol) was added dropwise over 10 min and the mixture stirred for 2hr, resulting in a clear solution. This solution was then used immediately in situ for subsequent reactions but could be isolated as follows. The solvent was removed under reduced pressure and the solid washed with hexane (2 x 20ml) leaving $[C_5H_4(CH_2)_3N(H)Me]Li$, **1.2**, (0.81g, 5.7mmol, 95% yield) as a white powder.

1.6.3 Preparation of $[C_5H_4(CH_2)_3NMe]Li_2$, 1.3

A solution of **1.1** (0.82g, 6mmol) in THF (30ml) was cooled to 0°C. ^nBuLi (7.5ml of a 1.6M solution in hexane, 12mmol) was added dropwise over 10 min and the mixture stirred for 2hr forming a white suspension. This suspension was then used immediately in situ for subsequent reactions but could be isolated as follows. The solvent was removed under reduced pressure and the solid washed with hexane (20ml) leaving $[C_5H_4(CH_2)_3NMe]Li_2$, **1.3**, (0.86g, 5.8mmol, 96% yield) as a white powder.

1.6.4 Preparation of $[C_5H_4(CH_2)_3NMe](SiMe_3)_2$, 1.4

A suspension of **1.3** (ca. 6mmol) in THF (30ml) was cooled to 0°C, Me_3SiCl (1.52ml, 12mmol) added dropwise and the mixture stirred at room temperature for 24hr. The solvent was removed under reduced pressure and the product extracted with toluene (2 x 20ml). Removal of the solvent under reduced pressure gave $[C_5H_4(CH_2)_3NMe](SiMe_3)_2$, **1.4**, (1.8g, 5.1mmol, 85% yield with respect to **1.1**) as a pale yellow oil (pure by ^1H NMR).

^1H NMR δ/ppm C_6D_6; 6.45 (t, 2H, C_5H_4), 6.14 (t, 2H, C_5H_4), 2.77 (m, 2H, NCH_2), 2.39 (s, 3H, NCH_3), 2.28 (m, 2H, $C_5H_4C\underline{H_2}$), 1.75 (m, 2H, $CH_2C\underline{H_2}CH_2$), 0.10 (s, 9H, $C_5H_4Si\underline{Me_3}$), -0.06 (s, 9H, $NSi\underline{Me_3}$).

1.7 References

1 a) G. Wilkinson, M. Rosenblum, M. C. Whiting and R.B. Woodward, *J. Am. Chem. Soc.*, 1952, **74**, 2125; b) A personal account of G. Wilkinson's early work, *J. Organomet. Chem.*, 1975, **100**, 273.

2 a) T.J. Marks, *Prog. Inorg. Chem.*, 1979, **25**, 223; b) R. Poli, *Chem. Rev.*, 1991, **91**, 509; c) B.E. Burston and R.J. Strittmatter, *Angew. Chem., Int. Ed. Engl.*, 1991, **30**, 1069.

3 a) J. Okuda, *Angew. Chem., Int. Ed., Engl.*, 1992, **31**, 47; b) J. Okuda, *Nachr. Chem. Tech. Lab.*, 1993, **41**, 8; c) R. Mülhaupt, *Chimia.*,1993, **41**, 1341; d) A.M. Thayer, *Chimia. Eng. News*, 1995, Sept. 11, 15; e) R. Mülhaupt and B. Rieger, *Chimia.*,1996, **50**, 10; f) W. Kaminsky, *Macromol. Chem. Phys.*, 1996, **197**, 3907.

4 a) H.H. Brintzinger, D. Fischer, R. Mülhaupt, B. Rieger and R. Waymouth, *Angew. Chem.*,1995, **107**, 1255, *Angew. Chem., Int. Ed. Engl.*, 1995, **34**, 1652; b) P.C. Möhring, N.J. Coville, *J. Organomet. Chem.*, 1976, **479**. 1.

5 J.W. Lauher and R. Hoffmann, *J. Am. Chem. Soc.*, 1976, **98**, 1729.

6 W.E. Piers, P.J. Shapiro, E.E. Bunel and J.E. Bercaw, *Synlett.*, 1990, **2**, 74.

7 a) Chapter 2, figure 2.2; b) Chapter 6, figure 6.9.

8 P.J. Shapiro, J.E. Bercaw, Abstracts of Papers, 195th Meeting of the American Chemical Society, Toronto, Canada, American Chemical Society, Washington, D.C., 1988, INOR 584.

9 P.J. Shapiro, W.D. Cotter, W.P. Schaefer, J.A. Labinger and J.E. Bercaw, *J. Am. Chem. Soc.*, 1994, **116**, 4623.

10 a) J.C. Stevens, F.J. Timmers, G.W. Rosen, G.W. Knight and S.Y. Lai (Dow Chemical Co.), *European Patent Application.*, 1991, EP 0 416815 A2 (filed August 30, 1990) b) J.A. Cannich (Exxon Chemical Co.), *European Patent Application*, 1991, EP 0 420 436 A1 (filed September 10, 1990).

11 J. Okuda, *Chem. Ber.*, 1990, **123**, 1649.

12 a) J. E. Bercaw, R.H. Marvich, L.G. Bell and H.H. Brintzinger, *J. Am. Chem. Soc.*, 1972, **94**, 1219; b) I.F. Urazowski, V.I Ponomaryov, O.G. Ellert, I.E. Niant'ev and D.A. Lemenovski, *J. Organomet. Chem.*, 1988, **356**, 181.

13 G. A. Luinstra and J.H. Teuben, *J. Chem. Soc., Chem Commun.*, 1990, 1470.

14 F. Amor and J. Okuda, *J. Organomet. Chem.*, 1996, **520**, 245.

15 K.E. du Plooy, U. Moll, S. Wocadlo, W. Massa and J. Okuda, *Organometallics,* 1995, **14**, 3129.

16 J. Okuda, S. Verch and T.P. Spaniol, *Chem. Ber/Recueill.,* 1996, **129**, 1429.

17 J. Okuda, T. Eberle and T.P. Spaniol, *Chem. Ber.*, 1997, **130**, 209.

18 D.W. Carpenetti, L. Kloppenburg, J.T. Kupec and J.L. Peterson, *Organometallics,* 1996, **15**, 1572.

19 J. Okuda, F.J. Schattenmann, S. Wocadlo and W. Massa, *Organometallics,* 1995, **14**, 789.

20 H.V.R. Dias, Z. Wang and S.G. Bott, *J. Organomet. Chem.*, 1996, **508**, 91.

21 a) G. Chandra and M.F. Lappert, *J. Chem. Soc.A.*, 1968, 1940; b) P.B. Power, A.R. Sanger and R.C. Srivastava, Metal and Metalloid Amides, E. Hoewood, Chicester, West Sussex, U.K. 1980.

22 G.M. Diamond, S. Rodewald and R.F. Jordan, *Organometallics*, 1995, **14**, 5.

23 A.K. Hughes, A. Meetsma and J.H. Teuben, *Organometallics*, 1993, **12**, 1936.

24 P.J. Sinnema, L. Van der Veen, A.L. Spek, N. Veldman and J.H. Teuben, *Organometallics,* in press.

25 A. K. Hughes, S.M.B. Marsh, J.A.K. Howard and P.S. Ford., *J. Organomet. Chem.*, 1997, **528**, 195.

26 a) S. Ciruelos, T. Cuenca, P. Gomez-Sal, A. Manzanero and P. Royo, *Organometallics*, 1995, **14**, 177; b) S. Ciruelos, T. Cuenca, R. Gomez, P. Gomez-Sal, A. Manzanero and P. Royo, *Organometallics*, 1996, **15**, 5577.

27 H.V.R. Dias, Z. Wang and S.G. Bott, *J. Organomet. Chem.*, 1996, **508**, 91.

28 L. Kloppenburg and J.L. Peterson, *Organometallics*, 1996, **15**, 7.

29 P.J. Sinnema, Organometaalchemie en Homogene Katalyse, Verslagen Wergroep, Rijksuniversiteit Gronigen, 1995, **7**, 23.

30 a) H. Bürger, K.Wiegel, U. Thewalt and D. Schomburg, *J. Organomet. Chem.*, 1975, **87**, 301; b) J. Feldman and J.C. Calabrese, *J. Chem. Soc., Chem. Commun.*, 1991, 1042.

31 R.M. Pulpi, J.N. Coalter and J.L. Peterson, *J. Organomet. Chem.*, 1995, **497**, 17

32 a) J.C. Stevens, *Metcon 93,* Houston, 26-28 May, 1993, 157., b) J.C. Stevens, *Stud. Surface Sci. Cat.* 1994, **89**, 277.

33 D.M. Giolando, K. Kirschbaum, L.J. Graves and U. Bolle, *Inorg. Chem.*, 1992, **31**, 3887.

34 R. Fandos, A. Meetsma and J.H. Teuben, *Organometallics,* 1991, **10,** 59.

35 G. Trouvé, D.A. Laske, A. Meetsma and J.H. Teuben, *J. Organomet. Chem.*, 1996, **511,** 255.

36 B. Rieger, *J. Organomet. Chem.*, 1991, **420,** C17.

37 J.W. Pattiansina, C.E. Hissink, J.L.de Boer, A. Meetsma and J.H. Teuben, *J. Am. Chem. Soc.*, 1985, **107,** 7758.

38 G. Erker and U. Korek, *Z. Naturforsch.*, 1989, **44b,** 1593.

39 Y. Qain, J. Huang, X. Chen, G. Li, W. Chen, B. Li, X. Jin and Q. Yang, *Polyhedron,* 1994, **13,** 1105.

40 K.E. du Plooy, U. Moll, S. Wocadlo, W. Massa and J. Okuda, *Organometallics,* 1995, **14,** 3129.

41 F. Amor, T.P. Spaniol and J. Okuda, unpublished results.

42 F. Amor, K.E. du Plooy, T.P. Spaniol and J. Okuda, unpublished results.

43 B.L. Goodall, *J. Chem. Educ.*, 1986, **63,** 191.

44 K. Soga, T. Uozumi, S. Nakamura, T. Toneri, T. Teranishi, T. Sano and T. Arai, *Macromol. Chem. Phys.*, 1996, **197,** 4237.

45 a) Y.X. Chen, C.L. Stem, S. Yang and T.J. Marks, *J. Am. Chem. Soc.*, 1996, **118,** 12451; b) L. Jai, X. Yang, C.L. Stem and T.J. Marks, *Organometallics*, 1997, **16,** 842.

46 a) T.K. Woo, L. Fan and T. Ziegler, *Organometallics,* 1994, **13,** 2252; b) T.K. Woo, P.M. Margi, J.C.W. Lohrenz, P.E. Blöch and T. Ziegler, *J. Am. Chem. Soc.*, 1996, **118,** 13021.

47 F.G. Sernetz, Mülhaupt, F. Amor, T. Eberie and J. Okuda, *J. Polym. Sci.*, Part A, 1997, **35,** 1571.

48 A.H. Hoveyda and J.P. Morken, *Angew. Chem. Int. Ed. Chem.*, 1996, **35,** 1262.

49 E.A. Bijpost, R. Duchateau and J.H. Teuben, *J. Mol. Cat. A.*, 1995, **95,** 121.

50 M. Osaga, D.T. Mallin, D.W. Macomber, M.D. Rausch, R.D. Rogers and A.D. Rollins, *J. Organomet. Chem.*, 1991, **405,** 41.

51 S.M.B. Marsh, Ph.D. Thesis, University of Durham, 1997.

52 U. Seimeling, O. Vorfield, B. Neumann and H.G. Stammler, *Chem. Ber.*, 1995, **128,** 481.

53 L. Angiolini, A.R. Katritzky and D.M. Read, *Gazz. Chim. Ital.*, 1976, **106,** 111.

54 F. Cortese, *Org. Synth. Coll.*, 1940, **II,** 91.

55 J.C. Stevens, F.J. Timmer, G.W. Rossen, G.W. Knight and S.Y. Lai, , *European Patent,* 5504224, to the Dow Chemical Company

56 R.E. Dessey, Y. Okuzami and A. Chen, *J. Am. Chem. Soc.,* 1962, **84**, 2899.

57 S.H. Pine, J.B. Hendrickson, D.J. Cram and G.S. Hammond, *"Organic Chemistry"*, 4th Edition, McGraw and Hill (Singapore), 1985, 200.

Chapter 2

Group 6 – Tungsten and Molybdenum Amide Functionalised Cyclopentadienyl Complexes.

2.1 Introduction

Compared with the wealth of donor functionalised cyclopentadienyl complexes of Group 4 transition metals, such complexes of Group 6 have been much less widely studied. There are only three publications relating to nitrogen functionalised cyclopentadienyl complexes of tungsten or molybdenum, and relatively few examples of linked bis-cyclopentadienyl complexes. This chapter is aimed at redressing this balance.

There are two main reasons for the lack of study into Group 6 donor functionalised cyclopentadienyl complexes. Firstly, the starting materials for the Group 6 reactions are more difficult to prepare than for Group 4. For example, $M(NMe_2)_4$ (M = Zr, Ti) is relatively easy to synthesise from MCl_4 (M = Ti, Zr, Hf) and $Li(NMe_2)$, whereas with the analogous MCl_6 (M = W, Mo), mixtures of $M(NMe_2)_6$ and $M_2(NMe_2)_6$ are produced. Therefore $M(NMe_2)_6$ (M = W, Mo) is prepared from MCl_4L_2 (L = THF, Et_2O) and $LiNMe_2$ giving very low yields (16% for W).[1] Furthermore, M(IV) complexes such as the homoleptic amides $M(NMe_2)_4$ (M = W, Mo) are paramagnetic.

Secondly, the potential catalytic applications for Group 6 complexes have been explored less, than for those of Group 4. In Chapter 1 Group 4 metallocenes and their domination of the industrial and academic scene, are discussed. In comparison, Group 6 cyclopentadienyl compounds have received little attention. However, among the transition metals that catalyse the polymerisation of olefins, chromium occupies a prominent position. This is discussed in more detail in Chapter 5, which focuses on chromium and vanadium chloro complexes.

2.1.1 Bis-cyclopentadienyl *(ansa)* complexes

To date, the only published work on such complexes has been from the reaction of MCl_4L (M = W, Mo; L = dme, THF) with linked bis-cyclopentadienyl dianions.[2,3] For example, Green and co-workers reacted MCl_4dme (M = Mo, W) with $[C_5H_4CMe_2C_5H_4]Li_2$,[2] and from this further reactions were carried out, a selection of which are shown in figure 2.1.

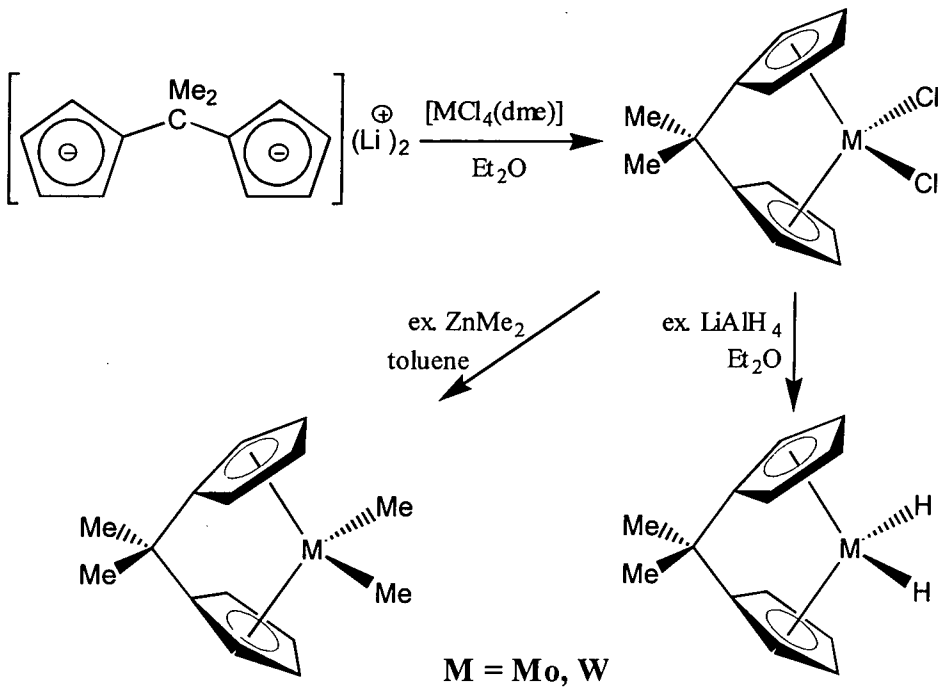

Figure 2.1

The *ansa* bridge causes modification of the electronic structures and studies found that compared to their non-*ansa* analogues, the *ansa* bridged bis-cyclopentadienyl complexes showed marked differences in their reactivity and structure. Similar work has also been carried out with the linked bis cyclopentadienyl ligand, $[C_5H_4SiMe_2OSiMe_2C_5H_4]Li_2$ and MCl_4THF (M = Mo, W).[3]

2.1.2 Nitrogen functionalised cyclopentadienyl complexes

The three publications on donor functionalised cyclopentadienyl complexes of molybdenum or tungsten, are of molybdenum nitrogen functionalised complexes, and two, by Wang and co-workers, discuss molybdenum amino complexes.[4] Reaction of the monolithiated ligand, $[\eta^5\text{-}C_5H_4CH_2CHRNMe_2]Li$, with a molybdenum carbonyl complex, followed by removal of carbon monoxide by i) oxidation, **A**, or ii) irradiation, **B**, provided a route to the amino functionalised *ansa* complexes (figure 2.2).

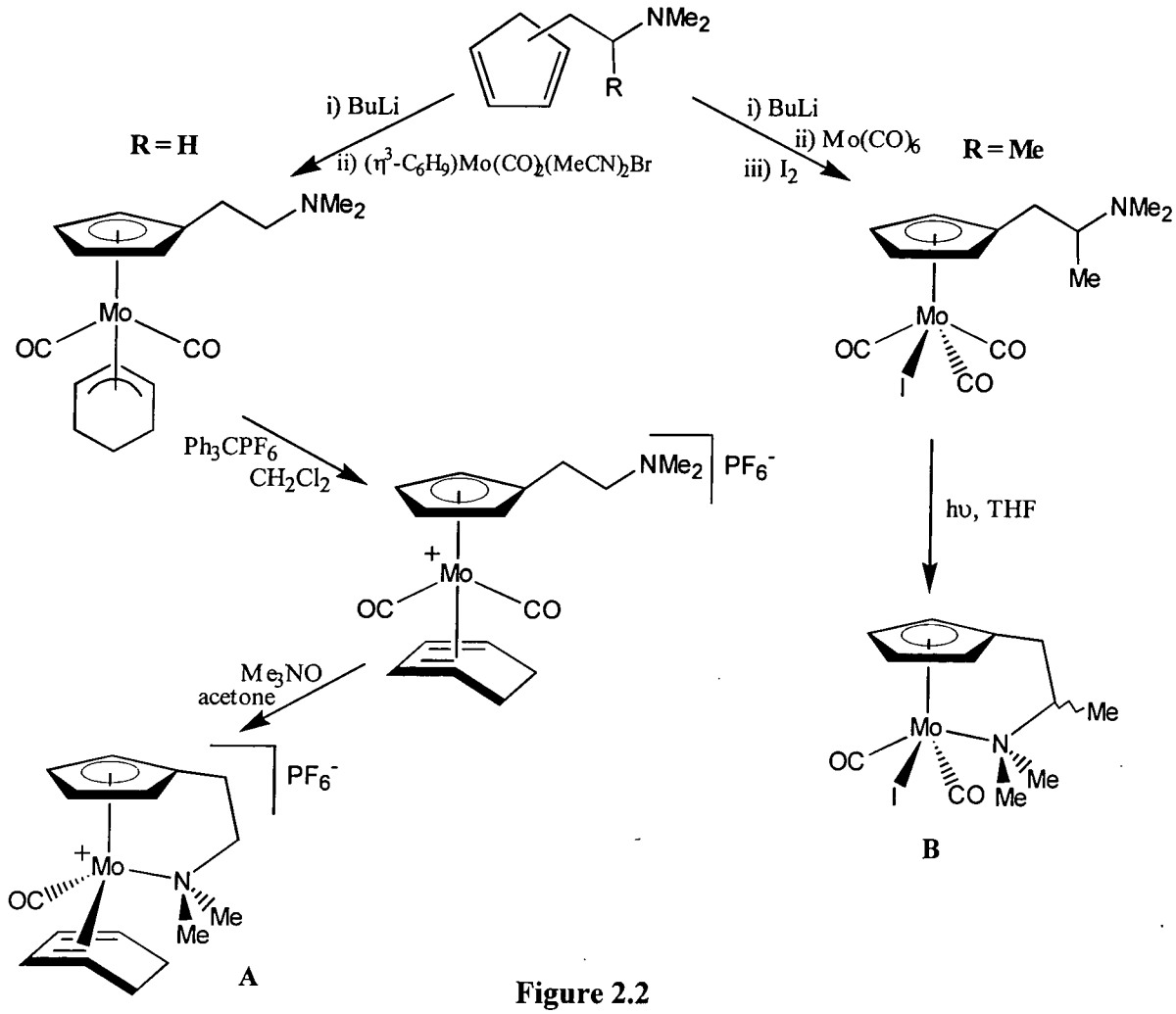

Figure 2.2

The only amide functionalised cyclopentadienyl complex of molybdenum or tungsten, was reported by Herrmann and co-workers.[5] The metal amide route, making use of the parent CH-/NH acidic ligand precursor (figure 2.3), provided a way of avoiding any redox process encountered with compounds such as molybdenum(IV) halides.

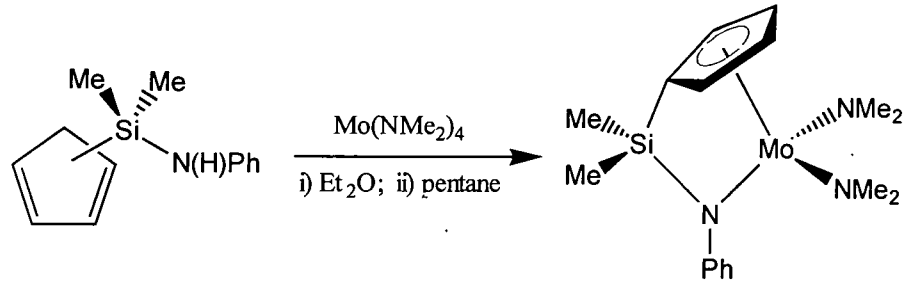

Figure 2.3

The molybdenum(IV) species formed has a formal electron count of 18 and a pseudo tetrahedral geometry, therefore making NMR spectroscopy possible. Again, compared with the unbridged derivative, the *ansa*-bridged cyclopentadienyl ligands were found to stabilise metal complexes in medium oxidation state. The linked complex decomposed when heated above 100°C, whereas the unbridged derivative, $(C_5H_5)Mo(NMe_2)_3$, disproportionates in solution at room temperature within several hours, yielding $Mo(NMe_2)_6$.[5]

2.1.3 Aims

Given the lack of well characterised amide functionalised cyclopentadienyl complexes the aim of this part of the project is to synthesise such complexes by making use of the acidic CH/NH of the neutral ligand, $C_5H_5(CH_2)_3N(H)Me$, **1.1**, and reacting it with a readily available tungsten or molybdenum(VI) amide. Alternatively the dianion, $[C_5H_4(CH_2)_3NMe]^{2-}$, **1.3**, could be reacted with a tungsten or molybdenum(VI) halide complex.

2.2 Synthesis of amide functionalised cyclopentadienyl complexes

2.2.1 Reaction between $W(N^tBu)_2(NH^tBu)_2$ and $C_5H_5(CH_2)_3N(H)Me$, 1.1

Difficulties synthesising $M(NMe_2)_6$ (M = Mo, W) led us to seek alternative molybdenum and tungsten(VI) amide reagents as starting materials to react with the neutral ligand. The bis-t-butyl amide bis-t-butyl imido tungsten(VI) complex can be readily synthesised from the reaction of tungsten hexachloride and ten equivalents of t-butylamine.[6]

$$WCl_6 + 10\ {}^tBuNH_2 \xrightarrow[\text{ii) Pentane}]{\text{i) } Et_2O} W(N^tBu)_2(NH^tBu)_2 + 6\ {}^tBuNH_3Cl$$

A solution of $W(N^tBu)_2(NH^tBu)_2$ in toluene and one equivalent of $C_5H_5(CH_2)_3N(H)Me$, **1.1**, was stirred at 55°C. After 3 days an aliquot was taken for NMR spectroscopic analysis. A ^1H NMR spectrum in $CDCl_3$ showed an approximate 50:50 mixture of two new products, along with a very small amount of the starting material, $W(N^tBu)_2(NH^tBu)_2$. This evidence indicates that the reaction had not gone to completion, and although no free ligand, **1.1**, was observed in the spectrum, this would be removed during sample preparation. Continued heating (up to 100°C) over several days, with occasional removal of any volatile products (i.e. t-butylamine) did not cause the reaction to go to completion.

After standing at ambient temperature for 10 days, ^1H and $^{13}C\{^1H\}$ NMR analysis of the mixture of products in the $CDCl_3$ solution, now found it to contain mainly one product. The ^1H NMR spectrum shows the complex signals observed in the olefinic region of the free ligand, **1.1**, has now simplified into a AA'BB' spin system (figure 2.4). This indicates that the cyclopentadienyl ring has been deprotonated, and is now coordinated to the metal centre. A singlet at 3.23ppm, integrating to three protons is assigned to a NMe fragment that is now attached to the metal. Comparison with ^1H NMR data on other complexes in this thesis demonstrate that the N(H)Me of the free ligand (^1H δ/ppm = 2.43) shifts to lower frequencies when it is deprotonated and coordinated to the metal. Three sets of multiplets, each integrating to two protons, are assigned to the trimethylene backbone of the ligand. Apart from some t-butylamine, there is only one singlet integrating to 18 protons for the two metal imido groups, indicating the displacement of two equivalents of

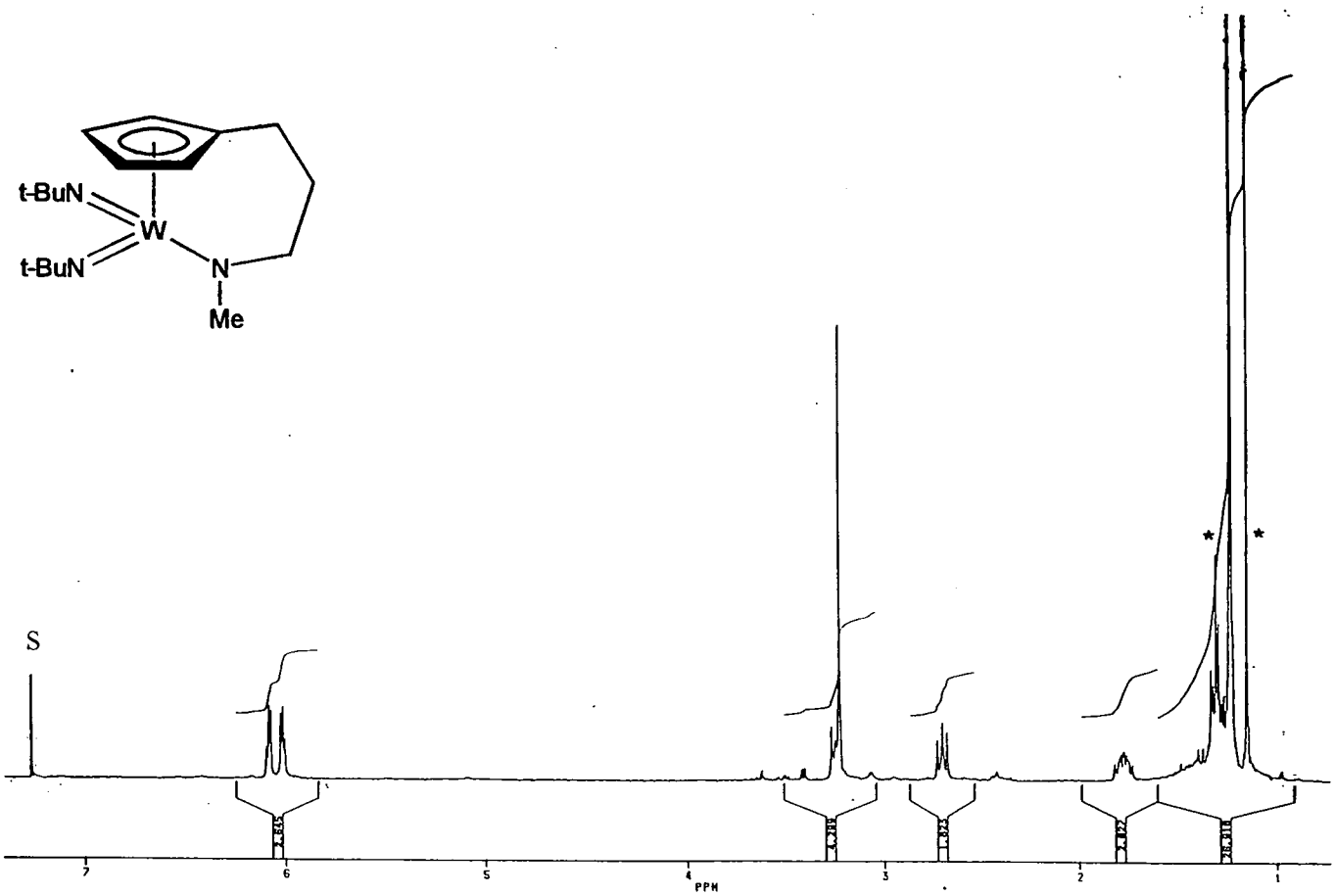

Figure 2.4 ^{1}H NMR spectrum of **2.2** in $CDCl_3$ at 250MHz

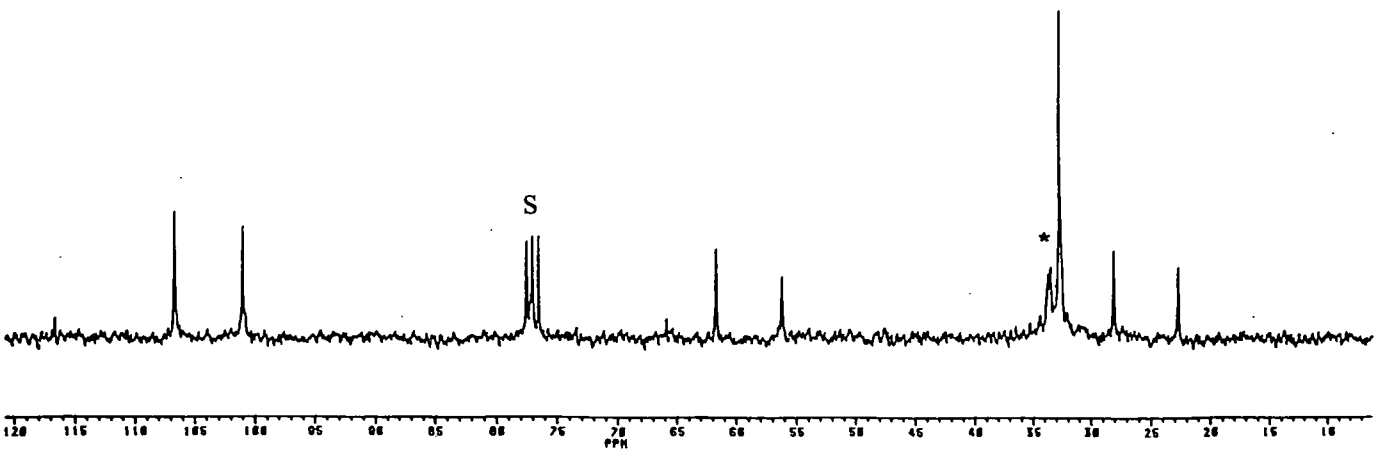

Figure 2.5 $^{13}C\{^{1}H\}$ NMR spectrum of **2.2** in $CDCl_3$ at 62.5MHz

t-butylamine. The $^{13}C\{^1H\}$ NMR spectrum exhibits three resonances for the cyclopentadienyl fragment, with the *ipso*-carbon observed (figure 2.5). Peaks for the quarternary carbons and methyl groups of t-butyl groups were also observed at 66.6 and 33.4ppm respectively. From the above evidence it was concluded that the ligand eliminates two equivalents of t-butyl amine forming $W[\eta^5:\eta^1\text{-}C_5H_4(CH_2)_3NMe](N^tBu)_2$, **2.2** (figure 2.6).

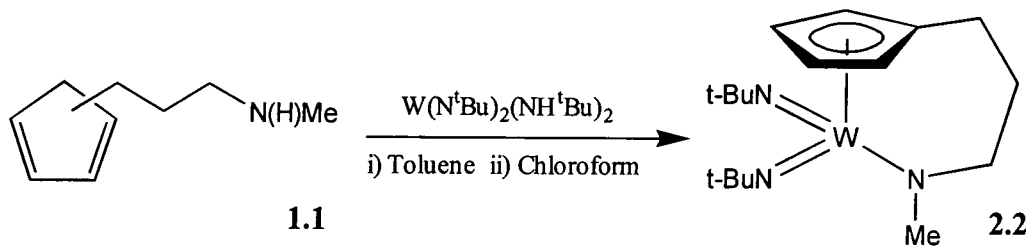

1.1 **2.2**

Figure 2.6

Similarly, IR spectroscopy showed no bands that could be attributed to N-H stretches, confirming this displacement and also the metallation of the secondary amine. Mass spectroscopy also confirmed the presence of **2.2**, with masses at 463, 448 and 321, corresponding to the cations $[\mathbf{2.2}]^+$, $[W(CpN)(N^tBu)_2]^+$, and $[W(N^tBu)_2]^+$ respectively.

The two stage nature of the reaction is reproducible on a larger scale (i.e. 3mmol), the second stage being carried out in $CHCl_3$. It has proved possible to isolate moderate quantities of the final product (1.20g, 87% yield), up to 95% pure by NMR, as a pale yellow oil. However such results were only obtained using a scaled-up version of the NMR tube experiment. The reaction mixture was transferred into a 20ml ampoule and $CHCl_3$ transferred under reduced pressure, the system sealed and left at room temperature for 10 days. In a system at atmospheric pressure, or a larger ampoule, the reaction did not go to completion even with longer reaction times, indicating that the pressure or presence of t-butylamine produced may have an effect on the reaction equilibrium. Attempts to reproduce the reaction using a one stage reaction with $CHCl_3$ or CH_2Cl_2 as the solvent gave a mixture of products, only a relatively small percentage of which was **2.2**.

Although a mixture of two products were formed from the reaction of **1.1** and $W(N^tBu)_2(NH^tBu)_2$ in toluene, only **2.2** was isolated pure. However, ^1H NMR analysis provides evidence for the second product being the intermediate, $W(\eta^1\text{-}C_5H_5(CH_2)_3NMe)(NH^tBu)(N^tBu)_2$, **2.1**, forming as a mixture of two isomers **A**, and **B** (figure 2.7).

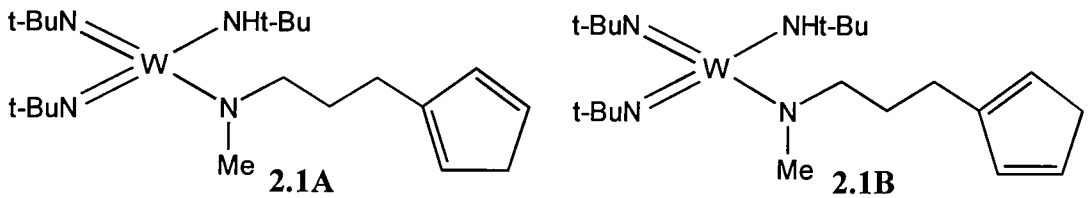

Figure 2.7

As discussed in Chapter 1 (section 1.4.5), the neutral ligand, $C_5H_5(CH_2)_3N(H)Me$, **1.1**, contains two acidic centres, the cyclopentadiene ($pK_a \sim 16$) and the secondary amine ($pK_a \sim 35\text{-}40$). Whereas the reaction between $Zr(NMe_2)_4$ and $Hf(NMe_2)_4$ and the neutral ligand gave access to good yields of thermodynamic products where it is assumed that the more acidic cyclopentadiene reacts initially followed by the less acidic amine, this presumption does not hold true for the tungsten reaction. If the reaction were thermodynamically controlled, then the more acidic cyclopentadiene would react first forming an attached cyclopentadienyl and an unattached amine (figure 2.8). This would give an AA'BB' or ABCD spin system for the C_5H_4 fragment in the ^1H NMR spectrum, but no such intermediate is observed.

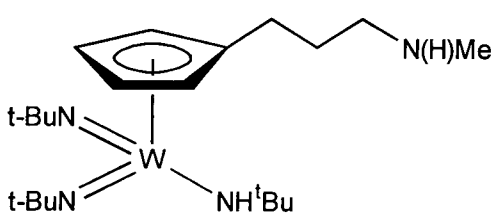

Figure 2.8

By contrast, the ^1H NMR spectrum of **2.1** shows the presence of a free cyclopentadiene (as a mixture of isomers), together with a tungsten amide as shown by the chemical shift of the

NMe protons (δ = 3.23ppm) characteristically shifted with respect to that of the free amine group, NHMe (δ = 2.43ppm). This observation suggests that the intermediate, **2.1**, is the product of a kinetic deprotonation reaction. The presence of **2.1** was also verified by mass spectroscopy, with a mass of 533 being that of the cation $[\mathbf{2.1}]^+$.

The advantages of the aminolysis route for the metallation of cyclopentadienes are that they are clean reactions with the elimination products, in this case t-butylamine, forming as low boiling liquids and, therefore, easily removed from the reaction, thus making purification of the final product easier. However the disadvantage of this process for the tungsten reaction is the slow reaction of the metal amides. This is also complicated by the variable yields of the final product in certain solvents and reaction volumes, where only a reaction carried out in toluene followed by chloroform in 20ml vessel gave **2.2** in a yield of 87%. These disadvantages led us to seek an alternative reaction yielding Group 6 complexes similar to **2.2**.

2.2.2 Reaction between $Mo(N^tBu)_2Cl_2dme$ and $[C_5H_4(CH_2)_3NMe]Li_2$, 1.3

In Chapter 1, many functionalised cyclopentadienyl complexes were successfully prepared from reactions between metal chlorides and lithium salts, with the formation of lithium chloride being the driving force for the reaction. In the past, $Mo(NR)_2Cl_2dme$, (R = ^{t}Bu, 2,6-^{i}Pr$_2$C$_6$H$_3$) has been used as a starting material for preparing a variety of substituted bis imido molybdenum complexes.[7] Reactions with alkylating agents, Grignards or lithium salts, produce bis alkyl bis imido molybdenum complexes, with formation of magnesium or lithium chloride, and displacement of 1,2-dimethoxyethane. By reacting $[C_5H_4(CH_2)_3NMe]Li_2$, **1.3**, with $Mo(N^tBu)_2Cl_2dme$, a similar reaction was therefore feasible.

$$Na_2MoO_4 + 4NEt_3 + 8TMSCl + 2\,{}^tBuNH_2 \xrightarrow[\text{ii) } Et_2O]{\text{i) dme}} Mo(N^tBu)_2Cl_2dme + 4NEt_3HCl + 4(TMS)_2O + 2NaCl$$

The reaction between sodium molybdate, triethylamine, trimethylsilylchloride and t-butylamine, in dimethoxyethane, gave crude $Mo(N^tBu)_2Cl_2dme$ in 98% yield.[8] Recrystallisation from diethyl ether gave amber coloured crystals of the pure complex. Although, $Mo(N^tBu)_2Cl_2dme$ is a well-used starting material, the molecular structure of this complex has not been determined. A crystal structure of what was thought to be the pure product was carried out recently, and was found to contain a 2:1 ratio of $Mo(N^tBu)_2Cl_2dme$ and $[Mo(^tNBu)_2(NH_2{}^tBu)_2Cl]_2(\mu\text{-}Cl)_2$ respectively.[9] Analysis of the amber crystals showed it to contain pure $Mo(N^tBu)_2Cl_2dme$, and molecular structure determination was carried out. The data was collected, and the structure solved by Prof. J.A.K. Howard and P.S. Ford within this department. The molecular structure is illustrated in figure 2.9, and the full data shown in the appendices.

Molecular Structure of $Mo(N^tBu)_2Cl_2dme$

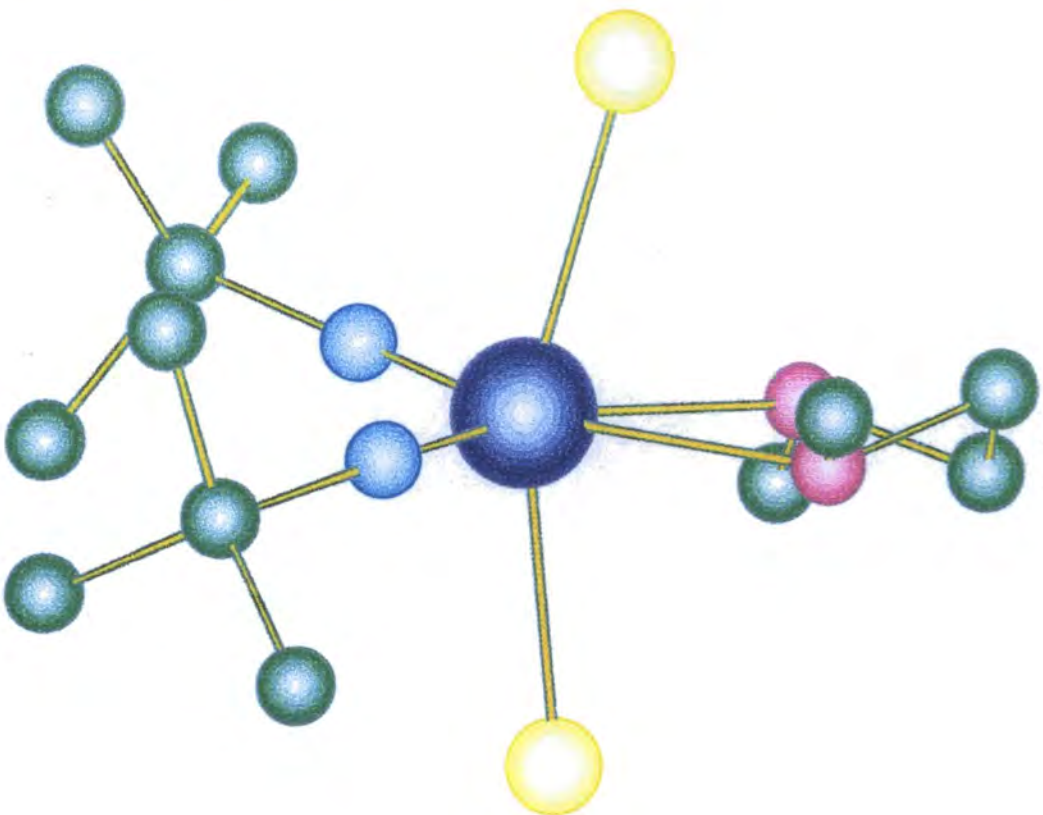

Figure 2.9

The complex was found to adopt a highly distorted octahedral geometry, possessing two mutually cis imido ligands, two approximately trans chloride ligands and a chelating dimethoxyethane group. The Cl-Mo-Cl bond angle of 159.0° deviates markedly from linearity, and the N-Mo-N angle of 107.1° is much greater than expected for an octahedral geometry,[10] although similar assymetry has been noted in other bis imido complexes of Group 6.[10] This has been attributed to repulsion between the π electron density in the two bonds leading to an opening of the N-Mo-N wedge. The chelating dme ligand has a relatively small bite angle of 68.9°, and this is most likely due to the observed distortion, an effect noted by Wentworth and co-workers with chelating dithiocarbamate ligands.[11]

Furthermore, if both imido ligands are described as bonding to the metal centre through triple bonds (1σ, 2π), then the complex becomes "formally" a 20 electron species. However, it is impossible to locate two formally triple bonds in a *cis*-orientation, in an octahedral geometry, there being only 3 dπ symmetry orbitals available for bonding. The electronic saturation can be relieved with more of the nitrogen lone pair density located on one of the nitrogen atoms. Both of these factors will contribute to the observed distortion in the bond angles for the two imido ligands. The M-N-^{t}Bu bond angles were each found to be 162.9°, and the M-N bond lengths of 1.72Å are consistent with those of two imido ligands bonding to the metal centre via pseudo triple bonds. Often a low M-N bond order is associated with bending of the M-N-R bond angle, leaving the nitrogen with a lone pair of electrons and hence sp^2 hybridised. These factors are discussed in further detail later, in the context of complex **2.2** having a formal electron count of 22 electrons (section 2.2.4).

The reaction between $Mo(N^tBu)_2Cl_2dme$ and $[C_5H_4(CH_2)_3NMe]Li_2$, **1.3**, in THF, gave a colour change from yellow to dark orange. Extraction of the product into hexane gave a brown oil and a stoichiometric amount of lithium chloride. Analysis of the oil showed it to be the desired molybdenum analogue of the tungsten complex, $Mo[\eta^5:\eta^1\text{-}C_5H_4(CH_2)_3NMe](N^tBu)_2$, **2.3**, (figure 2.10).

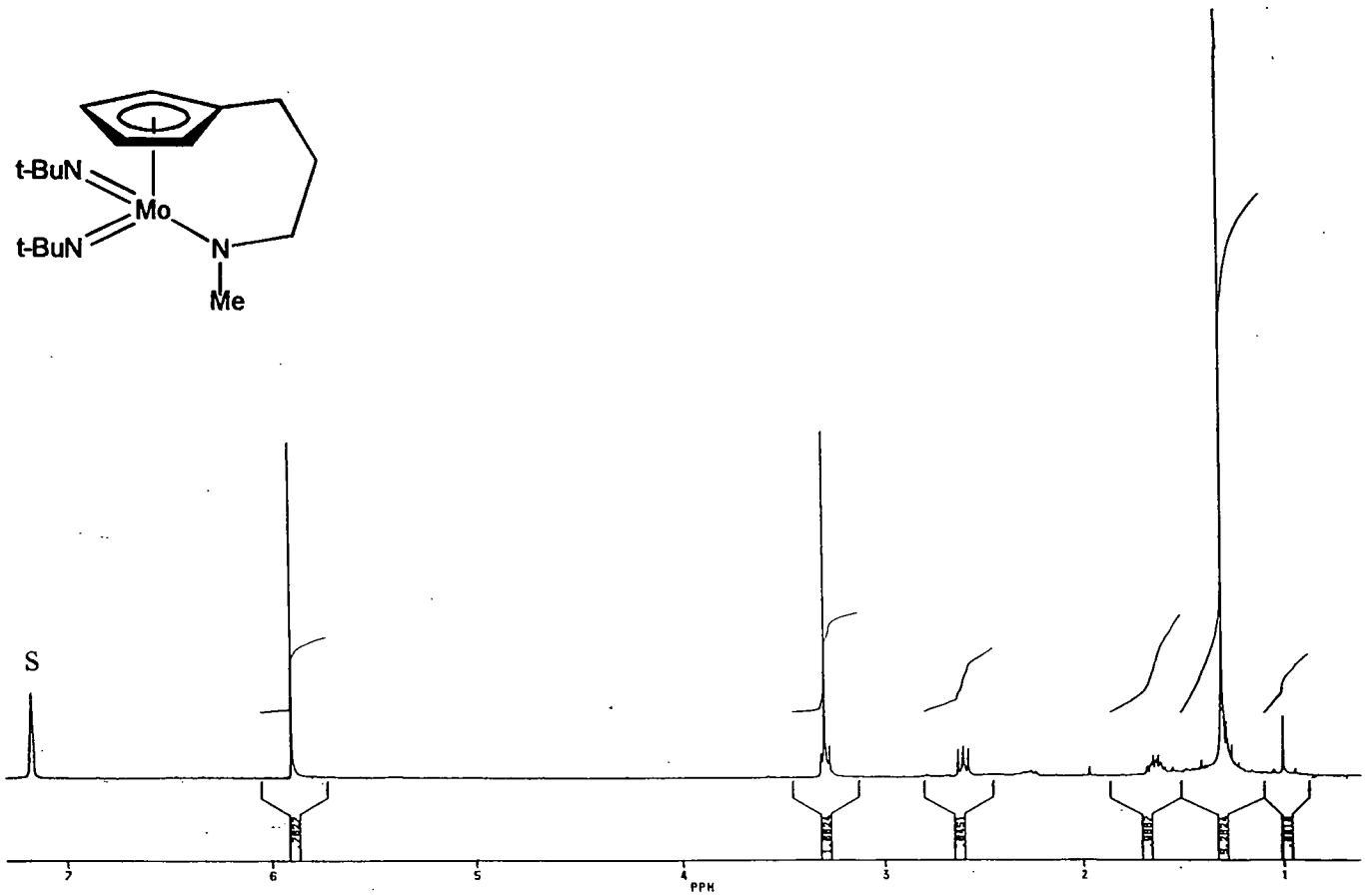

Figure 2.11 ^{1}H NMR spectrum of **2.3** in C_6D_6 at 250MHz

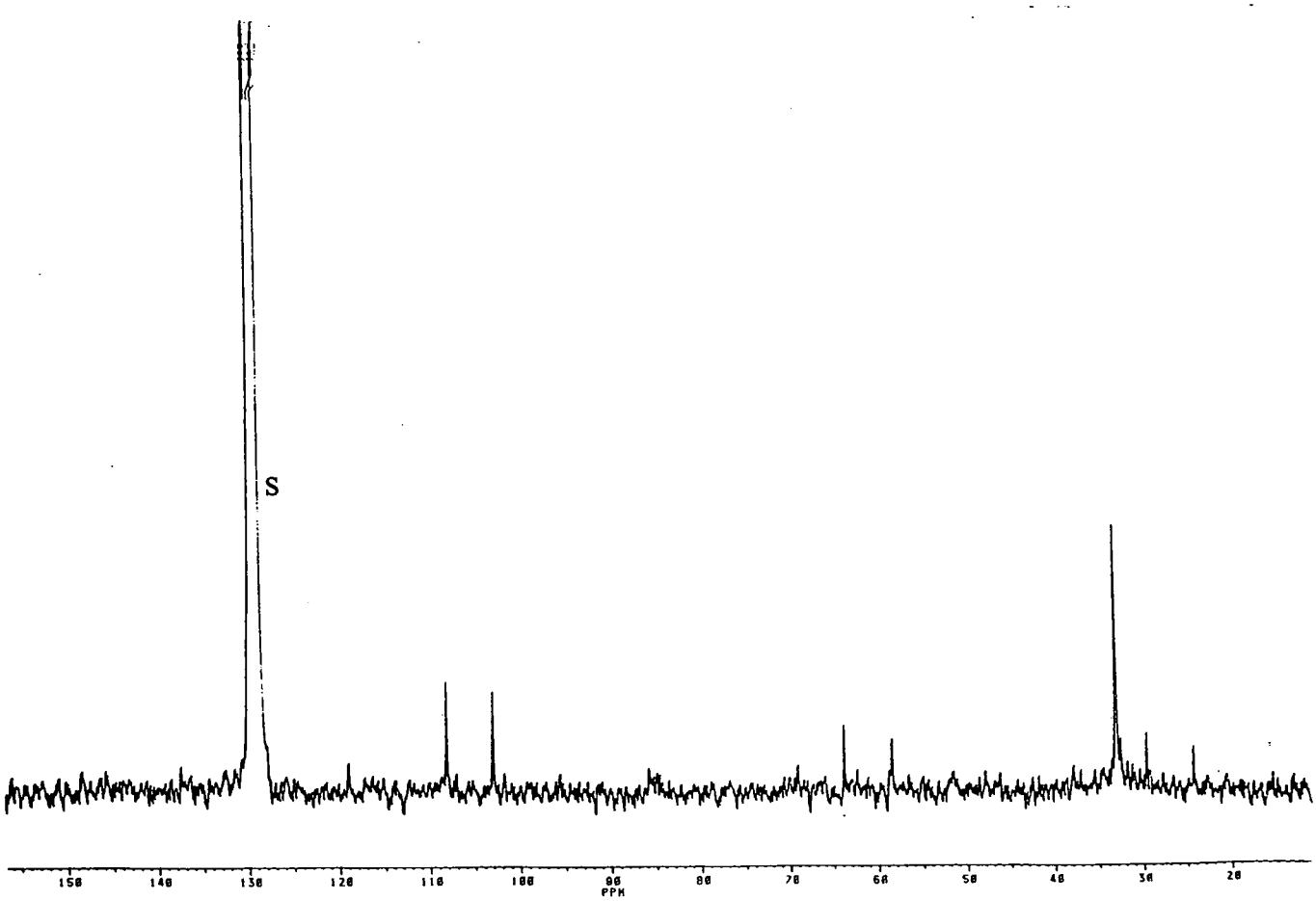

Figure 2.12 $^{13}C\{^{1}H\}$ NMR spectrum of **2.3** in C_6D_6 at 62.5MHz

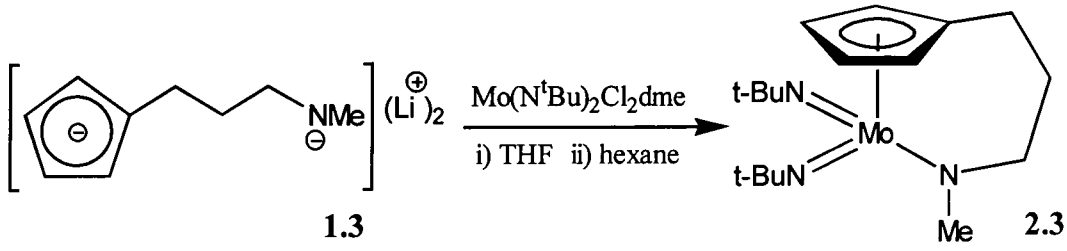

1.3 2.3

Figure 2.10

The relatively pure crude material was isolated in 95% yield (pure by ^{1}H NMR). An analytically pure sample for elemental analysis was obtained by sublimation onto a liquid nitrogen cooled probe giving a yellow solid which on warming gave pure **2.3** as a yellow oil which remained an oil and did not crystallise. This gave C,H and N values within 0.5% of those calculated. However much decomposition occurred during sublimation causing a large reduction in yield. The EI mass spectrum showed masses centred at m/e = 375, 360 and 302, corresponding to $[\mathbf{2.3}]^+$, $[Mo(CpN)(N^tBu)_2]^+$ and $[Mo(CpNMe)(N^tBu)]^+$ respectively.

Both the molybdenum (**2.3**) and tungsten (**2.2**) complexes have a molecular mirror plane, as indicated by the solution NMR spectra. The ^{1}H NMR spectrum is very similar in both complexes, apart from some accidental overlap of signals in the molybdenum analogue. Only one resonance was observed for the C_5H_4 fragment, at 5.90ppm, and the singlet for the NMe group coincides with the N-CH_2 triplet, at 3.29 and 3.27ppm respectively (figure 2.11). The $^{13}C\{^1H\}$ NMR spectrum for **2.3** is also similar to **2.2**, with one resonance observed for the NMe fragment and three for the C_5H_4 group and also for the trimethylene backbone (figure 2.12).

2.2.3 Reaction between $Mo(NAr)_2Cl_2dme$ and $[\eta^5:\eta^1\text{-}C_5H_4(CH_2)_3NMe]Li_2$, 1.3

Both $W[\eta^5:\eta^1\text{-}C_5H_4(CH_2)_3NMe](N^tBu)_2$, **2.2**, and $Mo[\eta^5:\eta^1\text{-}C_5H_4(CH_2)_3NMe](N^tBu)_2$, **2.3** are oils, and therefore molecular structure determinations were unobtainable. In an attempt to synthesise a crystalline material the t-butyl substituents were replaced by bulky aryl groups. Reactions were carried out using 2-$CF_3C_6H_4N$ and 2,6-$^iPr_2C_6H_3N$ as the aryl

imido functionalities. The aryl complexes $Mo(N\text{-}2\text{-}CF_3C_6H_4)_2Cl_2dme$ and $Mo(N\text{-}2,6\text{-}{}^iPr_2C_6H_3)_2Cl_2dme$ were prepared in an analogous fashion to $Mo(N^tBu)_2Cl_2dme$, by substituting t-butyl amine for 2-trifluoromethylaniline and 2,6-diisopropylaniline respectively.

The reaction between $Mo(N\text{-}2\text{-}CF_3C_6H_4)_2Cl_2dme$ and $[C_5H_4(CH_2)_3NMe]Li_2$, **1.3**, in THF gave a dark red solution. Extraction of the product into hexane yielded $Mo[\eta^5{:}\eta^1\text{-}C_5H_4(CH_2)_3NMe](NAr^f)_2$ (Ar^f = 2-$CF_3C_6H_4$), **2.4**, as a dark red oil/solid in 93% yield (figure 2.13). The ^1H NMR spectrum of **2.4**, showed the phenyl group observed as a series of multiplets in the aromatic region, and the C_5H_4 fragment as AA'BB' spin system with two triplets at 5.91 and 6.61ppm (figure 2.13). The attached amide appears as a singlet at 3.46ppm with the bridge of the ligand seen as a series of multiplets. Four resonances were observed for the phenyl group in the $^{13}C\{^1H\}$ NMR spectrum, the two quaternary carbons not appearing (figure 2.14). A m/z centred at 549 for $[\mathbf{2.4}]^+$ with the correct isotope distribution was also observed in the mass spectrum. Numerous attempts were made at crystallisation of the product using hexane, a hexane/toluene mixture, and diethyl ether, but to no avail.

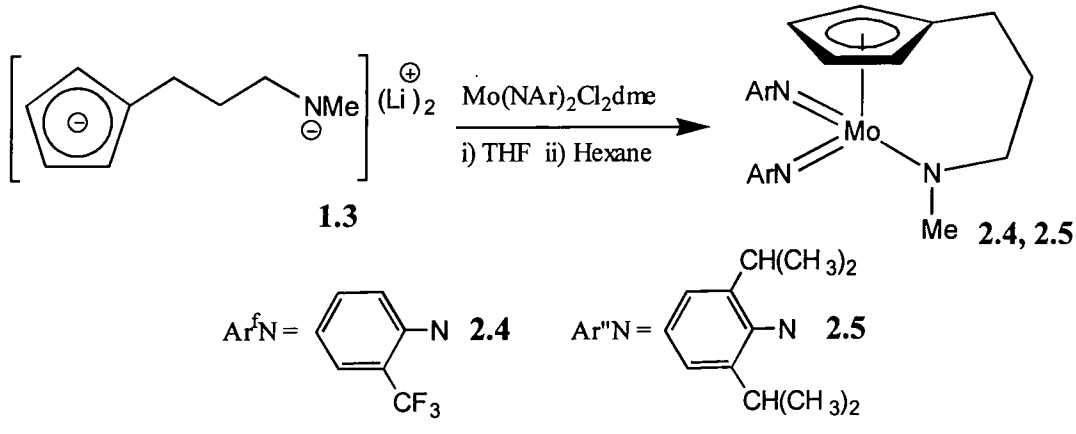

Figure 2.15

A similar reaction between $Mo(N\text{-}2,6\text{-}{}^iPr_2C_6H_3)_2Cl_2dme$ and $[C_5H_4(CH_2)_3NMe]Li_2$, **1.3**, yielded $Mo[\eta^5{:}\eta^1\text{-}C_5H_4(CH_2)_3NMe](NAr")_2$, **2.5**, as a dark red oil/solid in 94% yield (figure 2.15). Once again, attempts at recrystallisation were unsuccessful.

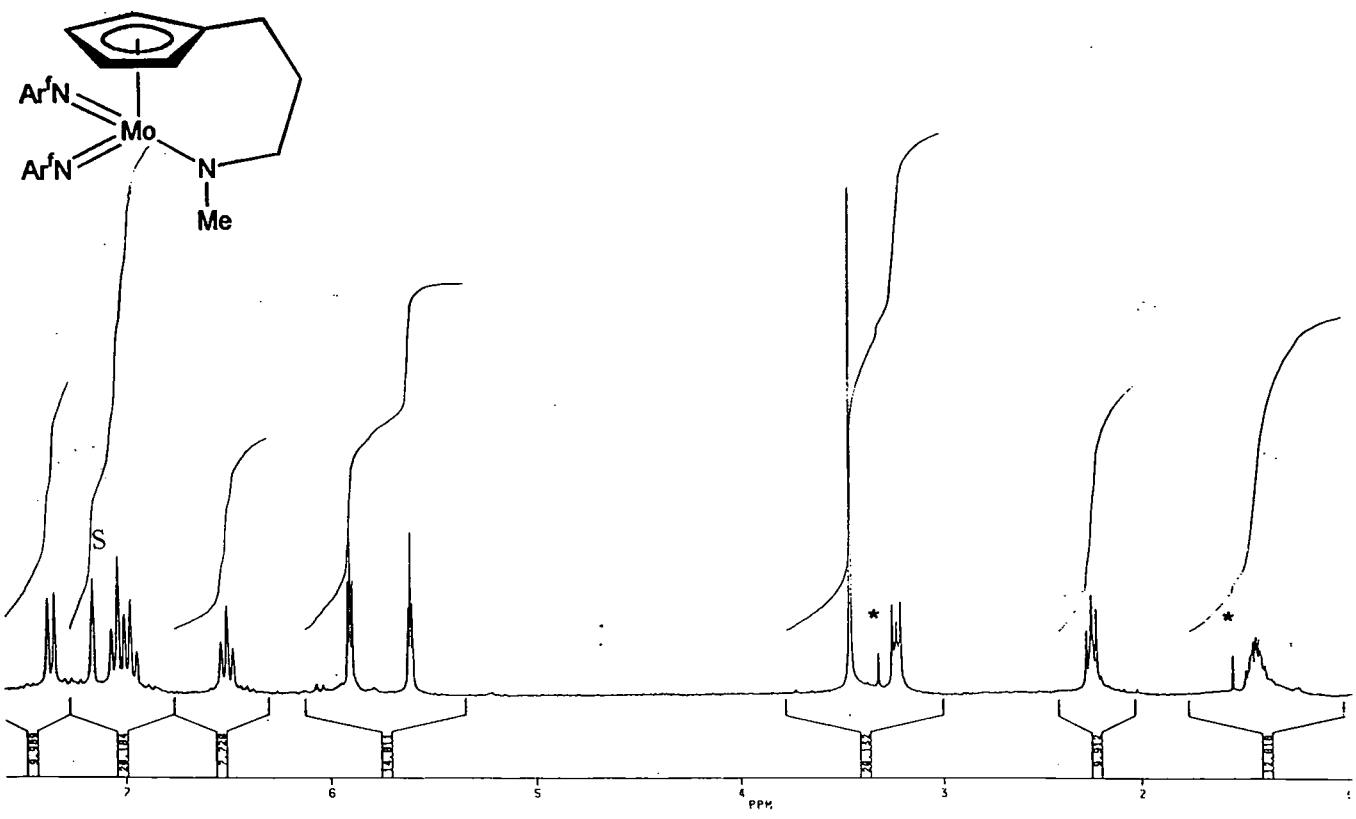

Figure 2.13 ^{1}H NMR spectrum of **2.4** in C_6D_6 at 250MHz

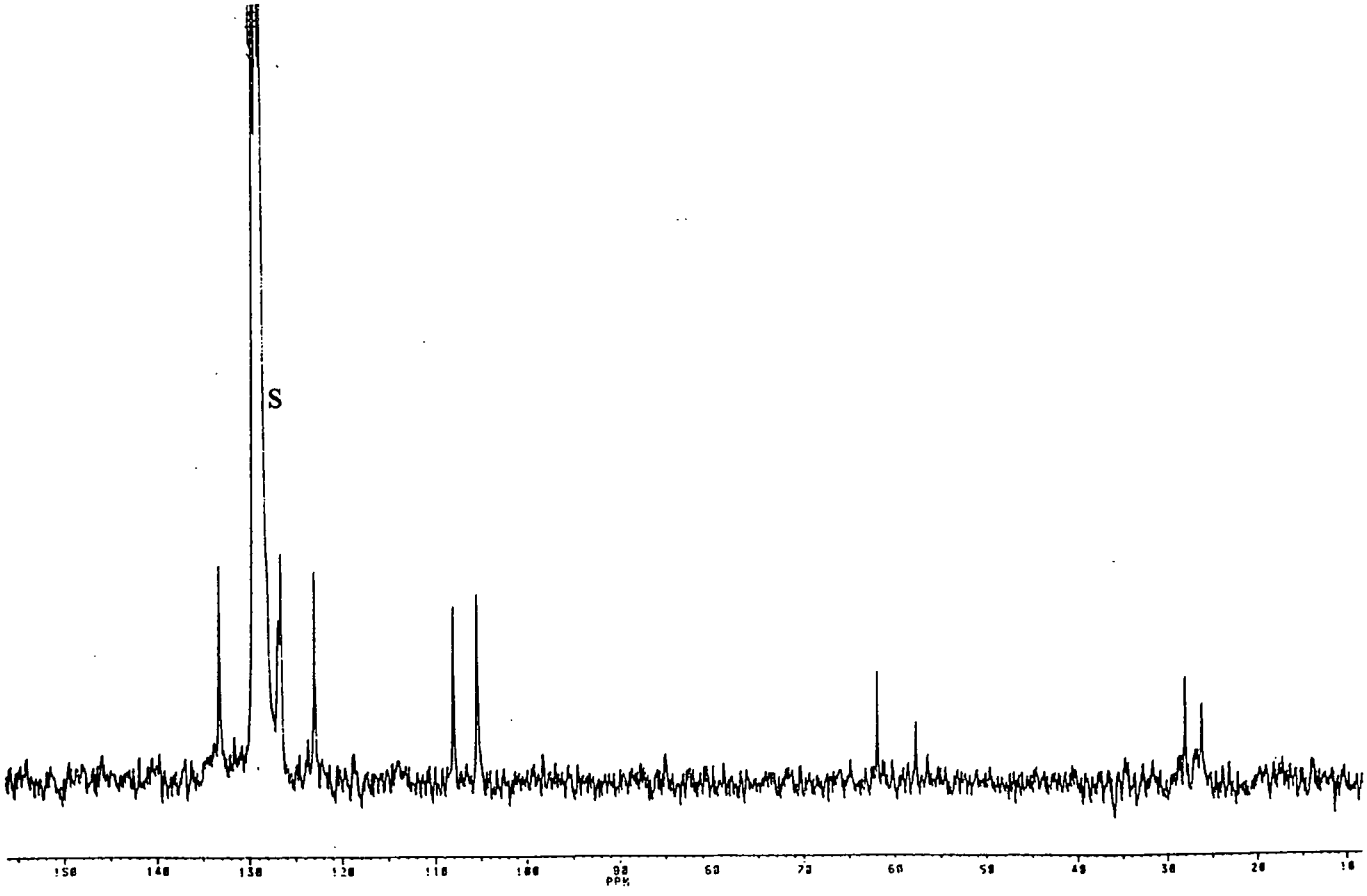

Figure 2.14 $^{13}C\{^{1}H\}$ NMR spectrum of **2.4** in C_6D_6 at 62.5MHz

2.2.4 Molecular and electronic structures of 2.2 – 2.5

The four Group 6 bis imido cyclopentadienyl amide complexes **2.2**, **2.3**, **2.4** and **2.5** were found to be isolobal and isoelectronic with the Group 7 complexes, $[M(N^tBu)_3(NH^tBu)]$ (M = Mn, Re) which are known, where the 5 electron cyclopentadienyl moiety has been replaced by another four electron bis imido.[12] Molecular structure determination found these complexes to be of pseudo tetrahedral geometry and therefore **2.2** – **2.5** are expected to be similar.

Electron count

In the absence of structural data, it could be assumed that both the imido ligands are linear, the amide ligand planar, and the cyclopentadienyl coordinated in a η^5 fashion, therefore potentially donating all available electrons to the metal centre. If this were the case then complexes **2.2**, **2.3**, **2.4** and **2.5** would be formally 22 valence electron species, apparently contradicting the 18 electron rule.

It is now well established that in complexes containing multiple π-donor ligands, there are only a limited number of linear combinations of ligand based π-orbitals which have symmetry matches with the metal s, p and d orbitals. Both the imido and cyclopentadienyl ligands are σ^2,π^4 ligands, and the amide ligand is a σ^2,π^2 ligand. Comparison of complexes **2.2**, **2.3**, **2.4** and **2.5** with examples studied by Lin and Hall suggests that there will be two combinations of ligand-based π orbitals which do not have symmetry matches with the metal-based orbitals.[13]

Consider the simpler example of the tetrahedral "MT_4" $Os(N^tBu)_4$ molecule, where if the imido ligands donate their full complement of electrons to the metal, this would make a 24 electron complex. However figure 2.16 shows that symmetry considerations reveal that three combinations of nitrogen pπ have t_1 symmetry, and therefore have no corresponding metal d orbital with which to interact. The molecule is therefore best considered an 18 electron complex and the maximum bond order in the molecule is therefore 2.25 [i.e. $(4\sigma + 5\pi)/4$], with three of ligand-based π orbitals.

ligand σ	ligand π	metal s + p	metal d	max M-T bond order	max d electron for max bond order
$a_1 + t_1$	$e + t_2 + \mathbf{t_1}$	$a_1 + t_2$	$e + t_2$	2.25	0

Figure 2.16

The analogy between the imido and cyclopentadienyl ligand, discussed in detail in Chapter 3 (section 3.1) means that this orbital analogy should hold for the cyclopentadienyl ligand. Therefore complexes **2.2** – **2.5** can be classed as 18 valence electron complexes with 4 electrons occupying ligand–based orbitals. Structural determination by X-ray diffraction may demonstrate that the electron-loading of these complexes is relieved in the following ways:

i) Metal imido bonds that are longer than that expected for M-N triple bonds and/or bent imido ligands.
ii) Cyclopentadienyl ring slippage.
iii) Pyramidalisation of the amide nitrogen.

Bent imido ligands were demonstrated in the formally 20 electron complex $MoCl_2(N^tBu)_2dme$ discussed earlier (section 2.2.2, figure 2.9). Although the M-N bond distances were consistent with those of imido triple bonds, Mo-N-C angles of 162.9° were observed. A low M-N bond order is often associated with bending of the M-N-R bond angle, leaving the nitrogen with a lone pair of electrons and hence sp^2 hybridised (this arises if the imido bond is described in valence bond terms).

^{13}C NMR studies

It has been reported that the difference between the ^{13}C chemical shifts for α and β carbon atoms of d^0 transition metals t-butylimido complexes can be used as an appropriate probe into the electronic structure of the ligand.[14] The difference in the ^{13}C NMR chemical shift (Δδ) between the quaternary carbon and the methyls of the t-butylimido group [δ($\underline{C}Me_3$ - δ($C\underline{Me}_3$)] has been proposed to afford a qualitative indication of the degree of electron donation from the imido group to the metal centre. The contribution from the lone pair of the nitrogen in a metal-imido bond has an effect on the electronic nature of the adjacent quarternary carbon and therefore the chemical shift. The greater the contribution of the lone pair the more electropositive the quarternary carbon becomes, causing a ^{13}C shift to higher frequencies and in turn a higher Δδ value. The Δδ values have been measured for a number of t-butylimido complexes and the following observations were made:

i) In a series of complexes where the imido ligand has a similar bond order (e.g., monoimido complexes) the value of Δδ is sensitive to the identity of the metal atom and the magnitude of Δδ increases with increasing electronegativity of the metal atom. For example in the series of related compounds $M(N^tBu)_2(OSiR_3)_2$ where M = W, Mo, Cr, the electronegativity increases 1.5 < 1.75 < 2.3 and Δδ increases 33 < 37 < 46.[15]

ii) As the number of imido ligands in a complex increases (and hence as their π-bond order decreases) the value of Δδ falls. This is seen most clearly in the series $Os(N^tBu)_nO_{(4-n)}$; the magnitude of Δδ decreases 55 > 46 > 41 for n = 1, 2 and 3 respectively.[12]

iii)There is some dependence on the ancillary ligands present but their effect is much smaller than that of the nature of the metal atom.

In general, the lower the electronegativity of the metal atom and the more t-butylimido groups and ancillary groups present, the smaller the contribution is from the imido lone pair and consequently a smaller Δδ value will be observed. The magnitudes of Δδ were measured for the tungsten and molybdenum complexes, **2.2**, **2.3** and also for $Mo[\eta^5:\eta^1\text{-}C_5H_4(CH_2)_3N(Et)Me]Br(N^tBu)_2$, **2.6** (discussed in section 2.3.1). To gain a qualitative

indication of electron donation from the imido group to the metal centre and the effects of ancillary ligands, the results were tabulated against other molybdenum and tungsten bis t-butyl imido complexes, so that comparisons can be drawn (Table 2.1). Included in the table are the starting materials $W(N^tBu)_2(NH^tBu)_2$ and $Mo(N^tBu)_2Cl_2dme$, from which **2.2** and **2.3** were prepared, and also a couple of mono t-butyl imido complexes, $M(N^tBu)Cl_3(C_5H_5)$ (M = Mo, W).

$Mo(N^tBu)_2$ complexes [(i)]	Δδ/ppm	$W(N^tBu)_2$ complexes [(i)]	Δδ/ppm
$Mo(CpNMe)(N^tBu)_2$ **2.3** (22)	34.0	$W(N^tBu)_2(CpNMe)$ **2.2** (22)	33.2
$Mo[CpN(Et)Me]Br(N^tBu)_2$ **2.6** (20)	40.2		
$Mo(N^tBu)_2Cl_2dme$[(ii)] (20)[16]	41.6	$W(N^tBu)_2(NH^tBu)_2$[(ii)] (20)	32.2
$Mo(N^tBu)Cl_3(C_5H_5)$[(iii)] (18)[17]	57.1	$W(N^tBu)Cl_3(C_5H_5)$[(iii)] (18)[17]	49.1
$Mo(N^tBu)_2Cl_2$ (16)[18]	44.0	$W(N^tBu)_2Cl_2py$ (18)[19]	37.9
$Mo(N^tBu)_2(C_5H_5)Cl$ (20)[19]	40.8	$W(N^tBu)_2(C_5H_5)Cl$ (20)[19]	35.8
$Mo(N^tBu)_2(C_5H_5)Me$ (20)[17]	36.2	$W(N^tBu)_2(C_5H_5)Me$ (20)[17]	33.9
$[Mo(N^tBu)(\mu\text{-}N^tBu)Me_2]_2$ (16)[20]	35.0	$[W(N^tBu)(\mu\text{-}N^tBu)Me_2]_2$ (16)[20]	33.8
$[Mo(N^tBu)(\mu\text{-}N^tBu)_3(\mu\text{-}Li)_2]_2$[(iv)]	b 24.0	$[W(N^tBu)(\mu\text{-}N^tBu)_3(\mu\text{-}Li)_2]_2$[(iv)]	b 24.0
	l 14.7		l 13.2

i) formal electron count in brackets

ii) starting materials used for the synthsis of **2.3** and **2.2**

iii)mono t-butyl imido complexes

iv)Δδ for both bridging and terminal imido groups, b = bent (i.e. terminal N^tBu), l = linear (i.e. bridging N^tBu)

Table 2.1

Table 2.1 lists the Δδ values for the three new complexes and for our fairly limited series, the values for **2.2**, **2.3** and **2.6** lie within the range previously recorded for t-butyl imido species, 25ppm for $[Hf(\mu\text{-}N^tBu)_2(NMe)_2]$ to 55ppm for $[CrO(N^tBu)(OSiMe_3)_2$. As expected, the molybdenum species, **2.3**, having a higher electronegativity, also has a higher

$\Delta\delta$ value than the tungsten complex, **2.2**. Also, the $\Delta\delta$ values for the new bis imido complexes, **2.2**, **2.3** and **2.6**, are lower than for the mono imido complexes, and lie within the range of 44.0-24.0ppm for molybdenum, and 37.9-23.6ppm for tungsten bis imido complexes.

Apart from the notable exception of the electronically saturated dimers, $[M(N^tBu)(\mu\text{-}N^tBu)_3(\mu\text{-}Li)_2]_2$ (M = Mo, W), which have extremely low $\Delta\delta$ values for the bridging imidos, the values for **2.2** and **2.3** are some of the lowest. This indicates a metal nitrogen bond where there is a small contribution from the nitrogen lone pair to the metal d orbitals, as would be expected for a formally 22 electron complex. This may be observed in the molecular structure as either a lengthening of the M-N bond and/or bending of the M-N-C bond. Being formally a 20 electron species, complex **2.6** has a higher $\Delta\delta$ value of 40.2, a value similar to the analogous complex $Mo(N^tBu)_2(C_5H_5)Cl$. This indicates a larger contribution from the nitrogen lone pair and, therefore, stronger imido bonding than in **2.2** or **2.3**. However, this value is not as high as, for example, the formally 20 electron complex, $Mo(N^tBu)_2Cl_2dme$, indicating that the contribution from the chlorides and dimethoxyethane group is smaller than the cyclopentadienyl and bromide group in **2.6**..

2.3 Reactions of $Mo[\eta^5:\eta^1\text{-}C_5H_4(CH_2)_3NMe](N^tBu)_2$, 2.3

Transition metal imido complexes, (M=NR), constitute one of the richest classes of compounds, both in variety of structural possibilities and the diversity of the chemistry associated with them.[21] Complexes containing this ligand have been proposed as intermediates in a variety of processes including selective oxidation,[22] ammoxidation,[23] and enzymatic transformations.[24] The $[NR]^{2-}$ ligands can be thought to coordinate with a metal-nitrogen multiple bond consisting of one σ and either one or two π interactions. A unique set of properties are imparted to the imido ligand and the complex itself from these M(dπ)-N(pπ) interactions-ranging from remarkable stability to extreme reactivity. Therefore many reactions of imido ligands are known, but the reactivity is a sensitive function of the chemical environment and found to depend on the following:

i) The nature of the transition metal to which it is bound.
ii) The oxidation state of the metal.
iii) The nature of other ligands that are present.

These three factors are important because they control the nature of the ligand-*p* to metal-*d*π interaction, which can sometimes even encompass both the HOMO and LUMO of the complex. For example a more electronegative metal in a higher oxidation state with less competitive π-bonding ligands will increase the π-bonding capability of the nitrogen in the imido. These chemical effects of increasing π donation are summarised in figure 2.17

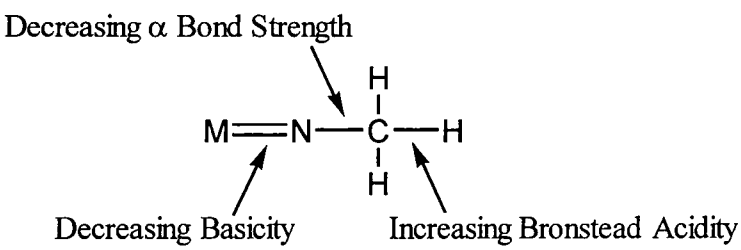

Figure 2.17

A good illustration of the effect of increasing the electronegativity of the metal was provided by Henderson. In the complex *trans*-$[M(NH)X(dppe)_2]^+X^-$ on changing M from tungsten to molybdenum, the acidity of the imido proton is increased 1000-fold.[25]

Numerous reactions of imido complexes with electrophiles have been reported, and reactions with excess electrophile often result in complete removal of the imido ligand from the metal. With this in mind reactions were carried between $Mo[\eta^5:\eta^1\text{-}C_5H_4(CH_2)_3NMe](N^tBu)_2$, **2.3**, and a number of electrophiles. Although the aim was to replace the imido ligand, reaction at the amide substituent was expected initially leaving a pendant amine, followed by reaction at the imido group.

2.3.1 Reaction between ethyl bromide and 2.3.

Imido ligands can be alkylated, with alkyl electrophiles attacking imido ligands and removing the ligand completely from the metal in some cases. Treatment of the molybdenum imido complex, shown in figure 2.18, with an excess of methyl bromide results in permethylation of one imido nitrogen.[26]

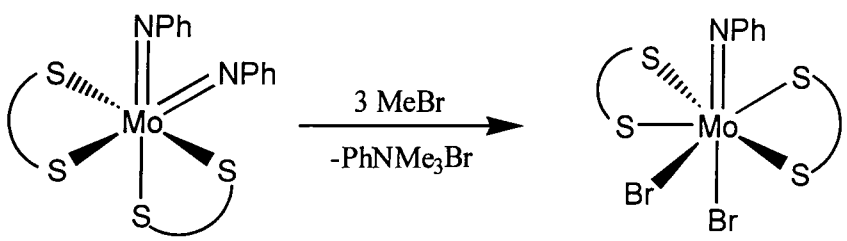

Figure 2.18

Since methyl bromide is a gas at room temperature and, therefore, difficult to handle, **2.3** was reacted with 10 equivalents of ethyl bromide (b.pt. 37-40°C), in toluene for 2 days. Upon work-up a brown oil/solid formed. Both the ^1H NMR and $^{13}C\{^1H\}$ NMR spectra, (figure 2.19 and 2.20 respectively) show little change in the cyclopentadienyl and imido regions, compared to that of **2.3**. However, significant shifts of the NCH_3 fragment to lower frequencies, 2.10 and 42.3ppm in the ^1H and $^{13}C\{^1H\}$ NMR spectra respectively,

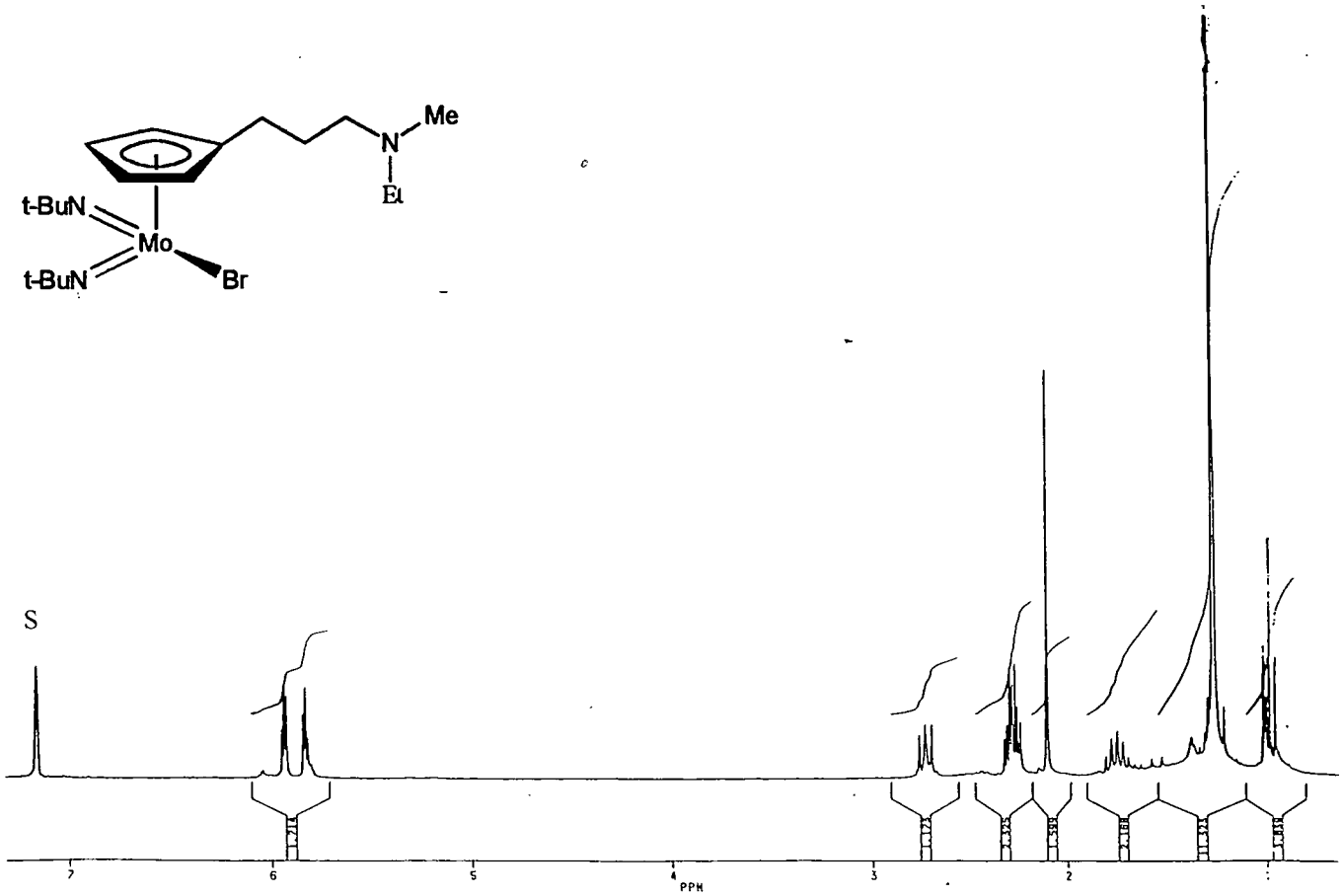

Figure 2.19 ^{1}H NMR spectrum of **2.6** in C_6D_6 at 250MHz

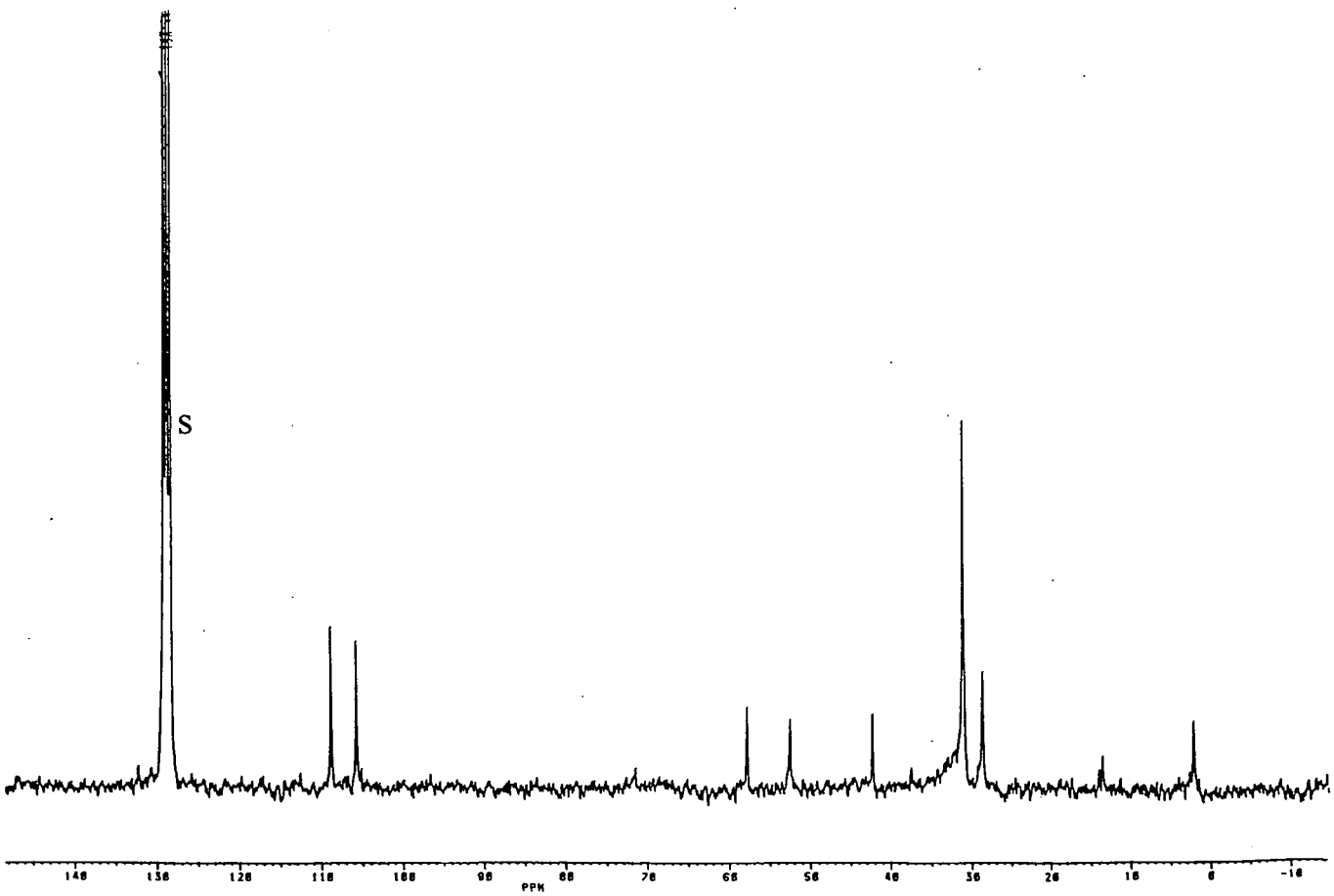

Figure 2.20 $^{13}C\{^{1}H\}$ NMR spectrum of **2.6** in C_6D_6 at 62.5MHz

indicate the presence of a pendant amine substituent. Two new sets of multiplets indicate the presence of an ethyl group attached to the nitrogen forming a tertiary amine. Resonances at 2.28 and 0.99ppm in the ^{1}H NMR spectrum are assigned to the NCH_2 and $NCH_2C\underline{H}_3$ groups respectively. From this evidence it was concluded that ethyl bromide had reacted with only the amide functionality, forming a molybdenum bromide and pendant ethyl amine, $Mo[\eta^5\text{-}C_5H_4(CH_2)_3N(Et)Me](N^tBu)_2$, **2.6**, in 94% yield (figure 2.21).

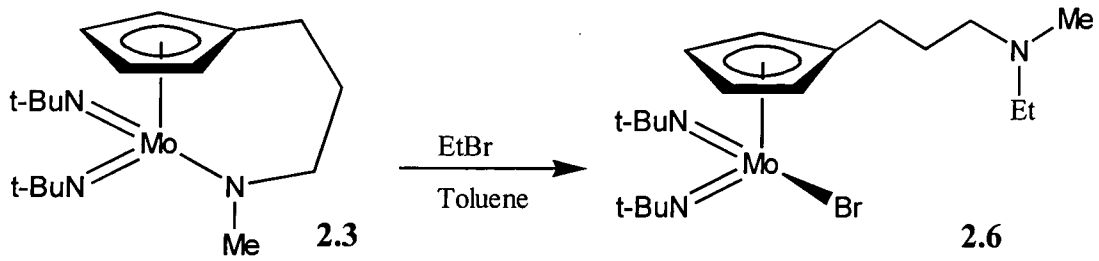

Figure 2.21

The product, **2.6**, was also confirmed by mass spectroscopy, with a mass centred at m/z = 482 for the cation, $[\mathbf{2.6}]^+$. No reaction of the imido groups with ethyl bromide was observed even when heated for several days in a closed system (ethyl bromide having a boiling point of 37-40°C allowing a reaction temperature of no more than 40°C). This lack of reactivity may be due to diminished π donation of the imido substituents caused by competitive π bonding ligands. As discussed earlier, these complexes are formally 22 electron complexes and are therefore likely to have diminished π donation from the imido substituents. The effect of the second imido substituent is evident from the reaction between $Mo(dtc)_2(NPh)_2$ and methyl bromide (figure 2.18), where the reaction stops cleanly after the replacement of a single imido substituent.

2.3.2 Attempted reactions between dimethyl ammonium chloride and 2.3

The molybdenum complex, **2.3**, is a low bond order polyimido complex and such complexes can also be cleaved by acids, as shown in figure 2.22.

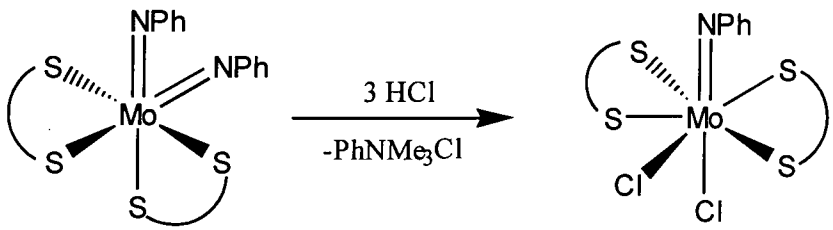

Figure 2.22

In an attempt to replace each imido ligand for two chloride ligands, **2.3** was reacted with 5 equivalents of dimethyl ammonium chloride for two days in THF. Analysis of the crude product by NMR showed the presence of an attached cyclopentadienyl group and pendant amine, with both imido ligands remaining intact. No product could be isolated pure from the reaction.

2.3.3 Attempted reactions between aniline and 2.3

Also included in the reactions with electrophiles is the formal attack of the imido nitrogen by protons of an amine. Imido ligands have been observed to undergo exchange, as shown in figure 2.23.

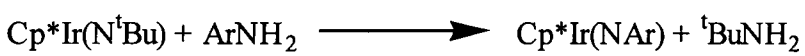

Figure 2.23

Complex **2.3** was reacted with 3 equivalents of aniline for 4 days. An aliquot was taken, the ^{1}H NMR analysis of which showed no evidence for a metal bonded cyclopentadienyl ligand, indicating that the dissociation of the metal ligand bonds had occurred.

2.3.4 Attempted reaction of benzophenone and 2.3

The majority of imido complexes will react with aldehydes and ketones to form the corresponding metal oxide. There are exceptions such as $O_3Os(NR)$ and $(Me_3SiO)_2CrO(NR)$ which contain less electropositive metal atoms, and therefore do not react. The mechanism is thought to involve a type of "Wittig-like" (2 + 2) process shown schematically in figure 2.24.

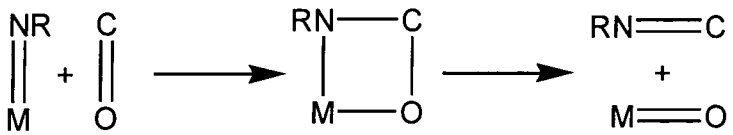

Figure 2.24

In an attempt to replace the imido ligands for oxo ligands, **2.3** was stirred with 2 equivalents of benzophenone in toluene for two days. Analysis of an aliquot by ^1H NMR spectroscopy showed the presence of both starting materials. No reaction was observed following reflux of the solution for three days.

2.4 Summary

The complexes $[M(C_5H_4(CH_2)_3NMe)(NR)_2]$ (M = W, R = ^{t}Bu; M = Mo, R = ^{t}Bu, Ar", Ar^f) have been successfully prepared using two very different approaches, the tungsten analogue from an amide route follow a kinetic pathway, and the molybdenum complexes using the chloride route follow a thermodynamic pathway, both giving products in high yield. All are examples of a few linked cyclopentadienyl amide Group 6 complexes to be synthesised and the tungsten complex appears to be the first cyclopentadienyl bis-imido amide complex of tungsten. Reactions carried out to replace the imido groups proved unsuccessful and, therefore, their use in preparing catalyst precursors seem limited.

2.5 Experimental

2.5.1 Preparation of starting materials

Preparation of $W(N^tBu)_2(NH^tBu)_2$[6]

To a suspension of WCl_6 (10.0g, 23mmol) in diethyl ether (200ml) t-butyl amine (30ml, 285mmol) was added dropwise, then stirred for 48hr. The yellow solution was filtered and the solvent removed under reduced pressure to affording $W(N^tBu)_2(NH^tBu)_2$ (6.7g, 14mmol, pure by NMR, 57% yield) as a pale yellow crystalline solid. Recrystallisation could be carried out from toluene or pentane (2ml/g) at -40°C yielding pale yellow crystals.

^1H NMR: δppm, C_6D_6; 5.2 (br s, 2H, NH), 1.40 (s, 18H, $NHCMe_3$), 1.25 (s, 18H, $N(CMe_3)$.

Preparation of $Mo(N^tBu)_2Cl_2dme$[8]

Solutions of NEt_3 (27.1ml, 194mmol), TMSCl (55.5ml, 437mmol) and t-butylamine (10.2ml, 97.1mmol) in dimethoxyethane (ca. 20ml each solution) were added sequentially to a stirred suspension of Na_2MoO_4 (10.0g, 48.6mmol) in dimethoxyethane (100ml). The mixture was then heated to 70°C for 12hr forming a pale yellow solution and a white precipitate. The solution was filtered and the solvent removed under reduced pressure to afford crude $Mo(N^tBu)_2Cl_2dme$ (15.35g, 40.1mmol, 82.5% yield) as a yellow crystalline solid. Recrystallisation from diethyl ether at -20°C gave amber coloured crystals suitable for X-ray diffraction studies.

^1H NMR: δppm, C_6D_6; 3.63 (s, 6H, CH_3), 3.38 (s, 4H, CH_2), 1.56 (s, 18H, $NCMe_3$).

Preparation of $Mo(NAr^f)_2Cl_2dme$

The method outlined for $Mo(N^tBu)_2Cl_2dme$ was employed for the reaction with 2-triflouromethylanaline (15.2g, 97mmol) used in exchange for t-butylamine. Crude Mo[N-2-$CF_3C_6H_4$]$_2Cl_2$dme (29.5g, 44mmol, 92% yield) formed as a dark red crystalline solid. Recrystallisation from diethyl ether could be carried out yielding dark red crystals.

^{1}H NMR: δppm, C_6D_6; 7.12 (m, 8H, C_6H_4), 3.43 (s, 4H, CH_2O), 3.27 (s, 6H, CH_3O).

Preparation of $Mo(NAr'')_2Cl_2dme$

The method outlined for $Mo(N^tBu)_2Cl_2dme$ was employed for the reaction with 2,6-diisopropylaniline (18.3ml, 97mmol) used in exchange for t-butylamine. Crude Mo[N-2,6-$^iPr_2C_6H_3$]$_2Cl_2$dme (27.3g, 45mmol, 96% yield) formed as a dark red crystalline solid. Recrystallisation from diethyl ether could be carried out yielding dark red crystals.

^{1}H NMR: δppm, C_6D_6; 6.96 (m, 6H, C_6H_3), 4.30 (sept, 2H, C<u>H</u>Me_2), 3.46 (s, 4H, CH_2O), 3.17 (s, 6H, CH_3O), 1.26 (d, 12H, CH<u>Me</u>$_2$).

2.5.2 Preparation of $W[\eta^5:\eta^1\text{-}C_5H_4(CH_2)_3NMe](N^tBu)_2$, 2.2, including the intermediate $W[\eta^1\text{-}C_5H_5(CH_2)_3NMe](NH^tBu)(N^tBu)_2$, 2.1

A solution of $W(N^tBu)_2(NH^tBu)_2$ (1.41g, 3.0mmol) and $C_5H_5(CH_2)_3N(H)Me$, **1.1**, in toluene (20ml) was heated under reduced pressure at 55°C for 3 days. The volatiles were removed under reduced pressure leaving an approximately 1:1 mixture of $W[\eta^1\text{-}C_5H_5(CH_2)_3NMe](N^tBu)_2(NH^tBu)$, **2.1**, and $W[\eta^5:\eta^1\text{-}C_5H_4(CH_2)_3NMe](N^tBu)_2$, **2.2**. Chloroform (10ml) was added to the mixture of **2.1** and **2.2**, and left to stand in a 20ml Young's ampoule under reduced pressure at room temperature for 10 days. The volatiles were removed under reduced pressure to afford $W[\eta^5:\eta^1\text{-}C_5H_4(CH_2)_3NMe](N^tBu)_2$, **2.2**, (1.20g, 2.6mmol, >95% pure by NMR, 87% yield) as a yellow oil.

Data characterising 2.1

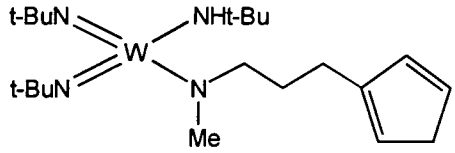

EI mass spec: m/z = 533 $[\mathbf{2.1}]^+$ with correct isotope distribution

^{1}H NMR: δ/ppm, 250 MHz, $CDCl_3$

ca. 6.2 [br m, 3H, (3 x CH in C_5H_5)]
5.03 [br s, 1H, ($N\underline{H}CMe_3$)]
3.63 [8 lines, 2H, (NCH_2)]
3.41 [s, 3H, (NCH_3)]
2.94 [dq, 2H, (2 x CH in C_5H_5)]
2.43 [m, 2H, ($C_5H_4CH_2$)]
1.78 [obscured by **2.2**, ($CH_2C\underline{H_2}CH_2$)]
1.30 [heavily obscured, ($NC\underline{Me_3}$)]

Data characterising 2.2

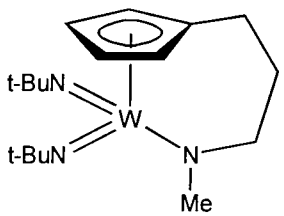

Description: Yellow oil

EI mass spec: m/z = 463 $[\mathbf{2.2}]^+$ with correct isotope distribution

Infra-red: 2921-2702 (aliphatic CH's); 1233, 1241, 788 (ring C-H bend)

^{1}H NMR: δ/ppm, 250 MHz, $CDCl_3$

6.09 [t, 2H, $^3J_{HH}$=2.7Hz), (C_5H_4)]
6.02 [t, 2H, $^3J_{HH}$=2.7Hz, (C_5H_4)]
3.25 [m, 2H, (NCH_2)]
3.23 [s, 3H, (NCH_3)]
2.71 [m, 2H, ($C_5H_4C\underline{H_2}$)]
1.78 [quin, 2H, $^3J_{HH}$=3.3Hz, ($CH_2C\underline{H_2}$)]
1.23 [s, 18H, (2 x $C\underline{Me_3}$)]

$^{13}C\{^1H\}$ NMR: δ/ppm, 62.5 MHz, $CDCl_3$

117.4 (C_5H_4 *ipso*)
107.4 (C_5H_4)
101.7 (C_5H_4)
66.6 ($\underline{C}Me_3$)
62.4 (NCH_2)
56.9 (NCH_3)
33.4 ($C\underline{Me_3}$)
28.8 ($C_5H_4\underline{C}H_2$)
23.4 ($CH_2\underline{C}H_2CH_2$)

2.5.3 Preparation of $Mo[\eta^5:\eta^1\text{-}C_5H_4(CH_2)_3NMe](N^tBu)_2$, 2.3

A solution of $Mo(N^tBu)_2Cl_2dme$ (2.30g, 6.0mmol) in THF (30ml) was cooled to -78°C (acetone/dry ice). A suspension of $[\eta^5:\eta^1\text{-}C_5H_4(CH_2)_3NMe]Li_2$, **1.3**, (0.89g, 6.0mmol) in THF (30ml) was added dropwise with vigorous stirring at -78°C. The mixture was warmed to room temperature over 2hr and then stirred for 24hr. The solvent was removed under reduced pressure and the product extracted into hexane (2 x 20ml) leaving LiCl (0.50g, 11.8mmol, 98% of theory) as an off-white solid. The solvent was removed from the combined extracts yielding $Mo[\eta^5:\eta^1\text{-}C_5H_4(CH_2)_3NMe](N^tBu)_2$, **2.3**, (2.15g, 5.7mmol, pure by NMR, 96% yield) as a dark orange oil. Distillation under reduced pressure (40°C, 10^{-3}mmHg) onto a sublimation probe at -196°C gave analytically pure **2.3** as a clear yellow oil.

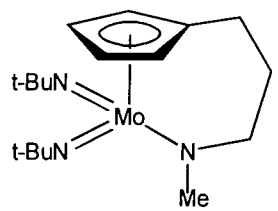

Data characterising 2.3

Description: Yellow oil. Sublimes 40°C, 10^{-3}mmHg

EI mass spec: m/z = 375 $[\mathbf{2.3}]^+$ with correct isotope distribution

Infra-red: 2966-2761 (aliphatic CH's); 1247, 1251, 799 (ring C-H bend)

Elemental analysis: Found($C_{17}H_{31}N_3Mo$ requires) C:55.1(54.7); H:8.2(8.3); N:10.9(11.3)

^{1}H NMR: δ/ppm, 250 MHz, C_6D_6

5.90	[s, 4H, (C_5H_4)]
3.29	[m, 2H, (NCH_2)]
3.27	[s, 3H, (NCH_3)]
2.60	[m, 2H, ($C_5H_4C\underline{H}_2$)]
1.62	[quin, 2H, $^3J_{HH}$=3.6Hz, ($CH_2C\underline{H}_2$)]
1.29	[s, 18H, (2 x $C\underline{Me}_3$)]

$^{13}C\{^1H\}$ NMR: δ/ppm, 62.5 MHz, C_6D_6

118.5 (C_5H_4 *ipso*)
107.3 (C_5H_4)
102.2 (C_5H_4)
66.3 ($\underline{C}Me_3$)
63.0 (NCH_2)
57.7 (NCH_3)
32.3 ($C\underline{Me}_3$)
28.8 ($C_5H_4\underline{C}H_2$)
23.4 ($CH_2\underline{C}H_2CH_2$)

2.5.4 Preparation of $Mo[\eta^5:\eta^1\text{-}C_5H_4(CH_2)_3NMe](NAr^f)_2$, 2.4

A solution of $Mo(NAr^f)_2Cl_2dme$ (1.15g, 2.0mmol) in THF (30ml) was cooled to -78°C (acetone/dry ice). A suspension of $[\eta^5:\eta^1\text{-}C_5H_4(CH_2)_3NMe]Li_2$, **1.3**, (0.30g, 2.0mmol) in THF (30ml) at -78°C was added dropwise with vigorous stirring. The mixture was warmed to room temperature over 2hr, then stirred for 24 hr. The solvent was removed under reduced pressure and the product extracted into hexane (2 x 30ml) leaving LiCl (0.16g, 3.8 mmol, 98% of theory) as an off-white solid. The solvent was removed from the combined extracts yielding $Mo[\eta^5:\eta^1\text{-}C_5H_4(CH_2)_3NMe](NAr^f)_2$, **2.4**, (1.03g, 1.9mmol, pure by NMR, 94% yield) as a dark red oily solid.

Data characterising 2.4

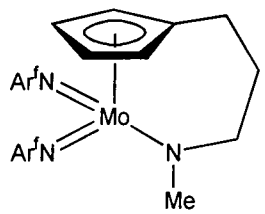

Description: Dark red oil/solid

EI mass spec: m/z = 548 $[\mathbf{2.4}]^+$ with correct isotope distribution

Infra-red: 3062 (aromatic C-H stretch); 2908-2743 (aliphatic CH's); 1298, 1256, 794 (ring C-H bends)

^{1}H NMR: δ/ppm, 250 MHz, C_6D_6

7.36	[d, 2 x 1H, $^3J_{HH}$=9.7Hz, (C_6H_4)]
7.03	[m, 2 x 2H, (C_6H_4)]
6.51	[t, 2 x 1H, $^3J_{HH}$=7.4Hz, (C_6H_4)]
5.91	[t, 2H, $^3J_{HH}$=2.5Hz, (C_5H_4)]
5.61	[t, 2H, $^3J_{HH}$=2.6Hz, (C_5H_4)]
3.46	[s, 3H, (NCH_3)]
3.24	[m, 2H, (NCH_2)]
2.25	[m, 2H, ($C_5H_4C\underline{H}_2$)]
1.43	[quin, 2H, $^3J_{HH}$=2.7Hz, ($CH_2C\underline{H}_2$)]

$^{13}C\{^1H\}$ NMR: δ/ppm, 62.5 MHz, C_6D_6

133.3	(C_6H_4)
126.6	C_6H_4)
123.0	(C_6H_4)
(C_5H_4 *ipso* not observed)	
108.0	(C_5H_4)
105.4	(C_5H_4)
61.7	(NCH_2)
57.7	(NCH_3)
28.0	($C_5H_4\underline{C}H_2$)
26.2	($CH_2\underline{C}H_2CH_2$)

2.5.5 Preparation of $Mo[\eta^5:\eta^1\text{-}C_5H_4(CH_2)_3NMe](NAr'')_2$, 2.5

A solution of $Mo(NAr'')_2Cl_2dme$ (3.64g, 6.0mmol) in THF (30ml) was cooled to -78°C (acetone/dry ice). A suspension of $[\eta^5:\eta^1\text{-}C_5H_4(CH_2)_3NMe]Li_2$, **1.3**, (0.89g, 6.0mmol) in THF (30ml) at -78°C was added dropwise with vigorous stirring. The mixture was warmed to room temperature over 2hr, then stirred for 24hr. The solvent was removed under reduced pressure and the product extracted into hexane (2 x 40ml) leaving LiCl (0.5g, 11.8mmol, 98% of theory) as an off-white solid. The solvent was removed from the combined extracts yielding $Mo[\eta^5:\eta^1\text{-}C_5H_4(CH_2)_3NMe](NAr'')_2$, **2.5**, (3.27g, 5.6mmol, pure by NMR, 94% yield) as a dark red oily solid.

Data characterising 2.5

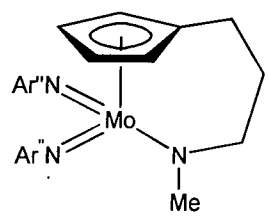

Description: Dark red oil/solid

EI mass spec: m/z = 384 $[\mathbf{2.5}]^+$ with correct isotope distribution

Infra-red: 3051 (aromatic C-H stretch); 2957-2772 (aliphatic CH's); 1327, 1266, 799 (ring C-H bends)

^{1}H NMR: δ/ppm, 250 MHz, C_6D_6

6.79	[m, 2 x 3H, (C_6H_3)]
5.90	[t, 2H, $^3J_{HH}$=2.5Hz, (C_5H_4)]
6.51	[t, 2H, $^3J_{HH}$=2.4Hz, (C_5H_4)]
3.61	[sept, 2 x 1H, (C<u>H</u>Me$_2$)]
3.10	[s, 3H, (NCH_3)]
3.06	[m, 2H, (NCH_2)]
2.29	[m, 2H, ($C_5H_4C\underline{H}_2$)]
1.32	[quin, 2H, $^3J_{HH}$=2.6Hz, ($CH_2C\underline{H}_2$)]
0.99	[s, 24H, (4 x CH<u>Me</u>$_2$)]

$^{13}C\{^1H\}$ NMR: δ/ppm, 62.5 MHz, C_6D_6

142.0	(C_6H_3)
124.6	C_6H_3)
123.1	(C_6H_3)
	(C_5H_4 *ipso* not observed)
107.1	(C_5H_4)
104.5	(C_5H_4)
70.9	(<u>C</u>HMe$_2$)
60.7	(NCH_2)
57.2	(NCH_3)
36.6	($C_5H_4\underline{C}H_2$)
29.9	($CH_2\underline{C}H_2CH_2$)
27.8	(CH<u>Me</u>$_2$)
24.1	(C<u>Me</u>$_3$)

2.5.6 Preparation of $Mo[\eta^5:\eta^1\text{-}C_5H_4(CH_2)_3N(Et)Me]Br(N^tBu)_2$, 2.6

A solution of **2.3** (0.37g, 1mmol) in toluene (20ml) was cooled to -78°C (dry ice/acetone). Ethyl bromide (0.34g, 3mmol, 3 x theory) was added dropwise and the solution allowed warmed to room temperature, then stirred for 24hr. The solvent was removed under reduced pressure and the product extracted with hexane (2 x 20ml). The extracts were combined and the solvent removed under reduced pressure to afford $Mo[\eta^5:\eta^1\text{-}C_5H_4(CH_2)_3N(Et)Me](N^tBu)_2Br$, **2.6**, (0.46g, 0.95mmol, pure by NMR, 94% yield) as a brown oil.

Data characterising 2.6

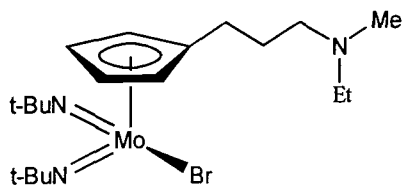

Description: Brown oil

EI mass spec: m/z = 482 $[\mathbf{2.6}]^+$ with correct isotope distribution

Infra-red: 2967-2788 (aliphatic CH's); 12244, 1206, 799 (ring C-H bends)

^{1}H NMR: δ/ppm, 250 MHz, C_6D_6

5.94	[t, 2H, $^3J_{HH}$=2.4Hz, (C_5H_4)]
5.83	[t, 2H, $^3J_{HH}$=2.5Hz, (C_5H_4)]
2.73	[m, 2H, ($NC\underline{H}_2CH_2$)]
2.28	[s, 2H, (NCH_2CH_3)]
2.28	[m, 2H, ($C_5H_4C\underline{H}_2$)]
2.10	[s, 3H, (NCH_3)]
1.74	[m, 2H, $^3J_{HH}$=3.9Hz, ($CH_2C\underline{H}_2$)]
1.29	[s, 18H, (2 x $C\underline{Me}_3$)]
0.99	[m, 3H, ($NCH_2C\underline{H}_3$)]

$^{13}C\{^1H\}$ NMR: δ/ppm, 62.5 MHz, C_6D_6

108.8	(C_5H_4)
105.7	(C_5H_4)
71.8	($N\underline{C}Me_3$)
57.8	($N\underline{C}H_2CH_2$)
52.5	($N\underline{C}H_2CH_3$)
42.3	(NCH_3)
37.9	($NCH_2\underline{C}H_3$)
31.6	($C\underline{Me}_3$)
28.6	($C_5H_4\underline{C}H_2$)
13.6	($CH_2\underline{C}H_2CH_2$)

2.5.7 Attempted reaction of dimethyl ammonium chloride and 2.3

A solution of **2.3** (0.37g, 1mmol) in THF (10ml) was cooled to -78°C (acetone/dry ice) and a suspension of Me_2NH_2Cl (0.40g, 5mmol) in THF (10ml) added dropwise. The mixture was allowed to warm to room temperature, then stirred for 48hr, forming a dark brown suspension. The product was filtered and solvent removed under reduced pressure, analysis of which showed reaction at the amide group had occurred, no product could be isolated.

2.5.8 Attempted reaction of aniline and 2.3

A solution of **2.3** (0.37g, 1mmol) in toluene (20ml) was cooled to 0°C and aniline (0.28ml, 3mmol) added dropwise, and the solution was stirred at ambient temperature for 4 days, forming a dark brown suspension. The solvent was removed under reduced pressure and analysis showed no evidence for a cyclopentadienyl ligand. No product could be isolated pure and characterised.

2.5.8 Attempted reaction of benzophenone and 2.3

A solution of **2.3** (0.37g, 1mmol) in toluene (10ml) was cooled to 0°C and benzophenone (0.37g, 2mmol) in toluene(10ml) was added dropwise and the solution stirred at ambient temperature for 48hr. An aliquot was taken for analysis and showed the presence of both starting materials. No reaction was observed following reflux of the solution for 3 days.

2.6 References

1 M.H. Chisholm, F.A. Cotton, M. Extine and B.R. Stults, *J. Am. Chem. Soc.*, 1976, **98**, 4477.

2 T. Mise, M. Maeda, T. Nakajima, K. Kobayashi, I. Shimizu, Y. Yamamoto and Y. Wakatsuki, *J. Organomet. Chem.*, 1994, **473**, 155.

3 a) L. Labella, A. Chernega and M.L.H. Green, *J. Organomet. Chem.*, 1995, **485**, C18; b) L. Labella, A. Chernega and M.L.H. Green, *J. Chem. Soc., Dalton Trans.*, 1995, 395.

4 a) T.-F. Wang, T.-Y. Lee, J.-W. Chou and C.-W. Ong, *J. Organomet. Chem.*, 1992, **423**, 31; b) T.-F. Wang and Y.-S. Wen, *J. Organomet. Chem.*, 1992, **439**, 155

5 W.A. Herrmann, W. Baratta and M.J.A. Morawietz, *J. Organomet. Chem.*, 1995, **497**, C4.

6 W.A. Nugent, *Inorg. Chem.*, 1983, **22**, 965.

7 G. Walker, Ph.D. Thesis, Imperial College, London, 1997.

8 J. Robbins, S. Cai and R.R. Schrock, *Inorg. Chem.*, 1992, **31**, 2287.

9 J.M. Rawson, University of Durham, 1995, unpublished results.

10 W.A. Nugent and J.M. Mayer, "Metal Ligand Multiple Bonds", John Wiley and Sons, New York, 1988.

11 E.A. Maata and R.A.D. Wentworth, *J. Am. Chem. Soc.*, 1979, **101**, 2063.

12 A. Danopoulos, C.J. Longley and G. Wilkinson, *Polyhedron*, 1989, **8**, 2657.

13 Z. Lin and M.B. Hall, *Coord. Chem. Rev.*, 1993, **123**, 149.

14 P. Klingelhofer and U. Müller, *Z. Anorg. Allg. Chem.*, 1984, **516**, 85.

15 L.Banci, A. Bencini, A. Dei and D. Gatteschi, *Inorg. Chim. Acta.*, 1984, **84**, L11.

16 H.H. Fox, K.B. Yap, J. Robbins, S. Cai and R.R. Schrock, *Inorg. Chem.*, 1992, **31**, 2287.

17 U. Radius and J. Sundermayer, *Chem. Ber.*, 1992, **125**, 2183.

18 G. Schoettel, J. Kress and J.A. Osborn, *J. Chem. Soc., Chem. Commun.*, 1989, 1062.

19 J. Sundermayer, *Chem. Ber.*, 1991, **124**, 1977.

20 W.A. Nugent and R.L. Harlow, *J. Am. Chem. Soc.*, 1980, **102**, 1759.

21 a) W.A. Nugent and B.L. Haymore, *Coord. Chem. Rev.*, 1980, **31**, 123; b) R.R. Schrock, J.S. Murdzek, G.C. Bazan, J. Robbins, M. DiMare and M. O'Regan, *J. Am. Chem. Soc.*, 1990, **112**, 3875; c) G.R. Clark, A.J. Nielson, C.E.F. Richards and D.C. Ware, *J.Chem. Soc., Chem. Comm.*, 1989, 343; d) D.N. Williams, J.P. Mitchell, A.D.

Poole, U. Siemeling, W. Clegg, D.C.R. Hockless, P.A. O'Neill and V.C. Gibson, *J. Chem. Soc., Dalton. Trans.*, 1992, 739.

22 J. Belgacem, J. Kress and J.A. Osborn, *J. Chem. Soc., Chem. Comm.*, 1993, 1125.

23 a) J.D. Burrington, C. Kartisek and R.K. Grasselli, *J. Catal.*, 1984, **87**, 363; b) D.M.T. Chan and W.A. Nugent, *Inorg. Chem.*, 1985, **24**, 1422.

24 D. Mansuy, P. Battioni and J.P. Mayer, *J. Am. Chem. Soc.*, 1982, **104**, 4487.

25 R.A. Henderson, *J. Chem. Soc., Dalton. Trans.*, 1983, 51.

26 E.A. Matta and R.A.D. Wentworth, *Inorg. Chem.*, 1979, **18**, 2409.

Chapter 3

Group 4 – Zirconium and Titanium Amide Functionalised Cyclopentadienyl Complexes.

3.1 Introduction

The isolobal relationship between the imido ligand and the cyclopentadienyl ligand has been widely exploited in recent studies of early transition metal organometallic and coordination chemistry.[1] The cyclopentadienyl ligand, ($C_5H_5^-$), is known to bind strongly to metals, generally being inert to both electrophiles and nucleophiles and, therefore, often regarded as a spectator ligand. In much the same way, organoimido ligands are also frequently becoming used as ancillary ligands. Like the Group 4 bent metallocenes discussed in Chapter 1, a number of homogeneous catalytic reactions are known to employ imido complexes, perhaps the most documented example being Schrock's well-defined four coordinate metathesis catalyst (figure 3.1).

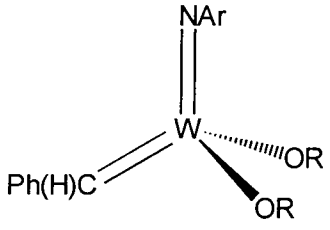

Figure 3.1

In general, imido ligands are "flexible" and can change the number of electrons they donate to the metal centre, readily allowing other species to coordinate (cf. ring slippage associated with the cyclopentadienyl ligand). This chapter outlines attempts to investigate the pseudo-isolobal relationship between Group 4 metallocenes and Group 6 bis imido complexes. As an introduction to this study the origins of this relationship are discussed.

3.1.1 The pseudo-isolobal relationship between MCp_2, M'Cp(NR), and M''$(NR)_2$

Two complex fragments are isolobal to each other if the number, the symmetry, the energy and the shape of the frontier orbitals are comparable. Simple MO calculations of the π-molecular orbitals of the cyclopentadienyl ligand ($C_5H_5^-$) reveal that it has an orbital of a_1 symmetry and a set of degenerate e_1 symmetry orbitals, the a_1 orbital is σ bonding and the e_1 pair are π bonding with respect to the metal ligand axis (figure 3.2). The ring system

also possesses an e_2 pair of δ symmetry unoccupied acceptor orbitals, although any interaction with these orbitals will be considerably weaker than those of π symmetry. The early transition metals have no filled δ symmetry orbitals on the metal that can donate into these orbitals and therefore it is unlikely that a significant bonding role is played by these levels. The frontier orbitals of the imido ligand (NR^{2-}) in a terminal geometry (sp hybridised nitrogen) resemble those of the cyclopentadienyl unit, and thus also bond to the metal via one σ and two π interactions (figure 3.2).[2]

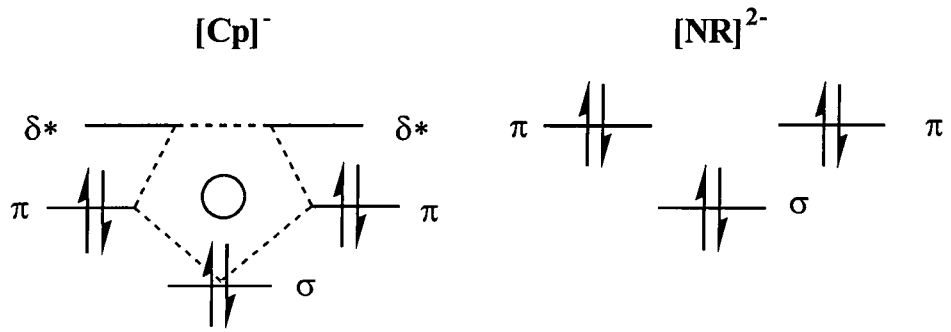

Figure 3.2 Representation of the frontier orbitals of the $[C_5H_5]^-$ and $[NR]^{2-}$ fragments

Detailed calculations have been performed which examine the bonding and resultant geometry of bent metallocenes. Using extended Hückel calculations, Lauher and Hoffmann have shown that as the angle between the normals to the rings in a metallocene decreases from 180° (i.e., a ferrocene-like structure), towards that of a bent metallocene, three new highly directional metal based orbitals result, $1a_1$, $2a_1$ and b_2 (figure 3.3).[3] These new orbitals are used to bind further ligands to the metal centre and are essentially directed in the yz plane, the b_2 orbital being mainly of d_{yz} character, while the two a_1 orbitals are formed from the metal's p_z, d_{z2} and d_{x2}-d_{y2} atomic orbitals. Thus, other ligands that bind to the metal centre should lie in the yz plane, bisecting the Cp-M-Cp wedge angle. The two remaining metal d orbitals remain essentially non-bonding.

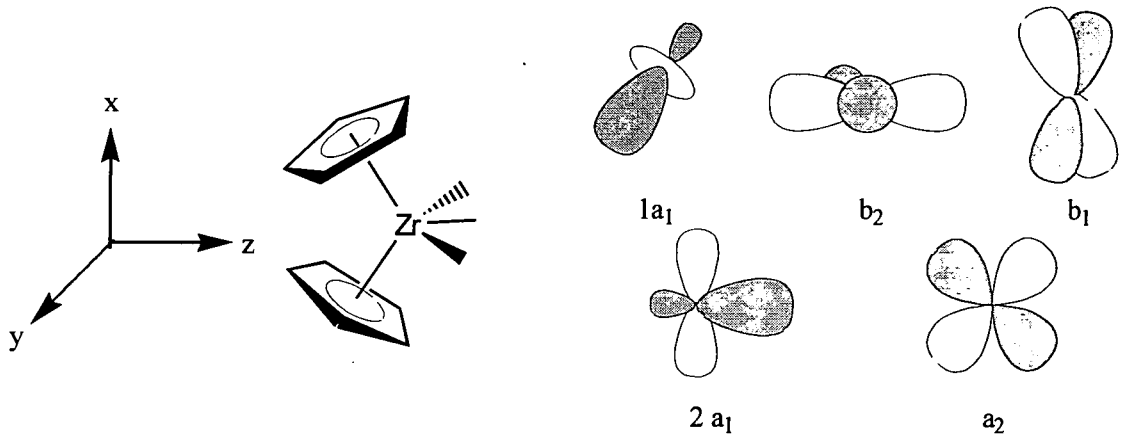

Figure 3.3 Frontier MO's of the $[Zr(C_5H_5)_2]^{2+}$ (most important contributions only)

Further Fenske-Hall quantum chemical calculations been performed which demonstrate that the frontier orbitals of Group 4 metallocene complexes are closely related to those of Group 5 half sandwich imido, and Group 6 bis imido complexes.[4] The frontier orbitals of the fragments $[Mo(NR)_2]^{2+}$,$[Nb(C_5H_5)(NR)]^{2+}$ and $[Zr(C_5H_5)]^{2+}$ are similar in their orientation (figure 3.4).

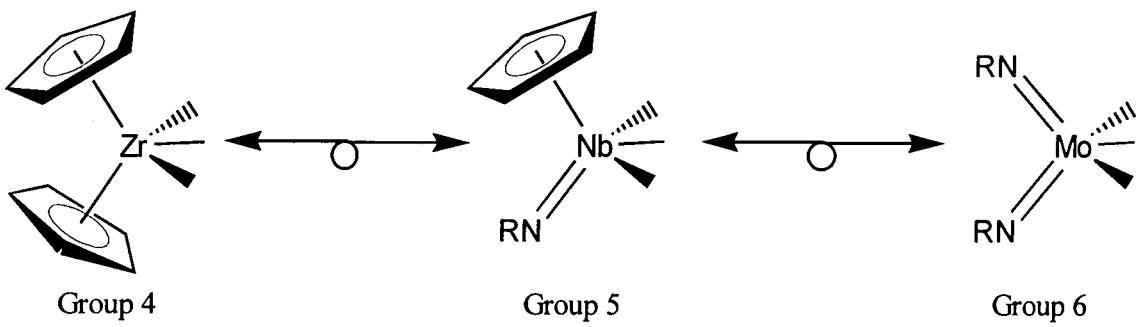

Figure 3.4

The cyclopentadienyl moiety formally donates five electrons to the valence electron count, whereas the linear imido ligand donates four electrons. Thus, in moving left to right across the series outlined in figure 3.4, the Group 4 bent metallocene fragment is formally valence isoelectronic and pseudo-isolobal to the Group 5 half-sandwich complex. This analogy can be carried out further to include Group 6 bis imido species, which possess two, formally four electron, donor ligands.

3.1.2 Aims

We sought to investigate the relationship between the tungsten and molybdenum complexes **2.1**, **2.3**, **2.4** and **2.5**, and complexes where the imido ligands (RN^{2-}) are replaced by cyclopentadienyl ligands (η-C_5H_5). In order to maintain an electron count of 14 electrons for each $M(NR_2)$ (M = W, Mo) fragment, the replacement of two imido ligands in the Group 6 transition metal complexes by two cyclopentadienyl ligands, requires the use of Group 4 metals.

In direct analogy to the reaction of $W(N^tBu)_2(NH^tBu)_2$ with $C_5H_5(CH_2)_3N(H)Me$ to give **2.2**, the reaction of $Zr(C_5H_5)_2(NMe)_2$ with $C_5H_5(CH_2)_3N(H)Me$ was investigated. Also, in analogy to the reaction of $Mo(NR)_2Cl_2dme$ (R = ^{t}Bu, Ar", Ar^f) with the dianion $[C_5H_5(CH_2)_3NMe]^{2-}$ yielding **2.3**, **2.4**, and **2.5**, we investigated the reaction of $Zr(C_5H_5)_2Cl_2$ and $Ti(C_5H_5)_2Cl_2$ with the dianion $[C_5H_5(CH_2)_3NMe]^{2-}$. These reactions could potentially allow us to explore the isolobal relationship shown in figure 3.5.

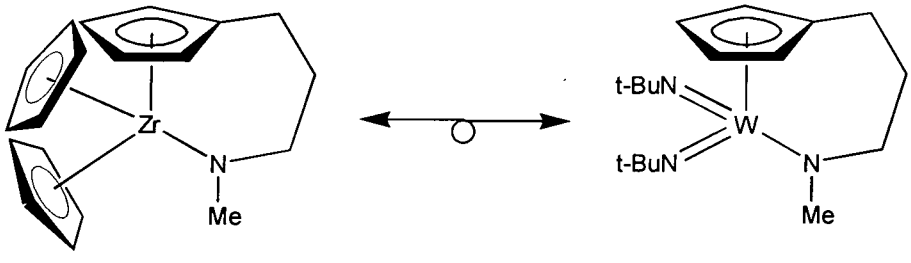

or Ti **or Mo**

Figure 3.5

As will be seen, the reactions of Group 4 complexes do not follow the pattern set by their "apparently related" Group 6 cousins.

3.2 Results and Discussion

3.2.1 Attempted reaction of $Zr(C_5H_5)_2(NMe_2)_2$ and $C_5H_5(CH_2)_3N(H)Me$, 1.1

In an attempt to substitute the two amide substituents of $Zr(C_5H_5)_2(NMe)_2$ for the cyclopentadienyl and amide groups of $C_5H_5(CH_2)_3N(H)Me$, one equivalent of the zirconocene complex and one equivalent of ligand **1.1**, were refluxed in toluene, in an ampoule under partial vacuum. Unlike the analogous tungsten reaction ^1H NMR analysis of an aliquot of the reaction mixture showed that no reaction had occurred, despite prolonged reflux over many days. The elimination of dimethylamine should be thermodynamically favourable and was expected to be the driving force for the reaction, but this is believed not to be a strong enough to counteract the steric and kinetic factors of the two cyclopentadienyl substituents on the metal. This might have been expected from the recent work of Jordan and coworkers who explored the influence of steric bulk on the reactions of $M(NR_2)_4$ with cyclopentadienyl ligands.[5]

3.2.2 Reaction between $Zr(C_5H_5)_2Cl_2$ and $[C_5H_4(CH_2)_3NMe]Li_2$, 1.3

It was thought that the problems encountered in the amide route would not be encountered in the reaction between zirconocene dichloride and one equivalent of the dianon $[C_5H_4(CH_2)_3NMe]Li_2$, **1.3**, in THF. It was expected that the formation of lithium chloride would be a strong driving force for a reaction to occur, in contrast to the non-formation of dimethylamine in the above reaction. The product was extracted into toluene leaving a dark orange oil and what was thought to be two equivalents of lithium chloride. Analysis of the crude material by ^1H NMR spectroscopy indicated the formation of a mixture of products. The oil was carefully sublimed (100-120°C, 10^{-3}mmHg) onto a liquid nitrogen cooled probe, producing a bright orange solid that formed an oil at room temperature (m.pt. ca.-20°C). Decomposition was observed during the sublimation with the formation of an intractable, involatile dark residue, ^1H NMR spectroscopic analysis of which showed no decipherable products.

Spectroscopic data indicate that the volatile product is not an analogue of replacing the $[Mo(N^tBu)_2]$ fragment in **2.3**, by a $[Zr(\eta\text{-}C_5H_5)_2]$ fragment as expected, since both ^1H and $^{13}C\{^1H\}$ NMR data show that the molecule does not possess a molecular mirror plane. The attached $\eta\text{-}C_5H_4$ moiety of the functionalised cyclopentadienyl is observed as an ABCD spin system. Four resonances each integrating to one proton are seen for the C_5H_4 fragment in the ^1H NMR spectrum (figure 3.6), and five carbon resonances, including the *ipso* carbon, in the $^{13}C\{^1H\}$ NMR spectrum (figure 3.7). The NCH_3 group is also attached intramolecularly forming a metal amide, with a singlet at 2.85ppm and 48.6ppm in the ^1H and $^{13}C\{^1H\}$ NMR respectively. In the ^1H NMR spectrum all of the hydrogens in the trimethylene backbone are inequivalent, with six sets of multiplets each integrating to one proton.

Most significantly a singlet integrating to only five protons in the ^1H NMR spectrum indicates that only <u>one</u> ($C_5H_5^-$) ligand per $[\eta^5\text{:}\eta^1\text{-}C_5H_4(CH_2)_3NMe]$ ligand is present in the complex. The complicated spectra led to further NMR studies being carried out, with a combination of HETCOR (figure 3.8), and COSY (figure 3.9), leading to all resonances being consistently assigned. Mass spectrometry and microanalytical data all identified $[Zr(\eta^5\text{:}\eta^1\text{-}C_5H_4(CH_2)_3NMe)(\eta^5\text{-}C_5H_5)Cl]$, **3.1**, as the isolated volatile product, forming in 42% yield (figure 3.10).

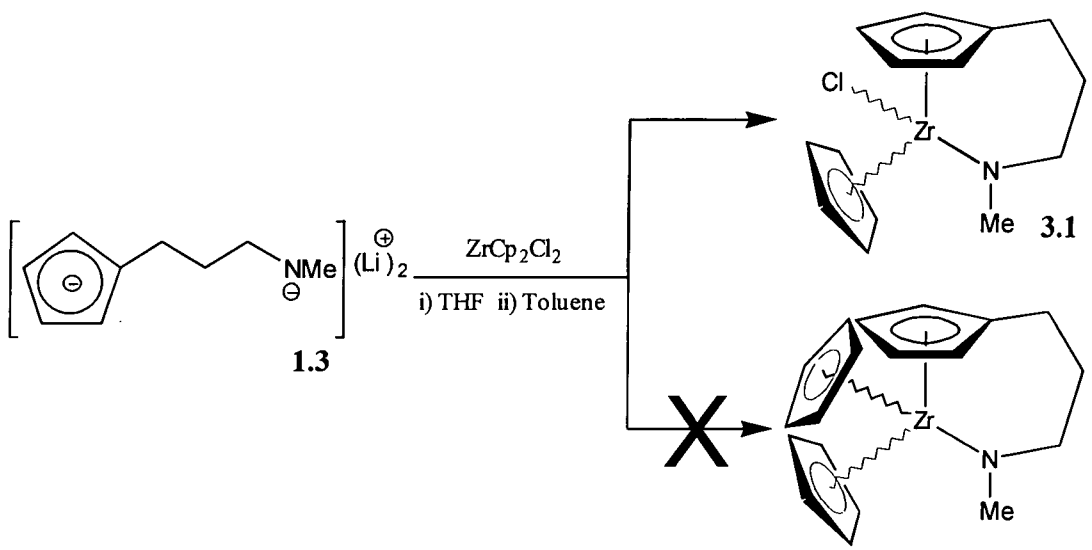

Figure 3.10

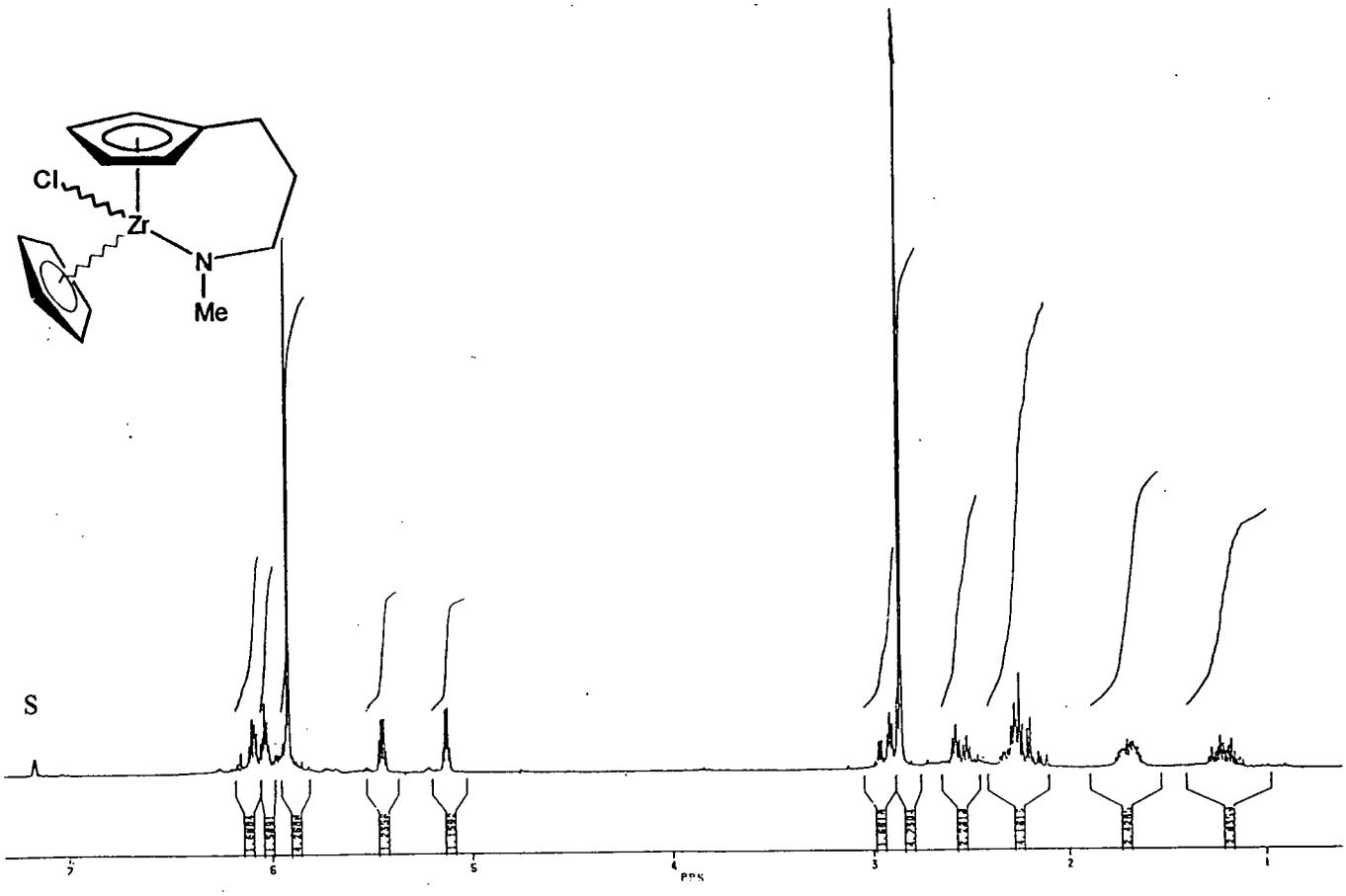

Figure 3.6 ^{1}H NMR spectrum of **3.1** in C_6D_6 at 250MHz

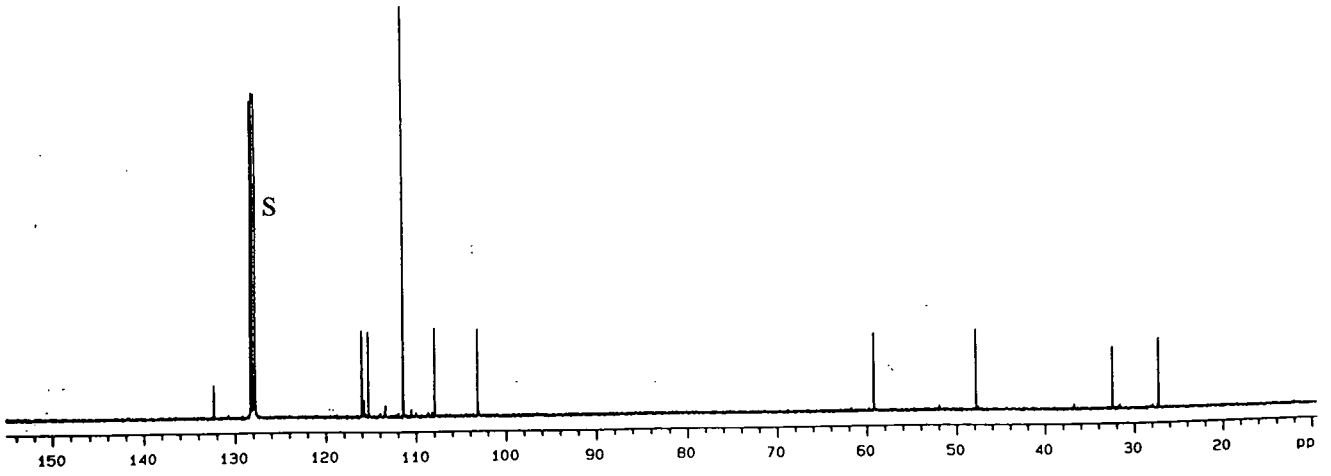

Figure 3.7 $^{13}C\{^{1}H\}$ NMR spectrum of **3.1** in C_6D_6 at 100MHz

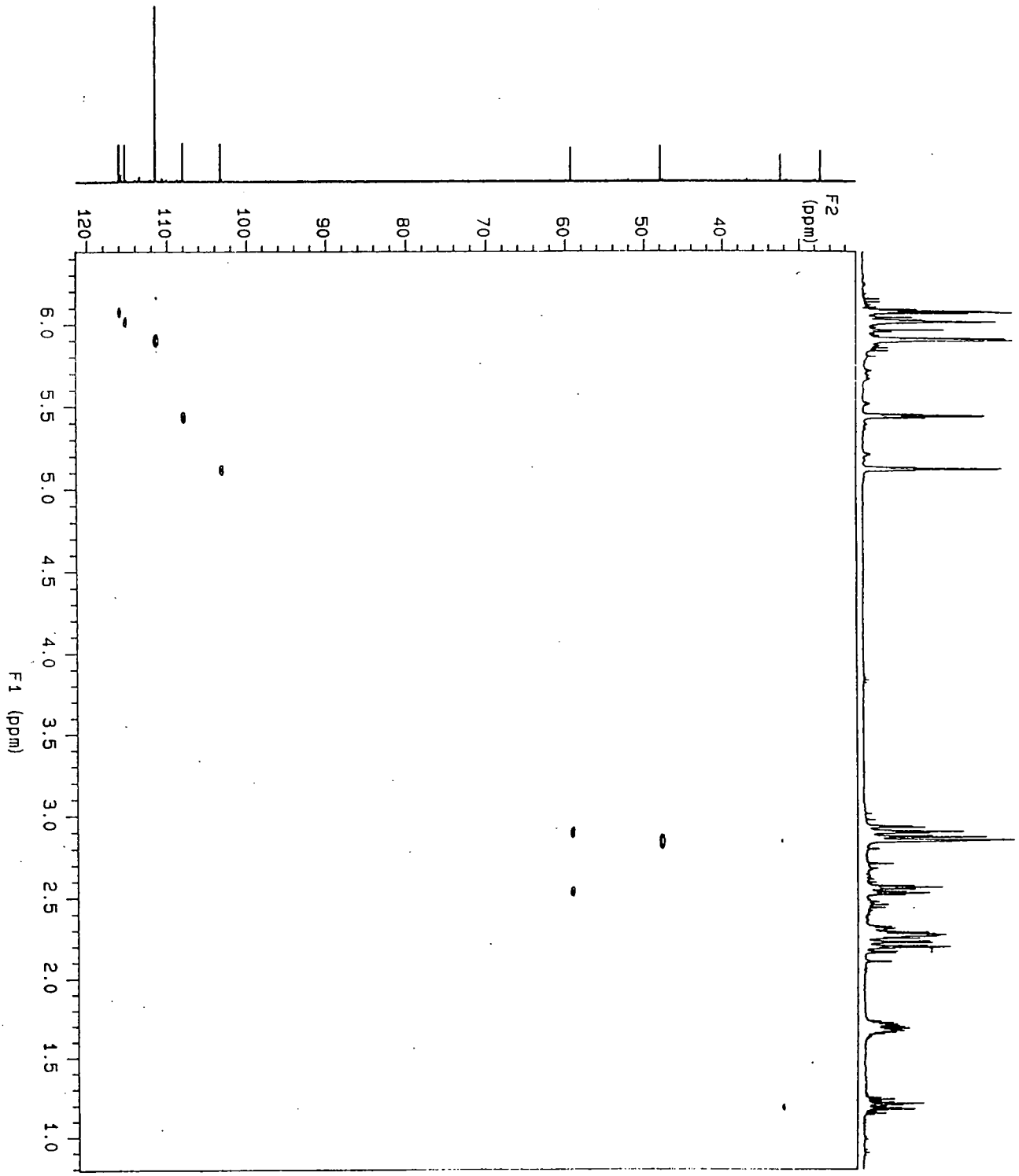

Figure 3.8 ^{1}H-^{13}C HETCOR of **3.1** in C_6D_6 at 400 and 100MHz

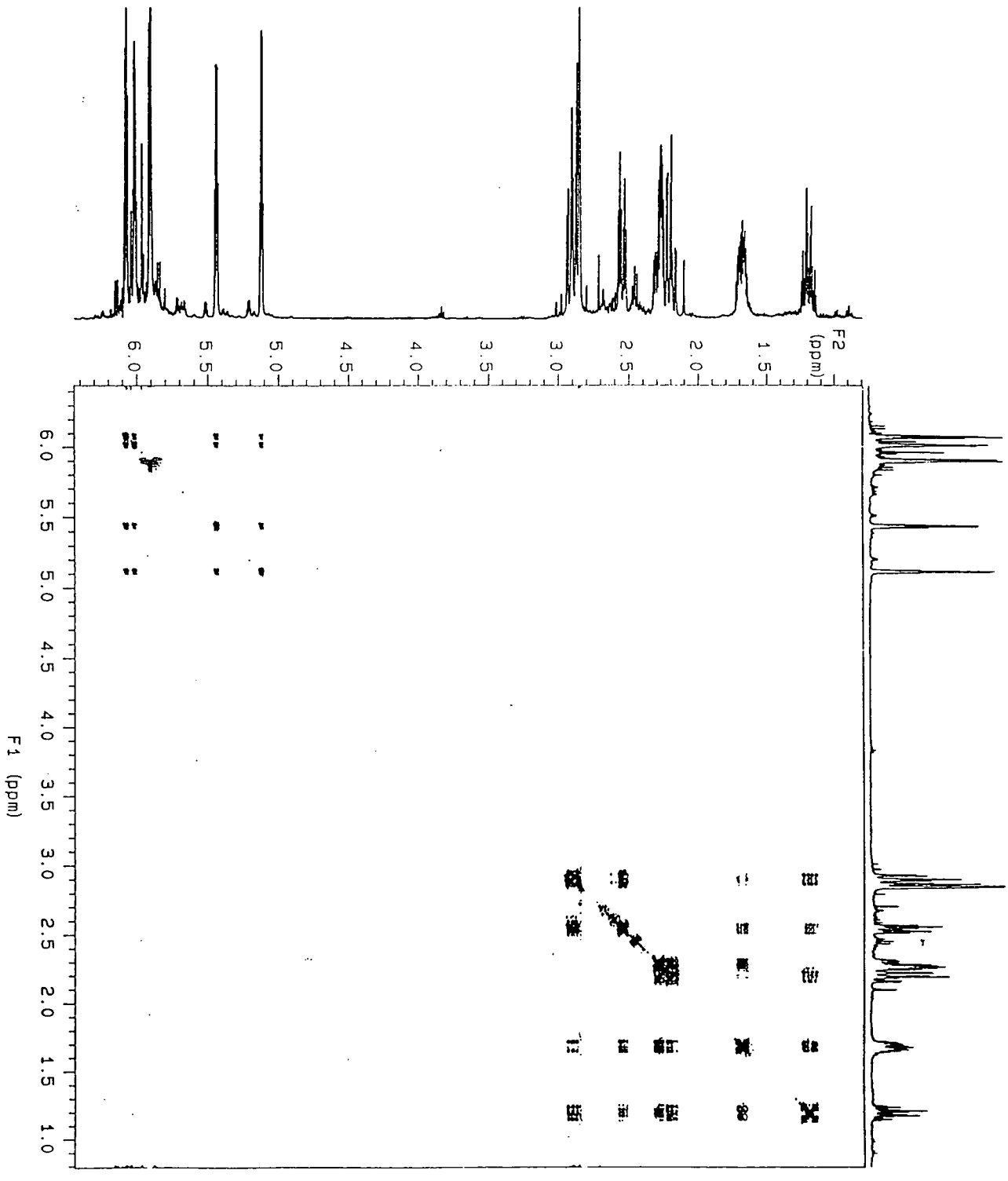

Figure 3.9 ^{1}H COSY of **3.1** in C_6D_6 at 400MHz

Figure 3.10 shows that the expected tris cyclopentadienyl zirconium complex is not made. Instead, there is a preference for one cyclopentadienide anion ($C_5H_5^-$) and one chloride anion (Cl^-) to act as leaving groups, rather than two chorides. This is in contrast to the synthesis of $Mo[\eta^5:\eta^1\text{-}C_5H_4(CH_2)_3NMe](N^tBu)_2$, **2.3**, where the choice between chloride ions or t-butyl imido dianions as leaving groups, leads to the loss of two chloride ions.

3.2.3 Cyclopentadienide ($C_5H_5^-$) as a leaving group

The cyclopentadienyl group is perhaps one of the most ubiquitous ligands in organometallic chemistry because of its ability to bind strongly to metals, stabilise high oxidation states, and because it is generally inert to both electrophiles and nucleophiles. For these reasons it is often regarded as a spectator ligand.

Despite these factors, in the reaction between zirconocene dichloride and the dianion, **1.3**, there is an opportunity for the stable cyclopentadienide anion ($C_5H_5^-$) to act as a leaving group, presumably with the formation of lithium cyclopentadienide. The loss of this ligand is favoured by electronic and steric factors. The loss of a cyclopentadienide removes four more electrons from the complex than a chloride anion producing a complex with a formal electron count of 18, rather than 22. It was thought that the reaction would have formed a product where one or more of the cyclopentadienyl fragments were not η^5-bonded to the metal (i.e., η^1 or η^3 bonded) which would also give a less electronically saturated complex. However, due to steric effects there is a preference for two rather than three cyclopentadienyl ligands.

In the synthesis of **3.1**, the reaction step in which the ($C_5H_5^-$) group is displaced by either the amide or cyclopentadienide part of the dianion, **1.3**, is probably favoured by the chelate effect. The formation of **3.1** allows an equilibrium to be set up in THF, where the displaced ($C_5H_5^-$) group can either replace the remaining cyclopentadienyl group, yielding the same product, **3.1**, or displace the functionalised cyclopentadienyl group, yielding a pendant cyclopentadienide (figure 3.11).

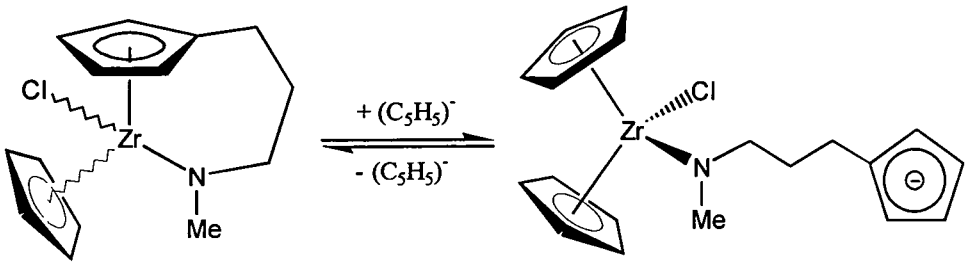

Figure 3.11

The pendant cyclopentadienide can then reattach itself displacing $(C_5H_5)^-$ and producing **3.1**. Upon work-up, extraction of the product with toluene will precipitate the $(C_5H_5)^-$, thereby breaking the equilibrium and producing **3.1** in solution. The chelate effect is thought to be one of reasons for the increased stability of *ansa* metallocenes over bis cyclopentadienyl systems.

In a recent patent by the Dow Chemical Company, displacement of a cyclopentadienide group from bis cyclopentadienyl titanium complexes was also found.[6] The reaction between the dianion $[(C_5Me_4)SiMe_2N^tBu]^{2-}$ and Cp_2TiCl_2, $Cp_2Ti(OMe)_2$, or $Cp_2TiCl(OEt)$, gives functionalised cyclopentadienyl titanium complexes where one cyclopentadienide fragment is eliminated (figure 3.12).

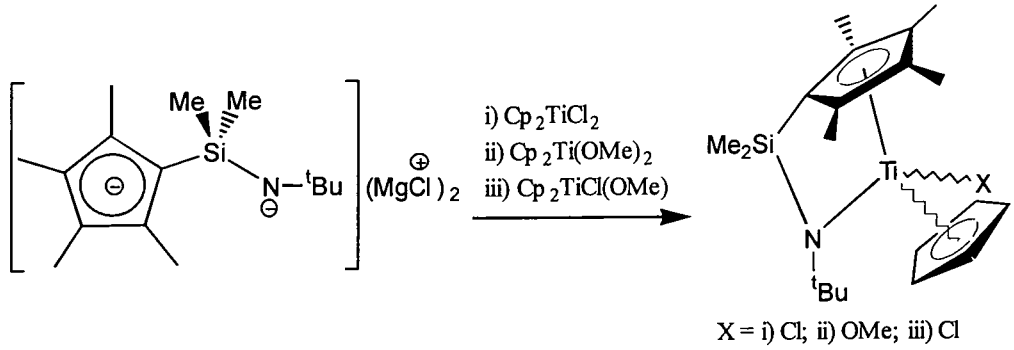

X = i) Cl; ii) OMe; iii) Cl

Figure 3.12

Green and co-workers have also observed cyclopentadienyl elimination occurring in the ring exchange of bis-cyclopentadienyl compounds.[7] Competition for metal acceptor orbitals by the imido ligand in the complexes $[Mo(\eta\text{-}C_5H_4R)_2(NR')]$ causes weakening of the metal-ring binding. This allows for the ring exchange reactions which are indicative of the inherent substitution lability of the η-cyclopentadienyl rings in the system (figure 3.13).

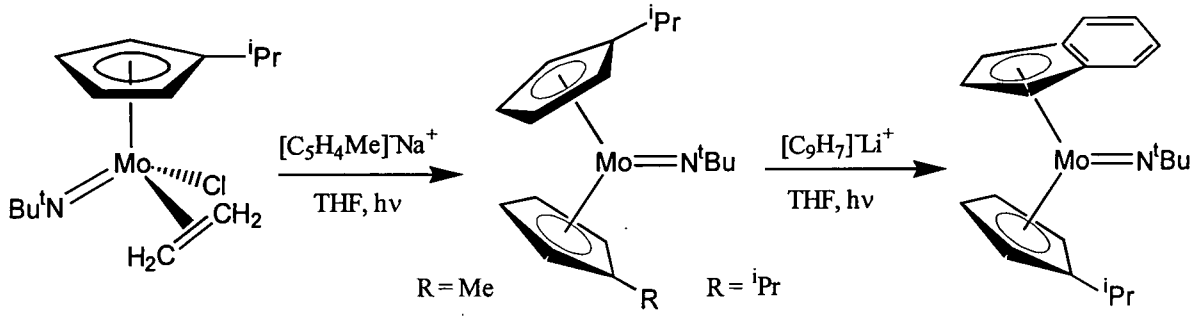

Figure 3.13

3.2.4 Reaction of $[Zr(\eta^5:\eta^1\text{-}C_5H_4(CH_2)_3NMe)(\eta^5\text{-}C_5H_5)Cl]$, 3.1, and $C_6H_5CH_2MgCl$

The cyclopentadienyl ($C_5H_5^-$) group in the zirconium complex **3.1** is expected to be reasonably labile, and therefore reactive. Reactions described in the patent by Dow chemicals have shown that a similar titanium complex reacts with two equivalents of an alkyl lithium salt to form the corresponding bis alkyl titanium complexes (figure 3.14).[6]

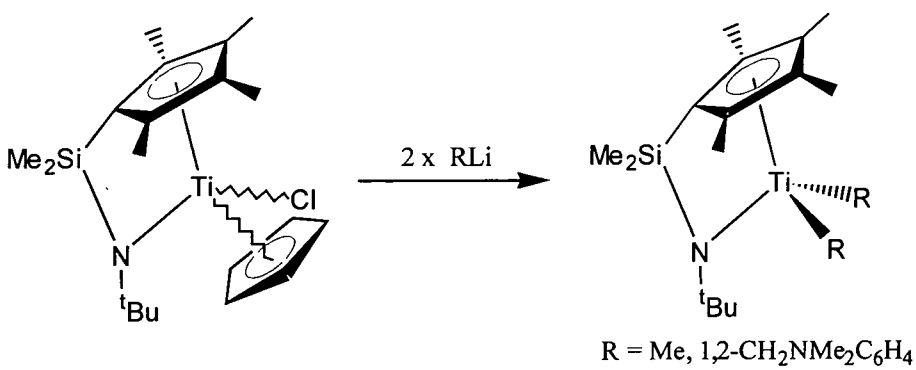

Figure 3.14

By reacting the **3.1** with two equivalents of an alkyl magnesium or lithium salt, the bis alkyl complexes $Zr[\eta^5:\eta^1\text{-}C_5H_4(CH_2)_3NMe]R_2$ (R = Me, $C_6H_5CH_2$ etc) may be synthesised. However the complexes $Zr[\eta^5:\eta^1\text{-}C_5H_4(CH_2)_3NMe]R_2$ (R = Me, $C_6H_5CH_2$ and CH_2SiMe_3), have previously been synthesised from similar reactions with $Zr[\eta^5:\eta^1\text{-}C_5H_4(CH_2)_3NMe]Cl_2(NHMe_2)$ and are described in Chapter 1 (section 1.4.5).[8]

Therefore by reacting **3.1** with only one equivalent of an alkyl Grignard or lithium salt it was thought possible to selectively react the metal chloride, leaving the cyclopentadienyl (C_5H_5) group intact. One equivalent of benzyl magnesium chloride was added to a solution of **3.1** in diethyl ether, and the reaction mixture stirred overnight, forming a yellow solution. The product was extracted into pentane, which on cooling gave crude $Zr[\eta^5:\eta^1\text{-}C_5H_4(CH_2)_3NMe](\eta^5\text{-}C_5H_5)(CH_2C_6H_5)$, **3.2**, as a pale yellow precipitate (figure 3.15).

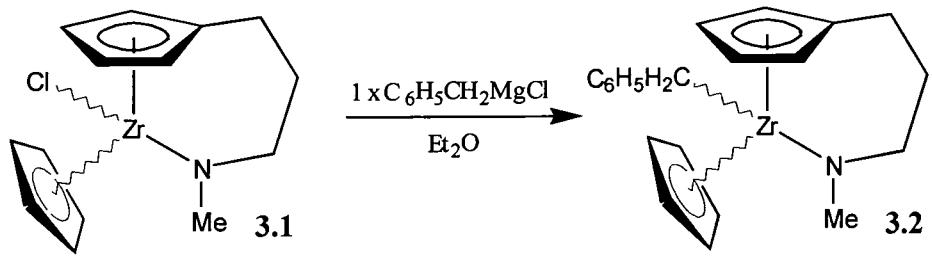

Figure 3.15

The ^1H NMR spectrum shows the presence of a benzyl group with resonances in the phenyl region of the spectrum and a singlet, due to accidental overlap, for the CH_2 group appearing at 2.27ppm. Due to the electronic and steric effects, the CH_2 group is probably η^1 bonded to the metal centre. A singlet at 6.18ppm is still observed for the C_5H_5 group, indicating the preference for chloride rather than cyclopentadienyl displacement. Resonances for the functionalised cyclopentadienyl group show evidence for the proposed molecular symmetry, with the C_5H_4 group seen as an ABCD spin system, and a series of six multiplets for the trimethylene backbone. The NMe group is observed as a singlet at 2.70ppm. Mass spectroscopy is consistent with the proposed formula **3.2**, with a mass of m/z = 381 being that of the cation $[\mathbf{3.2}]^+$.

The ^1H NMR spectrum also shows that a small amount of the previously reported disubstituted complex, $Zr[\eta^5:\eta^1\text{-}C_5H_4(CH_2)_3NMe](CH_2C_6H_5)_2$, was also produced.[8] Attempts to purify **3.2** by sublimation caused decomposition of the complex, presumably due to the reactive metal-alkyl bond which often makes such complexes light and thermally unstable.

3.2.5 Reaction between $Ti(C_5H_5)_2Cl_2$ and $[C_5H_4(CH_2)_3NMe]Li_2$, 1.3

In a reaction analogous to the formation of the zirconium complex, **3.1**, titanocene dichloride was reacted with one equivalent of the dianion, **1.3**, in THF for 1 day. Extraction of the product with toluene gave a dark red oil/solid, but unlike **3.1** purification by sublimation was not possible. Due to the ease with which Ti(IV) species are reduced [especially to Ti(III)], compared to Zr(IV), the product decomposes to an insoluble tar above 70°C. Purification of the titanium complex was possible using recrystallisation from toluene, forming $Ti[\eta^5:\eta^1\text{-}C_5H_4(CH_2)_3NMe](\eta^5\text{-}C_5H_5)Cl$, **3.3**, in 59% yield, as a dark red crystalline solid. (figure 3.16).

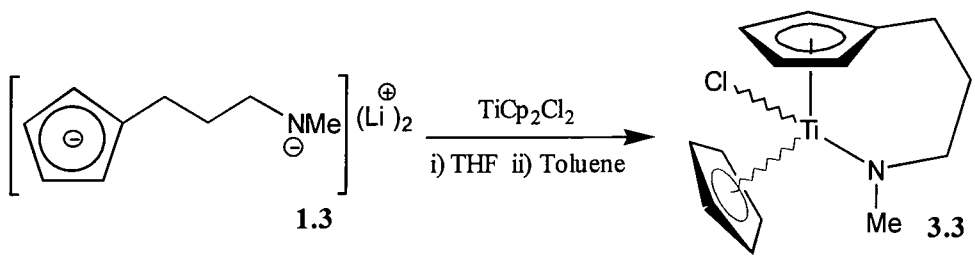

Figure 3.16

The $^{13}C\{^1H\}$ NMR spectrum of **3.3** (figure 3.17), has a very similar appearance to that of the zirconium analogue, **3.1**. Five resonances are observed for the attached functionalised cyclopentadienyl fragment, and one resonance appears at 114.2ppm, for the C_5H_5 group. Again the trimethylene backbone and attached amide appear as singlets in approximately the same region of the spectrum as **3.1**.

Due to the presence of some Ti(III) reduction product, that was found difficult to eliminate, the ^1H NMR spectrum of **3.3** is broad (figure 3.18). The presence of this reduction product could be due to **3.3** being unstable thermally, or to reduction, or contamination from the synthesis. Despite being broad, the ^1H NMR spectrum shows a similar spectrum to that of **3.1**, with four resonances for the functionalised cyclopentadienyl fragment and a singlet integrating to five protons, at 5.81ppm, for the C_5H_5 group. The attached amide is seen as a singlet at 3.28ppm with six broad resonances being observed for the trimethylene backbone.

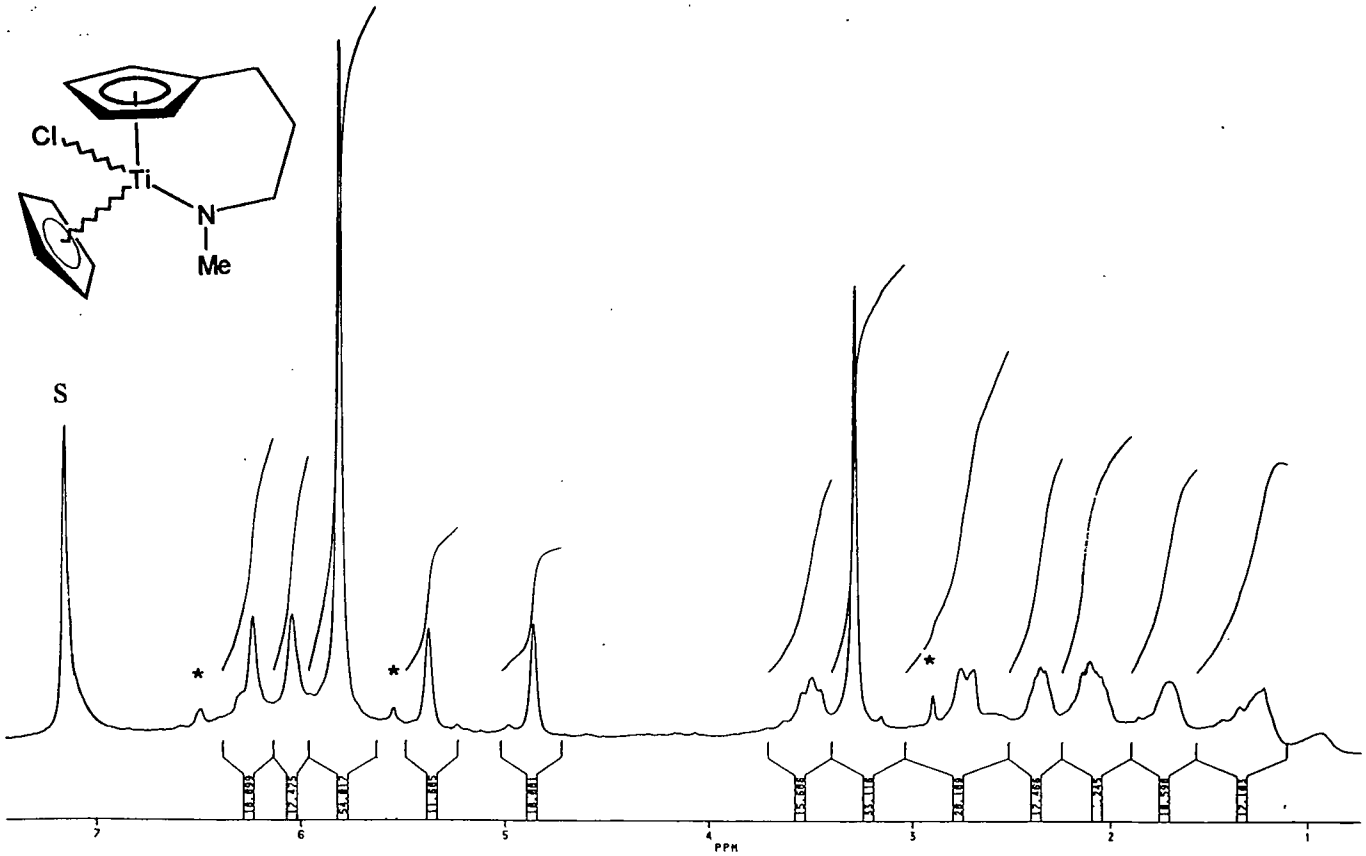

Figure 3.18 ^{1}H NMR spectrum of **3.3** in C_6D_6 at 250MHz

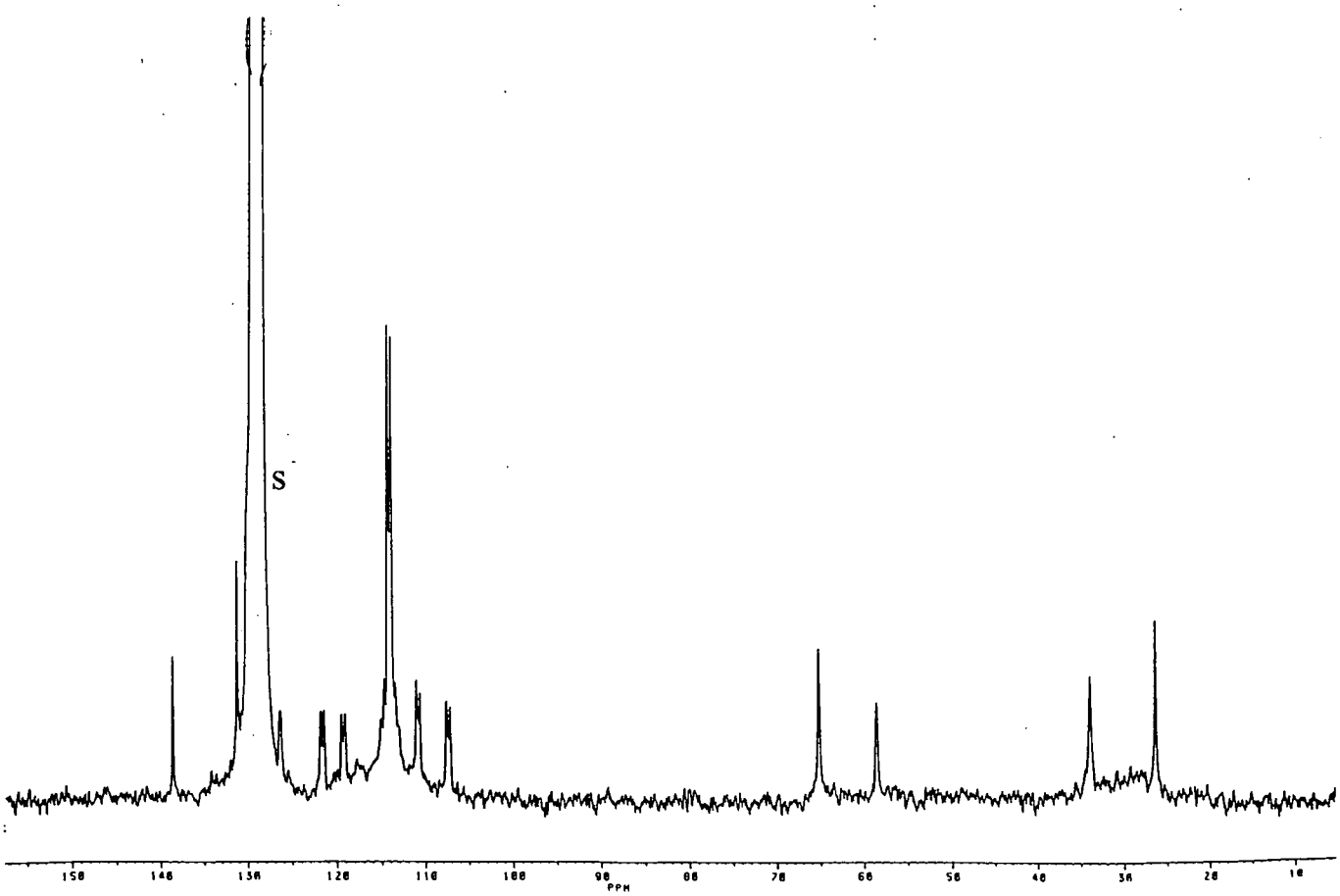

Figure 3.17 $^{13}C\{^{1}H\}$ NMR spectrum of **3.3** in C_6D_6 at 62.5MHz

3.2.6 Molecular structure of $Ti[\eta^5:\eta^1\text{-}C_5H_4(CH_2)_3N(H)Me](C_5H_5)Cl$, 3.4

Attempts to grow crystals of the dark red Ti(IV) complex $Ti[\eta^5:\eta^1\text{-}C_5H_4(CH_2)_3NMe](C_5H_5)Cl$, **3.3**, from toluene, suitable for X-ray crystallographic studies proved unsuccessful. However, pale green plate-like crystals formed over a period of a month from a dark red deutero-benzene NMR sample of **3.3** left standing at room temperature. A crystal of dimensions 0.25 x 0.2 x 0.1mm was sealed in a Lindemann capillary tube under an inert atmosphere. The molecular structure was determined by Mr A. McKinnon and Prof J.A.K. Howard within the department, and is shown in figure 3.19, with the full data shown in the Appendices.

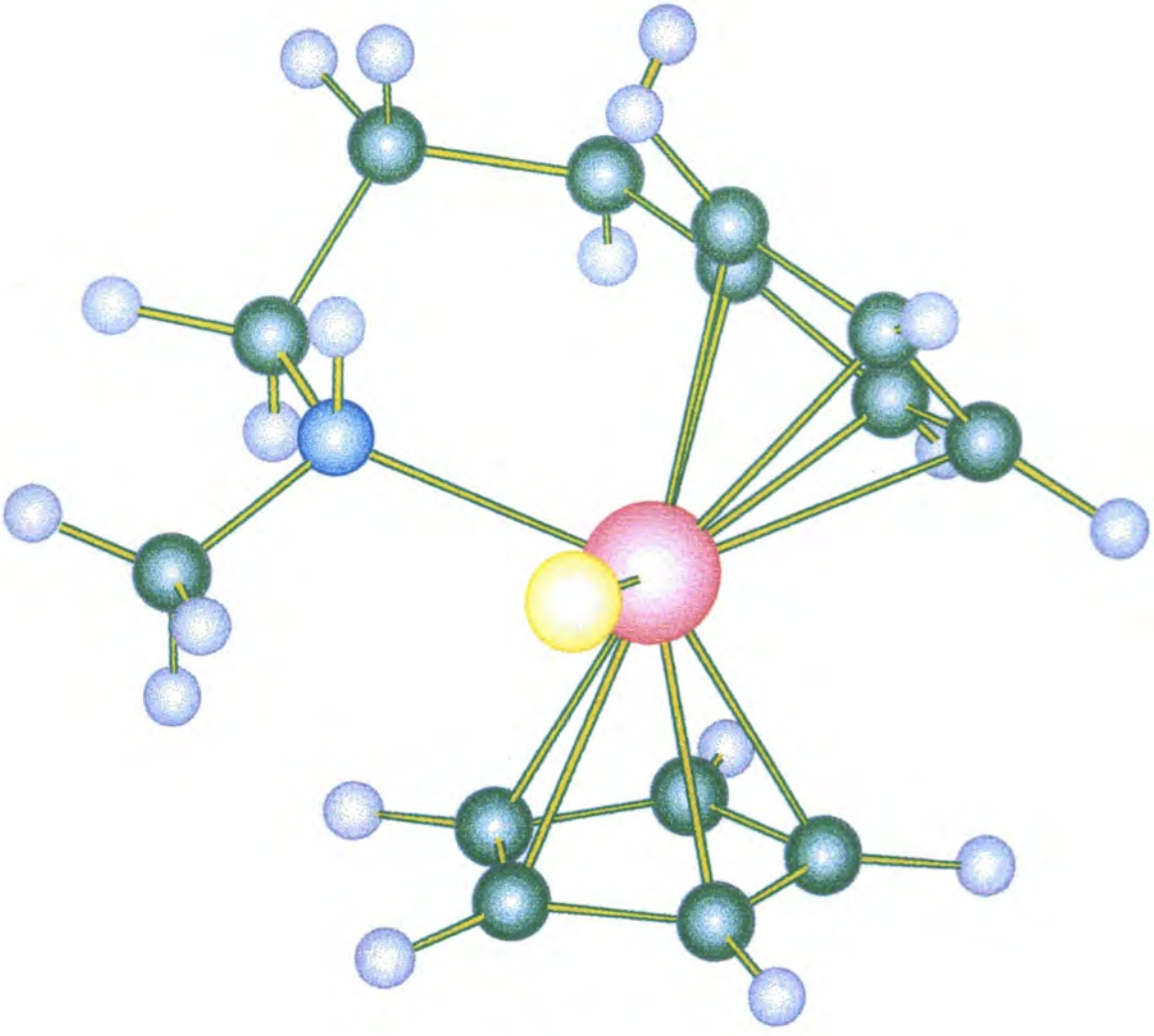

Figure 3.19

The structure shows the titanium(III) complex, $Ti[\eta^5:\eta^1\text{-}C_5H_4(CH_2)_3N(H)Me](C_5H_5)Cl$, **3.4**, with the nitrogen functioning as an L rather than LX, as can be seen from the Ti-N bond distance. For a titanium amide a Ti-N distance of approximately 1.93Å is expected whereas complex **3.4** shows a longer Ti-N bond of 2.312(4)Å, corresponding to that of a coordinated amine. The titanium chloride bond is also slightly longer, compared to other bis cyclopentadienyl titanium chloride complexes, which vary between 2.312(2)Å for $(C_5HPh_4)_2TiCl$,[9] and 2.364(3)Å for $(C_5H_5)_2TiCl$.[10] A longer Ti-Cl distance of 2.5064(14)Å in **3.4** is presumably caused by competition from the coordinated amine to donate electrons to the metal centre. The complex has a pseudo tetrahedral structure with a small N-Ti-Cl angle of 82.50(11) ° and a Cp-Ti-N bite angle 81.8(2)°, caused by the steric bulk surrounding the small metal centre.

Compared to bis cyclopentadienyl titanium(IV) complexes there are relatively few titanium(III) analogues. However many such complexes have been synthesised from the reaction of Cp_2TiCl_2 with ligands in the presence of a reducing agent. For example the reaction of Cp_2TiCl_2 and magnesium or magnesium chloride in THF gives light green crystals of the dimer $[Cp_2Ti(\mu\text{-}Cl)_2]_2Mg(THF)_2$.[11] Similarly the reaction of Cp_2TiCl_2 with magnesium in the presence of RPh_2 (R = Ph or c-C_6H_{11}) gives aquamarine crystals of $[Cp_2Ti(\mu\text{-}Cl)_2Mg(THF)_2(\mu\text{-}Cl)]_2$. Both complexes react with PMe_3 to give $[TiCp_2Cl(PMe_3)]$.[10] Furthermore, the reaction of Cp_2TiCl_2 with butyllithium in the presence of tertiary allylamines gives titanium(III) azametallacycles, **A** (figure 3.20), most notably via $TiHCp_2$ as an intermediate.[12] Allyl(butyl)ethylenediamine gives green crystals of the corresponding dinuclear complex, **B** (figure 3.20).[12]

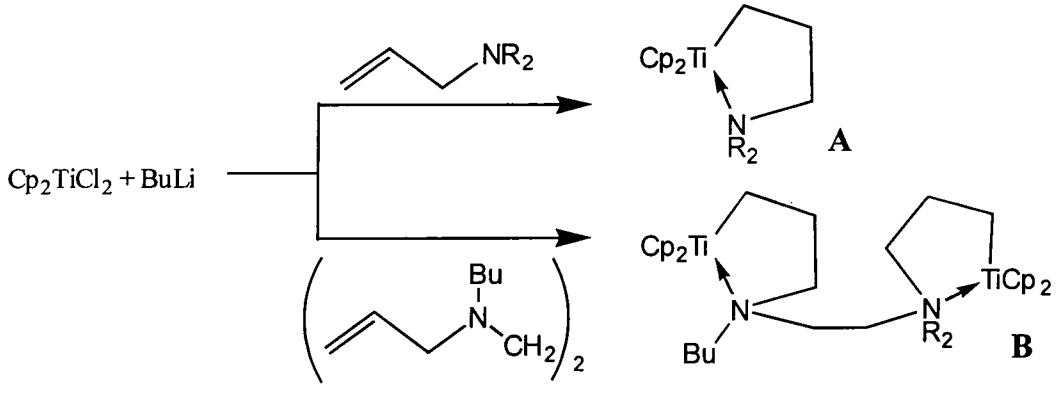

Figure 3.20

From the reactions shown in figure 3.20, it seems highly probable that some excess unreacted butyl lithium from the formation of the dilithiated ligand, **1.3**, is present during the preparation of **3.3**, and acting as a reducing agent. There is also the possibility the ligand, **1.1**, has not reacted fully, leaving the mono anion $[C_5H_4(CH_2)_3N(H)Me]Li$, **1.2**, and the unreacted butyllithium to react with one of the chlorides in Cp_2TiCl_2 forming lithium chloride. The lithium cyclopentadienide formed during the reaction could potentially act as a reducing agent. Either way this would allow for the formation of the titanium(III) amine complex.

3.2.7 Catalytic Applications

Previous reactions carried out with the titanium complex, $Ti[\eta^5:\eta^1\text{-}C_5Me_4(CH_2)_3NMe](\eta^5\text{-}C_5H_5)Cl$, and the reaction carried out with the zirconium complex, **3.1**, show that the zirconium and titanium complexes, **3.1** and **3.3**, are capable of reacting at both the cyclopentadienyl and chloride sites. This suggests they have the potential to fulfil the criteria needed to synthesise potential catalyst precursors, especially for olefin polymerisation.

In Chapter 1 the active Group 4 species for Ziegler Natta polymerisation was discussed as being the cation $[M(C_5H_5)_2R]^+$. The ability of complexes **3.1** and **3.3** to react with alkyl magnesium or lithium salts to form complexes of the type $M[\eta^5:\eta^1\text{-}C_5H_4(CH_2)_3NMe]R_2$ or $M[\eta^5:\eta^1\text{-}C_5H_4(CH_2)_3NMe](\eta^5\text{-}C_5H_5)R$ (M = Zr, Ti, R = Me, $SiMe_3$ or $CH_2C_6H_5$) suggests that the cation $[M(CpNMe)R]^+$ could be synthesised readily, and its catalytic ability examined.

3.3 Summary and Further Work

This study has underlined the fact that the relationship that links two seemingly unrelated fragments, $[M(C_5H_5)_2]$ and $[M'(NR)_2]$, is essentially a structural analogy and cannot be used to predict reaction pathways. Unlike the Group 6 complexes $M[\eta^5:\eta^1\text{-}C_5H_4(CH_2)_3NMe](N^tBu)_2$ (M = W or Mo) described in Chapter 2, the isolobal and isoelectronic Group 4 complexes $M[\eta^5:\eta^1\text{-}C_5H_4(CH_2)_3NMe](C_5H_5)_2$ (M = Zr or Ti) could not be synthesised.

Electronic, kinetic and steric influences prevent the formation of the desired compound and a reaction occurs where one of the cyclopentadienide ($C_5H_5^-$) groups is displaced, producing $M[\eta^5:\eta^1\text{-}C_5H_4(CH_2)_3NMe](\eta^5\text{-}C_5H_5)Cl$ (M = Zr, **3.1**; Ti, **3.3**). Studies on the zirconium analogue and previous work have shown that such complexes have potential as starting materials for the production of catalytic precursors for olefin polymerisation.

Much further work with the complexes **3.1** and **3.3** would be advantageous in the area of catalysts. Reactions with one or two equivalents of a variety of alkyl magnesium or lithium salts can be carried out, as well as further reactions (e.g. $NaBH_4$). Such complexes could then be tested for activity as olefin polymerisation caytalysts.

3.4 Experimental

3.4.1 Attempted reaction of $Zr(C_5H_5)_2(NMe_2)_2$ with $C_5H_5(CH_2)_3N(H)Me$, 1.1

Preparation of $Zr(C_5H_5)_2(NMe_2)_2$[13]

A solution of $Zr(C_5H_5)_2Cl_2$ (10.0g, 34mmol) in toluene (75ml) was added to a suspension of $LiNMe_2$ (78mmol, synthesis described in Chapter 4, section 4.5.1) in hexane (150ml) at 0°C. The mixture was stirred for 2hr, then refluxed for 6hr. The solution was filtered and the solvent removed under reduced pressure leaving a light brown oil. Sublimation (100°C, 10^{-3}mmHg) yielded yellow crystals of $Zr(C_5H_5)_2(NMe_2)_2$ (4.6g, 15mmol, 44% yield).

$Zr(C_5H_5)_2(NMe_2)_2$ and $C_5H_5(CH_2)_3N(H)Me$, **1.1**

A solution of $C_5H_5(CH_2)_3N(H)Me$, **1.1**, (0.27g, 2mmol) in toluene (5ml) was added to a solution of $Zr(C_5H_5)_2(NMe_2)_2$ (0.61g, 2mmol) in toluene (15ml), in an ampoule. The mixture was refluxed under partial vacuum for 48hr after which time an aliquot was taken, analysis of which showed that no reaction had occurred. Reflux for a further 10 days with the periodic removal of any volatiles during this time (i.e., dimethylamine) also gave no reaction.

3.4.2 Preparation of $Zr[\eta^5:\eta^1\text{-}C_5H_4(CH_2)_3NMe](\eta^5\text{-}C_5H_5)Cl$, 3.1

A solution of $Zr(C_5H_5)_2Cl_2$ (1.75g, 6.0mmol) in THF (30ml) was cooled to -78°C (acetone/dry ice). A suspension of $[C_5H_4(CH_2)_3NMe]Li_2$, **1.3**, (0.89g, 6.0mmol) in THF (30ml) at -78°C was added dropwise with vigorous stirring. The mixture was warmed to room temperature over 2 hr and stirred for 24 hr, forming a dark orange solution. The solvent was removed under reduced pressure, and the product extracted with toluene (2 x 20ml), then filtered. Removal of the solvent under reduced pressure gave a mixture of products. Distillation onto a sublimation probe at -196°C (100-120°C, 10^{-3}mmHg) gave analytically pure $[Zr(\eta^5:\eta^1\text{-}C_5H_4(CH_2)_3NMe](\eta^5\text{-}C_5H_5)Cl$, **3.1**, (0.82g, 2.5mmol, 42% yield) as a bright orange oil.

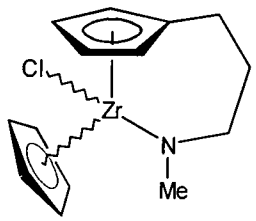

Data characterising 3.1

Description: Viscous orange oil. Sublimes 100-120°C, 10^{-3}mmHg

EI mass spec: m/z = 326 $[\mathbf{3.1}]^+$ with correct isotope distribution

Infra-red: 3086 (aromatic C-H stretch); 2924-2705 (aliphatic CH's); 1025, 998, 804 (ring C-H bends)

Elemental analysis: Found ($C_{14}H_{18}NClZr$ requires) C:51.6(51.4); H:5.8(5.5); N:4.1(4.3)

^{1}H NMR: δ/ppm, 250 MHz, C_6D_6		**^{13}C NMR: δ/ppm, 62.5 MHz, C_6D_6**
6.08	[q, 1H, $^3J_{HH}$=2.8Hz, (C_5H_4)]	120.3 (C_5H_4 *ipso*)
6.02	[q, 1H, $^3J_{HH}$=2.7Hz, (C_5H_4)]	116.7 (C_5H_4)
5.92	[s, 5H, (C_5H_5)]	116.0 (C_5H_4)
5.44	[q, 1H, $^3J_{HH}$=2.9Hz, (C_5H_4)]	112.1 (C_5H_5)
5.12	[q, 1H, $^3J_{HH}$=2.5Hz, (C_5H_4)]	108.7 (C_5H_4)
2.91	[m, 1H, (NCH$\underline{H}$)]	103.9 (C_5H_4)
2.85	[s, 3H, (NCH_3)]	60.0 (NCH_2)
2.56	[m, 1H, (NC$\underline{H}$H)]	48.6 (NCH_3)
2.21	[m, 2H, ($C_5H_4C\underline{H}_2$)]	33.1 ($C_5H_4\underline{C}H_2$)
1.66	[m, 1H, ($CH_2C\underline{H}HCH_2$)]	28.0 ($CH_2\underline{C}H_2CH_2$)
1.20	[m, 1H, ($CH_2CH\underline{H}CH_2$)]	

3.4.3 Preparation of $Zr[\eta^5:\eta^1\text{-}C_5H_4(CH_2)_3NMe](\eta^5\text{-}C_5H_5)(\eta^1\text{-}CH_2C_6H_5)$, 3.2

A solution of **3.1** (0.20g, 0.62mmol) in Et_2O (20ml) was cooled to -78°C. Benzyl magnesium chloride (0.7ml of a 0.97M solution in THF, 0.68mmol, 1.1 x theory) was added dropwise over a period of 10 mins. The mixture was warmed to room temperature over 2hr and stirred for 24hr. The solvent was removed under reduced pressure and the product extracted into pentane (2 x 15ml), filtered and cooled to -40°C. A pale yellow powder precipitated; this was filtered, dried under reduced pressure and was found to be crude $Zr[\eta^5:\eta^1\text{-}C_5H_4(CH_2)_3NMe](\eta^5\text{-}C_5H_5)(\eta^1\text{-}CH_2C_6H_5)$, **3.2**, (0.17g, 0.45mmol, 72% yield based on **3.1**) (containing a small amount of the disubstituted complex $Zr[\eta^5:\eta^1\text{-}C_5H_4(CH_2)_3NMe](CH_2C_6H_5)_2$.

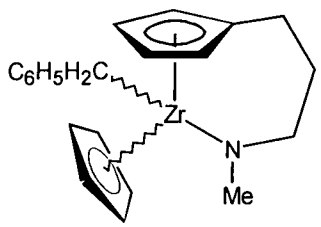

Data characterising 3.2

Description: Pale yellow powder

EI mass spec: m/z = 382 $[\mathbf{3.2}]^+$ with correct isotope distribution

^{1}H NMR: δ/ppm, 250 MHz, C_6D_6

ca.7.1 [m, 5H, (C_6H_5)]
6.33 [q, 1H, $^3J_{HH}$=2.6Hz, (C_5H_4)]
6.25 [q, 1H, $^3J_{HH}$=2.4Hz, (C_5H_4)]
6.18 [s, 5H, (C_5H_5)]
6.01 [q, 1H, $^3J_{HH}$=2.6Hz, (C_5H_4)]
5.98 [q, 1H, $^3J_{HH}$=2.5Hz, (C_5H_4)]
2.70 [s, 3H, (NCH_3)]
2.57 [m, 1H, ($NC\underline{H}H$)]
2.46 [m, 1H, ($NCH\underline{H}$)]
2.27 [s, 2H, ($C\underline{H}_2C_6H_5$)]
1.72 [m, 1H, ($C_5H_4C\underline{H}H$)]
1.65 [m, 1H, ($C_5H_4CH\underline{H}$)]
1.36 [m, 1H, ($CH_2C\underline{H}HCH_2$)]
1.06 [m, 1H, ($CH_2CH\underline{H}CH_2$)]

3.4.4 Preparation of Ti[η^5:η^1-$C_5H_4(CH_2)_3NMe$](η^5-C_5H_5)Cl, 3.3

A suspension of $Ti(C_5H_5)_2Cl_2$ (1.49g, 6.0mmol) in THF (30ml) was cooled to -78°C (acetone/dry ice). A suspension of $[C_5H_4(CH_2)_3NMe]Li_2$, **1.3**, (0.89g, 6.0mmol) in THF (30ml) at -78°C was added dropwise with vigorous stirring. The mixture was warmed to room temperature (2hr) and stirred in the absence of light for 24 hr, forming a dark red solution. The solvent was removed under reduced pressure and the product was then extracted into toluene (2 x 20ml). Some of the solvent was removed under reduced pressure (20ml) and the solution was cooled to -40°C. A dark red solid was precipitated, this was filtered off and dried under vacuum and found to be Ti[η^5:η^1-$C_5H_4(CH_2)_3NMe$](η^5-C_5H_5)Cl, **3.3**, (1.0g, 3.5mmol, 59% yield). The product was stored at -40°C in the absence of light.

Data characterising 3.3

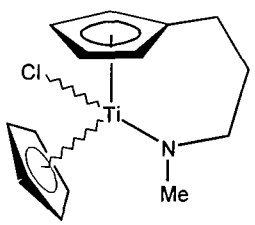

Description: Dark red solid.

EI mass spec: m/z = 284 $[\mathbf{3.3}]^+$ with correct isotope distribution

Infra-red: 3024 (aromatic C-H stretch); 2896-2745 (aliphatic CH's); 1034, 1011, 801 (ring C-H bends)

^{1}H NMR: δ/ppm, 250 MHz, C_6D_6

6.23 [br q, 1H, (C_5H_4)]
6.04 [br q, 1H, (C_5H_4)]
5.81 [br s, 5H, (C_5H_5)]
5.38 [br q, 1H, (C_5H_4)]
5.86 [br q, 1H, (C_5H_4)]
3.49 [br m, 1H, (NC<u>H</u>H)]
3.28 [br s, 3H, (NCH_3)]
2.76 [br m, 1H, (NCH<u>H</u>)]
2.34 [br m, 1H, (C_5H_4C<u>H</u>H)]
2.11 [br m, 1H, (C_5H_4CH<u>H</u>)]
1.71 [br m, 1H, (CH_2C<u>H</u>HCH_2)]
1.22 [br m, 1H, (CH_2CH<u>H</u>CH_2)]

^{13}C NMR: δ/ppm, 62.5 MHz, C_6D_6

138.6 (C_5H_4 *ipso*)
121.6 (C_5H_4)
119.2 (C_5H_4)
114.2 (C_5H_5)
110.7 (C_5H_4)
107.3 (C_5H_4)
65.2 (NCH_2)
58.6 (NCH_3)
34.0 (C_5H_4<u>C</u>H_2)
26.4 (CH_2<u>C</u>H_2CH_2)

3.5 References

1 a) P.J. Shapiro, W.D. Cotter, W.P. Schaefer, J.A. Labinger and J.E. Bercaw, *J. Am. Chem. Soc.*, 1994, **116**, 4623; b) Y. Mu, W.E.Piers, M.A. Macdonald and M.J. Zaworotko, *Can. J. Chem., 1995*, **73**, 2233; c) Y.Laing, G.P.A. Yap, A.L. Rheingold and K.H. Theopold, d) *Organometallics*, 1996, **15**, 5284; J.Okuda, T. Eberle and T.P. Spaniol, *Chem Ber.*, 1997, **130**, 209.

2 a) D.S. Williams, J.T. Anhaus, M.H. Schofield, R.R. Schrock and W.M. Davis, *J. Am. Chem. Soc.*, 1991, **113**, 5480. b) D.S. Glueck, J.C. Green, R.I. Michelman, and I.N. Wright, *Organometallics,* 1992, **11**, 4221.

3 J.W. Lauher and R. Hoffmann, *J. Am. Chem. Soc.*, 1976, **98**, 1729.

4 D.N. Williams, J.P. Mitchell, A.D. Poole, U. Siemeling, W. Clegg, D.C.R. Hockless, P.A. O'Neill and V.C. Gibson, *J. Chem. Soc. Dalton Trans.*, 1992, 739.

5 a) G.M. Diamond, R.F. Jordan and J.L. Peterson, *Organometallics*, 1996, **15**, 4030; b) J.N. Christopher, G.M. Diamond, R.F. Jordan and J.L. Peterson, *Organometallics*, 1996, **15**, 4038; c) G.M. Diamond, R.F. Jordan and J.L. Peterson, *Organometallics*, 1996, **15**, 4045.

6 D.R. Wilson, *U.S. Pat.*, 5504224, to the Dow Chemical Company.

7 M.L.H. Green, P.C. Kondaris, M. Michaelidou and P. Mountford, *J. Chem. Soc., Dalton Trans.*, 1995, 155

8 A.K. Hughes, A. Meetsma and J.H. Teuben, *Organometallics,* 1993, **12**, 1936.

9 M. Castellani, S.J. Geib, A.L. Arnold and W.C. Trogler, *Organometallics,* 1987, **6**, 2524.

10 A. Clearfield, D.K. Warner, C.H. Saldarriago, R. Ropal and I. Bernal, *Can. J. Chem.*, 1975, **97**, 6422.

11 D.W. Stephan, *Organometallics,* 1992, **11**, 996.

12 H. Lehmkuhl, Y.L. Tsien, E. Janssen and R. Mynott, *Chem. Ber.*, 1983, **116**, 2426.

13 G. Chandra and M.F. Lappert, *J. Chem. Soc. (A),* 1968, 1940.

Chapter 4

Group 5 – Niobium and Tantalum Amide Functionalised Cyclopentadienyl Complexes.

4.1 Introduction

In Chapter 1 the extensive literature available on Group 4 transition metal coordination chemistry with π-bonded *ansa* ligands, and their suitability for stereospecific α-olefin polymerisation, was discussed. By way of contrast, comparatively little is known about the chemistry of *ansa*-metallocenes of Group 5 transition metals. It was only recently that Group 5 metal systems such as vanadium alkylaluminium, $V(HBPz_3)(N^tBu)Cl_2$ /methylaluminoxane and $M(\eta^5\text{-}C_5H_5)(\eta^4\text{-diene})Me_2$/methylaluminoxane (M = Nb, Ta) were discovered to be precursors to catalysts for the polymerisation of ethylene.[1,2]

This Chapter outlines our attempts to redress this balance, by attempting to synthesise novel amide functionalised cyclopentadienyl complexes of tantalum and niobium. As an introduction to this work, previous related tantalum and niobium complexes will be discussed along with some applications to catalysis.

4.1.1 Mono-cyclopentadienyl complexes

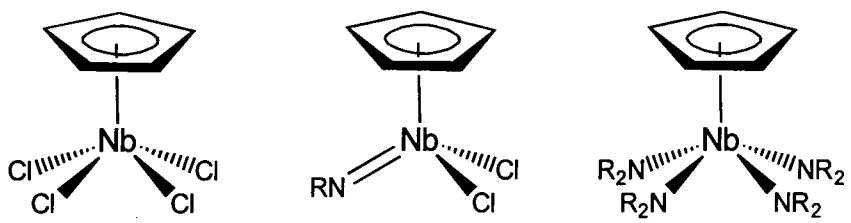

A **B** **C**

Niobium and tantalum monocyclopentadienyl compounds $CpMCl_4$, **A**, and their imido congeners $CpM(NR)Cl_2$, **B**, (M = Nb and Ta) are known,[3,4] but their amide congeners $CpM(NR_2)_{2\text{-}4}$, **C**, are rare. To the best of our knowledge only one has been reported to date. Lappert and coworkers have described the niobium complex $[Nb(C_5H_5)(NMe_2)_2]_3$, but the complex has not been fully characterised.[5]

4.1.2 Bis-cyclopentadienyl (*ansa*-) complexes

Although it has long been known that vanadocene complexes are capable of polymerising olefins,[6] there have been relatively few studies of *ansa*-bridged complexes of Group 5. An *ansa*-vanadocene complex has been reported and *ansa*-compounds of niobium with backbones of two or three bridging atoms are known.[7] Also, an *ansa*-bridged η^5:η^1-biscyclopentadienyl niobium complex containing a CMe_2 bridging group has been described.[8] Recently the first *ansa*-bridged η^5:η^5-biscyclopentadienyl complexes of niobium were reported (figure 4.1).[9]

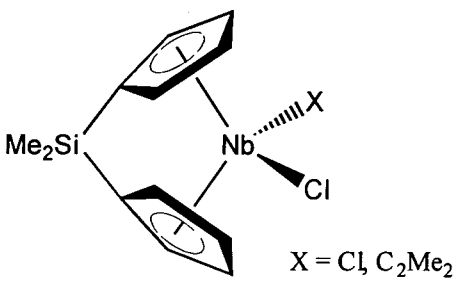

Figure 4.1

Green and co-workers have found that Group 5 *ansa*-bridged metallocenes exhibit markedly different structures and reactivities to their unbridged analogues.[10] For example, the angle subtended by the two ring centroids to niobium vectors in the *ansa*-bridged compound $Nb(\eta^5:\eta^5\text{-}C_5H_4CMe_2C_5H_4)(\eta^2\text{-}BH_4)$ is 125°, compared to 130° for the unbridged $Nb(\eta^5\text{-}C_5H_5)_2(\eta^2\text{-}BH_4)$. It was also found that $Nb(\eta^5:\eta^5\text{-}C_5H_4CMe_2C_5H_4)Cl_2$ is less conducive to ligand substitution than the non-*ansa* analogues.

4.1.3 Nitrogen functionalised cyclopentadienyl complexes

There have been only three publications on donor functionalised cyclopentadienyl complexes of Group 5, all of which describe nitrogen donors, with only one describing amide functionalised Group 5 complexes. The first such complexes were synthesised by Green and coworkers and show examples of η-cyclopentadienylimide and *ansa*-bridged η-cyclopentadienylimide niobium complexes.[11] Reaction of the ligand precursor, $(C_5H_4)TMS(CH_2)_3N(TMS)_2$, with $NbCl_5$ produced the *ansa*-complex $[Nb(\eta^5:\sigma\text{-}C_5H_4(CH_2)_3NCl_2]$, from which subsequent reactions were carried out (figure 4.2).

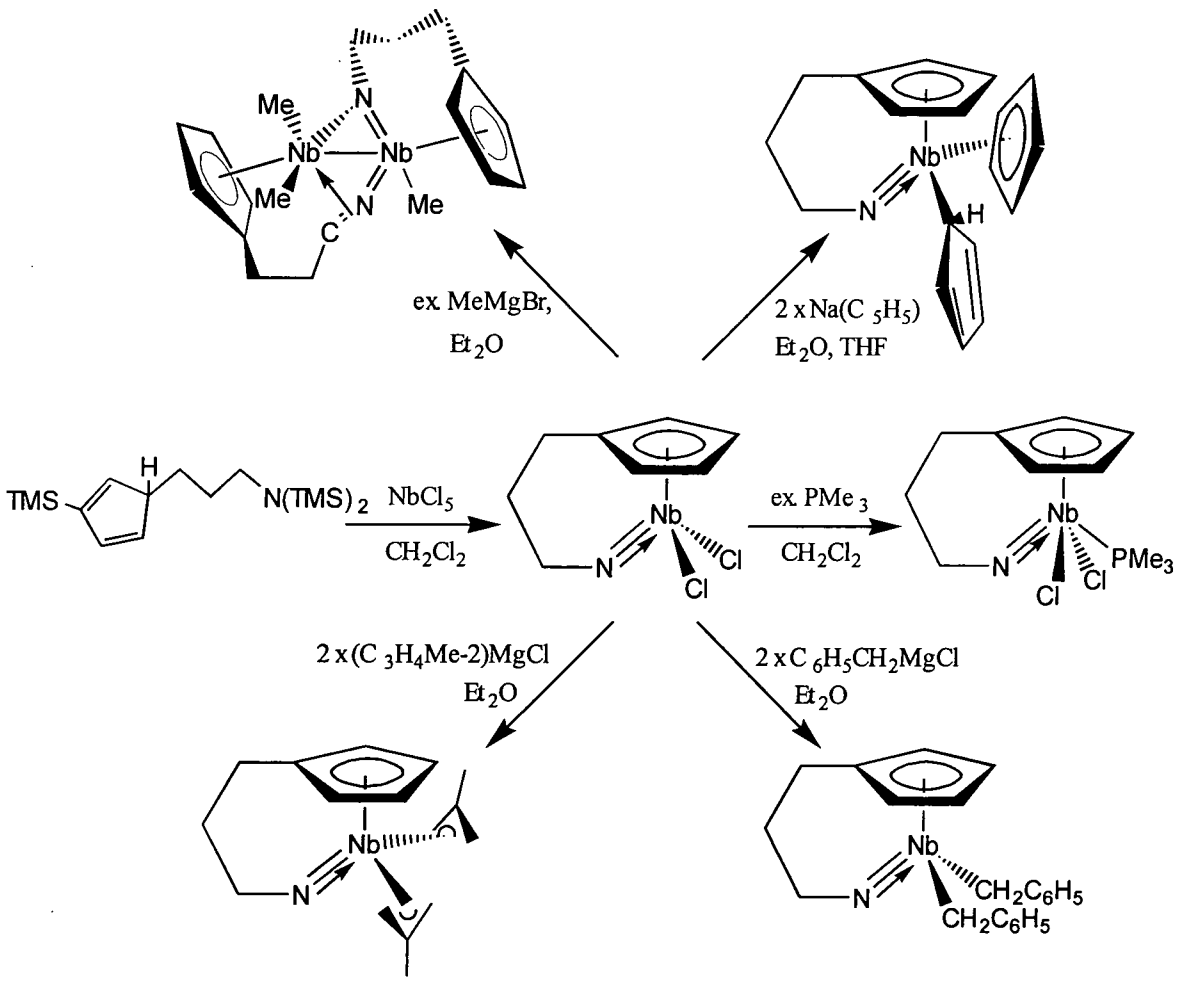

Figure 4.2

The second set of complexes reported by Herrmann and Baratta show the only examples of amide functionalised niobium and tantalum complexes.[12] The homoleptic amides $Nb(NMe_2)_5$ and $Ta(NMe_2)_5$ were treated with equimolar amounts of the protic ligand,

$C_5H_5SiMe_2N(H)C_6H_5$, forming niobium and tantalum *ansa*-type complexes as orange and yellow solids respectively (figure 4.3).

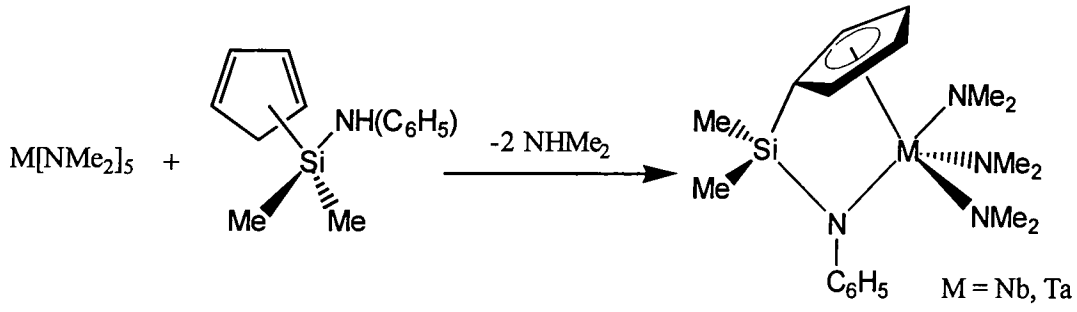

Figure 4.3

Isomerisation occurs in the presence of light, or at room temperature, cleaving the silicon-nitrogen bond, forming a cyclopentadienyl imido tantalum or niobium complex (section 4.2.2, figure 4.7)

4.1.4 Implications in catalysis

It is only recently that Group 5 metal systems have been investigated for catalytic activity. Unlike the 14 electron d^0 Group 4 metallocenes that are catalytically active species without the cocatalyst MAO, catalyst systems based on the 15 electron d^1 Group 5 tantalum and niobium metallocenes, e.g., $TaCp_2Cl_2$ and $NbCp_2Cl_2$, were found to exhibit no activity. Being d^1 metal complexes the metal is capable of π back donation to the incoming olefin thereby preventing polymerisation from occurring.

Recently, the capability of tantalum and niobium diene complexes as catalyst precursors for olefin polymerisation has been investigated. The cyclopentadiene systems $MX_2(\eta^5\text{-}C_5R_5)(\eta^4\text{-diene})$ (M = Ta and Nb; R = H and Me; X = Cl and CH_3; X_2 = 1,3-diene) in the presence of an excess of MAO were found to be new catalyst precursors for the living polymerisation of ethylene, and the narrowest polydispersity (M_w/M_n as low as 1.05) for polyethylene was accomplished. It was noticed that the fragments of these catalytically

active complexes, $MCp(1,3\text{-diene})^+$ (M = Ta and Nb), **C**, are isoelectronic to those of what are thought to be the active species in Group 3, **A**, and Group 4, **B**, catalysis (figure 4.4).

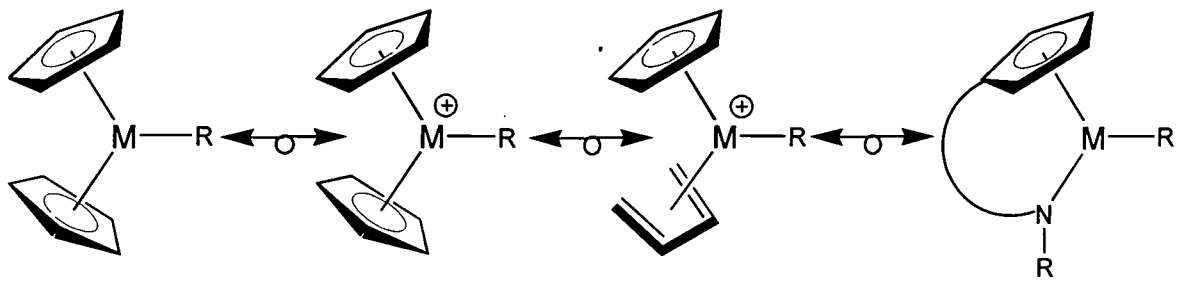

Group 3 **Group 4** **Group 5** **Group 5**

A **B** **C** **D**

Figure 4.4

In much the same way, amide functionalised cyclopentadiene complexes of niobium and tantalum, **D**, can also be isoelectronic with these complexes, and therefore may be potential olefin polymerisation catalysts.

4.1.5 Aims

There being only one example of an amide functionalised cyclopentadienyl niobium and tantalum complex, and this also being light and thermally unstable, we hoped to be able to produce the first stable complexes. By reacting the neutral ligand, **1.1**, and its dianion, **1.3**, with various tantalum and niobium amide and chloride complexes we hoped to be able to synthesise such complexes.

4.2 Attempted Synthesis of Amide Functionalised Cyclopentadienyl Complexes

4.2.1 Attempted reaction between $TaCl_5$ and $[C_5H_4(CH_2)_3NMe](SiMe_3)_2$, 1.4

In an attempt to carry out a similar reaction to that carried out by Green and coworkers for the synthesis of $[Nb(\eta^5{:}\sigma\text{-}C_5H_4(CH_2)_3NCl_2]$ (shown in section 4.1.3), a reaction between tantalum pentachloride and the disilylated ligand, **1.4**, was carried out. A solution of $[C_5H_4(CH_2)_3NMe](SiMe_3)_2$ in toluene (synthesis shown in section 1.6.4), was added to an equimolar amount of $TaCl_5$ in toluene. Although a colour change from orange to brown was observed during the reaction, no identifiable products could be isolated. A ^1H NMR spectrum of the crude material in deutero-benzene showed a number of unidentifiable products.

Similar reactions between the Group 4 metal chlorides ($TiCl_4$, $ZrCl_4$) and the dilithiated or disilylated ligands, $[C_5H_4(CH_2)_3NR]Li_2$ and $[C_5H_4(CH_2)_3NR](SiMe_3)_2$ (R = ^{t}Bu, Me), have been attempted in the past.[13] Again, unidentifiable products were obtained, none of which could be isolated, and it is thought the products of the reactions may be polymeric. For this reason alternative reaction procedures were sought, and in the case of Group 4 metals, these led to successful reactions using the homoleptic amides, $M(NMe_2)_4$ (M = Zr, Ti, Hf).

4.2.2 Attempted reaction between $Ta(NMe_2)_5$ and $C_5H_5(CH_2)_3N(H)Me$, 1.1

As discussed in detail in Chapter 1, the reaction between the Group 4 homoleptic amides, $M(NMe_2)_4$ (M = Ti, Zr and Hf), and the protic ligands $C_5H_5(CH_2)_3N(H)R$ (R = Me, ^{t}Bu), have been found to provide a quick and convenient route to the synthesis of functionalised cyclopentadienyl bis amide complexes (section 1.4.5). It was thought that a similar reaction might occur using the Group 5 homoleptic amides $M(NMe_2)_5$ (M = Ta, Nb), forming a tris rather than bis amide complex.

Using a method described by Bradley and Gilitz, $Ta(NMe_2)_5$ was prepared by reacting $TaCl_5$ and 5 equivalents of $Li(NMe_2)$.[14] Lithium dimethylamide was prepared from the

reaction of dimethylamine with a stoichiometric amount of n-butyl lithium in hexane. The $TaCl_5$ was then added, and stirred for a further two days. Unlike the preparation of $Nb(NR_2)_5$ (R = Me, Et, ^{n}Pr ,^{n}Bu),[15] where extensive reduction to Nb(IV) is observed, the +V oxidation state is retained for tantalum. Work-up of the brown suspension followed by sublimation gave pure $Ta(NMe_2)_5$ as large yellow crystals in 70% yield.

Molecular structure of $Ta(NMe_2)_5$

Interest within the group regarding metal amide structures led to the molecular structure of $Ta(NMe_2)_5$ being determined by X-ray diffraction. A crystal of dimensions 0.6 x 0.4 x 0.2mm was selected for study and the structure solved within the department, with the full data shown in the appendices. For pentacoordinated d^0 compounds, a trigonal bypyramidal arrangement is expected to be the most stable,[16] and $Ta(NEt_2)_5$ exhibits this geometry,[17] but $Nb(NMe_2)_5$ and $Nb(NC_5H_{10})_5$ approach square pyramidal geometry.[10] The structure of $Ta(NMe)_5$ was found to be between the two extremes, with a distorted square pyramidal structure (figure 4.5). Like all tantalum and niobium homoleptic amides, $Ta(NMe)_5$ was found to be a monomer, due to the steric requirements of the NR_2 group and their ability to form σ and π bonds.[12]

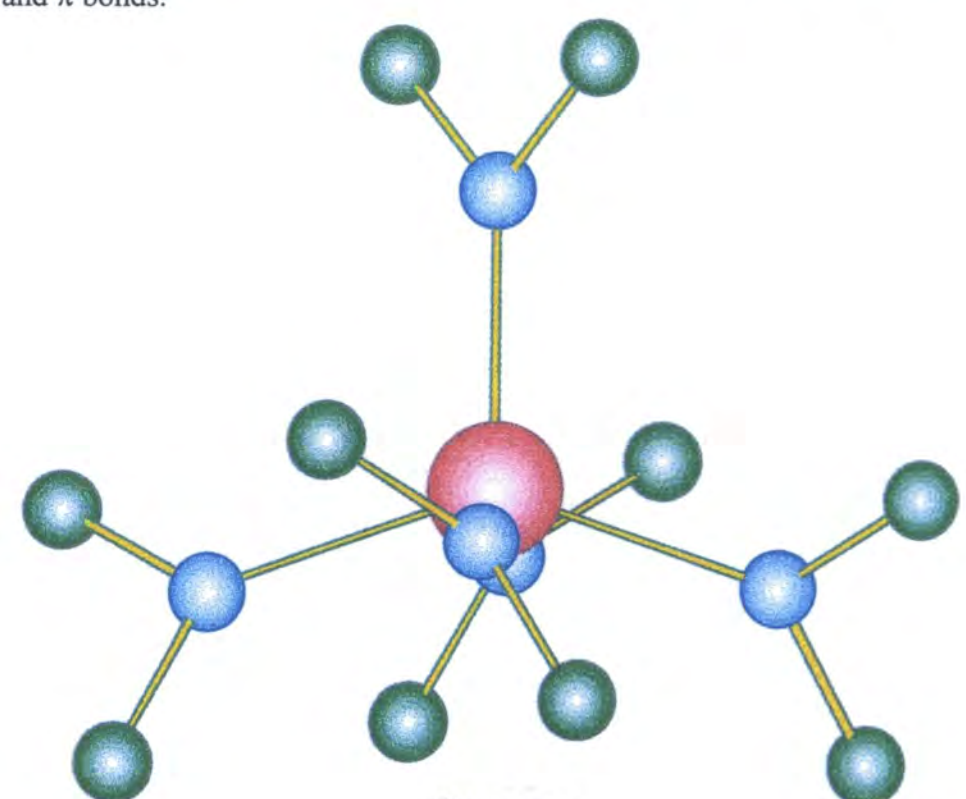

Figure 4.5

Although all the nitrogens have approximately planar geometry, one Ta-N bond appears to have greater π-character, on the basis of its shorter length. This Ta-N bond is 1.971(5)Å long (Ta-N double bonds average 1.947Å) whereas the other four Ta-N bonds are 2.041(8)Å long (Ta-N single bonds average 2.06Å), indicating little or no dπ-pπ interaction. The planar geometry of the nitrogen has been interpreted to result from the tight packing of the ligands around the metal.

The structure of $Ta(NMe_2)_5$ exhibits some disorder which needs to be described. The Ta and unique nitrogen atom, N1, are located at the intersection of two orthogonal crystallographic mirror planes, **A** and **B** (figure 4.6). The remainder of the asymmetric unit consists of two nitrogen atoms, N2 and N3, and their attached methyl groups, each of which is 50% occupancy, and represents disorder either side of one mirror plane. Construction of the whole molecular unit by applying the mirror planes to the asymmetric unit generates a total of nine NMe_2 groups, with 100% occupancy for the unique group and 50% occupancy for the other eight.

A more "correct" molecular unit can be constructed by taking the nitrogen atoms, N2 and N3, and their images alternatively around the four quadrants defined by the mirror planes. Thus one molecule contains N2, N3A, N2B and N3C, (figure 4.6, **A**) and the other contains N3, N2A, N2C and N3B, (figure 4.6, **B**) if the quadrants are to be labelled, as follows:

N2	N3A
N3C	N2B

N3	N2A
N2C	N3B

The two molecules which are generated by this interpretation of the disorder are found to be related to each other by a mirror plane, that is they are enantiomers.

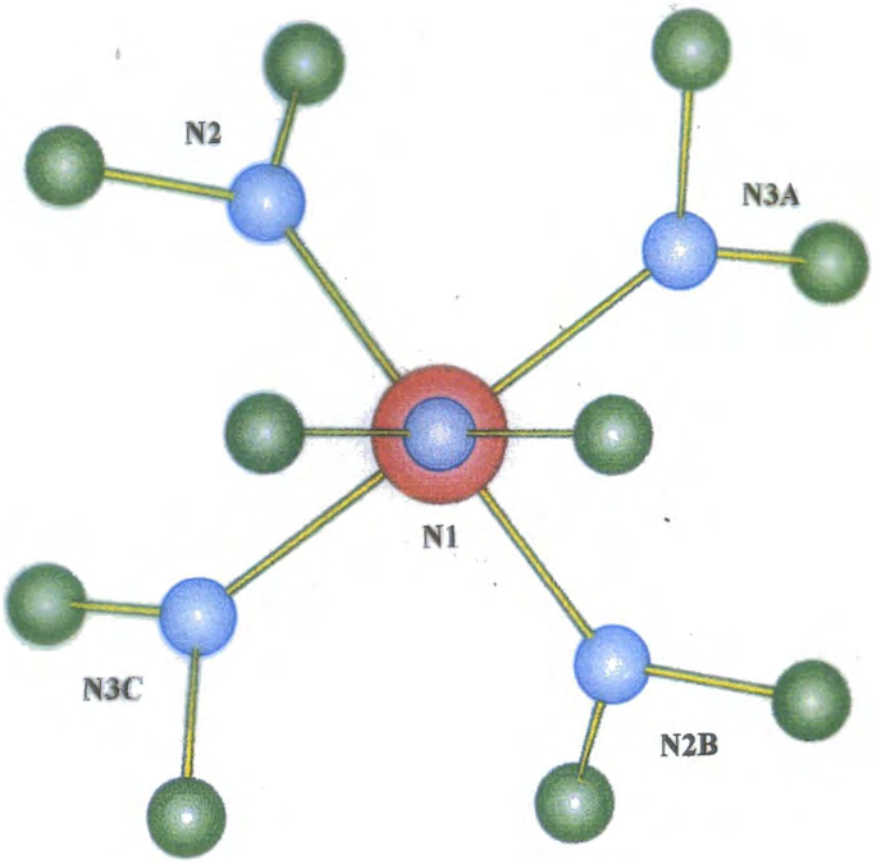

Figure 4.6 A

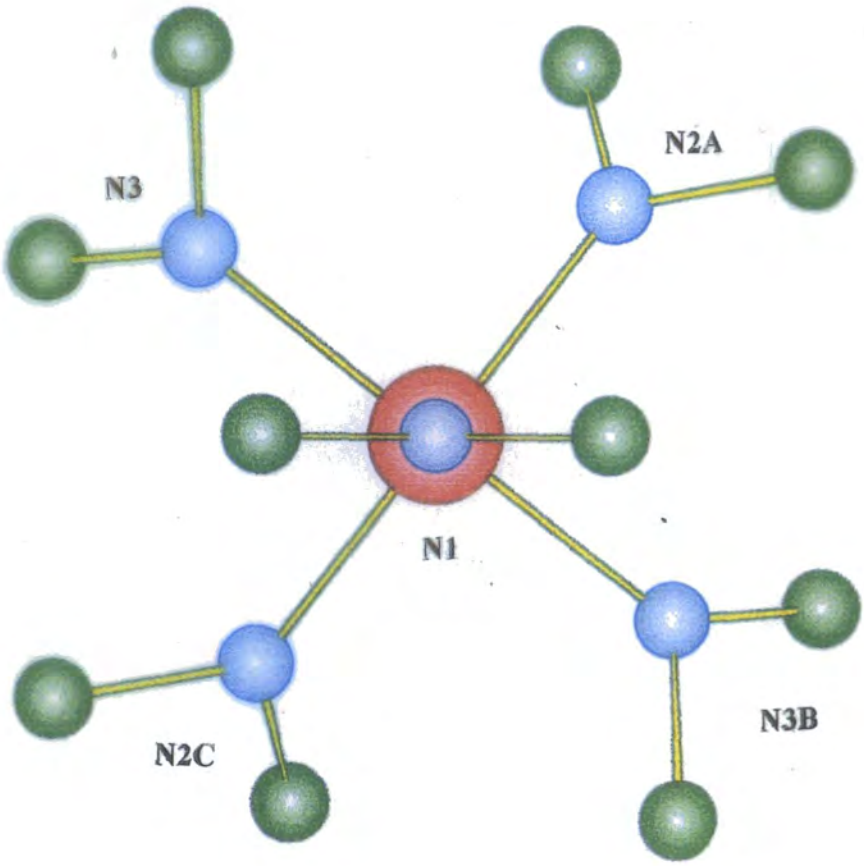

Figure 4.6 B

Herrmann and Baratta synthesised amide functionalised cyclopentadienyl complexes, $M(\eta^5:\eta^1\text{-}C_5H_4SiMe_2NC_6H_5)(NMe_2)_3$ (M = Nb, Ta), from the reaction of the tantalum and niobium homoleptic amides, $M(NMe_2)_5$, with equimolar amounts of the protic ligand, $C_5H_5SiMe_2N(H)C_6H_5$) (figure 4.3). By carrying out an analogous reaction using the ligand $C_5H_5(CH_2)_3N(H)Me$, a similar reaction was expected to occur.

Addition of the aprotic ligand, $C_5H_5(CH_2)_3N(H)Me$, **1.1**, to a toluene or hexane solution of $Ta(NMe_2)_5$, at 0°C, gave an immediate colour change from yellow to red. Stirring at ambient temperature for 24 hours gave a partially soluble dark red precipitate. An aliquot was taken for analysis, and the ^1H NMR spectrum in deutero-benzene gave a broad spectrum suggesting possible formation of some paramagnetic tantalum(IV) species. There was no evidence for an attached cyclopentadienyl group being present, or the free ligand, but this being volatile under reduced pressure, it would distill during the NMR sample preparation. New resonances were observed, but none that could be assigned to an attached ligand. Prolonged reflux of the reaction mixture over a number of days also gave no identifiable products.

In an attempt to try and understand the nature of this reaction, a reaction was carried out in an NMR tube using equimolar amounts of $Ta(NMe_2)_5$ and $C_5H_5(CH_2)_3N(H)Me$, **1.1**, in deutero-benzene, and monitored using ^1H NMR spectroscopy. Again the mixture turned dark red rapidly, with new resonances appearing in the NMe region of the ^1H NMR spectrum. There was no evidence for an attached cyclopentadienyl group with only the cyclopentadiene group of the free ligand being observed in the aromatic region.

Steric effects are thought to be the main cause for the failure of the reaction. Unlike the Group 4 homoleptic amides, which react with such ligands displacing two amide substituents, the Group 5 metals, despite being a similar size, have an extra amide group coordinated. The ^1H NMR spectroscopic evidence suggests that the amine group of the ligand reacts readily, substituting an amide group. A cyclopentadienyl group, however, occupies three coordination sites and is sterically likely to require displacement of more than one amide group. These requirements are therefore thought to prevent cyclopentadienyl attachment.

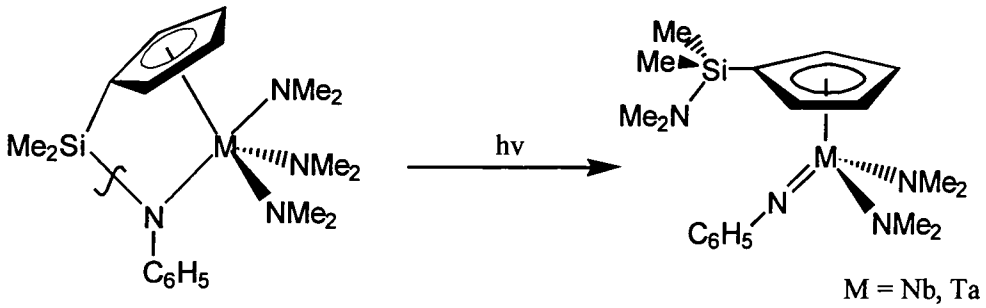

Figure 4.7

Steric crowding was found to cause isomerisation of the amide functionalised cyclopentadienyl tantalum complex discussed in section 4.1.3. The presence of the π-cyclopentadienyl group and four amide groups causes cleavage of the Si-N bond, in the presence of light or above room temperature, forming a less sterically strained four co-ordinate complex (figure 4.7).

4.3 Reactions between $[M(N^tBu)(NH^tBu)(NH_2{}^tBu)Cl_2]_2$ (M = Nb, Ta) and $[\eta^5:\eta^1\text{-}C_5H_4(CH_2)_3NMe]Li_2$, 1.3

The unsuccessful reactions described above led us to seek alternative reactants. The dimers $[M(N^tBu)(NH^tBu)(NH_2{}^tBu)Cl_2]_2$ (M = Nb, Ta), with two chloride groups per metal seem like possible candidates to react with the dilithiated ligand, $[C_5H_4(CH_2)_3NMe]Li_2$, **1.3**. To prevent steric and electronic crowding, displacement of the labile t-butylamine is also possible.

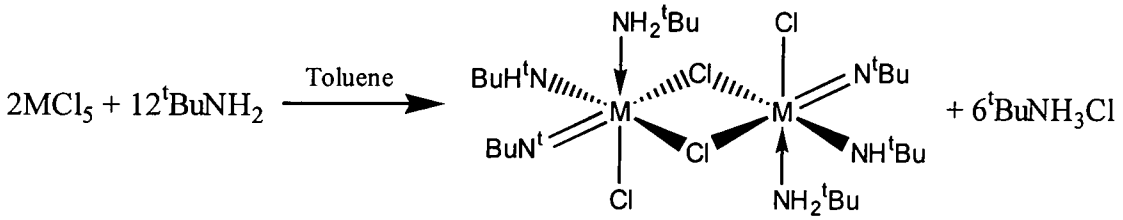

M = Ta, Nb

Figure 4.7

The starting materials, $[M(N^tBu)(NH^tBu)(NH_2{}^tBu)Cl_2]_2$ (M = Nb, Ta), were prepared using a method based on those by Nielson and coworkers (figure 4.7).[18,19] A suspension of MCl_5 (M = Nb, Ta) in toluene was reacted with 10 equivalents of t-butylamine. Removal of the solvent, followed by extraction with the minimum amount of cold toluene, was found to be unnecessary. Instead direct filtration of the solution left the desired quantity of t-butyl ammonium chloride. Removal of the solvent gave pure $[M(N^tBu)(NH^tBu)(NH_2{}^tBu)Cl_2]_2$ (M = Ta, Nb) in high yield, as white and yellow powders respectively.

4.3.1 Reaction between $[Ta(N^tBu)(NH^tBu)(NH_2{}^tBu)Cl_2]_2$ and $[\eta^5:\eta^1\text{-}C_5H_4(CH_2)_3NMe]Li_2$, 1.3

The reaction between $[Ta(N^tBu)(NH^tBu)(NH_2{}^tBu)Cl_2]_2$ and two equivalents of the dianion, $[C_5H_4(CH_2)_3NMe]Li_2$, **1.3**, in THF for two days, gave a clear, colourless solution. Extraction of the product into hexane left four equivalents of lithium chloride, and removal of the solvent gave an oily white solid. Analysis by ^1H NMR showed that the crude

material consisted of more than one product, and therefore sublimation onto a liquid nitrogen cooled probe was used as a means of separation. A white solid sublimed between 60-65°C, 10^{-3}mmHg, forming a clear colourless viscous oil at room temperature.

The ^{1}H NMR spectrum in C_6D_6 (figure 4.9) shows a clean but complicated spectrum that is characteristic of a chiral complex, and indicates the formation of an amide functionalised cyclopentadienyl complex. Four resonances each integrating as one proton appear in the aromatic region of the spectrum, indicating an ABCD spin system for the C_5H_4 group. A metal bonded NMe group is also evident at 3.74ppm, as a singlet integrating to three protons. Two separate resonances at 1.42ppm and 1.35ppm, are observed for the t-butyl groups, indicating that the two groups are in different environments. A broad singlet at 3.83ppm, integrating to one proton, suggests that one of these groups is present as a metal amide substituent (M-NH^{t}Bu). It seems likely that the second t-butyl resonance is for a metal imido group, (M-N^{t}Bu), given that such groups are generally spectator ligands.

The protons of the trimethylene backbone give a complicated series of multiplets in the ^{1}H NMR spectrum. Therefore selective proton decoupling experiments in the region 1.4ppm to 3.4ppm were used to identify protons coupled to each other. Figure 4.10 shows the results of the experiment, with all six hydrogens assigned to the relevant multiplets. ^{1}H COSY experiments was also used to confirm this (figure 4.11).

The $^{13}C\{^{1}H\}$ NMR spectrum shows a series of five resonances for each carbon in the cyclopentadienyl group, including the *ipso*-carbon (figure 4.12). Four resonances are also seen for two different t-butyl groups, one for each of the quarternary carbons, and one for each set of three fluxional methyl groups. To complete the assignment of the spectrum, ^{1}H-^{13}C HETCOR was used (figure 4.13), with each carbon of the trimethylene backbone being correctly assigned. From this evidence it was concluded that the chiral monomer Ta[η^5:η^1-$C_5H_4(CH_2)_3$NMe](N^{t}Bu)(NH^{t}Bu), **4.1**, had formed as the major product in 55% yield (figure 4.14).

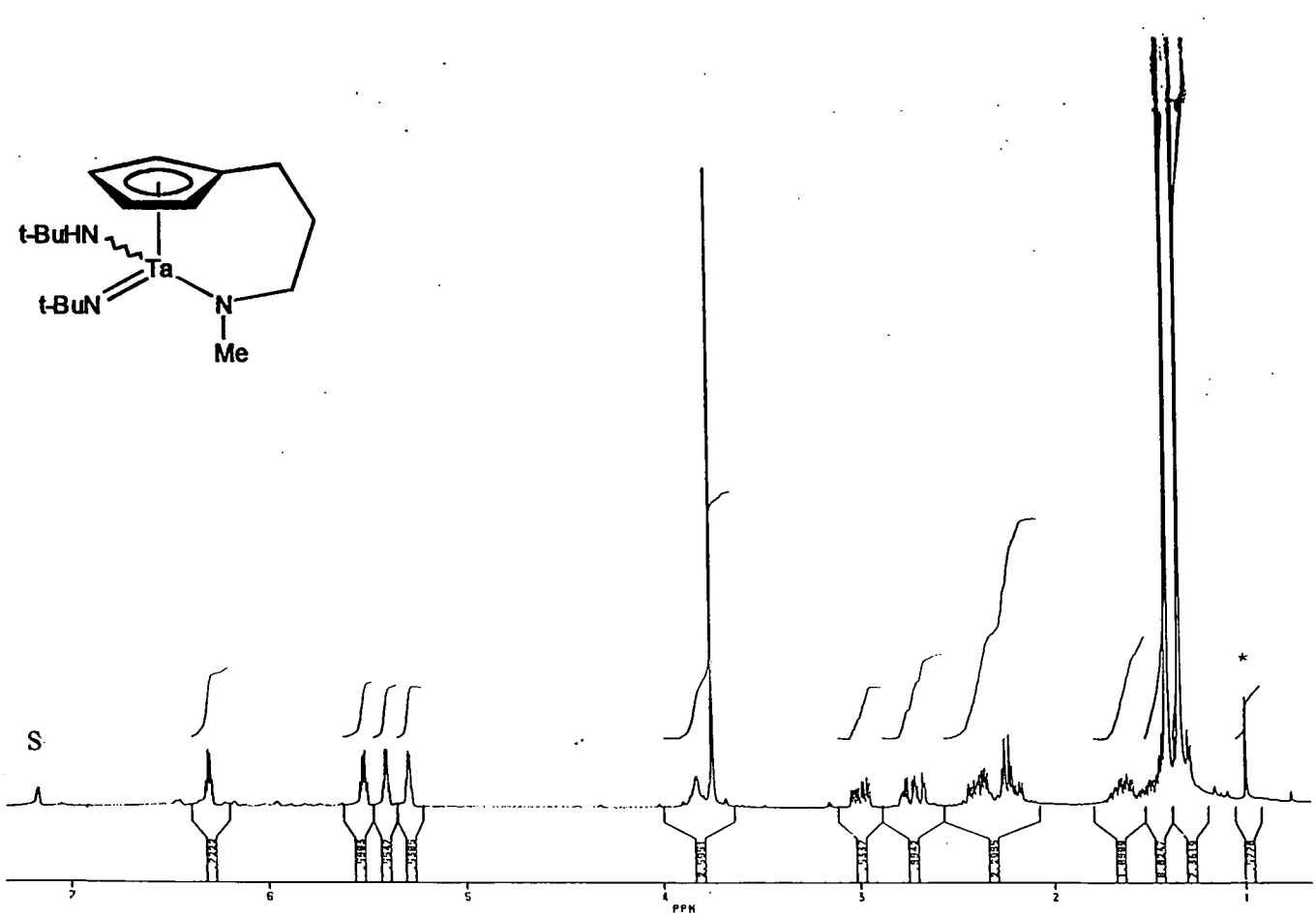

Figure 4.9 ^{1}H NMR spectrum of **4.1** in C_6D_6 at 250MHz

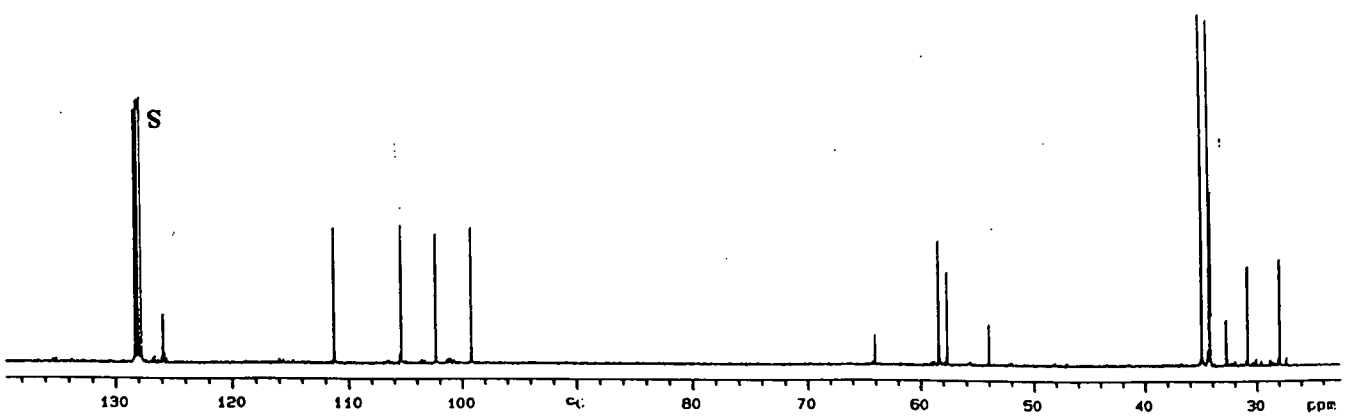

Figure 4.12 $^{13}C\{^{1}H\}$ NMR spectrum of **4.1** in C_6D_6 at 100MHz

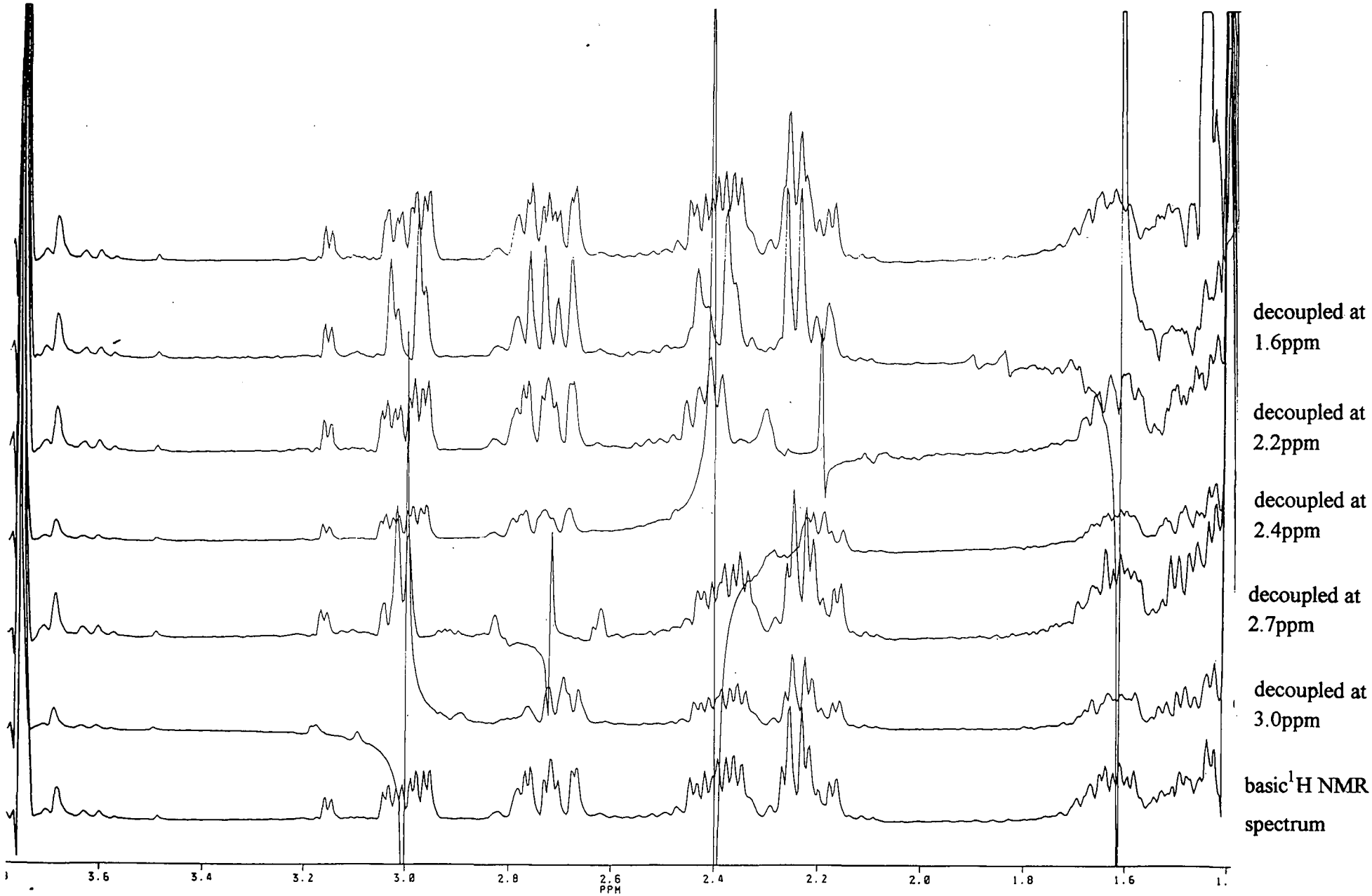

Figure 4.10 ^{1}H decoupled spectrum of **4.1** in C_6D_6 at 250MHz

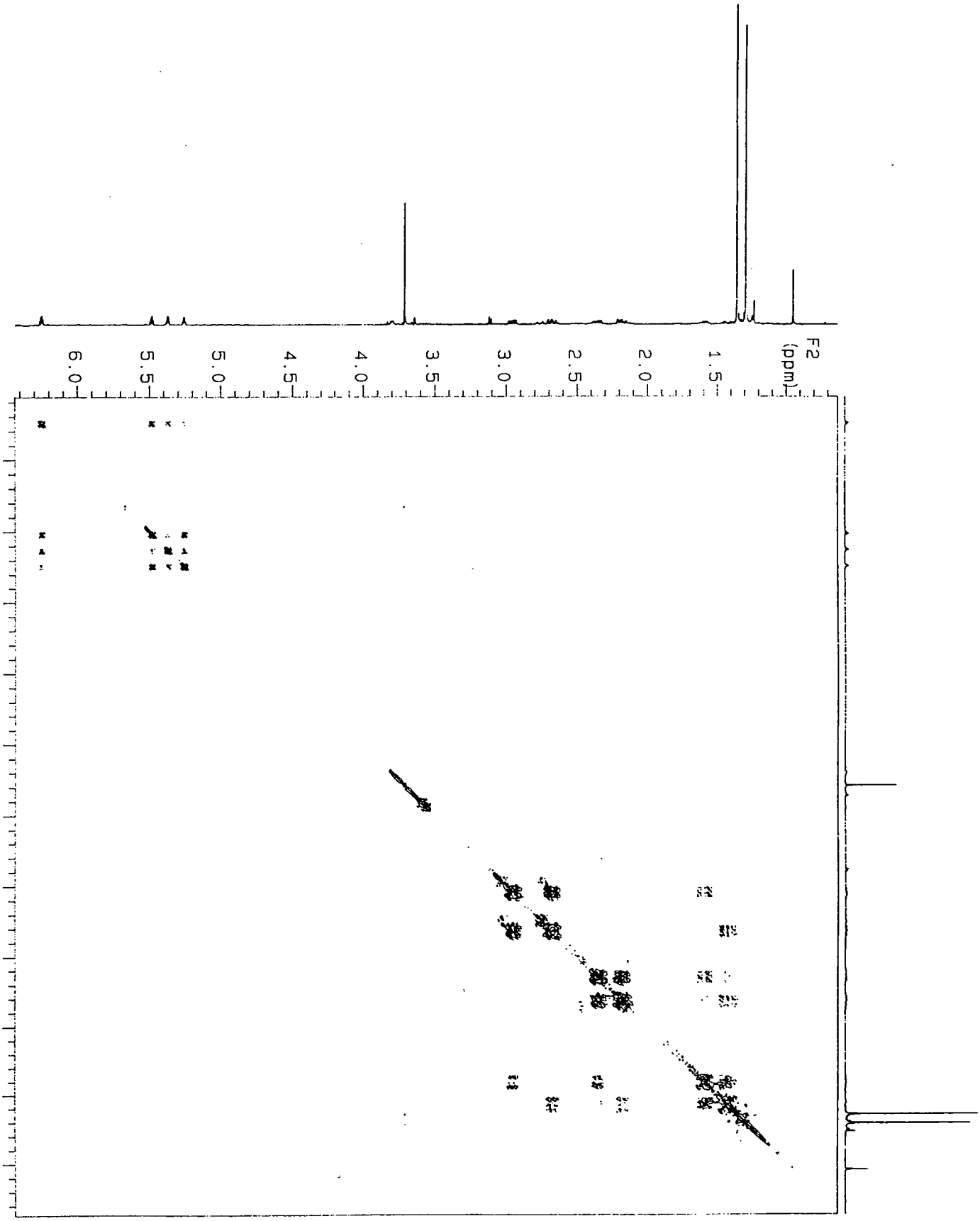

Figure 4.11 ^{1}H COSY of **4.1** in C_6D_6 at 400MHz

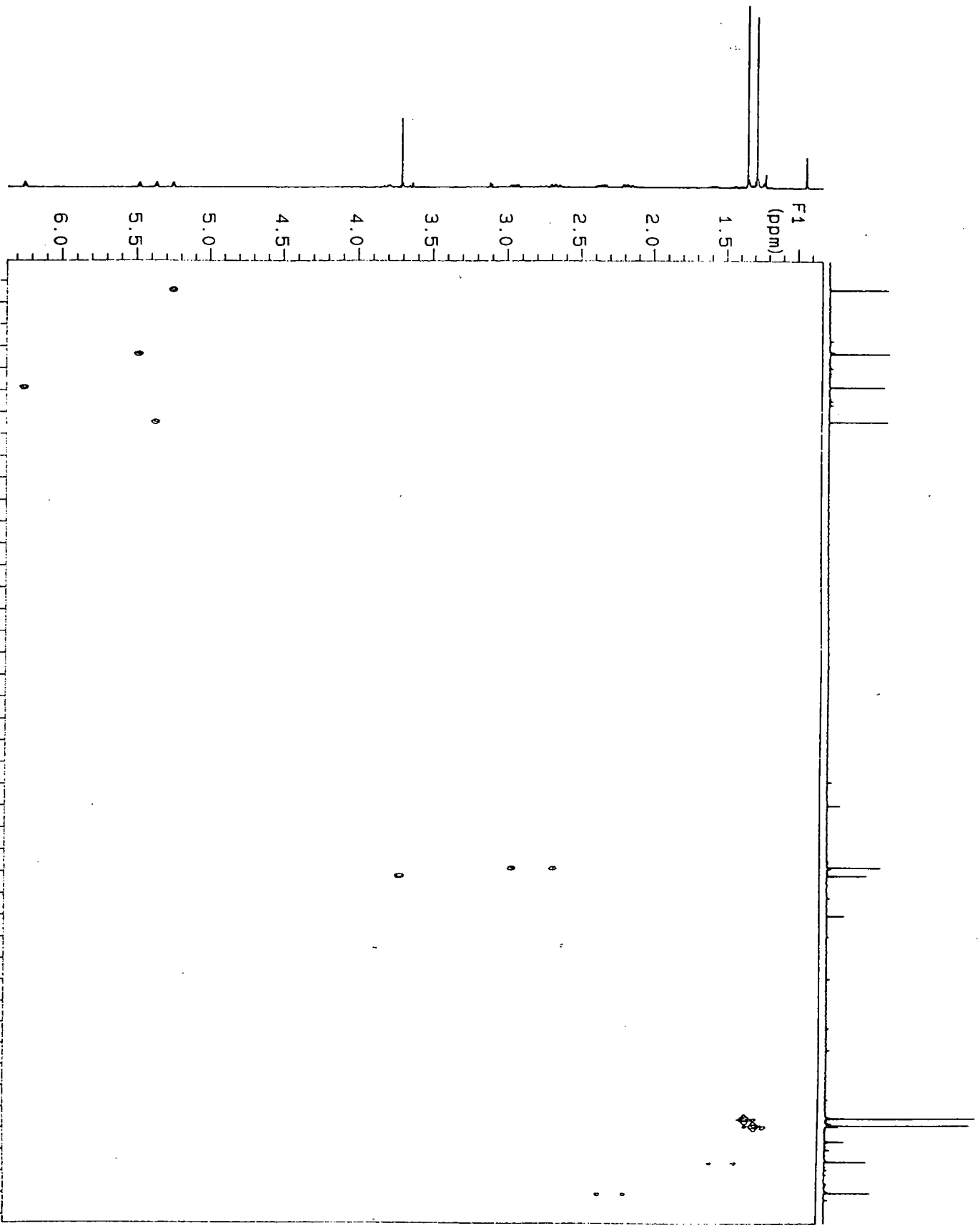

Figure 4.13 ^{1}H-^{13}C HETCOR of **4.1** in C_6D_6 at 400 and 100MHz

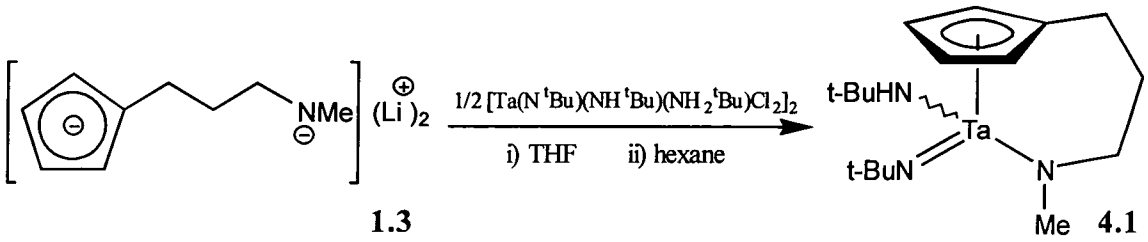

1.3 4.1

Figure 4.14

Infra-red spectroscopy also provided support for the formation of **4.1**. An N-H stretch at 3347cm^{-1} indicates the presence of an amine, presumably the M-NH^{t}Bu group. Strong bands at 804, 1211 and 1265cm^{-1} suggest the presence of a cyclopentadienyl group, with strong bands in the aliphatic region at 2703-2960cm^{-1} for the remainder of the ligand and t-butyl groups.

Mass spectroscopy confirmed the formation of **4.1**, with the cation [**4.1**]$^+$ appearing at a mass of 458. Masses were also observed for the break-up of the complex with [Ta(CpNMe)]$^+$, [Ta(N^{t}Bu)]$^+$, [Ta]$^+$, [CpNMe]$^+$ and [N^{t}Bu]$^+$, appearing at m/e = 319, 252, 180, 136, and 70, respectively, with the correct isotope distribution. Being an oil, accurate elemental analysis results proved difficult. Despite this, results recorded for the carbon and hydrogen percentages were within 0.2% of the required values, with the nitrogen value 0.8% lower than that calculated.

The possibility of another complex being formed could not be ruled out. A complex where both amide and amine groups are replaced, and amine coordinating again, would give a product with an indistinguishable elemental analysis and mass spectra to that of **4.1**. However such a complex would be a tantalum(IV) species and would therefore give paramagnetic NMR spectra, which is not the case.

Earlier, the discussion of two products being produced during the reaction was mentioned. Although, not isolated pure, it is proposed that this second product is a dimer. This will be discussed in detail in section 4.3.5

4.3.2 Reaction between $[Nb(N^tBu)(NH^tBu)(NH_2{}^tBu)Cl_2]_2$ and $[\eta^5:\eta^1\text{-}C_5H_4(CH_2)_3NMe]Li_2$, 1.3

In an attempt to synthesise the niobium analogue of **4.1**, the reaction between $[Nb(N^tBu)(NH^tBu)(NH_2{}^tBu)Cl_2]_2$ and $[C_5H_4(CH_2)_3NMe]Li_2$, **1.3**, was carried out in a similar manner. Similarly, ^1H NMR analysis of the crude material showed it to contain more than one product. Sublimation onto a liquid nitrogen cooled probe between 60-65°C, 10^{-3}mmHg, produced a yellow solid, which on warming gave $Nb[\eta^5:\eta^1\text{-}C_5H_4(CH_2)_3NMe](N^tBu)(NH^tBu)$, **4.2**, as a yellow oil in 65% yield (figure 4.15).

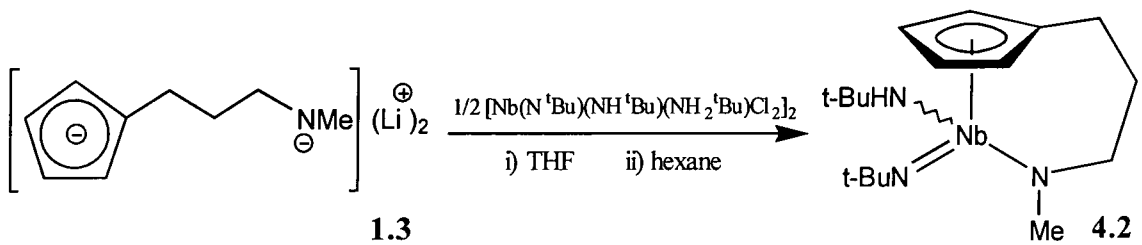

1.3 **4.2**

Figure 4.15

The ^1H and $^{13}C\{^1H\}$ NMR analysis gave very similar spectra to that of the tantalum complex, **4.1**. In the ^1H NMR spectrum four resonances are observed for the C_5H_4 group, and a singlet at 3.67ppm for a coordinated NMe group (figure 4.16). Two singlets at 1.39 and 1.28ppm are seen for each t-butyl group, with a broad singlet at 4.48ppm for an NH group, indicating the presence of a NH^tBu group. Again, a ^1H COSY spectrum aided in assigning the trimethylene backbone of the ligand. The $^{13}C\{^1H\}$ NMR spectrum (figure 4.17) was fully assigned with the aid of a ^1H-^{13}C HETCOR spectrum.

Mass spectroscopy gave the same fragments as **4.1**, except with the mass expected for niobium rather than for tantalum. The infra-red spectrum was also similar with cyclopentadienyl resonances observed at 1242-1134cm^{-1} and N-H stretch at 3352cm^{-1}, all aiding to prove that the niobium complex, $Nb[C_5H_4(CH_2)_3NMe](N^tBu)(NH^tBu)$, **4.2**, was synthesised. Again elemental analysis proved difficult to obtain, but results for nitrogen and hydrogen percentages were within 0.2% of calculated values, and the carbon percentage only slightly beyond the 0.5% range.

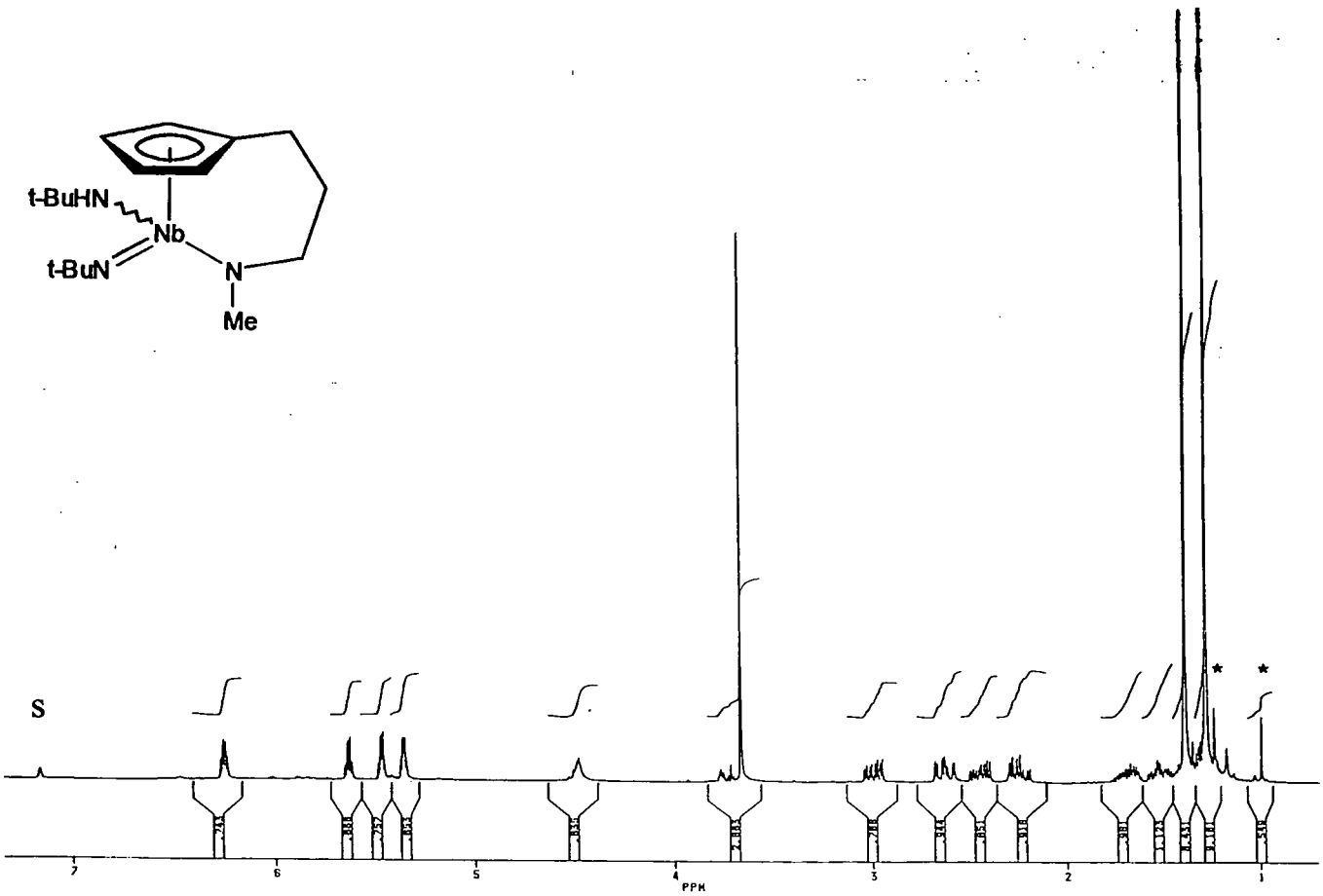

Figure 4.16 ^{1}H NMR spectrum of **4.2** in C_6D_6 at 250MHz

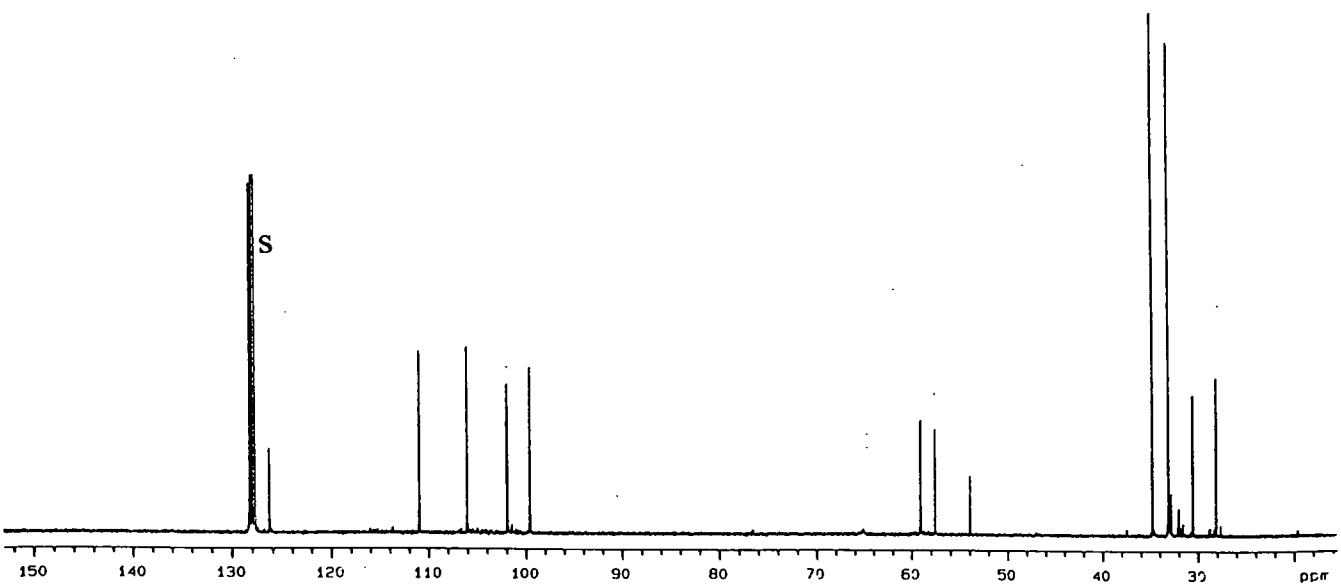

Figure 4.17 $^{13}C\{^{1}H\}$ NMR spectrum of **4.2** in C_6D_6 at 100MHz

4.3.3 Electronic structure

Like the tungsten and molybdenum complexes **2.2**, **2.3**, **2.4**, **2.5** and **2.6** discussed in Chapter 2, the monomers **4.1** and **4.2** have a formal electron count greater than 18. Again as we have no structural data the ^{13}C chemical shifts were taken, the $\Delta\delta$ values measured, and compared against other Group 5 mono imido systems to give an indication of the nature of the imido ligand (Table 4.1).

Nb(N^tBu) complexes [(i)]	$\Delta\delta$/ppm	Ta(N^tBu) complexes [(i)]	$\Delta\delta$/ppm
Nb(CpNMe)(N^tBu)(NH^tBu) (20)	30.4	Ta(CpNMe)(N^tBu)(NH^tBu) (20)	29.1
[Nb(N^tBu)(NH^tBu)($NH_2{}^tBu$)Cl_2]$_2$ (16)[(ii)]	37.1	[Ta(N^tBu)(NH^tBu)($NH_2{}^tBu$)Cl_2 (16)[(ii)]	32.0
Nb(N^tBu)Cl_3tmeda (16)[19]	41.2	Ta(N^tBu)Cl_3tmeda.1/6C_6H_6[19]	34.0
Nb(N^tBu)(dtc)$_3$ (16)[20]	35.9	Ta(N^tBu)(dtc)$_3$ (16)[20]	30.8
Nb(N^tBu)(NMe_2)$_3$ (15)[20]	35.1	Ta(N^tBu)(NMe_2)$_3$ (15)[20]	32.1
Nb(N^tBu)(NH^tBu)Cl_2(PMe_3)$_2$ (18)[21]	32.7	Ta(N^tBu)(NH^tBu)Cl_2(PMe_3)$_2$ (18)[21]	32.7
Nb(N^tBu)(NH^tBu)Cl_3 (15)[21]	30.9	Ta(N^tBu)(NH^tBu)Cl_3 (15)[21]	25.7
Nb(N^tBu)Cl_3(PMe_3)$_2$ (16)[21]	30.3	Ta(N^tBu)Cl_3(PMe_3)$_2$ (16)[21]	23.4

i) formal electron count in brackets

ii) starting materials used for preparation of **4.2** and **4.1**.

Table 4.1

Like the values for the tungsten and molybdenum complexes, the $\Delta\delta$ values measured for the tantalum and niobium complexes, **4.1** and **2.2**, were found to be some of the lowest when compared against other monoimido complexes. This indicates that the imido nitrogen is not contributing 4 electrons to the metal centre.

4.3.4 Evidence for dimers

Although the monomers, **4.1** and **4.2**, were the main products to be isolated in the two reactions, in each case a second product was also produced in smaller quantities. Following the sublimation of **4.1**, analysis of the involatile residue showed it to contain small amounts of a second complex. ^{1}H NMR analysis of the crude material in C_6D_6, showed a similar but simpler spectrum to that of **4.1**, indicative of a complex that is not chiral. Two equally integrated multiplets at 5.89 and 5.64ppm were observed, indicating the presence of C_5H_4 group as an AA'BB' spin system. The trimethylene backbone is seen as a series of three sets of multiplets at 2.43, 2.25 and 1.53ppm for $NC\underline{H}_2$, $C_5H_4C\underline{H}_2$, and $CH_2C\underline{H}_2CH_2$ respectively. Assignment of the t-butyl groups proved difficult with resonances from small amounts of **4.1** overlapping, but there appears to be two of them. A similar spectrum was also observed from the residue of the niobium reaction.

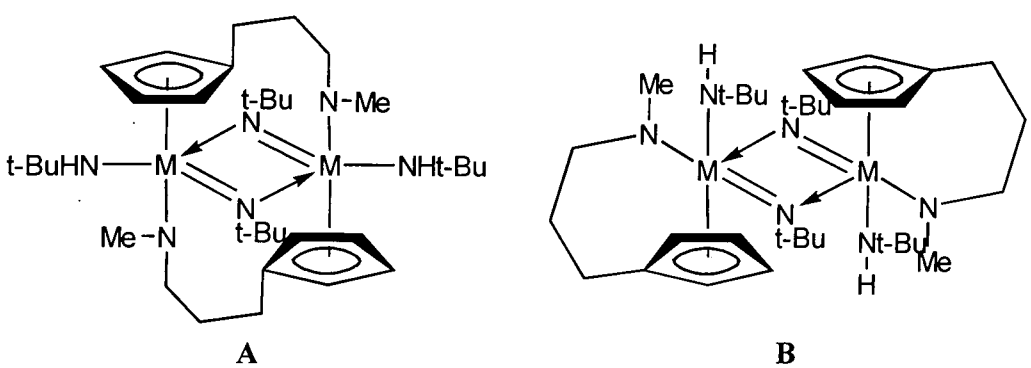

A B

Figure 4.18

From this evidence we propose that symmetrical tantalum and niobium dimers are the second products. Although the exact structure has yet to be diagnosed, two possible structures fit the available data, **A** and **B** (figure 4.18). Like many Group 5 imido complexes, including the reactants used for the reaction, a bridging imido group is thought to connect the two metals, in the form of a dimer.

4.4 Summary and Future Work

Although reactions of tantalum pentachlorides and amides with the disilylated and dilithiated ligands, **1.4** and **1.3** respectively, proved unsuccessful in synthesising amide functinalised cyclopentadienyl complexes of the ligand used, the reaction between the niobium and tantalum dimers $[M(N^tBu)(NH^tBu)(NH_2{}^tBu)Cl_2]_2$ and the dianion, **1.3**, provide a novel and successful route to such complexes. The chiral monomers $M[\eta^5:\eta^1\text{-}C_5H_4(CH_2)_3NMe](NH^tBu)(N^tBu)$ (M = Ta, **4.1**; M = Nb, **4.2**) formed as highly air and moisture sensitive oils. Evidence was also gained for a second minor product being formed as the tantalum and niobium dimers, with two imido ligands bridging each metal.

As discussed in the introduction, although Group 5 cyclopentadienyl amide complexes are known, only one example of a cyclopentadienyl amide compound exists. To our knowledge, apart from being one of very few Group 5 *ansa*-cyclopentadienyl compounds, complexes **4.1** and **4.2** are the first Group 5 cyclopentadienyl complexes to contain both an amide (-NMe) and an imido ($-N^tBu$) ligand.

Complexes **4.1** and **4.2** are formally 20 electron complexes and therefore unlikely to be catalytically active. Unlike the Group 6 complexes discussed in Chapter 2 that contain two imido groups, the Group 5 complexes **4.1** and **4.2** contain one imido and one amide substituent. Since metal amides are more reactive than imido ligands, it seems more likely that reactions carried out with **4.1** and **4.2** would be more successful. In Chapter 1 (section 1.4.5), reactions of the Group 4 bis amide complexes, $M[\eta^5:\eta^1\text{-}C_5H_4(CH_2)_3NMe](NMe_2)_2$ (M = Zr, Hf), with NH_4Cl gave the corresponding metal dichlorides from which further reactions could then be carried out. Such reactions could be carried out with **4.1** and **4.2**, although since primary amides (i.e. NH^tBu) are less basic than secondary amides (i.e.-CH_2NMe) it seems likely that the functionalised amide group would react preferentially. These reactions were not explored.

Although no reactions of the imido groups were successful in Chapter 2, such reactions do take place. It is more likely that complexes with one imido ligand will react, such as **4.1** and **4.2**, and therefore it may be possible for less electronically saturated complexes to be produced and are more likely to be potential catalysts.

Another reaction that would be of interest is the reaction of the tantalum or niobium dimer, used in the synthesis of **4.1** and **4.2**, with the ligand monoanion, **1.2**, rather than the dianion (figure 4.19).

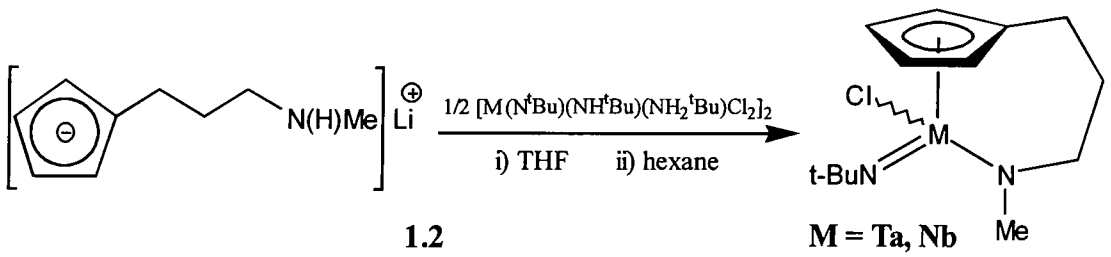

1.2 **M = Ta, Nb**

Figure 4.19

Rather than the amide complex forming, as in **4.1** and **4.2**, a chloride complex would be expected. Metal chlorides being more versatile ligands than metal amides (discussed in Chapter 1) further reactions could be carried out.

4.5 Experimental

4.5.1 Preparation of starting materials

Preparation of $Li(NMe_2)$

Pure dry dimethylamine was produced by adding 40% aqueous dimethylamine (32ml, 0.26mol) dropwise to NaOH (30g, 0.75mol), under reduced pressure. Throughout the addition the pressure of the gas was carefully monitored, such that the pressure did not exceed 150mmHg. The liberated gas was condensed into hexane (300ml) at -78°C (acetone/dry ice). The solution was allowed to warm to 0°C and $^{n}BuLi$ (137ml of a 1.6M solution in hexane, 0.22mol) was added dropwise over 2hr. The reaction mixture was then stirred at ambient temperature for 24hr. A white suspension of $Li(NMe_2)$ (ca. 0.22mol, assuming 100% completion) formed, and was not isolated but used in situ for the following reaction.

Preparation of $Ta(NMe_2)_5$[14]

$TaCl_5$ (14.4g, 40mmol) was added (in ca. 3g portions) over 3hr to a stirred suspension of $Li(NMe_2)$ (11.2g, 0.22mol) in hexane (300ml), at 0°C and the mixture stirred for 18hr. The pale yellow solution was then filtered and the solvent removed under reduced pressure leaving crude $Ta(NMe_2)_5$ as a light brown oil. Sublimation (60°C, 10^{-3}mmHg) gave pure $Ta(NMe_2)_5$ (11.2g, 28mmol, 70% yield) as large yellow crystals. Crystals suitable for X-ray diffraction studies were obtained.

^1H NMR: δ/ppm, C_6D_6, 3.27 (s, 30H, ($N\underline{Me_2}$)

Improved Synthesis of $[Ta(N^tBu)(NH^tBu)(NH_2{}^tBu)Cl_2]_2$

Neat $^tBuNH_2$ (14.9ml, 141mmol) was added dropwise to a stirred suspension of $TaCl_5$ (5.00g, 14.0mmol) in toluene (70ml) at 0°C forming a white turbid solution. The solution was allowed to reach ambient temperature and stirred for 16hr. The yellow solution was filtered from the $^tBuNH_3Cl$ (4.60g, 3 equivalents based on $TaCl_5$). The solvent was removed under reduced pressure and the resultant material was dried under reduced pressure for 24hr, leaving $[TaCl_2(N^tBu)(NH^tBu)(NH_2{}^tBu)_2]_2$ as a white powder (5.45g, 5.8mmol, 83% yield).

^1H NMR: δ/ppm, C_6D_6, 8.5 (s, 2H, NH), 3.70 (s, 4H, NH_2), 1.38 (s, 18H, $NC\underline{Me_3}$), 1.35 (s, 18H, $NHC\underline{Me_3}$), 1.32 (s, 18H, $NH_2C\underline{Me_3}$).

Improved Synthesis of $[Nb(N^tBu)(NH^tBu)(NH_2{}^tBu)Cl_2]_2$

Neat $^tBuNH_2$ (15.6ml, 148mmol) was added dropwise to a stirred suspension of $NbCl_5$ (5.00g, 18.5mmol) in toluene (70ml) at 0°C forming a yellow turbid solution. The solution was allowed to reach ambient temperature and stirred for 16hr. The yellow solution was filtered from the $^tBuNH_3Cl$ (5.9g, 3 equivalents based on $NbCl_5$). The solvent was removed under reduced pressure and the resultant material was dried under reduced pressure for 24hr leaving $[NbCl_2(N^tBu)(NH^tBu)(NH_2{}^tBu)_2]_2$ as a pale yellow powder (6.30g, 8.3mmol, 90% yield).

^1H NMR: δ/ppm, C_6D_6, 8.5 (s, 2H, NH), 4.0 (s, 4H, NH_2), 1.35 (s, 18H, $NC\underline{Me_3}$), 1.30 (s, 36H, $NHC\underline{Me_3}$ and $NH_2C\underline{Me_3}$).

4.5.2 Attempted reaction of $TaCl_5$ and $[C_5H_4(CH_2)_3NMe](SiMe_3)_2$, 1.4

A suspension of $TaCl_5$ (0.72g, 2mmol) in toluene (20ml) was cooled to -78°C (acetone/dry ice). A suspension of $[C_5H_4(CH_2)_3NMe](SiMe_3)_2$, **1.4**, (ca. 4mmol in toluene, from section 1.6.4) was added dropwise and the mixture allowed to warm to room temperature over 2hr, then stirred for 24hr. The brown suspension was filtered and the solvent removed under reduced pressure, leaving a brown oil, from which no products could be identified.

4.5.3 Attempted reaction of $Ta(NMe_2)_5$ and $C_5H_5(CH_2)_3N(H)Me$, 1.1

A solution of $Ta(NMe_2)_5$ (0.60g, 1.5mmol) in toluene (20ml), or hexane (20ml), was cooled to –40°C. Neat $C_5H_5(CH_2)_3N(H)NMe$, **1.1**, (0.21g, 1.5mmol) was added dropwise and the solution allowed to warm to room temperature. The mixture was stirred for 48hr producing a partially soluble dark red suspension. An aliquot (1ml) was taken, analysis of which showed no identifiable products. Reflux of the solution over several days also gave no identifiable products.

4.5.4 Preparation of Ta[η^5:η^1-$C_5H_4(CH_2)_3NMe$](N^{t}Bu)(NH^{t}Bu) 4.1

A solution of $[TaCl_2(N^tBu)(NH^tBu)(NH_2^tBu)_2]_2$ (2.81g, 3mmol) in THF (30ml) was cooled to -78°C (acetone/dry ice). A suspension of [η^5:η^1-$C_5H_4(CH_2)_3NMe$]Li_2, **1.3**, (0.89g, 6.0mmol) in THF (30ml) at -78°C was added dropwise with vigorous stirring. The solution was slowly warmed to room temperature (2hr) and stirred for 48hr. The solvent was removed under reduced pressure and the product was extracted into hexane (2 x 20ml). The colourless solution was filtered from the LiCl (0.51g, 12mmol, 2 eq. based on **1.3**) and the solvent was removed under reduced pressure giving a crude mixture of products. Distillation onto a sublimation probe at -196°C (60-65°c, 0.01mmHg) gave pure Ta[η^5:η^1-$C_5H_4(CH_2)_3NMe$](N^{t}Bu)(NH^{t}Bu), **4.1**, (1.71g, 4.6mmol, 76% yield) as a colourless oil.

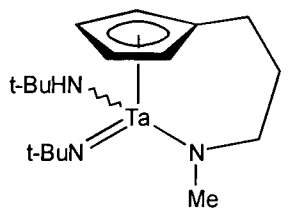

Data characterising 4.1

Description: Colourless oil. Sublimes 60-65°C, 10^{-3}mmHg
EI mass spec: m/z = 458 $[\mathbf{4.2}]^+$ with correct isotope distribution
Infra-red: 3347 (N-H); 2958-2783 (aliphatic C-H); 1267-1175 (C-H bends of C_5H_4)
Elemental analysis: Found ($C_{17}H_{32}N_3Ta$ requires); C:44.4(44.4); H:7.0(6.8); N:8.3(9.1)

^{1}H NMR: δ/ppm, 250 MHz, C_6D_6

6.30 [q,1H, $^3J_{HH}$=2.4Hz, (C_5H_4)]
5.52 [q, 1H, $^3J_{HH}$=2.6Hz, (C_5H_4)]
5.40 [q, 1H, $^3J_{HH}$=2.5Hz, (C_5H_4)]
5.29 [q, 1H, $^3J_{HH}$=2.4Hz, (C_5H_4)]
3.83 [br s, 1H, NH)]
3.74 [s, 3H, NCH_3)]
2.99 [m, 1H, (NC<u>H</u>H)]
2.70 [m, 1H, (NCH<u>H</u>)]
2.39 [m, 1H, (C_5H_4C<u>H</u>H)]
2.21 [m, 1H, (C_5H_4CH<u>H</u>)]
1.62 [m, 1H, (CH_2C<u>H</u>HCH_2)]
1.51 [m, 1H, (CH_2CH<u>H</u>CH_2)]
1.42 [s, 9H, (NC<u>Me</u>$_3$)]
1.35 [s, 9H, (NHC<u>Me</u>$_3$)]

^{13}C{^{1}H} NMR: δ/ppm, 62.5 MHz, C_6D_6

125.9 (C_5H_4 ipso)
111.2 (C_5H_4)
105.4 (C_5H_4)
102.3 (C_5H_4)
99.2 (C_5H_4)
64.0 (N<u>C</u>Me$_3$)
58.4 (NCH_2)
57.6 (NMe)
54.0 (NH<u>C</u>Me$_3$)
34.9 (NC<u>Me</u>$_3$)
34.3 (NHC<u>Me</u>$_3$)
30.8 (C_5H_4<u>C</u>H_2)
27.9 (CH_2<u>C</u>H_2CH_2)

4.5.5 Preparation of $Nb[\eta^5:\eta^1\text{-}C_5H_4(CH_2)_3NMe](N^tBu)(NH^tBu)$, 4.2

A solution of $[NbCl_2(N^tBu)(NH^tBu)(NH_2{}^tBu)_2]_2$ (2.28g, 3mmol) in THF (30ml) was cooled to -78°C (acetone/dry ice). A suspension of $[\eta^5:\eta^1\text{-}C_5H_4(CH_2)_3NMe]Li_2$, **1.3**, (0.89g, 6.0mmol) in THF (30ml) at -78°C was added dropwise with vigorous stirring. The solution was slowly warmed to room temperature (2hr) and stirred for 48hr. The solvent was removed under reduced pressure and the product extracted into hexane (2 x 20ml). The yellow solution was filtered from the LiCl (0.51g, 12mmol, 2eq. based on **1.3**) and the solvent removed under reduced pressure giving a crude mixture of products. Distillation onto a sublimation probe at -196°C (60-65°c, 10^{-3}mmHg) gave pure $Nb[\eta^5:\eta^1\text{:-}C_5H_4(CH_2)_3NMe](N^tBu)(NH^tBu)$, **4.2**, (1.71g, 4.6mmol, 76% yield) as a viscous yellow oil.

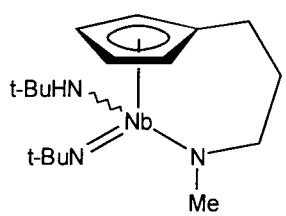

Data characterising 4.2

Description: Yellow oil. Sublimes 62°C, 10^{-3}mmHg
EI mass spec: m/z = 371 $[\mathbf{4.2}]^+$ with correct isotope distribution
Infra-red: 3352 (N-H); 2964-2753 (aliphatic C-H); 1242-1134 (C-H bends of C_5H_4)
Elemental analysis: Found ($C_{17}H_{32}N_3Nb$ requires): C:53.4(55.0); H:8.4(8.6); N;11.2(11.3)

^{1}H NMR: δ/ppm, 250 MHz, C_6D_6

6.25 [q,1H, $^3J_{HH}$=2.6Hz, (C_5H_4)]
5.63 [q, 1H, $^3J_{HH}$=2.5Hz, (C_5H_4)]
5.46 [q, 1H, $^3J_{HH}$=2.4Hz, (C_5H_4)]
5.35 [q, 1H, $^3J_{HH}$=2.5Hz, (C_5H_4)]
4.48 [br s, 1H, NH)]
3.67 [s, 3H, NMe]
2.99 [m, 1H, (NCHH)]
2.63 [m, 1H, (NCHH)]
2.44 [m, 1H, (C_5H_4CHH)]
2.25 [m, 1H, (C_5H_4CHH)]
1.66 [m, 1H, (CH_2CHHCH_2)]
1.49 [m, 1H, (CH_2CHHCH_2)]
1.39 [s, 9H, ($NCMe_3$)]
1.28 [s, 9H, ($NHCMe_3$)]

^{13}C{^{1}H} NMR: δ/ppm, 100 MHz, C_6D_6

126.3 (C_5H_4 ipso)
110.9 (C_5H_4)
106.0 (C_5H_4)
101.9 (C_5H_4)
99.6 (C_5H_4)
65.1 ($NCMe_3$)
59.1 (NCH_2)
57.6 (NMe)
53.9 ($NCHMe_3$)
34.8 ($NCMe_3$]
33.1 ($NHCMe_3$]
30.5 ($C_5H_4CH_2$)
28.1 ($CH_2CH_2CH_2$)

4.5.6 Preparation of dimers

Following sublimation of the tantalum and niobium complexes, **4.1** and **4.2** respectively, a pale yellow involatile residue was left behind. Spectroscopic analysis indicated that the dimers $\{M[\mu\text{-}\eta^5\text{:}\eta^1\text{-}C_5H_4(CH_2)_3NMe](\mu\text{-}N^tBu)(NH^tBu)]_2$ or $\{M[\eta^5\text{:}\eta^1\text{-}C_5H_4(CH_2)_3NMe](\mu\text{-}N^tBu)(NH^tBu)\}_2$ (M = Ta, Nb) had formed. Due to small amounts of **4.1** and **4.2** and other impurities in the residue isolation of the pure product was not possible, and full characterisation was not obtained. Attempts to crystallise the dimers from pentane were unsuccessful.

Data characterising Ta dimer

^{1}H NMR: δ/ppm, 250 MHz, C_6D_6

5.89 [br t, 2H, (C_5H_4)]
5.64 [br t, 2H, (C_5H_4)]
3.76 [br s, 3H, (NCH_3)]
2.43 [br m, 2H, (NCH_2)]
2.25 [br m, 2H, ($C_5H_4C\underline{H_2}$)]
1.53 [br m, 2H, ($CH_2C\underline{H_2}CH_2$)]
ca. 1.4 [NH^tBu, N^tBu obscured by **4.1**]

Data characterising Nb dimer

^{1}H NMR: δ/ppm, 250 MHz, C_6D_6

5.77 [br t, 2H, (C_5H_4)]
5.62 [br t, 2H, (C_5H_4)]
3.82 [br s, 3H, (NCH_3)]
2.40 [br m, 2H, (NCH_2)]
2.35 [br m, 2H, ($C_5H_4C\underline{H_2}$)]
1.44 [br m, 2H, ($CH_2C\underline{H_2}CH_2$)]
ca. 1.4 [NH^tBu, N^tBu obscured by **4.2**]

4.6 References

1 S. Scheuer, J. Fischer and J. Kress, *Organometallics,*1995, **14**, 2627.

2 K. Mashima, S. Fujikawa, Y. Tanaka, H. Urata, T. Oshiki, E. Tanaka and A. Nakamura, *Organometallics,* 1995, **14**, 2633.

3 M.J. Bunker, A. De Cian, M.L.H. Green, J.J.E. Moreau and N. Siganporia, *J. Chem. Soc., Dalton Trans.,* 1980, 2155.

4 a) D.N. Williams, J.P. Mitchell, A.D. Poole, U. Siemeling, W. Clegg, D.C. Hockless, P.A. O'Neill and V.C. Gibson, *J. Chem. Soc., Dalton Trans.,* 1992, 739. b) J. Sundermeyer and D. Runge, *Angew. Chem., Int. Ed. Engl.,* 1994, **33**, 1255.

5 A.D. Jenkis, M.F. Lappert, R.C. Srivastava, *J. Organomet. Chem.,* 1970, **23**, 165.

6 a) D.S. Breslow, *Chem. Abstr.*, 1960, **54**, 507; b) G.L. Kaprinka and W.L. Carrick, *J. Polym. Sci.*, 1961, **55**, 145.

7 D.A. Lemenovskii, V.P. Fedin, A.V. Aleksandrov, Y.L. Slovohotov and Y.T. Struchkov, *J. Organomet. Chem.,* 1980, **201**, 257.

8 A.N. Chernega, M.L.H. Green and A.G. Saurez, *Can. J. Chem.,* 1995, **73**, 1.

9 A. Antinolo, M. Martinez-Ripoll, Y. Mugnier, A. Otero, S. Prashar and A.M. Rodriquez, *Organometallics*, 1996, **15**, 3241.

10 N.J. Bailey, M.L.H. Green, M.A. Leech, J.F. Saunders and H.M. Tidswell, *J. Organomet. Chem.,* 1997, **538**, 111.

11 a) D.M. Antonelli, M.L.H. Green and P. Mountford, *J. Organomet. Chem.,* 1992, **438**, C4-C8; b) D.M. Antonelli, P.T. Gomes, M.L.H. Green, A.M. Martins, P. Mountford, *J. Chem. Soc., Dalton Trans.,* 1997, 2435.

12 W.A. Herrmann, W. Baratta, *J. Organomet. Chem.,*1996, **506**, 357.

13 S.M.B. Marsh, Ph. D. Thesis, University of Durham, 1997; b) A.K. Hughes, Postdoctoral Report, University of Groningen, 1992.

14 D.C. Bradley and M.H. Gilitz, *J. Chem. Soc.*, (A), 1969, 980.

15 a) D.C. Bradley and I.M. Thomas, *Can. J. Chem.,* 1962, **40**, 449; b) D.C. Bradley and M.H. Chrisholm, *J. Chem. Soc.* (A), 1971, 1511.

16 C.E. Heath and M.B. Hursthouse, *J. Chem. Soc., Chem. Commun.*, 1971, 143

17 D.C. Bradley and M.H. Chisholm, *Acc. Chem. Res.,* 1976, **9**, 273.

18 P.A. Bates, A.J. Nielson, J.M. Waters, *Polyhedron.*, 1985, **8**, 1391.

19 A.J. Neilson, *Polyhedron,* 1988, **7**, 67.

20 W.A. Nugent and R.L. Harlow, *J. Chem. Soc., Chem. Commun.*, 1978, 579.

21 a) T.C. Jones, A.J. Nielson and C.E. F. Pickard, *J. Chem. Soc., Chem. Commun.*, 1984, 205; b) P.A. Bates, A.J. Nielson and J.M. Waters, *Polyhedron,* 1985, **4**, 1391.

Chapter 5

Chromium and Vanadium Amide Functionalised Cyclopentadienyl Complexes.

5.1 Introduction

Among the transition metals that catalyse the polymerisation of olefins, chromium occupies a prominent position. Broadly speaking, two classes of chromium-based heterogeneous catalysts are used commercially. The so-called Phillips catalyst is prepared by deposition of CrO_3 on silica followed by activation with hydrogen,[1] and is commercially more important than Ziegler-Natta catalysts. On the other hand, Union Carbide has developed catalysts formed by the treatment of silica with low-valent organometallic compounds, most notably chromocene, $Cr(C_5H_5)_2$.[2] The species thus generated is thought to retain one cyclopentadienyl ligand, which is not incorporated into the growing polymer chain. Questions about the chemical nature of the active site(s), the oxidation state of the active chromium, and the mechanism of initiation have been the subject of a longstanding debate to this day.[3]

Despite the commercial significance of chromium based ethylene polymerisation catalysts, investigations into their chemistry on a molecular level remain grossly outnumbered by studies of Ziegler-Natta catalysts containing d^0, Group 4 elements. Much of the known organometallic chemistry of chromium concerns low-valent carbonyl derivatives and/or diamagnetic complexes with 18-electron configurations.[4] Such molecules are unlikely candidates for modelling highly reactive (coordinatively unsaturated) and oxide-supported alkylchromium compounds.

Likewise, the chemistry of vanadium hydrocarbyl complexes is poorly developed compared to that of most other transition metals. The reason for this probably lies both in the fact that vanadium has the tendency to form paramagnetic V(III) and V(IV) complexes that are not easily studied by NMR spectroscopy and that vanadium hydrocarbyl complexes tend to be thermally quite labile. Silica-supported vanadium complexes have attracted attention as olefin polymerisation catalysts because of their excellent hydrogen response and high comonomer incorporation allowing greater control over the properties of the polymer.[5] Low-valent vanadium surface species have been implicated as active sites in many of these systems.[6]

On the basis that the general notion that open-shell (paramagnetic organometallics or "metallaradicals") may be more reactive, and thus more appropriate, models for catalytic intermediates, Chapter 5 aims to explore the reactivity of a class of paramagnetic chromium(III) and vanadium(III) chloro complexes. Organometallic derivatives of chromium in this oxidation state have been reported previously,[7] but their limited stability and paramagnetic nature have prevented the development of their chemistry.

5.1.1 Cyclopentadienyl complexes

Recently Theopold and coworkers have explored the reactivity of paramagnetic alkylchromium (III) compounds as catalytic intermediates and found that the availability of a coordination site for olefin polymerisation proved crucial. Their first highly active catalyst to be discovered was the cationic complex $[CrCp^*(THF)_2CH_3]^+BPh_4^-$. The mechanism for the polymerisation was probed in some detail and involves the dissociation of a THF ligand generating a 13 electron complex and opening up of a coordination site, which rapidly undergoes multiple insertions of ethylene. The polymer was found to have narrow molecular weight distribution and exhibited little branching. It was suggested that the trivalent chromium was probably responsible for the activity of the catalyst. Further work found that $CrCp^*(THF)(Bz)_2$ and $Li[CrCp^*(Bz)_3]$ were also active catalyst precursors. As these three complexes include a cation, a neutral complex, and an anion then the charge on the chromium cannot be an important variable.

Initially the majority of vanadium complexes reported were bis-cyclopentadienyl V(III) and V(IV), Cp_2V, Cp^*_2V and Cp_2VR_2 (R = hydrogen, alkyl, aryl, σ-allyl, benzyl, alkynyl; $Cp^* = \eta^5\text{-}C_5Me_5$). Complexes of this type were not found to be active olefin polymerisation catalysts, for example $(\eta^5\text{-}C_5Me_5)_2VH$ does not react with ethylene at pressures up to 17atm. Recently attention has turned to half-sandwich imido vanadium complexes, CpV(NR) (R = alkyl or aryl), due to their isolobal relationship with the Group 4 metallocene fragments $[MCp_2]$ (M = Ti, Zr and Hf). This relationship is discussed in Chapter 4 regarding niobium and tantalum complexes.

5.1.2 Nitrogen functionalised cyclopentadienyl complexes

In a quest to generate a new family of chromium-based copolymerisation catalysts Theopold and co-workers synthesised and characterised the first constrained-geometry chromium alkyl complexes. By reacting $[C_5Me_4SiMe_2N^tBu]Li_2$ with a suspension of $CrCl_3(THF)_3$ in THF the dark green complex, $Cr(\eta^5:\eta^1\text{-}C_5Me_4SiMe_2N^tBu)(THF)Cl$, **A**, was produced (figure 5.1). Alkylation of this starting material with various alkyl lithium salts yielded a new class of chromium(III) alkyls, **B**, **C**, **D** and **E** (figure 5.1), and the only functionalised cyclopentadienyl complexes of chromium. Depending on steric bulk of the alkyl group, the complexes either retained or lost the THF ligand.

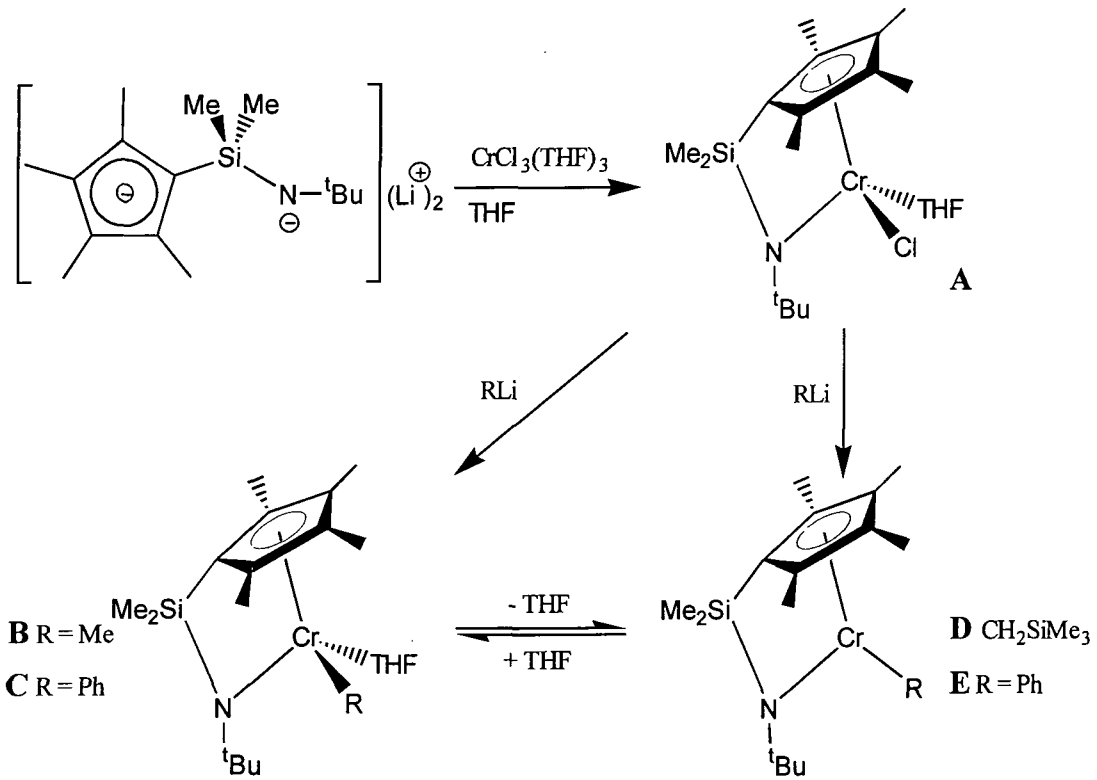

Figure 5.1

Complexes **D** and **E** belong to a new class of coordinatively unsaturated chromium(III) alkyl complexes that fulfil the previously established minimum requirements for ethylene polymerisation, namely a chromium(III)-carbon σ-bond and coordinative unsaturation (i.e. pseudo-five-coordination in a cyclopentadienyl complex). In the X-ray structure of **D**, an angle of 115.9° is observed for the $Cp_{centroid}$-Cr-N angle giving an indication of the "openness" of the structure i.e. the anticipated site of catalytic activity.

Accordingly complex **E** catalyses the polymerisation of ethylene, with high quantities of polyethylene being produced at room temperature and 500psi, in both toluene and 1:1 toluene:hexane solutions. Although attempts at polymerising propene were unsuccessful, monitoring of the reaction showed that an olefin dimerisation reaction was occurring with complete conversion to 2-methyl-1-pentene being observed over several hours. The reaction of **D** with 1-hexene not only gave the expected product of head-to-tail dimerisation, i.e. 2-butyl-1-octene but also a mixture of isomeric internal hexenes. Thus **D** not only catalyses olefin polymerisation, but also the dimerisation and isomerisation of olefins as well, which may also have applications in organic synthesis. Furthermore, both the dimerisation and isomerisation were accelerated by the addition of hydrogen. On the basis of these observations, it was suggested that the actual catalyst may be the hydride $[Cr(\eta^5:\eta^1\text{-}C_5Me_4SiMe_2N^tBu)H)]_n$, small quantities of which may be formed by β-elimination from $(\eta^5:\eta^1\text{-}C_5Me_4SiMe_2N^tBu)CrCH_2CH_2CHRCH_2SiMe_3$, i.e. the product of insertion of an olefin in the chromium-carbon bond.

5.1.3 Aims

Our aim was to synthesise geometrically constrained chromium(III) complexes with the ligand system, $C_5H_5(CH_2)_3N(H)Me$, **1.1**, and also to attempt to extend the study to their vanadium analogues. From these systems, reactions could then be carried out and potential catalytic precursors synthesised, e.g. the chromium(III) and vanadium(II) alkyl analogues.

5.2 Reaction of $MCl_3(THF)_3$ (M = Cr, V) and $[\eta^5:\eta^1\text{-}C_5H_4(CH_2)_3NMe]Li_2$, 1.3

In order to prepare geometrically constrained coordinatively unsaturated chromium(III) and vanadium(III) alkyl complexes of the ligand, $C_5H_5(CH_2)_3N(H)Me$, **1.1**, the substituted metal chloro complexes had to be synthesised initially. These were prepared from the reaction of the chromium and vanadium chloro complexes, $MCl_3(THF)_3$ and the dilithiated ligand, $[C_5H_4(CH_2)_3NMe]Li_2$, **1.3**. $MCl_3(THF)_3$ (M = Cr or V), was prepared in high yield from the soxhlet extraction of commercial chromium and vanadium trichlorides with tetrahydrofuran. Removal of the solvent followed by washing with hexane yielded $CrCl_3(THF)_3$ as a pink/purple powder and $VCl_3(THF)_3$ as a pink/brown powder.

5.2.1 Reaction between $CrCl_3(THF)_3$ and $[\eta^5:\eta^1\text{-}C_5H_4(CH_2)_3NMe]Li_2$, 1.3

The addition of $[\eta^5:\eta^1\text{-}C_5H_4(CH_2)_3NMe]Li_2$, **1.3**, in THF to a suspension of $CrCl_3(THF)_3$ in THF, at low temperature, gave an immediate colour change from purple to blue/green, and on stirring for two days at ambient temperature a dark blue solution formed. The product was found to be insoluble in less polar solvents such as hexane and only partially soluble in moderately polar solvents such as toluene, and therefore multiple hot toluene extractions were used. On cooling the solution, thin, square, dark blue plate-like crystals formed. Unfortunately, despite numerous attempts at recrystallisation, each plate contained a number of very thin crystals which were too thin (<0.1mm) for X-ray diffraction studies to be carried out.

As expected, a number of problems were encountered in the characterisation of such complexes, that made structure assignment appreciably more difficult than for other complexes described in this thesis. The paramagnetism of such Cr(III) complexes makes NMR-spectroscopy considerably less useful, with the ^1H NMR resonances usually being very broad ($\Delta\nu_{1/2}$ of 300-7000Hz) and chemical shifts varying over a wide range (±1200ppm). Relaxation phenomena may also cause resonances to be unobservable.[8] In favourable cases, when resonances are sufficiently well separated ^1H NMR can be used to

check sample purity and in some complexes stoichiometry of the complex may be obtained as well.

Attempts at ^1H NMR analysis of the complex in C_7D_8 were made, using a spectrometer with a large spectral width and fast scanning. The partial solubility and rather complicated ligand system meant that although some small broad resonances were observed, assignment of them was impossible. For this reason, characterisation of such paramagnetic compounds often relies heavily on functional group identification by elemental analysis, infra-red and mass spectroscopy, to determine the stoichiometry of the compounds.

An infra-red spectrum of a KBr disc of the complex provided evidence for the presence of an amide functionalised cyclopentadienyl chromium system. Absorbances in the region 897-1063cm^{-1} and a strong band at 822cm^{-1} are evident of the C-H bends of the cyclopentadienyl ring and stretches in the aliphatic region, between 2793-2975cm^{-1}, are evident of the trimethylene backbone. Further, no N-H stretches were observed, therefore indicating an attached amide group. Metal chloride stretches occur at low wavenumbers (<200cm^{-1}) no Cr-Cl stretching frequencies were observed (the spectrometer records a minimum of 450cm^{-1}). The product being of a crystalline nature, elemental analysis proved invaluable for characterisation, with recorded C, H, and N values being within 0.2% of calculated values for Cr[η^5:η^1-$C_5H_4(CH_2)_3NMe$]Cl, **5.1** (figure 5.2).

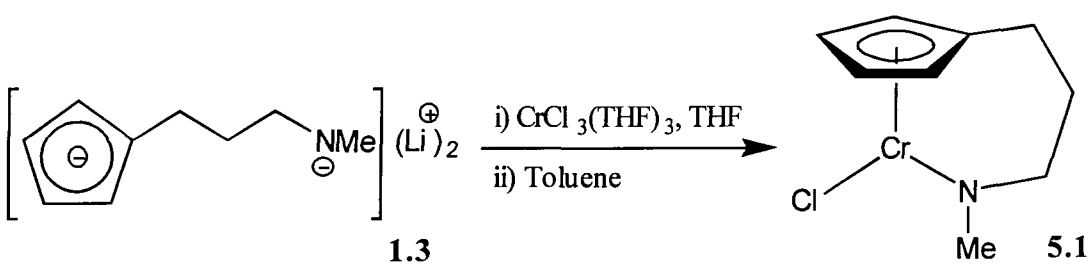

1.3 **5.1**

Figure 5.2

The mass spectrum of the complex shows evidence for Cr[η^5:η^1-$C_5H_4(CH_2)_3NMe$]Cl being the dimer, {Cr[η^5:η^1-$C_5H_4(CH_2)_3NMe$](μ-Cl)}$_2$, where the two chromium atoms are assumed to be joined by two bridging chlorides (figure 5.3). Although no peaks were observed for the actual dimer itself (m/e = 445), presumably due to bridging chlorides

forming weak covalent interactions and therefore easily breaking up to form a monomer, peaks were observed for the chromium dichloride cation, $[Cr(CpNMe)Cl_2]^+$ with a mass of m/e = 258 (figure 5.4). A mass of m/e = 223 corresponds to the monomer $[Cr(CpNMe)Cl]^+$, while further peaks at m/e = 186, 136 and 52 correspond to the break up of the monomer into the cations $[Cr(CpNMe)]^+$, $[CpNMe]^+$, and $[Cr]^+$ respectively.

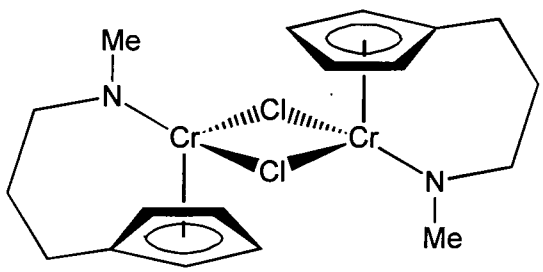

Figure 5.3: 5.1 shown in the form of a dimer

Some metal chloride complexes, particularly those that are electronically and coordinatively unsaturated, form bridging chlorides in the form of a dimer. Theopold and coworkers found that many of their coordinatively unsaturated chromium complexes were dimers. For example the molecular structures of Cp*CrCl and $Cp^*Cr(CH_2C_6H_5)Cl$ were found to be $[Cp^*Cr(\mu\text{-}Cl)Cl]_2$,[9] and $[Cp^*Cr(CH_2C_6H_5)(\mu\text{-}Cl)]_2$,[10] respectively. Both complexes were found to be representative of a class of dimeric chromium (III) chloro and/or alkyl complexes, and most were found to be blue or purple.

Unlike $Cr[\eta^5:\eta^1\text{-}C_5Me_4SiMe_2N^tBu](THF)Cl$ (figure 5.1, **A**) which is produced with one THF ligand coordinated, evidence suggests that all three THF ligands have been displaced in **5.1**, presumably due to the trimethylene backbone forming a ligand system with a larger bite angle. With **5.1** therefore being more coordinatively and electronically unsaturated it is more likely to form the dimer (figure 5.3). The same elemental analysis results would also be observed and no observable differences would be seen in the infra-red spectrum. It was concluded that $[\eta^5:\eta^1\text{-}C_5H_4(CH_2)_3NMe]Li_2$ had reacted with $CrCl_3(THF)_3$ displacing all three THF ligands and formation of two equivalents of lithium chloride, forming an amide functionalised cyclopentadienyl complex, **5.1**, as a dimer with two bridging chloride ligands.

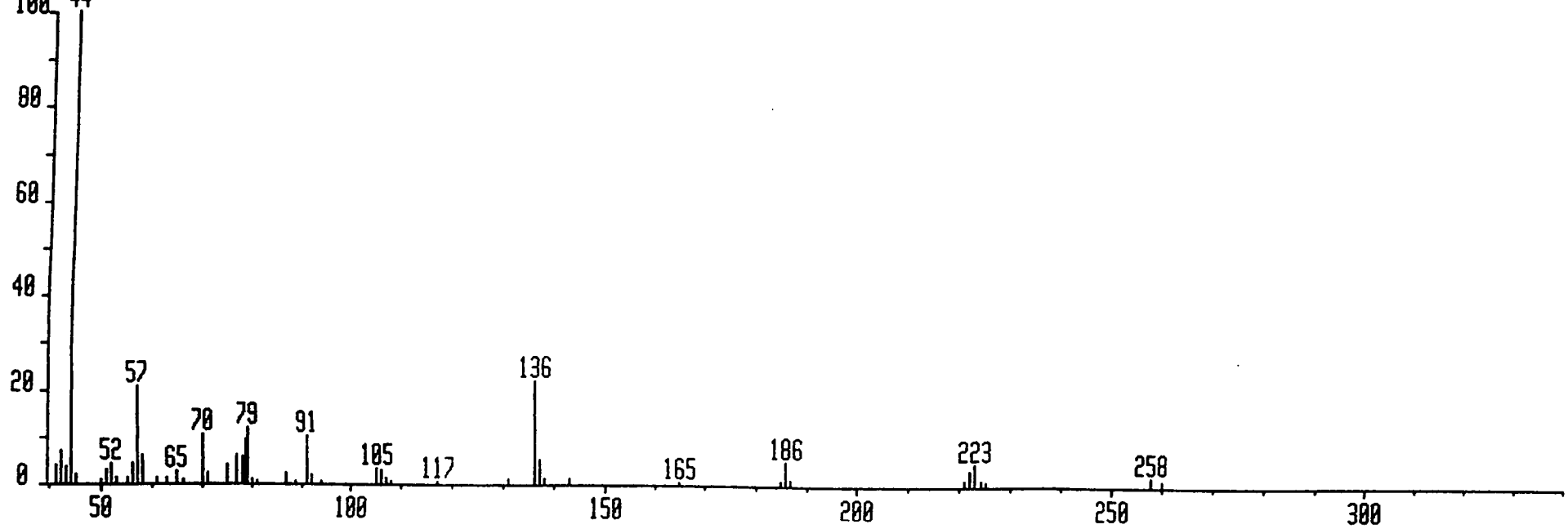

Figure 5.4 EI mass spectrum of **5.1**

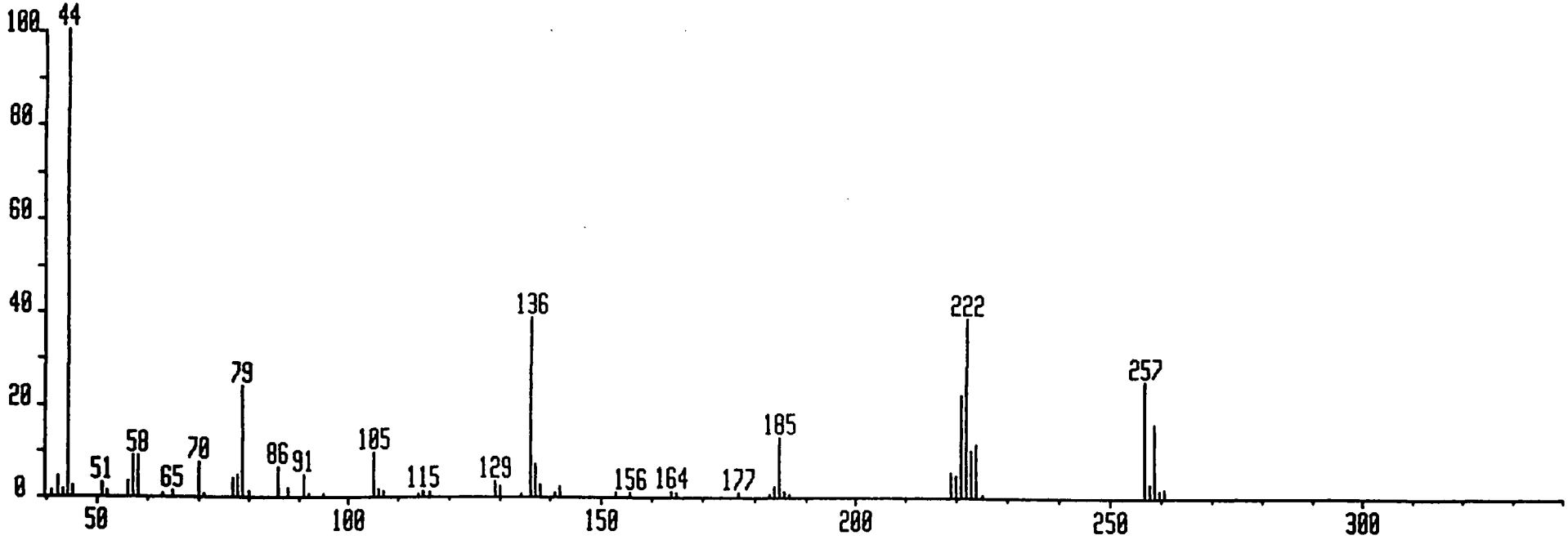

Figure 5.6 EI mass spectrum of **5.2**

5.2.2 Reaction between $VCl_3(THF)_3$ and $[\eta^5:\eta^1:C_5H_4(CH_2)_3NMe]Li_2$, 1.3

In an attempt to synthesise the vanadium analogue of **5.1**, the reaction of $VCl_3(THF)_3$ and $[\eta^5:\eta^1:C_5H_4(CH_2)_3NMe]Li_2$, **1.3**, was carried out in a similar manner. On addition, a colour change from pink to purple was observed, and upon stirring for two days a dark green solution was produced. Again the product was found to be insoluble in hexane but was more soluble in toluene, forming a purple solution. The colour changes from purple to green and back to purple are indicative of purple/green dichroism. On cooling the solution $V[\eta^5:\eta^1\text{-}C_5H_4(CH_2)_3NMe]Cl$, **5.2**, was produced as a purple microcrystalline solid.

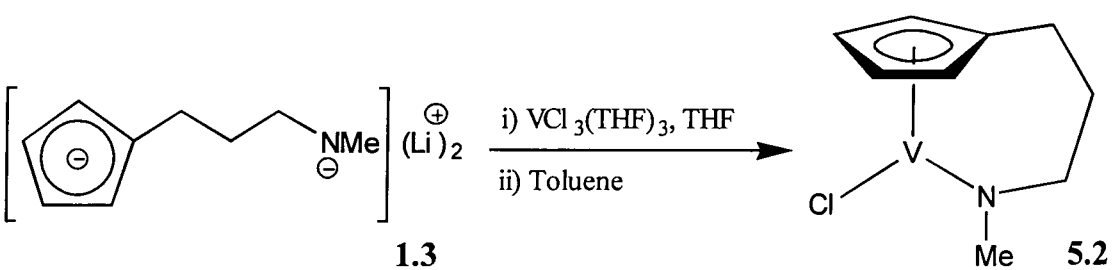

1.3 **5.2**

Figure 5.5

Despite being more soluble than the chromium species, **5.1**, ^1H NMR spectroscopic studies of the vanadium complex in C_7D_8 were unsuccessful, due to the paramagnetic nature of the complex. Although some small broad resonances were observed, assignment was not possible. Evidence for an amide functionalised cyclopentadienyl complex was obtained from infra-red spectroscopy. An IR spectrum of a KBr disc of the complex, shows strong bands at 796, 1030 and 1493cm^{-1} which were assigned to the C-H bends of the cyclopentadienyl ring. Stretches in the region 2853-2921cm^{-1} could be assigned to aliphatic groups of the ligand, and like the spectrum of chromium complex, **5.1**, there is no evidence of an N-H stretch for an unattached amine group. Elemental analysis values close to those predicted for $V[\eta^5:\eta^1\text{-}C_5H_4(CH_2)_3NMe]Cl$, **5.2**, indicate that the vanadium analogue of the chromium complex, **5.1**, has been synthesised (figure 5.5).

Evidence from mass spectroscopy again suggested that like the chromium complex, **5.1**, $V[\eta^5:\eta^1\text{-}C_5H_4(CH_2)_3NMe]Cl$, **5.2**, is in the form of a dimer, $\{V[\eta^5:\eta^1\text{-}C_5H_4(CH_2)_3NMe](\mu\text{-}Cl)\}_2$. With vanadium being on the left of chromium in the periodic table, their atomic weights are ~51 and ~52 respectively. The mass spectrum of **5.2** is nearly identical to that of **5.1** with all the relevant peaks for the vanadium complex appearing 1a.m.u. lower than for the chromium complex (figures 5.6). Peaks were observed for the vanadium dichloride cation, $[V(CpNMe)Cl_2]^+$ at m/e = 257, with peaks for the monomer $[V(CpNMe)Cl]^+$ at m/e = 222. Further peaks corresponding to the break up of the complex were seen at m/e = 185, 135 and 51 for $[V(CpNMe)]^+$, $[CpNMe]^+$, and $[V]^+$ respectively.

From the above evidence it is clear that the reaction of the dianion $[\eta^5:\eta^1:C_5H_4(CH_2)_3NMe]Li_2$, **1.3**, and $VCl_3(THF)_3$ produces $V[\eta^5:\eta^1:C_5H_4(CH_2)_3NMe]Cl$, **5.2**, probably as the dimer, with bridging chloride groups. The reaction and the product is directly analogous to the chromium complex, **5.1**, and shows that a close link exists between Group 5 vanadium and Group 6 chromium chemistry. The vanadium complex, **5.1**, appears to be the first donor functionalised cyclopentadienyl vanadium complex, and one of relatively few vanadium (III) complexes to be studied and characterised.

5.3 Reactions of M[η^5:η^1-$C_5H_4(CH_2)_3NMe$]Cl (M = Cr, 5.1; V, 5.2)

The chromium and vanadium complexes, **5.1** and **5.2**, are both potential olefin polymerisation precursors. Like the catalyst precursor Cr[η^5:η^1-$C_5Me_4SiMe_2N^tBu$](THF)Cl described in the introduction (figure 5.1, **A**), the chromium complex Cr[η^5:η^1:$C_5H_4(CH_2)_3NMe$]Cl, **5.1**, has the potential to fulfil the criteria for organo-chromium catalysts, set by Theopold, namely a chromium(III)-carbon σ-bond with coordinative and electronic unsaturation. The reaction of **A** with various alkylating agents produced a number of chromium (III) alkyl complexes (figure 5.1, **B**, **C**, and **D**), one of which was studied and found to be an active olefin polymerisation catalyst (figure 5.1, **D**). It is therefore expected that **5.1** will form similar catalytically active alkyl complexes.

Likewise, the vanadium complex, **5.2**, being a coordinatively and electronically unsaturated vanadium(III) complex, it is also thought to have the potential to be an active catalyst when alkylated, forming a vanadium(III) alkyl complex. With both titanium(III) and chromium(III) complexes used in catalysis [titanium(III) in Ziegler Natta catalysis and chromium(III) as mentioned in the introduction], and these being adjacent to vanadium in the periodic table, it is thought that such vanadium(III) complexes will be. However, due to difficulties in synthesising and characterising such complexes, few studies have been carried out in this area in comparison.

Initially the chromium complex, **5.1**, was reacted with a number of alkylating reagents, with the aim of preparing active geometrically constrained chromium alkyl catalysts. To prevent β-hydrogen elimination from occurring once the chromium-alkyl bond had formed, alkylating reagents with no hydrogens on the β-carbon atom were used.

5.3.1 Reaction between $C_6H_5CH_2MgCl$ and $Cr[\eta^5:\eta^1\text{-}C_5H_4(CH_2)_3NMe]Cl$, 5.1

The addition of one equivalent of $C_6H_5CH_2MgCl$ to a solution of **5.1** in THF formed a violet solution. Extraction of the product into toluene gave a violet solution and a stoichiometric amount of magnesium chloride. On cooling, the chromium-benzyl complex $Cr[\eta^5:\eta^1\text{-}C_5H_4(CH_2)_3NMe](CH_2C_6H_5)$, **5.3**, precipitated as a violet powder (figure 5.7).

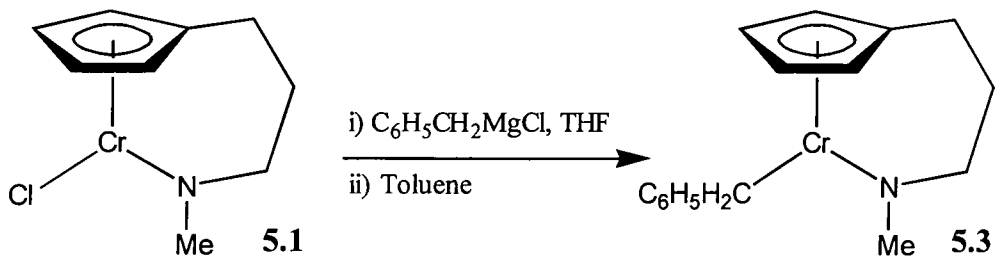

Figure 5.7

Elemental analysis of the complex gave values very close to those calculated for **5.3**, with both nitrogen and hydrogen values exactly the same as those calculated, and a carbon percentage within 0.4%. An infra-red spectrum of the product showed the presence of both aliphatic stretches in the region 2853 to 2922cm^{-1}, and bands 803 and 1030 to 1544cm^{-1} attributed to a cyclopentadienyl group. Although no masses for **5.3** were seen in the mass spectrum, such chromium alkyl complexes have been found to break up easily, e.g Cp_2CrR complexes often appears as the cation $[Cp_2Cr]^+$. Masses for the cations $[Cr(CpNMe)]^+$, $[CpNMe]^+$ and $[CH_2C_6H_5]^+$ were observed at m/e = 186, 136 and 91 respectively (figure 5.8).

There is no evidence to suggest that a THF ligand is coordinated, but such complexes have been found to retain or lose the THF ligand depending on the steric bulk of the alkyl group. For example in the similar chromium methyl complex, $Cr(\eta^5:\eta^1\text{-}C_5Me_4SiMe_2N^tBu)Me(THF)$ (figure 5.1, **B**) the solvent molecule is retained whereas with the bulkier (trimethylsilyl)methyl ligand the THF ligand is lost, $Cr(\eta^5:\eta^1\text{-}C_5Me_4SiMe_2N^tBu)CH_2SiMe_3$ (figure 5.1, **D**). Further examples have also been found in similar complexes (Chapter 1, section 1.2.2). Another factor is the trimethylene backbone

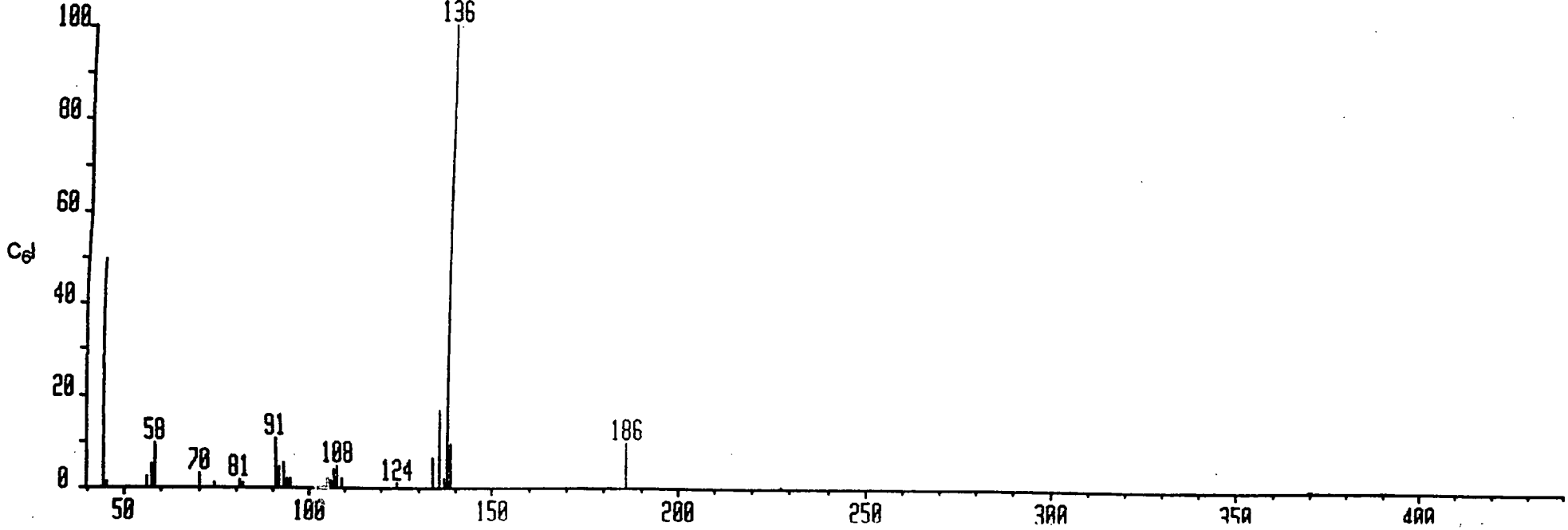

Figure 5.8 EI mass spectrum of **5.3**

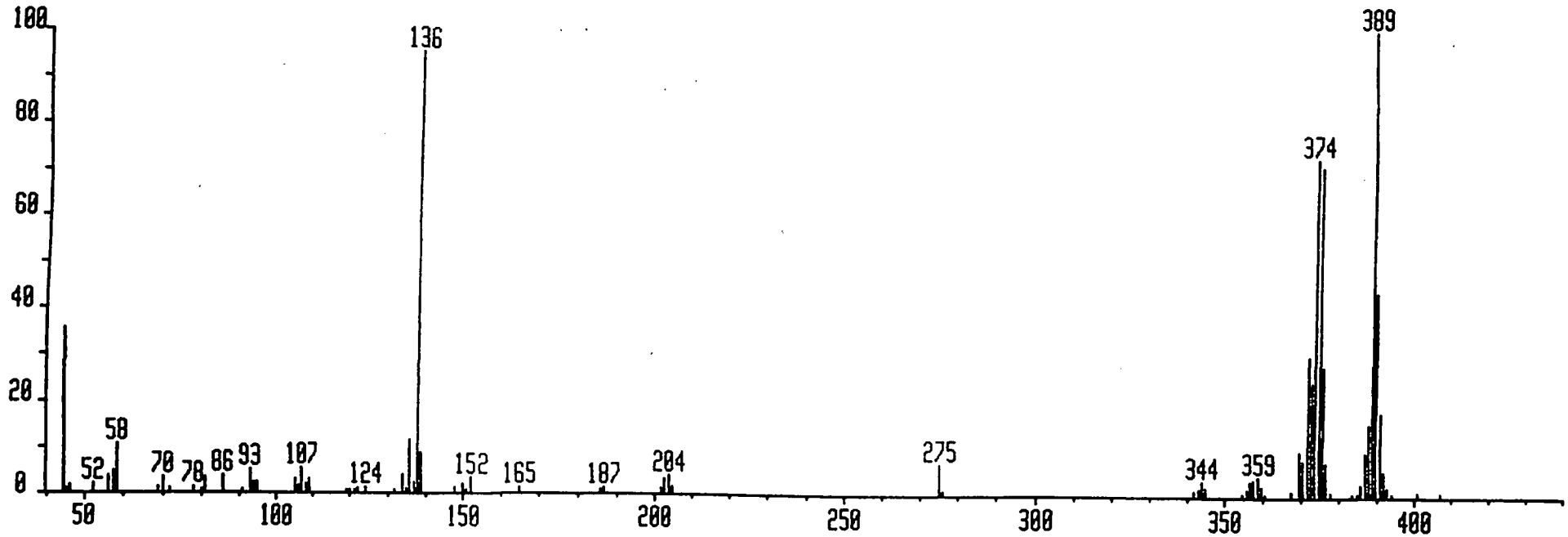

Figure 5.10 EI mass spectrum of **5.4**

of the ligand (link Z), which will form a complex with a larger bite angle than those with a two carbon link, or one silicon link like those mentioned earlier (figure 5.1). This in turn will form a less "open" structure adjacent to the Cr-N bond and therefore is less likely to coordinate a THF ligand. Therefore in **5.3** with a bulky benzyl substituent present, it is likely that the THF ligand will lost.

It is likely that the benzyl group in **5.3** will be bonded to the metal in an η^3 fashion but only X-ray and NMR data would data would be able to confirm this. Many similar benzyl complexes relieve their electronic and coordinative unsaturation by forming this allyl bond.

Complex **5.3** fits the description set by Theopold, for an active olefin polymerisation chromium catalyst, of a chromium(III)-carbon σ-bond and coordinative unsaturation (i.e. pseudo-five-coordination in a cyclopentadienyl complex). Like $Cr(\eta^{5}:\eta^{1}\text{-}C_5Me_4SiMe_2N^tBu)CH_2SiMe_3$ it would be expected to readily form the 13-electron cationic species, $Cr[\eta^{5}:\eta^{1}\text{-}C_5H_4(CH_2)_3NMe]^+$, in the presence of MAO, producing a sterically unencumbered coordination site available for olefin insertion. The absence of the THF ligand will also help facilitate binding of the olefin with polymerisation reactions found to be strongly inhibited by coordinated THF. The coordinatively unsaturated 13-electron complex, $[Cp^*Cr(THF)Me]^+$ is a highly active catalyst,[11] comparable to that of $CrCp_2/SiO_2$. However addition of THF forms the inactive 15-electron species, $[Cp^*Cr(THF)_2Me]^+$, and the rate of polymerisation at a constant chromium concentration was found to be inversely proportional to the THF concentration.

5.3.2 Reaction between MeLi and $Cr[\eta^5:\eta^1\text{-}C_5H_4(CH_2)_3NMe]Cl$, 5.1

The addition of one equivalent of methyl lithium to a solution of **5.1** in THF gave a dark red solution. The product was extracted into hexane from which a dark pink/red powder precipitated on cooling. An infra-red spectrum of the product, although not diagnostic, indicate the presence of both aliphatic stretches in the region 2829 to 2921cm^{-1}, and bands in the region 801 and 1020 to 1540cm^{-1} attributed to a cyclopentadienyl group. Elemental

analysis results gave values within 1% for the chromium methyl complex, and therefore $Cr[\eta^5:\eta^1\text{-}C_5H_4(CH_2)_3NMe]Cl$, **5.4**, was assigned as the product (figure 5.9).

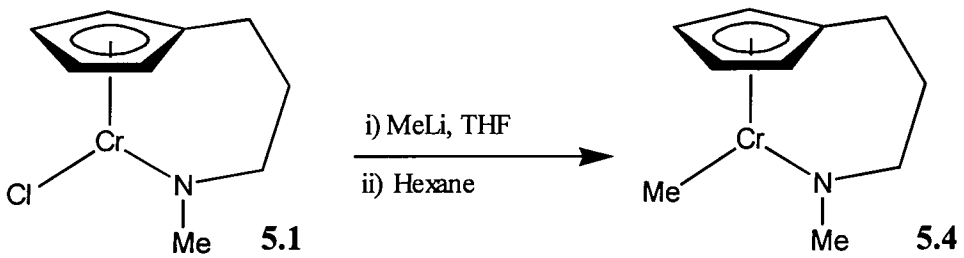

Figure 5.9

An insight into the possible structure of the complex came from the mass spectrum (figure 5.10). Although peaks for corresponding to the monomer, $[\mathbf{5.4}]^+$, and breakup into the fragments $[Cr(CpNMe)]^+$ and $[CpNMe]^+$ were observed at m/e = 202, 187, and 138 respectively, the largest peaks appear at higher masses, indicating that **5.4** is in the form of a dimer so that a chromium-chromium interaction exists. No peaks were observed for the complete dimer, but similar chromium alkyl complexes have also been found to dissociate easily (see **5.3**). Peaks corresponding to $[Cr_2(CpNMe)_2Me]^+$ and $[Cr_2(CpNMe)_2]^+$ at me = 389 and 374 respectively indicate that **5.4** may be the dimer $\{Cr[C_5H_4(CH_2)_3NMe](\mu\text{-}CH_3)\}_2$ (figure 5.11).

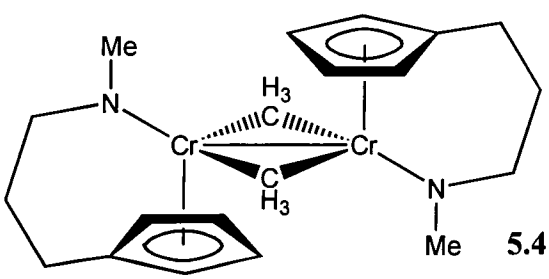

Figure 5.11 Complex **5.4** in the form of a dimer

Unlike the chromium methyl complex, $Cr(\eta^5:\eta^1\text{-}C_5H_4SiMe_2N^tBu)(CH_3)(THF)$ (figure 5.1, **B**), described by Theopold, where a coordinated THF ligand relieves the electronic and coordinative unsaturation, **5.4** appears to have no coordinated THF, but the electronic and coordinative unsaturation appears to be relieved in the form of a chromium-chromium interaction and bridging methyl groups. Metal-metal interactions have been observed in

similar cyclopentadienyl methyl chromium complexes. The dimer $[Cp^*Cr(CH_3)(\mu\text{-}CH_3)]_2$ was found to have a chromium-chromium distance of 2.606Å, while in $[Cp^*Cr(\mu\text{-}CH_3)]_2(\mu\text{-}CH_2)$ the Cr(III)-Cr(III) distance was found to be the shortest known at 2.39Å.[12] On the basis of theoretical analysis,[13] it is believed that significant metal-metal bonding occurs in these types of complexes. The key to forcing the metal atoms together appears to be the bridging ligands which engage in three-centre, two-electron bonding, (e.g. bridging methyls in these cases).[14] This core level effect increases the splitting of the frontier d orbitals, leading to pairing of electrons in MOs which are metal-metal bonding in character. Until recently Cr(III) complexes with bridging ligands were thought to exhibit repulsive interactions between the metal centres.[15]

Chromium-chromium interactions sometimes exist in bridging chloride complexes, although less commonly, e.g. $[CpCr(\mu\text{-}Cl)]_3(\mu\text{-}CH)$ where the Cr-Cr distances are 2.837Å and 2.793Å. Therefore, although less likely than in **5.4**, a chromium-chromium interaction cannot be ruled out in the dimer $\{Cr[\eta^5:\eta^1\text{-}C_5H_4(CH_2)_3NMe](\mu\text{-}Cl)\}_2$, **5.1** (figure 5.3).

If **5.4** is dimeric, it would be less electronically and coordinatively unsaturated than the chromium benzyl complex, **5.3**, and therefore seem less likely to be a suitable olefin polymerisation catalyst. However, depending on the strength of the dimer interactions, olefin insertion may be possible and therefore tests on the complex would be advantageous.

5.3.3 Attempted reaction between $LiBH_4$ and $Cr[\eta^5:\eta^1\text{-}C_5H_4(CH_2)_3NMe]Cl$, 5.1

In transition metal chemistry, alkali- or alkaline-earth metal borohydrides, usually $LiBH_4$ or $NaBH_4$, are commonly used as reagents in the synthesis of metal borohydrides and polyhydrides by reaction with metal halides. Such reactions have led to a wide structural range of complexes. For simple metal-borohydrides, the borane moiety can be attached to the metal centre in a number of ways. The most common is as a bidentate ligand $M(\eta^2\text{-}BH_4)$ but monodentate $M(\eta^1\text{-}BH_4)$ and tridentate bonding $M(\eta^3\text{-}BH_4)$ have also been observed (figure 5.12)

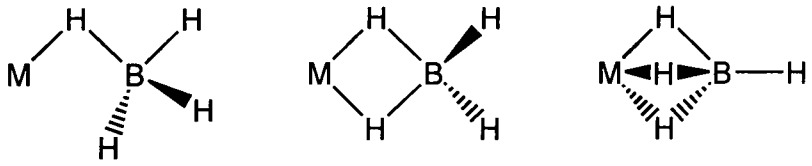

η^1-BH_4 η^2-BH_4 η^3-BH_4

Figure 5.12

It was hoped that such a metal borohydride complex could be prepared from the reaction of the chromium chloride group of **5.1** and $LiBH_4$. A similar reaction has previously been carried out on the complex $Zr[\eta^5:\eta^1\text{-}C_5H_4(CH_2)_3NMe]Cl_2(NHMe_2)$ producing a bis η^3-borohydride complex, $Zr[\eta^5:\eta^1\text{-}C_5H_4(CH_2)_3NMe](\eta^3\text{-}BH_4)_2$.

Three equivalents of lithium borohydride were added to a solution of **5.1** in THF, forming a purple solution. The product was extracted into toluene forming a dark green solution (like the synthesis of **5.2** this is another example of purple/green dichroism), from which a dark green solid precipitated at low temperature. Unfortunately identification of the product has so far been unsuccessful.

Unfortunately mass spectroscopy has not been able to identify the product with no masses above 137 occurring [that of the free ligand, $C_5H_5(CH_2)_3N(H)Me$], indicating possible break-up of the complex during analysis. Attempts to purify the compound from the minimum amount of toluene were also unsuccessful.

5.3.4 Attempted reaction between PMe_3 and $V[\eta^5:\eta^1\text{-}C_5H_4(CH_2)_3NMe]Cl$, 5.2

Theopold and coworkers found that some of their chromium(III) complexes also had a coordinated THF ligand (figure 5.1) which in some cases was reasonably labile, being able to coordinate reversibly to the chromium. The vanadium complex was reacted with an three equivalents of PMe_3, in toluene, in an attempt to add a strongly coordinating phosphine ligand. No colour change was observed during the reaction and ^{31}P NMR analysis of an aliquot showed that no reaction had occurred, even after heating the solution to 50°C.

5.4 Summary and Future Work

Reaction of $CrCl_3(THF)_3$ with the dianion, $[C_5H_4(CH_2)_3NMe]^{2-}$, **1.3**, gives an amide functionalised cyclopentadienyl complex as the dimer $\{Cr[\eta^5:\eta^1\text{-}C_5H_4(CH_2)_3NMe](\mu\text{-}Cl)\}_2$, **5.1**. The reaction can also be extended to Group 5, with the $VCl_3(THF)_3$ forming the first amide functionalised cyclopentadienyl vanadium complex, $\{V[\eta^5:\eta^1\text{-}C_5H_4(CH_2)_3NMe](\mu\text{-}Cl)\}_2$, **5.2**. Both the chromium(III) and vanadium(III) complexes are precursors to potential catalysts.

Reactions of the chromium complex with the alkylating reagents, $(C_6H_5CH_2)MgCl$ and CH_3Li, produced the corresponding chromium(III) alkyls, $Cr[\eta^5:\eta^1\text{-}C_5H_4(CH_2)_3NMe](\eta^3\text{-}CH_2C_6H_5)$, **5.3**, and the dimer $\{Cr[\eta^5:\eta^1\text{-}C_5H_4(CH_2)_3NMe\}(\mu\text{-}CH_3)\}_2$, **5.4**, respectively. **5.3** is a geometrically constrained, chromium(III) alkyl complexes, and fits the criteria set by Theopold, for chromium olefin polymerisation catalysts, with the cation, $Cr[\eta^5:\eta^1\text{-}C_5H_4(CH_2)_3NMe]^+$, the likely active species. In an attempt to make a chromium borohydride complex $LiBH_4$ was reacted with **5.1** but the product has not yet been fully characterised.

From these preliminary studies, it can be seen that there is much scope for further work with these complexes, despite their paramagnetic nature. The vanadium complex, **5.2**, has much potential for further reactions, especially with alkylating agents, to create new, exciting and possible active catalysts in the future. Work within the group is currently under way on the vanadium complex and with its chromium analogue, **5.2**. Tests within the research group are being carried into the catalytic activity of the chromium(III) benzyl complex, **5.3**.

5.5 Experimental

5.5.1 Preparation of $Cr[\eta^5:\eta^1\text{-}C_5H_4(CH_2)_3NMe]Cl$, 5.1

A suspension of $CrCl_3(THF)_3$ (2.30g, 6.0mmol) in THF (30ml) was cooled to -78°C (acetone/dry ice). A suspension of $[C_5H_4(CH_2)_3NMe]Li_2$, **1.3**, (0.89g, 6.0mmol) in THF (30ml) at -78°C was added dropwise with vigorous stirring. The mixture was warmed to room temperature (2hr) and stirred for 48hr forming a dark blue solution. The solvent was removed under reduced pressure and the product was extracted with hot toluene (3 x 100ml at 60°C). Removal of the solvent under reduced pressure yielded $Cr[\eta^5:\eta^1\text{-}C_5H_4(CH_2)_3NMe]Cl$, **5.1**, probably in the form of the dimer $\{Cr[C_5H_4(CH_2)_3NMe](\mu\text{-}Cl)\}_2$, (1.25g, 93% yield) as a dark blue crystalline solid. Pure **5.1** suitable for elemental analysis was obtained by recrystallisation from a toluene solution at -40°C.

Data characterising 5.1

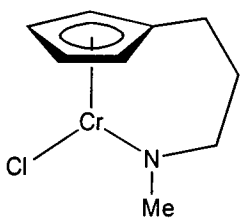

Description: Dark blue crystalline solid

Elemental analysis: Found ($C_9H_{13}NCrCl$ requires) C:48.6(48.5); H:6.0(5.8); N:6.3(6.3)

EI mass spec: m/z (intense peaks)

258 $[CrCl_2(CpNMe)]^+$
223 $[CrCl(CpNMe)]^+$
186 $[Cr(CpNMe)]^+$
136 $[CpNMe]^+$

Infra-red: ν/cm^{-1} (relevant bands)

3111 (aromatic C-H stretch)
2793-2975 (aliphatic C-H stretch)
822, 897-1489 (C-H bends of aromatic ring)

^{1}H NMR: δ/ppm, 250 MHz, C_7D_8: Partially soluble paramagnetic Cr(III) complex giving a broad unassignable spectrum.

5.5.2 Preparation of V]η^5:η^1-$C_5H_4(CH_2)_3NMe]Cl$, 5.2

A suspension of $VCl_3(THF)_3$ (2.24g, 6.0mmol) in THF (30ml) was cooled to -78°C (acetone/dry ice). A suspension of $[\eta^5:\eta^1\text{-}C_5H_4(CH_2)_3NMe]Li_2$, **1.3**, (0.89g, 6.0mmol) in THF (30ml) at -78°C was added dropwise with vigorous stirring. The mixture was warmed to room temperature (2hr) and stirred for 48hr, forming a dark green solution. The solvent was removed under reduced pressure and the product was extracted with toluene (2 x 20ml). Removal of the solvent under reduced pressure yielded $V[\eta^5:\eta^1\text{-}C_5H_4(CH_2)_3NMe]Cl$, **5.2**, possibly in the form of the dimer $\{V[C_5H_4(CH_2)_3NMe](\mu\text{-}Cl)\}_2$, (1.2g, 90% yield) as a purple crystalline solid. Pure **5.2** suitable for elemental analysis was obtained from recrystallisation of a toluene solution at -40°C.

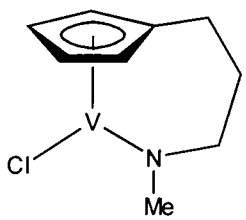

Data characterising 5.2

Description: Purple solid

Elemental analysis: Found ($C_9H_{13}NClV$ requires) C:49.6(48.8); H:6.3(5.9); N:5.9(6.3)

EI mass spec: m/z (intense peaks)

257 $[VCl_2(CpNMe)]^+$
222 $[VCl(CpNMe)]^+$
185 $[V(CpNMe)]^+$
136 $[CpNMe]^+$
51 $[V]^+$

Infra-red: ν/cm^{-1} (relevant bands)

3080 (aromatic C-H stretch)
2853-2921 (aliphatic C-H stretch)
796, 1030-1493 (C-H bends of aromatic ring)

^{1}H NMR: δ/ppm, 250 MHz, C_7D_8: Partially soluble paramagnetic V(III) complex giving a broad unassignable spectrum.

5.5.3 Preparation of $Cr[\eta^5:\eta^1\text{-}C_5H_4(CH_2)_3NMe](CH_2C_6H_5)$, 5.3

A solution of $C_6H_5CH_2MgCl$ (0.47ml of a 0.97M solution in THF, 0.46mmol) was added dropwise over 10mins.to a solution of **5.1** (0.10g, 0.45mmol) in THF (30ml) at -10°C (salt/ice bath). The mixture was stirred at room temperature for 24hr producing a violet suspension. The solvent was removed under reduced pressure and the product was extracted into toluene (3 x 20ml) and filtered leaving behind $MgCl_2$. Removal of the solvent under reduced pressure yielded $Cr\{C_5H_4(CH_2)_3NMe\}(CH_2C_6H_5)$, **5.3** probably as the η^3-bonded complex $Cr\{C_5H_4(CH_2)_3NMe\}(\eta^3\text{-}CH_2C_6H_5)$(0.11g, 89% yield) as a violet powder. Product suitable for elemental analysis was prepared from precipitation from the minimum amount of toluene at -40°C.

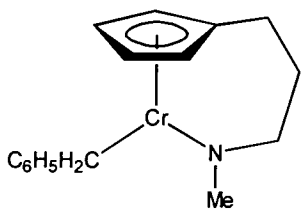

Data characterising 5.3

Description: Violet powder

Elemental analysis: Found ($C_{16}H_{20}NCr$ requires) C:68.6(69.0); H:7.2(7.2); N:5.0(5.0)

EI mass spec: m/z (intense peaks)

186 $[Cr(CpNMe)]^+$
136 $[(CpNMe)]^+$
91 $[CH_2C_6H_5]^+$
52 $[Cr]^+$

Infra-red: ν/cm^{-1} (relevant bands)

2853-2922 (aliphatic C-H stretch)
803, 1030-1544 (C-H bends of aromatic ring)

^{1}H NMR: δ/ppm, 250 MHz, C_6D_6: Paramagnetic Cr(III) complex giving a broad unassignable spectra.

5.5.4 Preparation of $Cr[\eta^5:\eta^1\text{-}C_5H_4(CH_2)_3NMe](CH_3)$ 5.4

A solution of CH_3Li (0.7ml of a 1.6M solution in THF, 1.1mmol, 1.1 x theory) was added dropwise over 10mins.to a solution of **5.1** (0.23, 1.0mmol) in THF (30ml) at -10°C (salt/ice bath). The mixture was stirred at room temperature for 24hr forming a dark red suspension. The solvent was removed under reduced pressure and the product was extracted into hexane (2 x 20ml), filtered leaving 1 equivalent of LiCl. Removal of the solvent under reduced pressure yielded crude $Cr[\eta^5:\eta^1\text{-}C_5H_4(CH_2)_3NMe](CH_3)$, **5.4**, probably as the dimer $\{Cr[C_5H_4(CH_2)_3NMe](\mu\text{-}CH_3)\}_2$ (0.18g, 89% yield), as a dark pink/red solid. Product suitable for elemental analysis was prepared from precipitation of **5.4** from the minimum amount of hexane at -40°C.

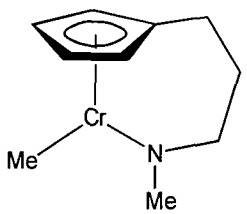

Data characterising 5.4

Description: Dark pink/red powder

Elemental analysis: Found ($C_{10}H_{16}NCr$ requires) C:60.4(59.4); H: 8.8(7.9); N: 6.7(6.9)

EI mass spec: m/z (intense peaks)

389 $[Cr_2(CpNMe)_2Me]^+$
374 $[Cr(CpNMe)Me]^+$
187 $[Cr(CpNMe)]^+$
136 $[CpNMe]^+$
52 $[Cr]^+$

Infra-red: ν/cm^{-1} (relevant bands)

2829-2921 (aliphatic C-H stretch)
801, 1020-1540 (C-H bends of aromatic ring)

^{1}H NMR: Not attempted due to paramagnetic Cr(III).

5.5.5 Attempted reaction between $LiBH_4$ and $Cr[\eta^5:\eta^1\text{-}C_5H_4(CH_2)_3NMe]Cl$, 5.1

A solution of **5.1** (0.23g, 1.0mmol) in THF (30ml) was cooled to -78°C (dry ice/acetone). A solution of $LiBH_4$ (0.1g, 4.6mmol) in THF (10ml) was added dropwise and the solution was allowed to warm to room temperature, then stirred for 24hr forming a purple solution. The solvent was removed under reduced pressure and the product was extracted with toluene (2 x 20ml) and filtered forming a dark green solution and leaving a white solid. The solvent was removed under reduced pressure leaving an unidentified dark green crystalline solid (0.25g). Attempts to recrystallise the product from the minimum amount of toluene proved unsuccessful.

5.4.6 Attempted reaction between PMe_3 and $V[\eta^5:\eta^1\text{-}C_5H_4(CH_2)_3NMe](THF)Cl$, 5.2

Neat PMe_3 (0.23g,. 3mmol) was added to a solution of **5.2** (0.30g, 1mmol) in toluene (20ml) at 0°C and the solution stirred at room temperature for 48hr with the solution remaining a dark purple. An aliquot was removed and analysed with ^{31}P NMR showing only the presence of uncoordinated PMe_3. Heating the solution to 50°C in a sealed system for 4 days also gave no reaction.

5.6 References

1 A. Clark, *Cat. Rev.*, 1969, **3**, 145.

2 a) F.J. Karol, G.L. Karapinka, C. Wu, W. A. Dow, N.R. Johnson and W.L. Carrick, *J. Polym. Sci., Part A-1,* 1972, **10**, 2621; b) F.J. Karol, G.L. Brown and J. M. Davidson, *J. Polym. Sci., Polym. Chem. Ed.,* 1973, **11**, 413.

3 a) H.L. Kraus and H. Stach, *Inorg. Nucl. Chem. Lett.,* 1968, **4**, 393; b) M. P. McDaniel and M.B. Welch, *J. Catal.,* 1983, **82**, 98 and 110; c) D.L. Myers and J.H. Lunsford, *J. Catal.*, 1985, **92**, 260; d) H. L. Kraus, K. Hagen and E.J. Hums, *J. Mol. Catal.,*1985, **28**, 233; e) D.L. Myers and J.L. Lunsford, *J. Catal.,* 1986, **99**, 140; f) J.H. Lunsford, S.-L. Lu and D.L. Myers, *J. Catal.,* 1989, **111**, 231; g) B. Rebenstorf, *J. Catal.*, 1989, **117**, 71.

4 a) S.W. Kirtley, *Comprehensive Organometallic Chemistry*; b) G. Wilkinson, F.G.A. Stone and E.W. Abel, Eds., Pergamon: Oxford, 1982, Vol. 3, p783.

5 W. Kaminsky and H. Sinn, Eds., Springer-Verlag: New York, 1988, p149.

6 a) P.D. Smith, J.L. Martin, J.C. Huffmann, R.L. Bansemer and K.G. Caulton, *Inorg. Chem.,* 1984, **24**, 2997; b) Y. Doi, S. Suzuki and K. Soga, *Macromolecules*, 1986, **19**, 2896.

7 a) T.G. Gardner and G.S. Girolami, *J. Chem. Soc., Chem. Commun.*, 1987, 1758; b) W.A. Herrmann, W.R. Thiel and E.J. Herdtweck, *J. Organomet. Chem.* 1988, **353**, 323; c) E.G. Thaler, K. Folting, J.C. Hoffman and K.G. Caulton, *J. Organomet. Chem.,* 1992, **30**, 189.

8 a) G.N. La Mar, W.D. Horrocks and R.H. Holm, *NMR of Paramagnetic Molecules*, Academic Press, New York, 1972; b) F.H. Köhler, P. Hoffman and W.J. Prössdorf, *J. Am. Chem. Soc.,* 1981, **103**, 6359.

9 D.S. Richeson, J.F. Mitchell and K.H. Theopold, *Organometallics,* 1989, **8**, 2570.

10 G. Bhandari, Y. Kim, J.M. McFarland, A.L. Rheingold and K.H. Theopold, *Organometallics,*1995, **14**, 738.

11 B.J. Thomas, S.K. Noh, G.K. Schulte, S.C. Sendlinger and K.H. Theopold, *J. Am. Chem. Soc.,* 1991, **113**, 893.

12 K.H. Theopold, *Acc. Chem. Res.,* 1990, **23**, 263.

13 C. Janiak, J. Silvistre and K.H. Theopold, *Comments Inorg. Chem.,* submitted for publication.

[14] S.K. Noh, S.C. Sendlinger, C. Janiak and K.H. Theopold, *J. Am. Chem. Soc.*, 1989, **111**, 9127.

[15] F.A. Cotton and G. Wilkinson, *Advanced Inorganic Chemistry*, 5th Ed., Wiley: New York, 1988, 689.

Chapter 6

Group 8 – Substituted Cyclopentadienyl Iron Complexes.

6.1 Introduction

6.1.1 Substituted ferrocenes

There are many examples of cyclopentadienyl iron complexes, particularly ferrocene-type complexes, since they are easily synthesised and unusually stable organometallic compounds. Recent annual surveys of ferrocene chemistry by Rocket and Marr average over 200 citations per year.[1] Substituted ferrocenes have been synthesised with a variety of donor-functionalities including pyridyl, **A**,[2] phosphine, **B**,[3] carboxylic-acid amides, **C**,[4] and vinyl, **D**[5] (figure 6.1).

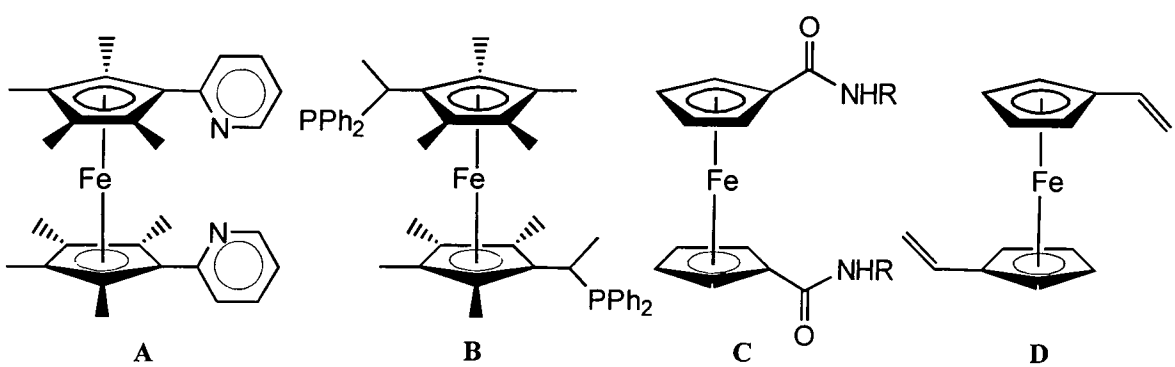

Figure 6.1

There are many examples of Lewis-base substituted ferrocenes and such complexes are of particular interest since they have the potential to be used as redox-active ligands for other transition–metal ions.[6]

6.1.2 Nitrogen functionalised cyclopentadienyl complexes

Whereas functionalised ferrocene complexes are common, complexes of iron where an intramolecularly coordinated functionalised cyclopentadienyl ligand is present are much rarer. However, there is an example where a cyclopentadienyl ligand with a primary amine group attached to the ring by a [$SiMe_2$] spacer unit has been used to prepare an iron (II) carbonyl complex, where the ligand is coordinated through the ring and intramolecularly through the amine nitrogen. This was prepared by reacting the dilithiated ligand with

ferrous chloride, followed by the reaction with carbon monoxide, yielding $Fe[\eta^5:\eta^1\text{-}C_5H_3(CMe_3)SiMe_2N^tBu](CO)_2$ as dark brown crystals (figure 6.2).[7]

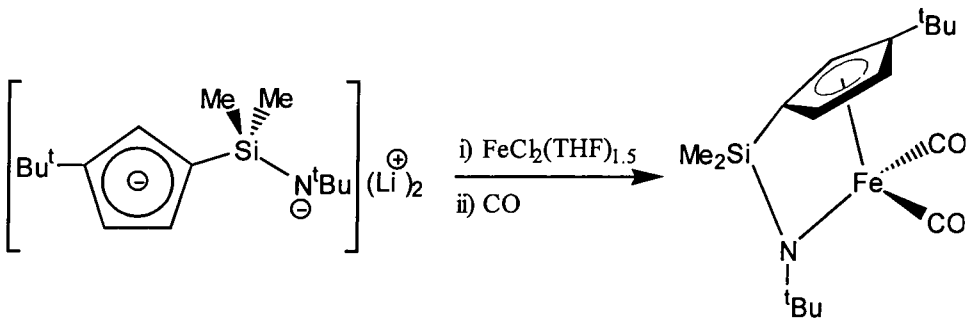

Figure 6.2

6.1.2 Aims

With few intramolecularly coordinated functionalised cyclopentadienyl iron complexes known, one of the aims was to synthesise a complex with the ligand $C_5H_5(CH_2)_3N(H)Me$, where both the cyclopentadienyl and amine groups are coordinated to the iron intramolecularly. Since Lewis-base substituted ferrocenes and other complexes of this type have the potential to be used as redox-active ligands for other transition–metal ions another aim was to prepare an amine functionalised ferrocene with the ligand $C_5H_5(CH_2)_3N(H)Me$.

6.2 Synthesis of Substituted Cyclopentadienyl Complexes

6.2.1 Reaction between $FeCl_2$ and $[C_5H_4(CH_2)_3N(H)Me]Li$, 1.2

The ferrocene, **6.1**, was prepared using a modified literature synthesis for $Fe(C_5H_5)_2$,[8] which is known to be readily adaptable to the synthesis of Lewis-base substituted ferrocenes. Two equivalents of $[C_5H_4(CH_2)_3N(H)Me]Li$, **1.2**, were added to anhydrous $FeCl_2$ in THF and the dark solution stirred overnight. Upon work-up, the desired ferrocene, $Fe[\eta^5\text{-}C_5H_5(CH_2)_3N(H)Me]_2$, **6.1**, was produced as an orange oil (figure 6.3).

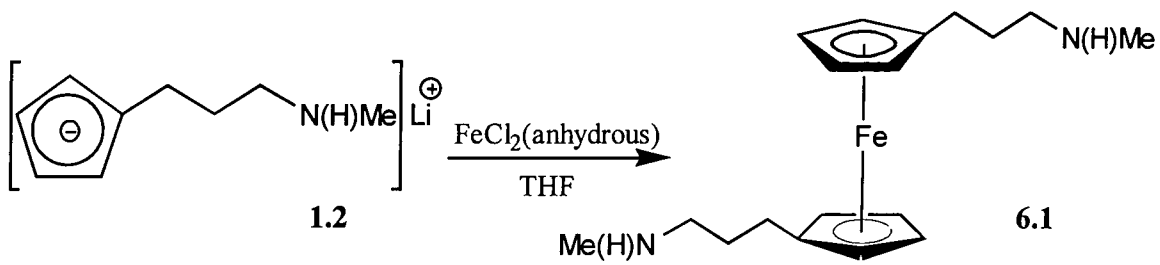

1.2 **6.1**

Figure 6.3

The ^1H NMR spectrum of **6.1**, proved misleading at first, since the cyclopentadienyl ring appears as a singlet when an AA'BB' system is expected (figure 6.4). However, the product is obviously not the free ligand, **1.1**, as this gives complex multiplets in this region of the ^1H spectrum, and since the singlet integrates to four protons, accidental overlapping of the resonances is thought to occur. As expected the resonance for the uncoordinated methylamine appears in a similar position to that in the free ligand, with a broad singlet at 1.36ppm for the NH group. The $^{13}C\{^1H\}$NMR spectrum gives the expected three signals for the cyclopentadienyl ring, one weak resonance for the *ipso* carbon, and two other resonances for the ring carbons (figure 6.5). The chemical shift values for the ring carbons were both comparable to those of ferrocene, $Fe(C_5H_5)_2$ (δ^1H/ppm, $CDCl_3$ = 4.28 compared to 3.98 for **6.1**; $\delta^{13}C$/ppm = 67.9 compared to 68.5, 69.3 and 89.4 for **6.1**).[9]

The IR spectrum of **6.1** shows strong bands assignable to aliphatic and aromatic C-H stretches and to the C-H bends of a coordinated cyclopentadienyl ring at 804cm^{-1}, with a broad band at 3316cm^{-1} exhibited for the N-H stretches. The EI mass spectrum clearly shows the molecular ion, m/z = 328 and also a mass of 192 attributable to the loss of one $C_5H_4(CH_2)_3NH(Me)$ fragment.

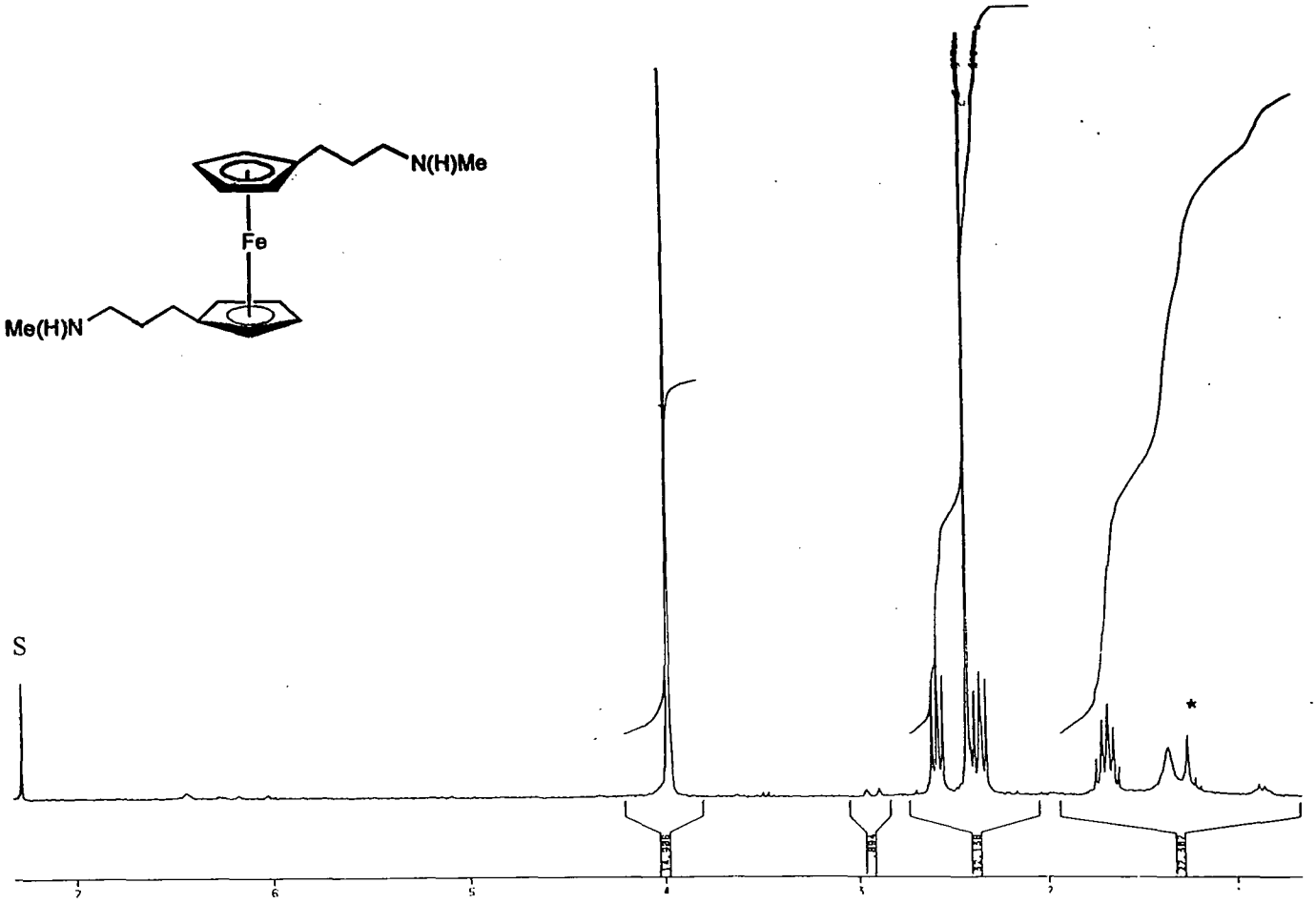

Figure 6.4 ^{1}H NMR spectrum of **6.1** in $CDCl_3$ at 250MHz

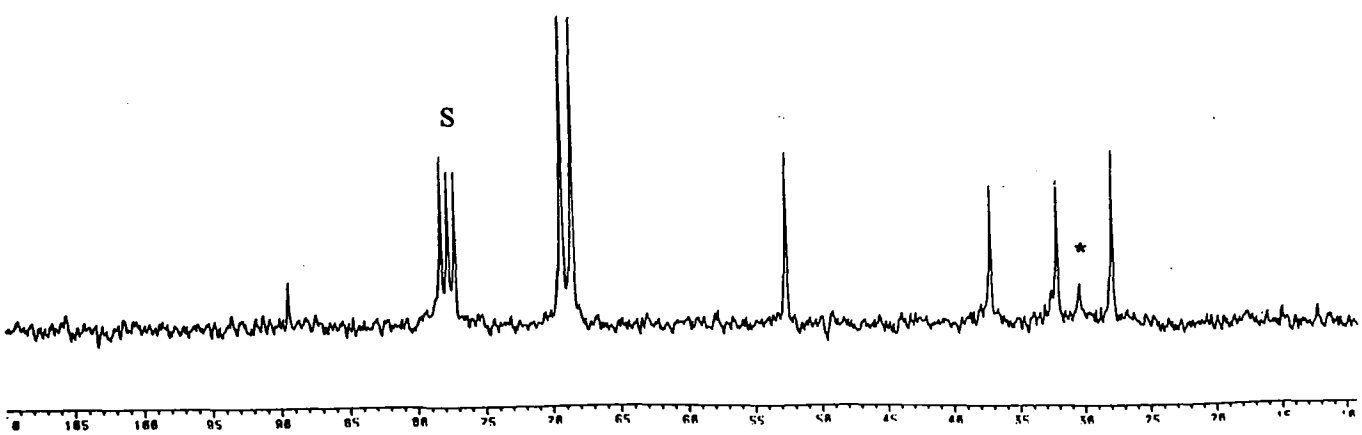

Figure 6.5 $^{13}C\{^{1}H\}$ NMR spectrum of **6.1** in $CDCl_3$ at 62.5MHz

6.2.2 Reaction between $Fe(CO)_5$ and $C_5H_5(CH_2)_3N(H)Me]$, 1.1

Many complexes of the type $[FeCp(CO)(\mu\text{-}CO)]_2$ have been synthesised with substituents on the cyclopentadienyl ring. Substituted cyclopentadienes suitable for conversion to the iron dimer derivatives have been reviewed.[10] Three general methods for preparing such compounds have been used:

i) synthesis from the substituted cyclopentadiene
ii) functionalisation of the cyclopentadienyl ring in the $[FeCp(CO)(\mu\text{-}CO)]_2$ compound
iii) intramolecular migration of a group from iron to the ring subsequent to deprotonation

In an attempt to synthesise the iron dimer with a substituted cyclopentadiene, $Fe_2(CO)_9$ and two equivalents of $C_5H_5(CH_2)_3N(H)Me$, **1.1**, were refluxed in toluene. Although the reaction was successful sizeable quantities of impurity were produced, making purification difficult. Iron pentacarbonyl was found to be the preferred reagent and was refluxed in toluene with one equivalent of neutral ligand, **1.1**. On cooling, the toluene solution yielded the iron dimer, $\{Fe[\eta^5\text{-}C_5H_4(CH_2)_3N(H)Me]CO(\mu\text{-}CO)\}_2$, **6.2**, as a dark brown microcrystalline solid (figure 6.6).

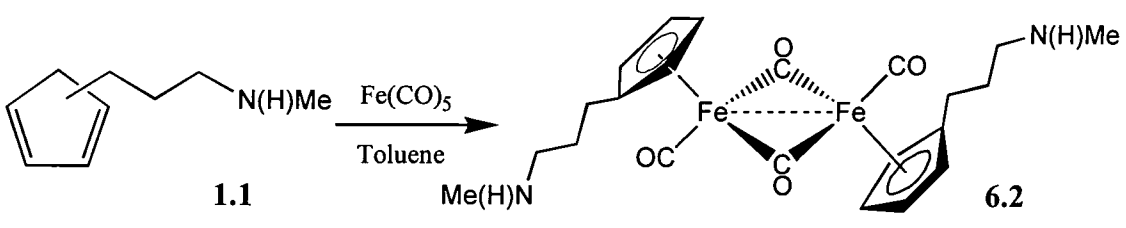

Figure 6.6

Both ^1H and $^{13}C\{^1H\}$ NMR spectroscopic analysis of **6.2** showed that the desired product had been produced, although small amounts of impurity were seen in the region for the trimethylene backbone of both spectra. The complex signals seen in the aromatic region of the ^1H NMR spectrum of the free ligand simplify into an AA'BB' spin system, showing that the cyclopentadienyl ring has undergone deprotonation and is now coordinated to the

metal centre. Three signals are also observed for the cyclopentadienyl ring in the $^{13}C\{^1H\}$ NMR spectra, two for the cyclopentadienyl C-H's, and one for the *ipso*-carbon.

The infra-red spectrum of **6.2** shows evidence for the functionalised ligand with stretches in both aromatic and aliphatic regions, and also at 3281cm^{-1} for the N-H stretch (figure 6.7). The IR spectrum in the carbonyl stretching region also provides a strong diagnostic tool. The peaks at 1943 and 1987cm^{-1} correspond to terminal carbonyl groups which are in the region observed for various $[CpFe(CO)_2]_2$ complexes of 1900-2100cm^{-1}. The peak at 1771cm^{-1} corresponds to the bridging carbonyls, which are found in the region 1750-1800cm^{-1}. There were no bands assignable to the $Fe(CO)_5$ starting material which appear at 2013 and 2034cm^{-1}.

Interestingly, the mass spectrum shows no masses for the dimer, **6.2**, which should appear at m/z = 496. However peaks appearing at 274 and 246 correspond to the cations $\{Fe[CpN(H)Me](CO)_3\}^+$ and $\{Fe[CpN(H)Me](CO)_2\}^+$ respectively, indicating the ease with which the dimer is oxidised.

Structure

IR and NMR spectroscopy can provide an insight into the structure and bonding of the compound under study, including the fluxional behaviour as depicted in figure 6.8.

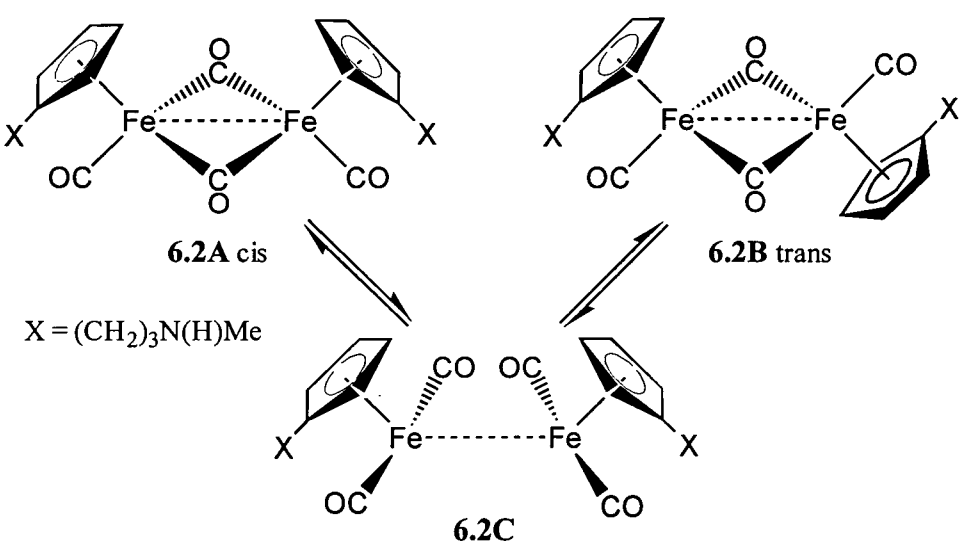

Figure 6.8

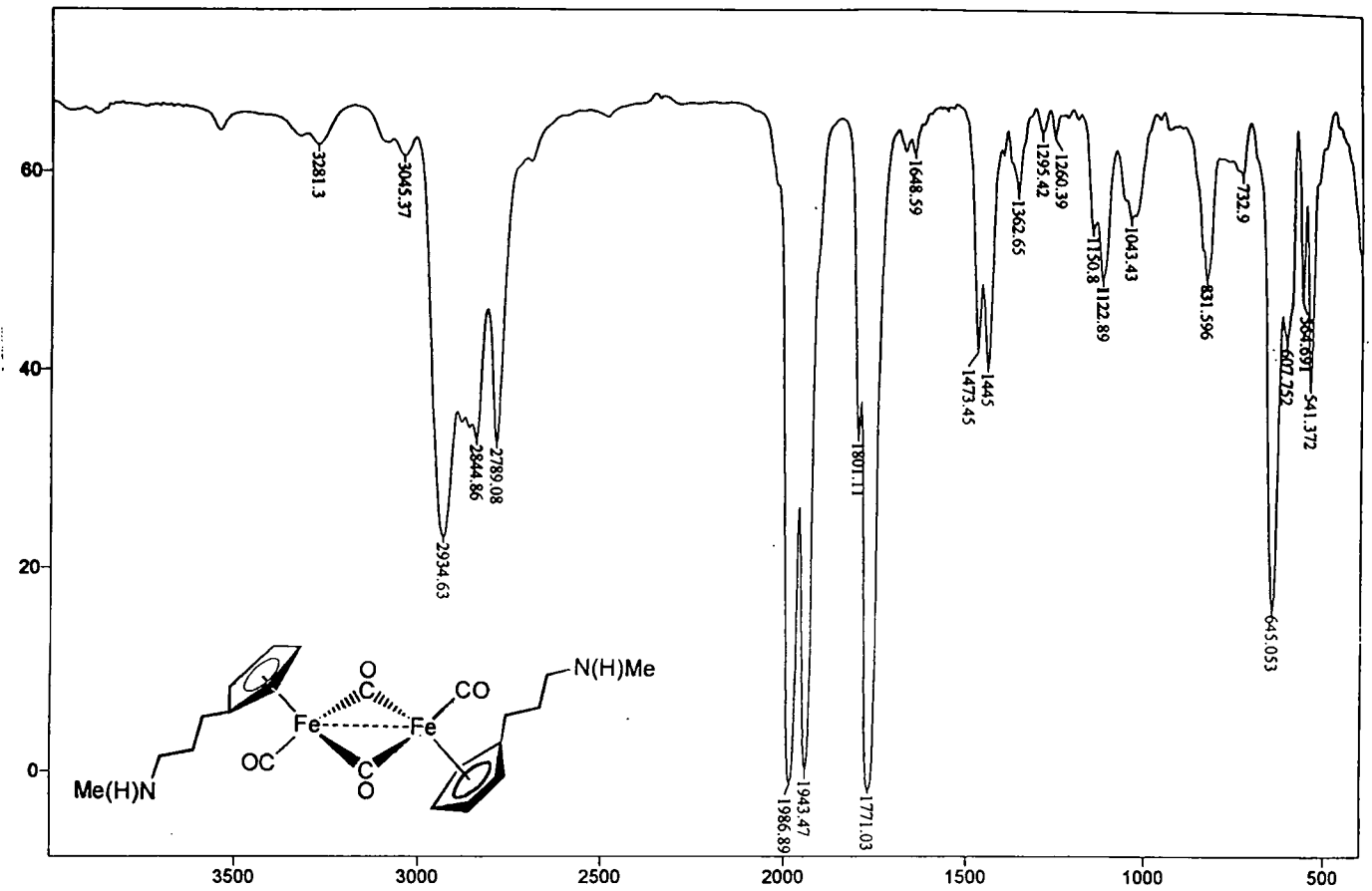

Figure 6.7 Infra-red spectrum of **6.2**

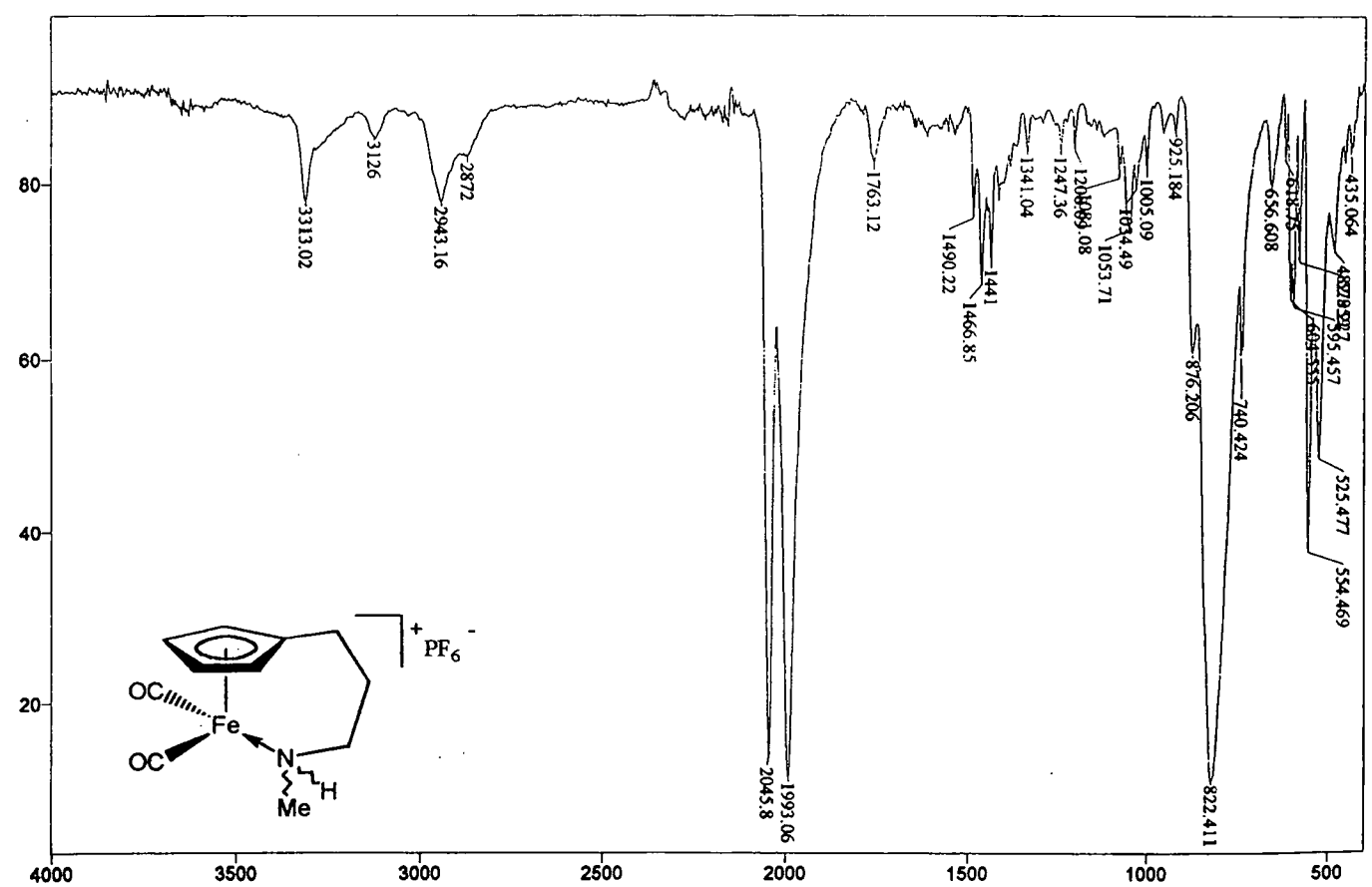

Figure 6.10 Infra-red spectrum of **6.3**

The cyclopentadienylirondicarbonyl dimer, **6.2**, exists in solution as a solvent dependent mixture of *cis*- and *trans*- CO-bridged isomers, **6.2A** and **6.2B** respectively, and to a lesser extent as the postulated transition state **6.2C**, as shown in figure 6.8, which includes structures and chemical conversions. Previous studies have found that the non-polar *trans* form dominates in non-polar solvents, and the polar *cis* form is stabilised in polar solvents.[11]

The ^{1}H NMR and $^{13}C\{^{1}H\}$ NMR spectra demonstrate the rapid interconversion of the principal isomers. In the ^{1}H NMR spectrum of $[(C_5H_5)Fe(CO)_2]_2$ a singlet is observed due to equivalent cyclopentadienyl protons. At -95°C, however, the singlet splits into two separate singlets in a 1:4 ratio, indicating the presence of both *cis* and *trans* isomers respectively.[12] The relative intensities of the ν(MC-O) terminal bands can also be used to calculate the relative *cis/trans* ratio. Studies carried out on the $[(C_5R_5)Fe(CO)_2]_2$ (where R = H, or Me or both) in solution, have shown that more methyl substituents on the cyclopentadienyl ring means that a larger quantity of the *trans* isomer is formed.[12] For example $[(C_5H_5)Fe(CO)_2]_2$ is 69% and 17% *trans* in hexane and acetonitrile respectively, whereas $[(C_5Me_5)Fe(CO)_2]_2$ is exclusively *trans* in both solvents.[13] The total exclusion of the *cis* form is assumed to be due to steric repulsions between the methyl groups. However, mono- and disubstituted cyclopentadienyl rings have been found to exert almost no steric influence. Therefore despite the length of the substituted chain in complex **6.2** it can be assumed there is little steric repulsion and therefore both *cis* and *trans* isomers are expected.

6.3.3 Reaction between $[Fe(C_5H_5)_2]^+PF_6^-$ and 6.2

Photolysis can sometimes dissociate metal carbonyl bonds thereby forming a vacant site for another molecule to coordinate. This could enable an uncoordinated amine to coordinate intramolecularly, similar to the molybdenum complex discussed in Chapter 2 (section 2.1), and manganese complex shown in figure 6.9.[14]

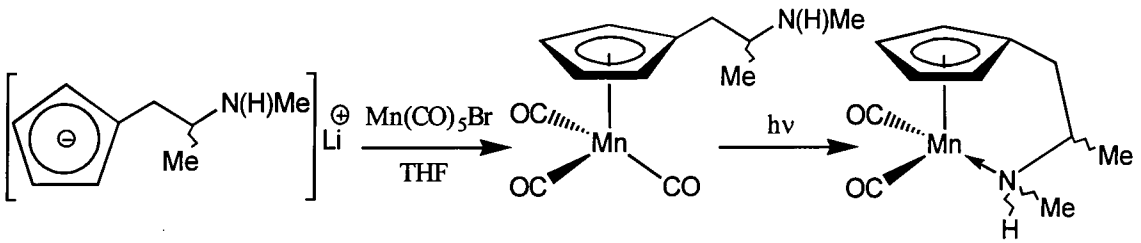

Figure 6.9

Oxidation of complex **6.2** may also allow intramolecular coordination of the amine. By breaking the Fe-Fe bond a monomer with a vacant coordination site will be formed. The ferrocenium ion as its hexafluorophosphate salt $[(C_5H_5)_2Fe]^+PF_6^-$ was used as the oxidising agent and reacted with half an equivalent of the dimer, **6.2**, in dichloromethane. On addition of diethyl ether a yellow solid precipitated and a yellow solution was produced. Infra-red analysis of the yellow solution confirmed the presence of ferrocene, $Fe(C_5H_5)_2$, confirming that an oxidation/reduction process had occurred.

Small amounts of paramagnetic material that could not be removed, presumably unreacted ferrocenium, prevented assignment of the complex by NMR spectroscopy. The product being ionic also meant that mass spectrometry was not possible. The infra-red spectrum provides strong evidence for the nature of the complex and is shown in figure 6.10 alongside that of complex **6.2**, for comparison. An N-H stretch is observed at 3313cm^{-1}, in addition to bands characteristic of the C-H bends of a coordinated cyclopentadienyl ring. More importantly a new stretch at 822cm^{-1} is characteristic of the presence of the PF_6 anion. Furthermore the large bridging carbonyl stretches observed for **6.2** are not seen, instead the spectrum exhibits two stretches at 1993 and 2046cm^{-1}, indicative of two terminal carbonyl groups.

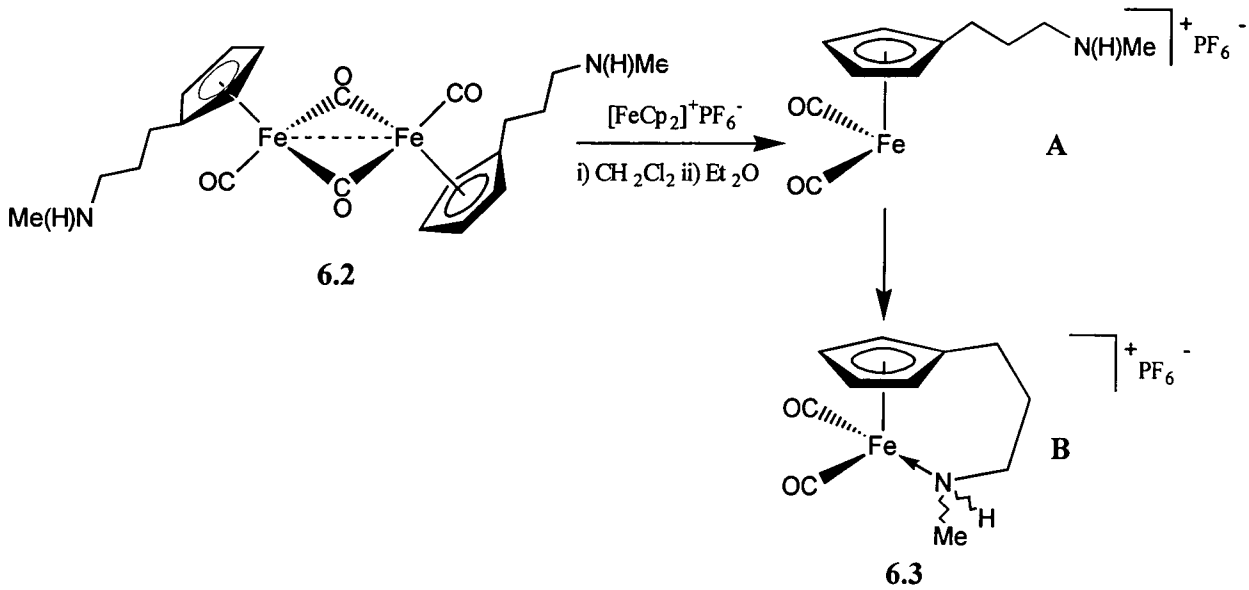

Figure 6.11

The above evidence indicates the formation of the monomer **6.3**, but does not show if the amine is pendant, **A**, or coordinated intramolecularly, **B**, (figure 6.11). Since the product is a monomer, **6.3A** will be coordinatively unsaturated and therefore likely to form a complex where the amine is coordinated forming $\{Fe[\eta^5:\eta^1\text{-}C_5H_4(CH_2)N(H)Me](CO)_2\}^+PF_6^-$, **6.3B.** X-ray diffraction studies would be one way of providing this evidence, but attempts made at growing crystals from a dichloromethane solution layered with diethyl ether were unsuccessful.

6.3 Summary

The substituted cyclopentadienyl iron complexes, $Fe[\eta^5\text{-}C_5H_4(CH_2)_3N(H)Me]_2$, **6.1**, and $\{Fe[\eta^5\text{-}C_5H_4(CH_2)_3N(H)Me](CO)(\mu\text{-}CO)\}_2$, **6.2**, have both been synthesised, according to other similar substituted ferrocenes and iron dimers. The oxidation of **6.2** with ferrocenium yielded what is thought to be the $\{Fe[\eta^5\eta^1\text{-}C_5H_4(CH_2)_3N(H)Me](CO)_2\}^+PF_6^-$, **6.3B**, but this has yet to be fully characterised.

6.4.Experimental

6.4.1 Preparation of $Fe[\eta^5\text{-}C_5H_4(CH_2)_3N(H)Me]_2$, 6.1

A solution of $[C_5H_5(CH_2)_3N(H)Me]Li$, **1.2**, (6mmol) in THF (20ml) was added dropwise to anhydrous $FeCl_2$ (0.38g, 3mmol) in THF (20ml), and stirred for 16hr forming a dark orange mixture. The solvent was removed under reduced pressure and water (15ml) was added (the product not being air or moisture sensitive), and the product was extracted with hexane (2 x 20ml). The solvent was removed under reduced pressure yielding $Fe[\eta^5\text{-}C_5H_4(CH_2)_3N(H)Me]_2$, **6.1**, (0.42g, 43% yield, pure by NMR) as a bright orange oil.

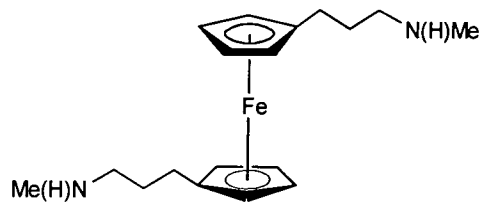

Data characterising 6.1

Description: Orange oil

EI mass spec: m/z = 328 $[\mathbf{6.1}]^+$; 192 $[Fe(CpNMe)]^+$ with correct isotope distribution

Infra-red: 3316 (N-H stretch); 3085 (aromatic C-H); 2961, 2928, 2851, 2792 (aliphatic C-H); 1109, 1038, 1021 (ring C-H bend)

^{1}H NMR: δ/ppm, 250 MHz, $CDCl_3$

3.98	[s, 4H, (C_5H_4)]
2.59	[t, 2H, $^3J_{HH}$=7.4Hz, ($C_5H_4C\underline{H}_2$)]
2.43	[s, 3H, (NCH_3)]
2.39	[t, 2H, $^3J_{HH}$=7.7Hz, (NCH_2)]
1.68	[quin, 2H, $^3J_{HH}$=7.6Hz, ($CH_2C\underline{H}_2$)]
1.36	[br s, 1H, (NH)]

$^{13}C\{^1H\}$ NMR: δ/ppm, 62.5 MHz, $CDCl_3$

89.4	(C_5H_4-*ipso*)
69.3	(C_5H_4)
68.5	(C_5H_4)
52.6	(NCH_3)
37.2	(NCH_2)
32.1	($C_5H_4C\underline{H}_2$)
27.9	($CH_2\underline{C}H_2CH_2$)

6.4.2 Preparation of $\{Fe[\eta^5\text{-}C_5H_4(CH_2)_3N(H)Me](CO)(\mu\text{-}CO)\}_2$, 6.2

Neat $Fe(CO)_5$ (0.53ml, 4mmol) was added dropwise to a solution of the neutral ligand $C_5H_5(CH_2)_3N(H)Me$, **1.1**, (0.55g, 4mmol) in toluene (40ml). The solution was refluxed under nitrogen, for 24hr. The dark brown mixture was filtered whilst hot, and the filtrant was extracted with toluene (2 x 15ml, at 70°C). The solvent was removed from the combined extracts under reduced pressure yielding crude $\{Fe[\eta^5\text{-}C_5H_4(CH_2)_3N(H)Me](CO)(\mu\text{-}CO)\}_2$, **6.2**, (0.78g, 1.6mmol, 78% yield) as a brown solid. Recrystallisation was carried out from toluene at -40°C giving **6.2** as a brown microcrystalline powder.

Data characterising 6.2

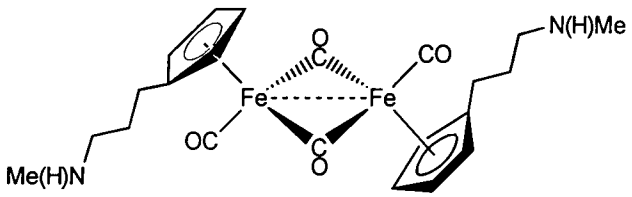

Description: Brown microcrystalline solid

EI mass spec: 274 $\{Fe[CpN(H)Me](CO)_3\}^+$, 246 $\{Fe[CpN(H)Me](CO)_2\}^+$, 191 $\{Fe[CpN(H)Me]\}^+$

Infra-red: 3281 (N-H stretch); 3045 (aromatic C-H); 2934, 2845, 2789 (aliphatic C-H); 1987, 1943 (C=O terminal); 1771 (C=O bridging); 1150, 1122, 1043 (ring C-H bend)

^{1}H NMR: δ/ppm, 250 MHz, $CDCl_3$		**$^{13}C\{^1H\}$ NMR: δ/ppm, 62.5 MHz, $CDCl_3$**	
4.59	[t, 2H, $^3J_{HH}$=2.7Hz, (C_5H_4)]	108.9	(C_5H_4-*ipso*)
4.41	[t, 2H, $^3J_{HH}$=2.6Hz, (C_5H_4)]	89.1	(C_5H_4)
2.70	[s, 3H, (NCH_3)]	88.1	(C_5H_4)
2.62	[t, 2H, $^3J_{HH}$=7.2Hz, ($C_5H_4C\underline{H}_2$)]	52.1	(NCH_3)
2.36	[t, 2H, $^3J_{HH}$=7.5Hz, (NCH_2)]	37.1	(NCH_2)
1.71	[quin, 2H, $^3J_{HH}$=7.3Hz, ($CH_2C\underline{H}_2$)]	32.0	($C_5H_4C\underline{H}_2$)
0.66	[br s, 1H, (NH)]	26.0	($CH_2\underline{C}H_2CH_2$)

6.5.3 Preparation of $\{Fe[\eta^5:\eta^1\text{-}C_5H_4(CH_2)_3N(H)Me](CO)_2\}^+PF_6^-$, 6.3

A suspension of $[Fe(C_5H_5)_2]^+PF_6^-$ (0.33g, 1.0mmol) in CH_2Cl_2 (15ml) was added slowly to a solution of **6.2** (0.25g, 0.5mmol) in CH_2Cl_2 (15ml). The mixture was stirred for 2hr, changing from blue/red to brown/yellow. The solution was filtered and the volume of the solvent reduced to approximately 10ml. Et_2O (50ml) was added precipitating a brown/yellow solid, which was filtered leaving crude $Fe[\eta^5:\eta^1\text{-}C_5H_4(CH_2)_3N(H)Me](CO)_2$, **6.3**, (0.14g, 58mmol, 58% yield) as a brown/yellow solid. The yellow filtrate was analysed and found to contain $Fe(C_5H_5)_2$.

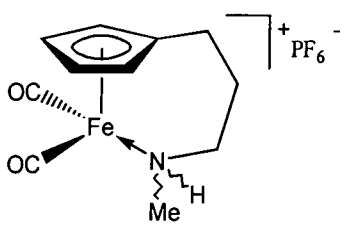

Data characterising 6.3

Description: Yellow solid

Infra-red: 3133 (N-H stretch)
3126 (aromatic C-H)
2943, 2872 (aliphatic C-H)
2046, 1993 (C=O terminal)
1081, 1054, 1005 (ring C-H bend)
822 (P-F stretch)

6.5 References

1 B.W. Rockett and G. Marr, *J. Organomet. Chem*, published each year.

2 a) U. Siemeling, B. Neumann and H.G. Stammler, *Z. Naturforsch.*, 1994, **49**, 683; b) U. Siemeling, O. Vorfield, B. Newmann and H.G. Stammler, *Chem. Ber.*, 1995, **128**, 481.

3 a) D.J. Harvan, J.R. Hass, K.L. Buisch, M.M. Bursey, F. Ramirez and S. Meyerson, *J. Am. Chem. Soc.*, 1979, **101**, 7410; b) D.M. Bensley and E.A. Mintz, *J. Organomet. Chem.*, 1988, **353**, 91.

4 M. Oberhoff, L. Duda, J. Karl, R. Mohr, G. Erker, R. Frölich and M. Grell, *Organometallics,* 1996, **15**, 4005.

5 M. Osaga, D.T. Mallin, D.W. Macomber, M.D. Rausch, R.D. Rogers and A.D. Rollins, *J. Organomet. Chem.*, 1991, **405**, 41.

6 U. Siemeling, O. Vorfield, B. Neumann and H.G. Stammler, *Chem. Ber.*, 1995, **128**, 481.

7 J. Okuda, *Chem. Ber.*, 1990, **123**, 1649.

8 a) G. Wilkinson, *Org. Synth.*, 1956, **36**, 31; b) W.L. Jolly, *Inorg. Synth.*,1968, **11**, 120.

9 Chemical shift values for commercially produced ferrocene at 250MHz in $CDCl_3$.

10 D.W. Macomber, W.P. Hart and D. Rousel, *Adv. Organomet. Chem.*, 1982, **21**, 1.

11 a) J.G. Bullit and F.A. Cotton, *J. Am. Chem. Soc.*, 1970, **92**, 2155; b) O.A. Gansow, A.R. Burke and W.D. Vernon, *J. Am. Chem. Soc.*, 1976, **98**, 5817; c) D.C. Harris, E. Rosenberg and J.D. Roberts, *J. Chem. Soc., Dalton Trans.*, 1974, 2398

12 A.R. Manning, *J. Chem. Soc. (A),* 1969, 1319

13 P. McArdle, L. O'Neill and D. Cunningham, *Organometallics,* 1997, **16**, 1335.

14 T.F. Wang, T.Y. Lee, Y.S. Yen and L.K. Liu, *J. Organomet. Chem.*, 1991, **403**, 353.

Chapter 7

Introduction to NMR Studies of Potentially α-Agostic Methyl and Neopentyl Complexes

7.1 Introduction

Carbon-hydrogen bonds, especially those of saturated (sp^3) carbon centres, are normally considered to be chemically inert. There is evidence however that C-H bonds can act as ligands to transition metal centres by forming three centre, two electron bonds (3c-2e), and that the extent of the interaction is such as to have a marked effect on the molecular and electronic structure, and reactivity of the molecule. The chemistry of such systems has recently been reviewed.[1,2,3] The term agostic, derived from the Greek word meaning to clasp, draw towards, is the name given to describe such a bond.

Recently α-agostic bonds, where there is an interaction between the hydrogen atom of an α-carbon atom and the transition metal centre, have been implicated in intermediates or transition states in the carbon-carbon bond forming step in Ziegler-Natta catalysis. Chapters 7 to 9 are therefore dedicated to investigating such interactions using NMR techniques, and begins with a general introduction to the subject.

7.1.1 Early Observations

Interactions between C-H bonds and coordinatively unsaturated metal fragments were first observed in the 1960's by Ibers and Maitlis.

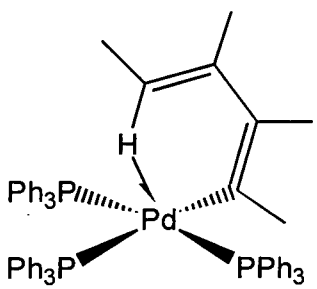

Figure 7.1

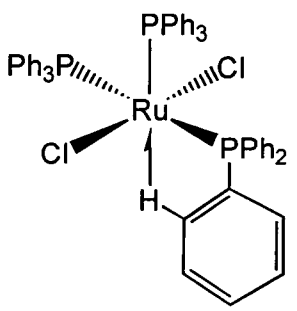

Figure 7.2

Maitlis and co-workers reported the crystal structure of trans-[Pd(CMeCMeCMeCMeH$_a$)Br(PPh$_3$)$_2$] (figure 7.1), and showed there to be close approach of the H$_a$ to the palladium metal centre estimated at 2.23Å.[4] ^{31}P-H$_a$ coupling was also observed in the ^{1}H NMR spectrum. Ibers and co-workers observed close approach of the ortho-hydrogen atoms of aryl phosphine ligands to the metal centre in the compound [RuCl$_2$(PPh$_3$)$_3$] (figure 7.2).[5]

7.1.2 α-Agostic interactions

Whilst there are now many examples of agostic alkyl complexes there are still relatively few simple α-agostic alkyls, where there is an interaction between the hydrogen atom of an α-carbon and the transition metal centre. However, α-agostic bonds have been implicated as intermediates or transition states in the carbon-carbon bond forming step in Ziegler Natta catalysis (section 7.3).

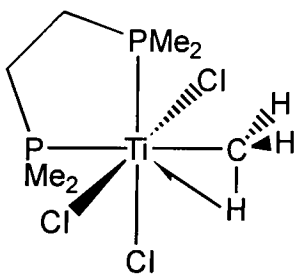

Figure 7.3

The first example of an α-agostic M←H-C bond to be fully characterised was the titanium compound [Ti(η^2-Me)Cl$_3$(dmpe)] (figure 7.3), the structure of which was determined by neutron diffraction.[6] It was shown that the methyl group was tilted such that one hydrogen atom approaches the metal giving a Ti-C-H angle of 93.5°.

7.2 Agostic Bonding

7.2.1 Three centre, two electron bond

Only recently has it become clear that σ bonding electron pairs can ligate to metals, the resultant structure being isolobal with H_3^+, a bent species having only two bonding electrons and three atoms (figure7.4). The ion is triangular due to considerable overlap between the terminal hydrogen 1s orbitals. This is in comparison to H_3^- in which the non-bonding level is filled and there is no overlap between the terminal hydrogens, hence the molecule is linear (figure 7.5).

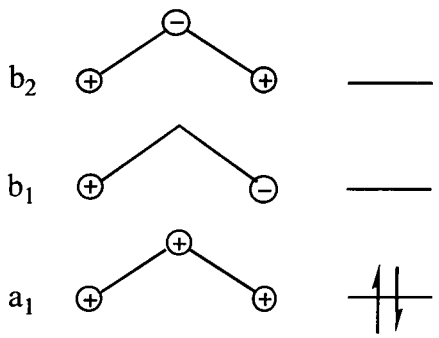

Bent H_3^+

Figure 7.4

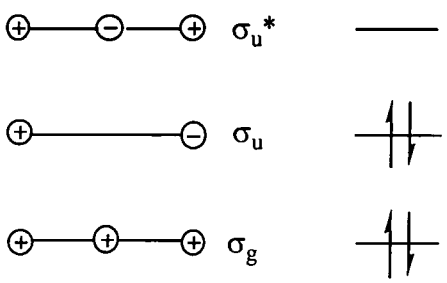

Linear H_3^-

Figure 7.5

The representation of such a bond in Lewis diagrams employs an arrow or half arrow. Thus H_3^+ can be written as $H_2 \rightarrow H^+$ in such a localised representation, although it is clearly a highly delocalised species. Analogous heteronuclear systems will adopt bent or linear structures according to whether they have 2 or 4 electrons. In all 3 centre 2 electron bonds the system is bent. For example, the classical situation of a 3 centre 2 electron bond in diborane (figure 7.6).

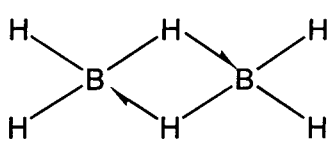

Figure 7.6

Agostic bonds arise from the presence of X-H bonds (X = mainly C but now recognised to include Si, N, B etc) in the vicinity of an electron deficient metal centre. In such cases the C-H bond can supply two electrons to the metal as a three centre two electron bond, in order to relieve electronic unsaturation. For example the absence of an agostic bond in figure 7.7 would leave a metal centre with an electron count of 16, whereas the agostic 3 centre 2 electron bond enables the 18 electron rule to be obeyed.

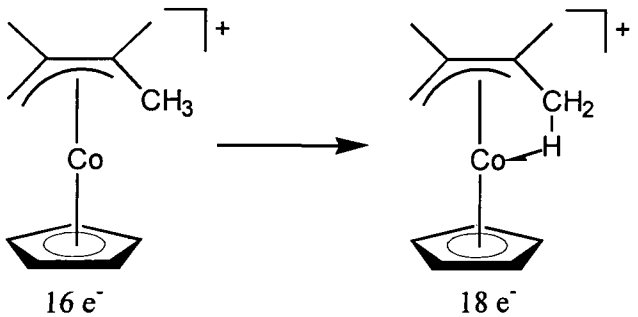

Figure 7.7

7.2.2 Representation

The half arrow convention, C-H–⇀M, was chosen to indicate that the formation of an agostic bond results in the formal donation of two electrons to the metal centre (figure 7.7). It is designed to facilitate electron counting in a molecule which is very important, for example, in the context of the 18 electron rule. Since the relative electron density distribution of the M-H, C-H and M-C components in agostic bonds will vary, it would be very difficult to indicate the strength of an agostic bond.

7.2.3 Factors favouring agostic interactions

The minimum requirement for an agostic interaction is that the metal centre should have an empty orbital with which to receive two electrons from the C-H bond. It is presumed that this orbital will be essentially of d character for transition metal complexes. The orbital should be a very good acceptor of electrons, and the energy and disposition should approach those of the C-H bonding orbitals as far as possible. Although the formation of an agostic group is sterically quite undemanding, it is possible from normal consideration of steric restrictions that the formation of an agostic alkyl group will be favoured when this bond results in the metal attaining a coordination number of six or less.

The requirement of an unsaturated 16 electron (or fewer) metal centre is a necessary but not sufficient condition for the occurrence of an agostic hydrogen. Eisenstein and co-workers have studied the model octahedral and tetrahedral complexes $[H_5TiCH_3]^{2-}$ and H_3TiCH_3 by extended Hückel calculations in order to understand the reason why the d^0 octahedral complex $MeTiCl_3(dmpe)$ forms an agostic interaction while the d^0 tetrahedral complex $MeTiCl_3$ shows no significant distortion.[7] They found that a distortion of a methyl group is likely to occur only if strong interaction between the σTi-C orbital and low lying d orbital of appropriate symmetry develops upon distortion. In both octahedral and tetrahedral complexes such an interaction exists but it is much larger in the former. The stability of the distorted structure originates more from an electronic reorganisation of the M-C bond than from a direct electron donation into the metal.

The effects of ligands on agostic interactions have also been analysed. Competition would be expected between the formation of an agostic bond and donation by lone pairs on ligands, such as halogen atoms or the oxo ligand. It is found in $MeTiCl_3(dmpe)$ that those lone pairs of electrons of the three chlorine ligands that have suitable symmetry to overlap with the titanium orbitals do not successfully compete with the agostic C-H electron pair.

7.3 Implications of α-Agostic Bonds in Ziegler Natta Catalysis

The traditional mechanism for the carbon-carbon bond forming step in Ziegler Natta polymerisation of olefins proposed by Cossee proceeds by simple alkyl migration to the coordinated olefin.[8] There is no direct involvement of the C-H bonds of the alkyl chain in this mechanism. However α-agostic bonds have been implicated in the carbon-carbon bond forming step in Ziegler-Natta catalysis. One proposed mechanism is the "Modified Green Rooney Mechanism" (figure 7.8).

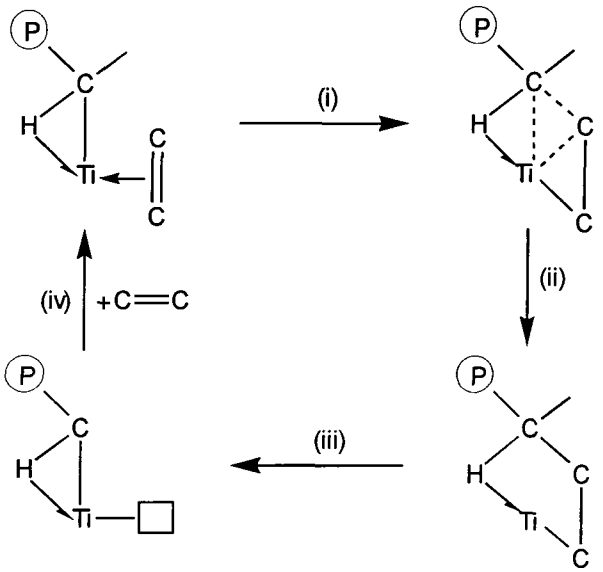

i) The C-C bond forming step assisted by partial migration of an α-H atom to the metal giving a C-H→Ti.

ii) The metallacycle intermediate with a γ C-H→Ti bond.

iii) Rearrangement of the agostic hydrogen from the γ to the α position.

iv) Addition of the next olefin.

Figure 7.8

Bercaw has shown that in the hydrocyclisation of 1,5-hexadiene to methyl cyclopentane using a scandium catalyst, a transition state containing an α-agostic hydrogen provides evidence for a Modified Green-Rooney Type Pathway for chain propagation within Ziegler-Natta systems.[9] Moreover these transition states suggest a rationale for the apparent requirement that active catalysts be 14 electron alkyl derivatives with 2 vacant orbitals; one to accommodate the incoming olefin, and one for the agostic interaction.

Bercaw probed the reaction using deuterated substrates and found that a transition state in which the hydrogen atom was agostically bonded was more stable than a system in which the deuterium was agostically bonded (figure 7.9).

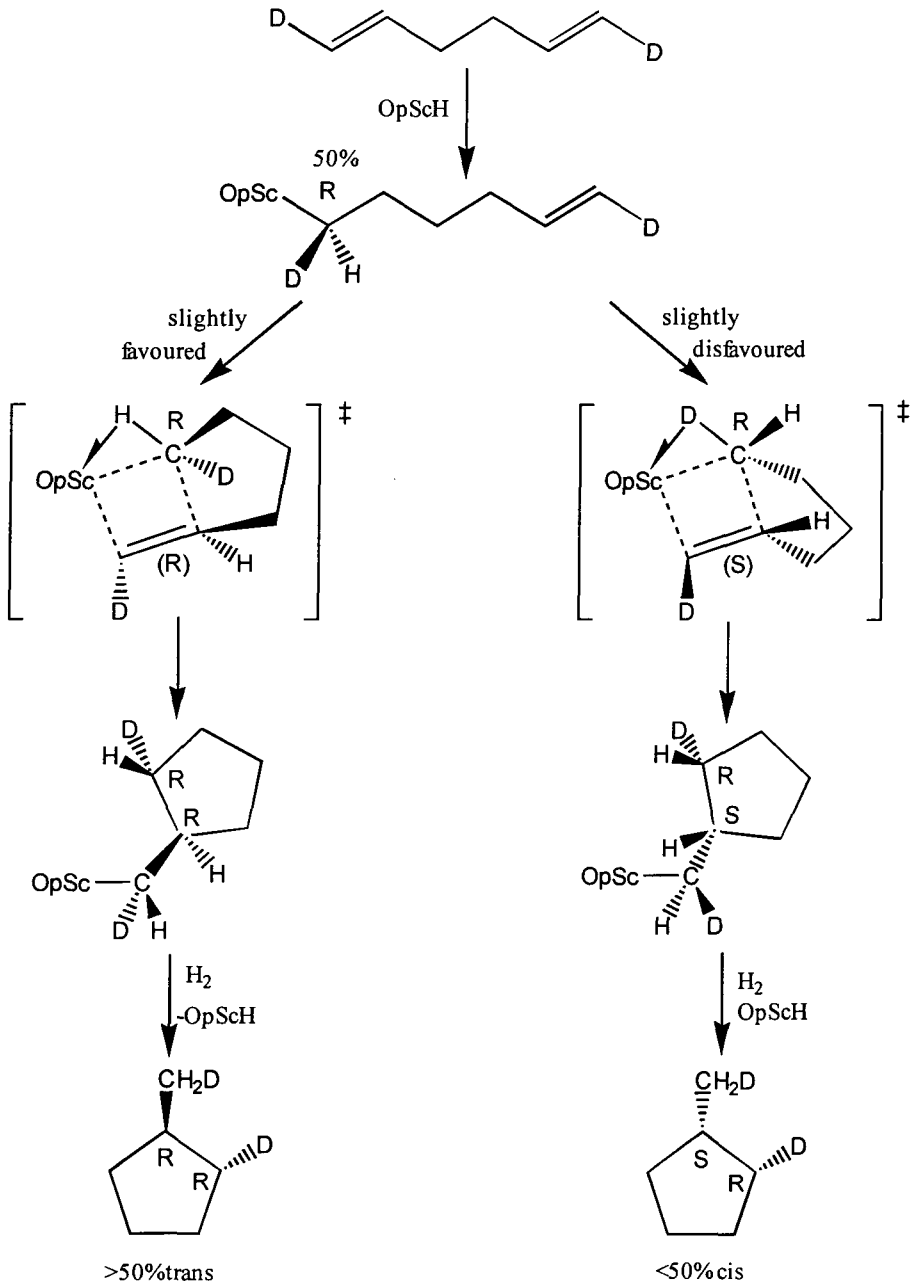

Figure 7.9

Due to ring strain there should be a strong preference for fusion of the pseudo 4,5 ring system in the transition state for olefin insertion as shown in the reaction scheme – here for the R isomer only. The face selection for insertion depends upon whether the hydrogen or deuterium atom occupies the agostic position. The preference for the hydrogen to occupy

the bridging site leads to an enantiomeric excess of the R,R-trans product. A similar analysis of the S enantiomer leads to the same conclusion, i.e., the trans isomer is produced in excess if an α-agostic interaction assists olefin insertion into the M-C bond.

Studies on α-agostic systems using Hückel MO methods on models of Ziegler-Natta catalysis have been carried out by Janiak.[10] Work on the cationic zirconium complex $[ZrCp_2(C_2H_4)CH_3]^+$ revealed the following:

i) α-agostic interactions may be unimportant in the ground state of the possible catalyst, $[ZrCp_2(C_2H_4)CH_3]^+$.
ii) The strong anti-bonding H^{α}-Zr in the HOMO is overcome only through a Zr-methyl weakening in the course of the C_{methyl}-C_{olefin} approach i.e. in the bond forming reaction. That is, α-agostic stabilisation becomes important through an increase in the electron density of the central metal, in this case the transformation of the 16 electron $[ZrCp_2(C_2H_4)CH_3]^+$ to the 14 electron $[ZrCp_2(CH_2)_2CH_3]^+$. Hence calculations strongly support the presence of an α-agostic H-Zr interaction around and beyond the transition state for olefin insertion.

More recent work investigating co-catalyst activity in Ziegler Natta polymerisation has shown the first evidence for α-olefin insertion in the titanium based Ziegler Natta catalyst systems.[11] Participation of α and β hydrogens in the intramolecular insertion of an α olefin into a Ti-C bond was examined through competitive cyclisation of isotopically labelled 2-alkyl-6-hepten-1-yl ligands. Comparison of cyclisation rates revealed deuterium isotope effects for both α and β sites of a propagating chain model. Through the use of MgX_2 to promote alkene insertion, mechanistic features of this insertion process were observed in which both α and β agostic interactions were involved in the rate-determining step of the olefin insertion. The values obtained are consistent with the α-agostic interactions or secondary isotope effects due to hyperconjunction with the proposed titanium intermediate cation.

7.4 Obtaining Evidence for α-agostic Interactions

7.4.1 Nuclear Magnetic Resonance studies

NMR spectroscopy is the most useful spectroscopic technique for detecting the presence of agostic systems. Where spectra of static systems can be obtained, the ^{1}H and ^{13}C chemical shifts and in particular J(C-H), which is expected to be reduced because of the reduced C-H bond order, can be used to assign them. Many agostic compounds are however, highly fluxional and undergo rapid exchange of the agostic hydrogen with other hydrogens. These fluxional compounds give only averaged spectra at 25°C and static spectra can only be obtained at low temperatures (-80 to -100°C). However, in simple methyl groups, even at the lowest attainable temperatures, static spectra cannot be observed and it is very difficult to distinguish between the agostic formulation and classical structures. Therefore it is difficult to establish α-agostic bonding spectroscopically as there are no examples of an agostic methyl group that is static on the NMR timescale.

When a spectrum of the static species cannot be obtained, then only an averaged value of the chemical shift and J(C-H) can be measured. This problem can make it difficult to distinguish between three possible structures namely the unsaturated **A**, the agostic **B**, and the terminal hydride **C** (figure 7.10).

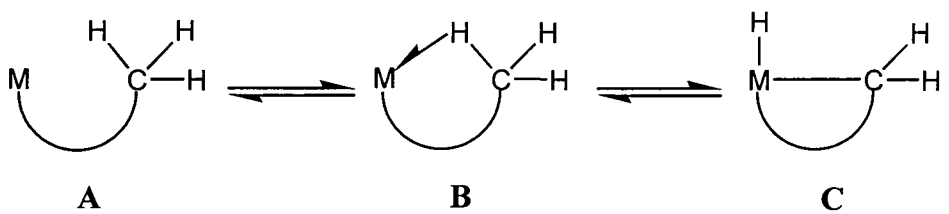

Figure 7.10

All three structures have overlapping ranges for the $J(C\text{-}H)_{average}$ value, and therefore this can seldom be used to assign agostic structures.

In compounds for which the metal has d^n n>0 configuration the average ^{1}H chemical shift for the fluxional methyl group of **B** is normally at a frequency lower than 0ppm and at a

lower frequency than the non-interacting methyl group of **A**. If **C** were highly fluxional then the averaged chemical shift of the methyl group would also be at a frequency lower than 0ppm, therefore not permitting a distinction to be made between these two systems. In d^0 systems where the structures **A** and **B** are favoured, the averaged chemical shift in each case will be at frequencies higher than 0ppm and this cannot be used to distinguish **A** from **B**.

The IPR Technique

For rapidly exchanging agostic alkyl groups the NMR technique of isotopic perturbation of resonance (IPR) originally described by Saunders,[12] and first applied to agostic systems by Calvert and Shapley,[13] on the trinuclear osmium system $[Os_3(CO)_{10}(CH_3)(H)]$, provides the most reliable spectroscopic evidence. In the IPR technique, the average ^1H NMR chemical shift values are quite sensitive to the extent of deuteration of the methyl group and fall in the order:

$$\delta CH_3 > \delta CH_2D > \delta CHD_2$$

high frequency $\longrightarrow$ **low frequency**

Further, partially deuterated agostic C-H groups may show a decrease in the value of the coupling constant J(C-H) in the sequence:

$$J(C\text{-}H)(CH_3) > J(C\text{-}H)(CH_2D) > J(C\text{-}H)(CHD_2)$$

Furthermore both the ^1H chemical shift and J(C-H) values of the partially deuterated species (but not CH_3) are strongly temperature dependent.

The IPR experiment consists of taking the proton spectrum of a mixture of isotopomers of the complex in which the methyl group has been partially substituted with deuterium. In the d_0 isotopomer, the observed chemical shift δ_0, is the average of the shifts for the bridging and terminal positions, with any given proton spending twice as long in the terminal site than bridging site (figure 7.11).

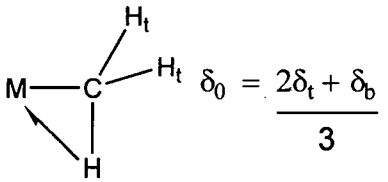

$$\delta_0 = \frac{2\delta_t + \delta_b}{3}$$

$$\delta_1 = \frac{\delta_b + \delta_t + A\delta_t}{2 + A}$$

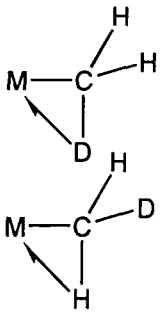

Figure 7.11 **Figure 7.12**

"In the d_1 isotopomer there is a thermodynamic preference for the deuterium atom to occupy terminal positions and hydrogen atoms to occupy the bridging, agostic site (figure 7.12). The reason is that the zero point energy of H is greater than that of D, and the stability difference depends on the strength of the C-(H,D) bond. The H/D zero point energy difference is greater for the terminal C-$(H,D)_t$ than for the weaker bridging C-$(H,D)_b$ bond and so there is an energy advantage for a hydrogen to be in a C-H_b site. This population shift translates into a chemical shift in the ^1H NMR resonance of the methyl group. The δ_1, shift for the d_1 complex is an average that we can calculate by looking at the equilibrium shown in figure 7.13. First we calculate the average shift observed for each form in the absence of IPR (figure 7.11). For example **Y** has one terminal and one bridging H and so the required average is $(\delta t+\delta b)/2$ (figure 7.13). We next apply a Boltzmann weighting A to the least stable form Z, with D in the bridge. The term A is $\exp(-\Delta E/RT)$, and is therefore always less than one. ΔE is the energetic preference for D being terminal, which is usually about 150 cal/mol, but the exact value is extracted from the data, and T is the absolute temperature. Finally, we need a statistical weighting for **Y** because there are two ways of having D terminal, since there are two terminal positions. Figure 7.12 gives the appropriate average. By putting A=1, the IPR goes to zero and $\delta_0=\delta_1$. As the temperature is lowered the population of agostic bonds falls, accentuating the chemical shift to a lower frequency."[2]

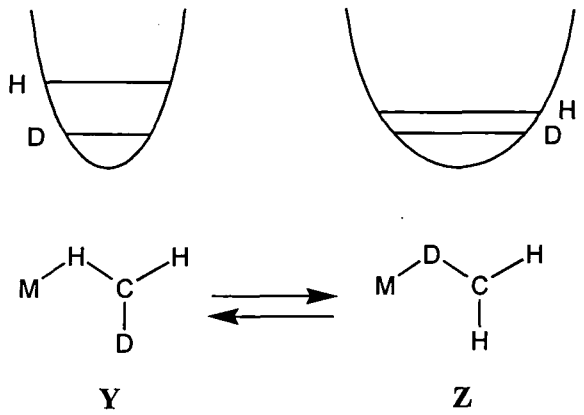

Y Z

Chemical shift:	$(\delta t + \delta b)/2$	δt
Boltzmann weighting	1	A
Statistical weighting	2	1
Overall weighting	2	A

Figure 7.13

The relative sign of the geminal ^2J(H-H) coupling constant of methyl groups also has the potential to be used as a probe for agostic bonding. Extended Hückel calculations indicate that increasingly acute M-C-H angles, a possible result of α-agostic metal methyl interaction, should lead to a more positive value for the geminal coupling constant.[14] The origin of the term 'relative' for the sign of the geminal coupling constants is as follows. Since known geminal coupling constants for hydrogen attached to both sp^2 and sp^3 carbons cover the range 0-20Hz,[15] it is possible that these values may be positive or negative. However, since the values of ^1J(C-H) coupling constants cover at an extreme, the range 60-200Hz, these values are all assumed to have the same sign; the sign of ^1J(C-H) has been determined to be positive for CH_3CN.[16] By using heteronuclear spin tickling and, more recently, two-dimensional NMR techniques, it is possible to determine the sign of ^2J(H-D) relative to that of ^1J(C-D). Since the ^1H, ^2D and ^{13}C nuclei all have positive magnetogyric ratios (γ), the sign of ^2J(H-H) is the same as that of ^2J(H-D), and the sign of ^2J(C-H) is the same as that of ^2J(C-D).

Partial deuterium labelling experiments must be interpreted critically since there are two specfic situations from which the wrong conclusions could be drawn. First, as Faller and co-workers noted,[17] if the hydrogen scrambling were occurring via unsaturated C (figure 7.10, **C**) then a Shapley effect would still be observed, since the M-H_a/M-D_a zero point energy difference would be significantly less than for C-H_t/C-D_t. In practice, there have been no cases where a classical olefin hydride has been established crystallographically, that cannot be 'frozen' out by low temperature NMR spectroscopy.

The second occurs in d^0 metal alkyl complexes, in which it is more difficult to distinguish between structures **B** and **C** (figure 7.10) as illustrated by the agostic complex [CH_2DTiCl_3(dmpe)]. No Shapley effect is observed, even though the neutron structure shows it to be agostic with one Ti-C-H angle of 93.5°. Interestingly the neutron structure shows that the C-H bond lengths are similar (Chapter 8, figure 8.1), and since the IPR method depends on there being a difference between the zero point energies (and hence bond lengths) of the agostic and non-agostic bonds, no Shapley effect is expected. In such d^0 systems crystal or molecular structure determinations may be required to establish the presence of distortions arising from agostic interactions.

Also small isotope shifts with no significant temperature dependence may be observed on deuteration. These shifts are due to a second-order isotope effect,[18] where the redistribution of vibrational energy levels on deuteriation causes minor changes in the electronic nature of the methyl group, and not from an agostic interaction. Such isotope effects are typically of the order 0.03 to 0.06ppm and are not temperature dependent, whilst IPR effects give rise to temperature dependent shifts of 0.1ppm or more.

7.4.2 X-ray, neutron and electron diffraction studies.

The most interesting structural feature of agostic bonds is the location of the hydrogen atom and the C-H and M-H bond distances. In several X-ray structure determinations, evidence for interaction of the C-H group with the metal was inferred from a close M-H distance. Many X-ray structures locate and refine hydrogen atom positions, but such data give only approximate M-H and C-H distances.

For more reliable r(C-H) and r(M-H) distances, neutron or possibly electron diffraction data are required. An agostic C-H bond distance lies in the range of 1.13-1.19Å and is elongated 5-10% relative to a non-bridging C-H bond. The M-H distances in agostic bonds are also substantially longer (10-20%) than expected for a normal terminal M-H bond, and all agostic bonds are bent. The effects are due to the presence of a 3c-2e agostic bond with the consequent reduction of the C-H and M-H bond orders. However agostic interactions do not always give rise to an elongated C-H bond as was shown by the usymmetrically distorted $MeTiCl_3(dmpe)$. The neutron structure (Chapter 8, figure 8.1) shows that all three C-H bonds do not deviate significantly from 1.10Å.

7.4.3 Infra-red spectroscopy

The stretching frequencies of agostic bonds have been reported for relatively few agostic compounds. Consequently υ(C-H) data is rarely used as a probe for agostic interactions. Bands assignable to an agostic C-H→M group are found at lower frequencies than for normal sp^3 C-H bonds and occur in the range 2250-2800cm^{-1}. However such bands frequently do not appear and therefore infra-red spectroscopy is an unreliable technique.

7.5 Aims and Objectives

The inaccuracy of X-ray structure characterisation, unreliabilty of infra-red spectroscopy, in searching for α-agostic interactions, and with neutron and electron diffraction studies being costly and not readily available, has led to isotopic perturbation of resonance being the technique widely used to investigate such interactions. This project is concerned with investigating α-agostic interactions in a number of electron deficient organometallic complexes containing hydrogens on the α-carbon atom, primarily using IPR analysis with variable temperature ^1H NMR studies being carried out on a number of mono-deuterated compounds. The investigation was split into two categories as follows;

Chapter 8 concerns the investigation into methyl complexes and focuses on two main areas. (i) The investigation of $MeTiCl_3$ with coordinated bidentate ligands and (ii) Group 6 dimethyl bis imido complexes.

Chapter 9 involves the investigation of neopentyl complexes. A series of neopentyl chloro complexes of titanium and zirconium, of the type $MNp_xCl_{(4-x)}$ (x = 0-4) were investigated for any α-hydrogen interactions.

In order to investigate such complexes using IPR analysis the monodeuterated methyl and neopentyl complexes were synthesised. These were prepared from reactions with the relevant alkyl magnesium halide or lithium salts. The methyl complexes discussed in Chapter 8 were synthesised from CH_2DMgCl or $(CH_2D)Li$, whereas the neopentyl complexes described in Chapter 9 were prepared from $(Me_3CCHD)MgCl$. The remainder of this chapter discusses the preparation of such starting materials, with some new improved methods and attempted alternative reactions, as well as those found in the literature.

7.6 Monodeuterated Methyl and Neopentyl Reagents

7.6.1 Preparation of $(CH_2D)MgCl$, 7.1a, and $(CH_2D)Li$, 7.1b

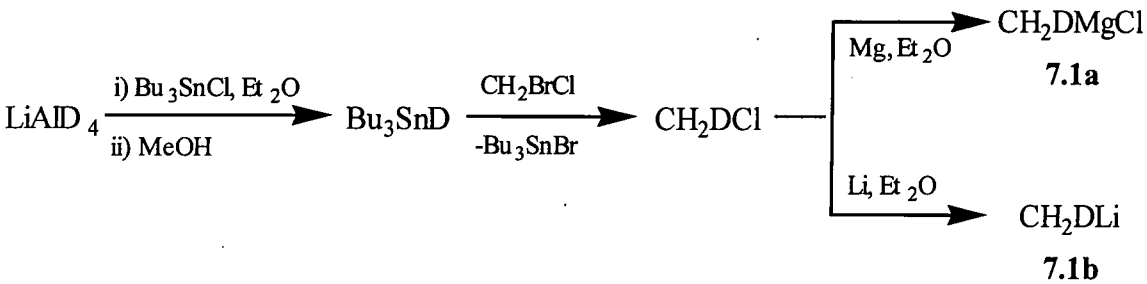

The monodeuterated Grignard and lithium salts were synthesised from a convenient preparation of CH_2DCl,[19] that avoided the use of ketene.[20] The reaction of Bu_3SnCl and $LiAlD_4$ in diethyl ether for 3 hours, followed by work-up with methanol, gave Bu_3SnD in 85% yield as a colourless oil. This was then reacted with a stoichiometric amount of CH_2BrCl producing $(CH_2D)Cl$ as a gas which was fractioned through traps and collected as a white solid at -196°C. The $(CH_2D)Cl$ was condensed directly onto a suspension of magnesium or lithium turnings in diethyl ether producing $(CH_2D)MgCl$, **7.1a** and $(CH_2D)Li$, **7.1b** respectively, as a diethyl ether solution. The resulting solutions were then titrated against n-propanol, using 1,10 phenanthroline as an indicator, to ascertain the exact molarity.

The preparation of $(CH_2D)Cl$ was successful on the whole, with the reaction of Bu_3SnD and CH_2BrCl producing $(CH_2D)Cl$ in good yield. Since the preparation of Bu_3SnD is a two stage reaction with the starting material, LiD, not being the cheapest form of deuterium, a more rapid and less expensive way of preparing CH_2DCl was investigated.

Stephenson and coworkers reduced a number of organic halides to alkanes using a zinc-copper couple in solvents containing H_2O and D_2O, and at varying temperatures depending on the ease with which the organic halide was reduced.[21] Although there are examples of dihaloalkanes being reduced to alkanes there are none where they are reduced to haloalkanes. It was found that simple haloalkanes and also dihaloalkanes required a somewhat higher temperature (>50°C) for full reduction to occur and with bromoalkanes

being easier to reduce than chloroalkanes it was thought that CH_2BrCl may be reduced to CH_2DCl at low temperatures (0°C) as follows:

$$CH_2BrCl \xrightarrow{Zn} Br\text{-}Zn\text{-}CH_2Cl \xrightarrow{D_2O} CH_2DCl$$

A reaction was carried out using a reaction procedure similar to that between Bu_3SnD and CH_2BrCl. Any CH_2DCl produced was collected at -196°C, unreacted CH_2BrCl at -78°C and any CH_2D_2 produced would not condense at these temperatures. A vigorous reaction commenced with some methane being produced and also a white solid forming at -196°C. ^1H NMR analysis showed it to contain approximately equal amounts of the desired product, CH_2DCl, and CH_2D_2, with small quantities of CH_2DBr and CH_2BrCl also produced. By using improved fractionation techniques this method could potentially provide a relatively easy and inexpensive way of producing CH_2DCl.

7.6.2 Preparation of $(Me_3CCHD)MgCl$, 7.2

$(Me_3CCHD)MgCl$, **7.2**, was prepared using an improved synthesis of $Me_3CCH(D)Cl$ from $Me_3CCH(D)OH$.

$$Me_3CC[O]H \xrightarrow[ii)\ H_2O]{i)\ LiAlD_4,\ Et_2O} Me_3CCHDOH \xrightarrow[ii)\ H_2O,\ Et_2O]{i)\ TsCl,\ pyridine} Me_3CCHDOTs$$

The reduction of pivaldehyde, $Me_3CC[O]H$ with $LiAlD_4$ followed by aqueous (H_2O) work-up gave $Me_3CCHDOH$, as a waxy white solid in 56% yield. An improved yield of alcohol was obtained when a solution of pivaldehyde, diluted with Et_2O, was added very slowly at 0°C. This method of preparing the deuterated alcohol is quicker and more convenient than that used by Weiss and Snyder, where a mixture of $Me_3CCH[O]$, $LiAlD_4$ and EtMgBr was refluxed in THF, followed by a complicated separation from the unreacted pivaldehyde giving Np(d)OH in a smaller yield of 39%.[22]

The alcohol was converted into the tosylate, $Me_3CCHDOTs$, in 80% yield by treatment with toluenesulphonyl chloride and pyridine using the standard procedure for the non-deuterated compound, with no need for further purification.

$$Me_3CCHDOTs \xrightarrow{LiCl,\ DMPU} Me_3CCHDCl \xrightarrow{Mg,\ Et_2O} Me_3CCHDMgCl$$

7.2

The conversion of the tosylate to neopentyl chloride, $Me_3CCHDCl$, was achieved using a novel synthesis. The displacement of tosylate by the chloride ion using LiCl was carried out using 1,3-dimethyl-3,4,5,6-tetrahydro-2(1H)-pyrimidinone (DMPU) as the solvent. The chloride was then distilled from the solvent in 96% yield. This method appears superior to previously reported syntheses. Stephenson and co-workers used dimethylsulphoxide (DMSO) as the solvent producing neopentyl chloride in 78% yield contaminated with small amounts of other volatile materials that were difficult to remove.[23] Our attempts to repeat this synthesis in DMSO also gave other volatile, and smelly products that could not be removed. Weis and Snyder achieved a yield of only 62%, not counting the significant amount of unreacted tosylate recovered from the reaction, using the hazardous hexamethylphosphoramide (HMPA) as the solvent.[22] Lee employed the use of triphenylphosphine and carbon tetrachloride and after two distillations the neopentyl chloride was still contaminated with CCl_4.

7.7 Experimental

7.7.1 Preparation of $(CH_2D)MgCl$, 7.1a and $(CH_2D)Li$, 7.1b

Preparation of Bu_3SnD

Initially $LiAlD_4$ was prepared. A suspension of finely ground LiD (2.0g, 0.22mol) in diethyl ether (60ml) was cooled to 0°C. It is essential to finely grind the LiD. A solution of $AlCl_3$ (7.0g, 52mmol) in diethyl ether (60ml) was then added dropwise over a period of 10min and the mixture was stirred at room temperature for 16hr. The $LiAlD_4$ formed as a white precipitate and was used in situ for the next stage of the reaction.

The $LiAlD_4$ suspension was cooled to 0°C and Bu_3SnCl (22ml, 80.6mmol) was added dropwise. The mixture was stirred at room temperature for 3hr, then cooled to 0°C, and methanol (10ml) was added dropwise. The solution was filtered and the residue was washed with diethyl ether (2 x 20ml). The solvent was removed from the combined washings on a rotary evaporator leaving pure Bu_3SnD (21g, 85% yield with respect to Bu_3SnCl) as a colourless oil.

^{119}Sn NMR δ/ppm, C_6D_6; -88.8ppm (t, SnD)

Preparation of CH_2DCl

a) Reaction between Bu_3SnD and CH_2BrCl[24]

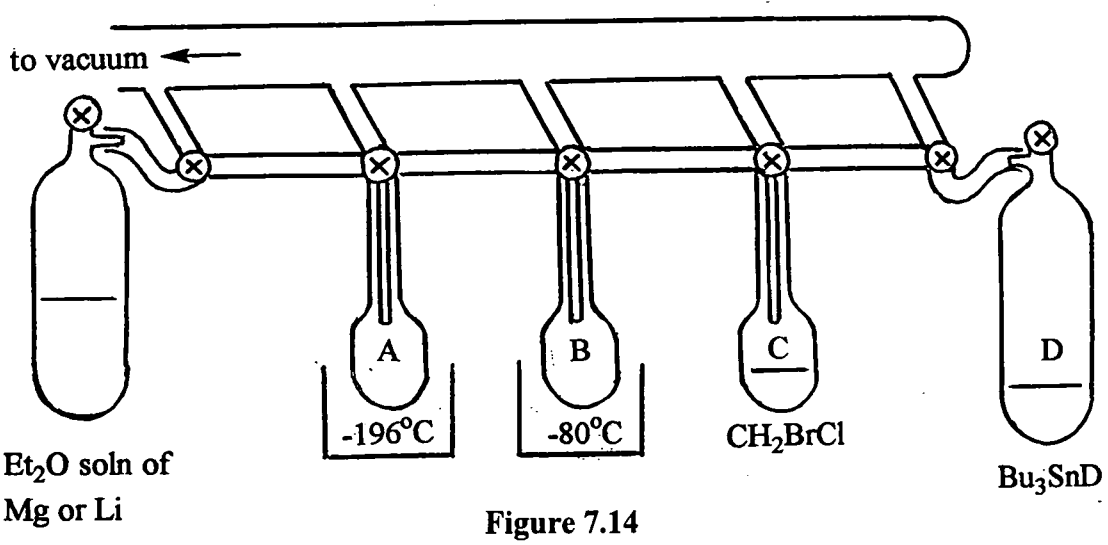

Figure 7.14

CH_2DCl (a gas at room temperature) was prepared using the apparatus shown in figure 7.14. Bu_3SnD (21.0g, 72mmol) was placed in D, cooled to -196°C and placed under reduced pressure. CH_2BrCl (4.65ml, 71.8mmol) was transferred under reduced pressure into trap C at -196°C, then slowly warmed and transferred onto the frozen Bu_3SnD. The frozen mixture was carefully melted and slowly warmed to room temperature, with stirring. At this stage a mildly exothermic reaction commenced and the resulting volatiles were fractioned through trap B at -78°C, and trap A at -196°C. Any unreacted CH_2BrCl was collected in trap B, whilst the CH_2DCl was collected in trap A as a white solid. After 30 min the contents of Schlenk D were cooled to -196°C and any unreacted CH_2BrCl from trap B was warmed and condensed onto it. The reaction was then allowed to proceed again as described above, to make sure all the Bu_3SnD had reacted. The yield of CH_2DCl was not determined but the product was transferred under reduced pressure either into a storage bulb (2L) at -196°C or used directly to react with magnesium or lithium.

^1H NMR δ/ppm, $CDCl_3$; 3.12 (s, CH_3 from 2% CH_3Cl), 3.10 (t, 2H, CH_2D)

b) Reaction between CH_2BrCl and D_2O

Initially the zinc-copper couple was prepared. Zinc dust (6.5g, 100mmol) was suspended in distilled water (10ml). Acidic cupric chloride solution (22ml of a 5%HCl solution, 0.15M) was added with vigorous stirring. When the evolution of gas had ceased the suspension was filtered and the black residue washed sequentially with H_2O (2 x 20ml), acetone (2 x 20ml) and D_2O (2 x 20ml) followed by acetone (2 x 20ml). Finally the Zn-Cu couple was washed with diethyl ether (2 x 20ml) and dried under reduced pressure. Diethyl ether (30ml) was added to the Zn-Cu couple, followed by D_2O (0.54ml, 27mmol), the mixture cooled to -196°C and placed under reduced pressure. CH_2BrCl (1.6ml, 25mmol) was condensed onto the frozen suspension and the reactants were allowed to warm slowly to 0°C at which point an exothermic reaction commenced. The volatiles were fractioned through traps at –78 and -196°C (using the apparatus shown in figure 7.14). Any methane produced would pass through these traps. When the evolution of gas had ceased any unreacted CH_2BrCl collected at –78°C was condensed onto the reactants at

-196°C, and the reaction was allowed to proceed once more. The white solid collected at -196°C was transferred into a storage bulb, and was found to contain mainly CH_2DCl, with small quantities of ethylene and CH_2DBr also produced.

^1H NMR δ/ppm, $CDCl_3$; 5.49 (s, C_2H_4), 3.10 (t, CH_2DCl), 2.74 (t, CH_2DBr).

Preparation of $(CH_2D)MgCl$, 7.1a[25]

Diethyl ether (50ml) was added to activated magnesium (2.6g, 0.108mol, stirred vigorously under nitrogen for 2hr) and the suspension was cooled to -196°C. A small amount of CH_2DCl was transferred under reduced pressure onto the frozen suspension. This was then allowed to warm to room temperature and stirred for 30 min before being cooled to -196°C and a second portion of CH_2DCl condensed onto it. This procedure was repeated until no further CH_2DCl remained after which the mixture was stirred for 12hr. The solution was filtered and the unreacted magnesium was washed with diethyl ether (2 x 25ml). The washings were combined and 0.5ml aliquots were titrated against n-propanol using 1,10-phenanthroline as an indicator. $(CH_2D)MgCl$, **7.1a**, (100ml of 0.4M solution, 40mmol, 55% yield with respect to Bu_3SnD) was produced as a pale yellow solution.

Preparation of $(CH_2D)Li$, 7.1b[25]

Under an atmosphere of argon, a suspension of lithium (1.4g, 0.2mol, finely cut) and diethyl ether (100ml) was cooled to -196°C and placed under reduced pressure. A small portion of CH_2DCl was transferred onto the frozen lithium suspension and allowed to warm to room temperature for 30 min with stirring before being cooled to -196°C and a second portion added. The procedure was repeated until no further CH_2DCl remained and finally the mixture was stirred at room temperature for 24hr. The solution was filtered and the molarity determined in the manner described for $(CH_2D)MgCl$. $(CH_2D)Li$, **7.1b**, (100ml of 0.55M solution, 55mmol, 76% yield with respect to Bu_3SnD) was produced as a pale yellow solution.

7.7.2 Preparation of $Me_3CCHDMgCl$, 7.2

Preparation of $Me_3CCHDOH$[26]

Diethyl ether (100ml) was added to $LiAlD_4$ (2.0g, 0.22mol) and the suspension was cooled to 0°C. $Me_3CCH[O]$ (12g, 0.14mol 0.65 x theory) in diethyl ether (80ml) at 0°C was then added dropwise over a period of 1hr and the mixture was stirred for 24hr. The flask was cooled to 0°C and H_2O (2ml in 50ml Et_2O) followed by NaOH (0.6g in 3ml H_2O) was added dropwise causing the contents to become viscous. Diethyl ether (300ml) was added to the mixture which was then filtered and the filtrate washed with diethyl ether (2 x 200ml). The combined ether extracts were dried over $MgSO_4$, filtered, and the solvent was removed under reduced pressure affording $Me_3CCHDOH$ (7.0g, 78.6mmol, 56% yield) as a waxy solid.

^1H NMR δ/ppm, $CDCl_3$; 3.29 (s, CH_2 from 2% Me_3CCH_2OH), 3.27 (t, 1H, CHD), 1.55 (s, 1H, OH), 0.92 (s, 9H, CMe_3).

Preparation of $Me_3CCHDOTs$[23]

$Me_3CCHDOH$ (7.0g, 78.6 mmol) and para-toluene sulphonyl chloride (15.0g, 79mmol) was stirred in pyridine (60ml) at 0°C for 24hr. The mixture was poured onto ice-water (1lt) and the product extracted into diethyl ether (3 x 200ml). The ether extract was washed with 1M HCl (4 x 100ml) followed by H_2O (3 x 100ml) and then dried over $MgSO_4$. The solvent was removed under reduced pressure yielding $Me_3CCHDOTs$ (15.3g, 62.9mmol, 80% yield) as a white solid.

^1H NMR δ/ppm, $CDCl_3$; 7.62 (d, 2H, C_6H_4), 7.50 (d, 2H, C_6H_4), 3.66 (s, CH_2 from 2% Me_3CCH_2OTs), 3.64 (t, 1H, CHD), 2.45 (s, 3H, CH_3), 0.90 (s, 9H, CMe_3).

Improved synthesis of $Me_3CCHDCl$

A solution of $Me_3CCHDOTs$ (15.3g, 62.9mmol) and dried LiCl (2.9g, 68mmol, 1.08 x theory) was stirred in 1,3-dimethyl-3,4,5,6-tetrahydro-2(1H)-pyrimidinone (DMPU) (30ml) at 90°C in a sealed ampoule under vacuum for 24hr. The product was carefully distilled under reduced pressure (23°C, 10^{-2}mmHg) to afford pure $Me_3CCHDCl$ (6.5g, 60.5mmol, 96% yield, >95 %D) as a colourless liquid.

^1H NMR δ/ppm, $CDCl_3$; 3.34 (s, CH_2 from 2% Me_3CCH_2Cl), 3.32 (t, 1H, CHD), 1.0 (s, 9H, CMe_3)

Preparation of $Me_3CCHDMgCl$, 7.2[27]

Diethyl ether (80ml) was added to activated magnesium (3.0g, 0.125mmol, stirred vigorously under nitrogen for 2hr), and the suspension was brought to reflux. A solution of $Me_3CCHDCl$ or Me_3CCH_2Cl (6.5g, 60.5mmol) and dibromoethane (1ml) in diethyl ether (20ml) was added dropwise to the refluxing mixture over 3hr, and the mixture was refluxed for 16hr. The resulting yellow solution was filtered at room temperature and washed with diethyl ether (20ml) The washings were combined and 0.5ml aliquots were titrated against n-propanol using 1,10-phenanthroline as an indicator. $Me_3CCHDMgCl$ and Me_3CCH_2MgCl, **7.2**, (120ml of 0.4M solution, 48mmol, 79% yield) was produced as a pale yellow solution.

7.8 References

1 M. Brookhart and M.L.H. Green, *J. Organomet. Chem.*, 1983, **250**, 395.

2 R.H. Crabtree and D.G. Hamilton, *Adv. Organomet. Chem.*, 1988, **28**, 299.

3 M. Brookhart, M.L.H. Green and L-L. Wong, *Prog. Inorg. Chem.*, 1988, **36**, 1.

4 N.A. Bailey, J.M. Jenkins, R. Mason and B.L. Shaw, *J. Chem. Soc., Chem. Commun.*, 1965, 237.

5 S.J. LaPlaca and J.A. Ibers, *Inorg. Chem.*, 1965, **4**, 778.

6 Z. Dawoodi, M.L.H. Green, V.S.B. Mtetwa, K. Prout, A.J. Schultz, J.M. Williams and T.F. Keotle, *J. Chem. Soc., Dalton Trans.*, 1986, 1629.

7 O. Eienstein, and Y. Jean, *J. Am. Chem. Soc.*, 1985, **107**, 1177.

8 A.D. Gaunt and C. Kemball, Catalysis (Special Periodical Reports), *The Chemical Society.*, 1977, **1**, 277.

9 W.E. Piers and Bercaw, *J. Am. Chem. Soc.*, 1994, **112**, 9406

10 a) C. Janiak, H.H. Brintzinger and M.H. Prosenc, *Organometallics*, 1992, **11**, 4036; b) C. Janiak, *J. Organomet. Chem.*, 1993, **452**, 63.

11 N.S. Barta, B.A. Kirk and J.R. Stille, *J. Am. Chem. Soc.*, 1994, **116**, 8912.

12 M. Saunders, L. Telkovski and M.R. Kates, *J. Am. Chem. Soc.*, 1977, **99**, 8070.

13 R.B. Calvert and J.R. Shapley, *J. Am. Chem. Soc.*, 1978, **100**, 7726.

14 J.C. Green and M.J. Payne, *Magn. Reson. Chem.*, 1987, **25**, 544.

15 R.C. Cookson, T.A. Crabb, J.J. Frankel and J. Hudec, *Tetrahedron Suppl. 7*, 1966, 355.

16 G. Englert and A. Sauppe, *Mol. Cryst.*, 1966, **1**, 503

17 C.A Tolman and J.W. Faller, *Homogeneous Catalysis with Metal Phosphine Complexes.*, L.H. Pignolet, Ed., New York, 1983, 2.

18 a) P.E. Harrison, *Annu. Rep. NMR. Spectros.*, 1983, **15**, 105. b) R.K. Harris, *Nuclear Magnetic Resonance Spectroscopy.*, Longman, London, 1986, 94.

19 M.L.H. Green, A.K. Hughes, N.A. Popham, A.H.H. Stephens and L.L. Wong, *J. Chem. Soc., Dalton Trans.*, 1992, 3077.

20 F.I. Anderson, *Nature (London)*, 1954, **173**, 541.

21 L.M. Stephenson, R.V. Gemmer and S.P. Current, *J. Org. Chem.*, 1977, **42**, 212.

22 R.G. Weiss and Snyder, *J. Org. Chem.*, 1971, **36**, 403.

23 B. Stephenson, G. Solladie and H.S. Mosher, *J. Am. Chem. Soc*, 1972, **94**, 4184.

24 H.G. Kuiliva, *Synthesis.*, 1970, 499.

25 M.J. Lusch, W.V. Phillips, R.F. Seiloff, G.S. Nomura and H.O. House, *Org. Synth.*, 1984, **62**, 101.

26 R.R. Schrock and J.D. Fellmann, *J. Am. Chem. Soc.*, 1978, **100**, 3359.

27 P. Legzdins, S.J. Rettig, J.E. Veltheer, R.J. Batchelor and F.W.B. Einstein, *Organometallics*, 1993, **12**, 3575.

Chapter 8

Investigation of Methyl Complexes for α-Agostic Interactions

Chapter 8 concerns an investigation into potential α-agostic interactions in some methyl complexes using the IPR technique, and is split into two sections. The first study is of the Group 4 complexes $MeTiCl_3L$ (where L is a bidentate ligand e.g dme, tmeda or diphos), **8.1**, and the second study is of the Group 6 complexes $M(NR)_2(Me)_2$ (where M = W, R = ^tBu; M = Mo, R = ^tBu, 2,6-$^iPr_2C_6H_3$), **8.2**.

8.1 Investigation of $MeTiCl_3L$ (L = dme, tmeda, diphos)

8.1.1 Introduction

The first fully characterised α-agostic complex was (η^2-Me)$TiCl_3$dmpe, the structure of which was determined by neutron diffraction.[1] This showed the methyl group being tilted such that one hydrogen approaches the metal giving a Ti-C-H_α angle of 93.5° (figure 8.1).

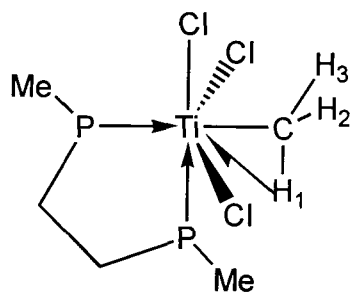

r(Ti-H_1)	2.447Å
r(C-H_1)	1.095Å
r(C-H_2)	1.090Å
r(C-H_3)	1.082Å
<(Ti-C-H_1)	93.5°
<(Ti-C-H_2)	112.9°
<(Ti-C-H_2)	118.4°

Figure 8.1

Two characteristics led to $MeTiCl_3$dmpe being studied. Firstly, titanium with its low atomic number means that X-ray diffraction will have a better chance of locating hydrogen atoms near to the metal centre in the form of an agostic bond. Secondly, being of d^0 configuration the complex has an empty orbital with which to accept electrons, but also means that an alkylidene hydride cannot be formed. The reversible 1,2 hydrogen shift takes place in certain metal alkyl complexes causing a formal increase in the electron count of the metal by two and a reduction of the d^n number of the metal by two. Therefore oxidative addition of the α-C-H bond can only take place if the metal centre has at least two electrons available, as well as an appropriate empty orbital.

However, IPR analysis of $(CH_2D)TiCl_3$dmpe has shown an isotope shift of only 0.057ppm at 233 K and 0.070ppm at 173 K.[2] An isotope shift of at least 0.1ppm with a large temperature dependence is required as evidence for an α-agostic bond. This led to our investigation of further bidentate ligands bonded to $MeTiCl_3$, using the IPR technique including the bidentate oxygen, nitrogen and phosphorus ligands, dimethoxyethane and tetramethylethylenediamine and 1,2 bis(diphenylphosphino)ethane respectively.

8.1.2 Preparation of $(CH_2D)TiCl_3L$ (L = dme, tmeda and diphos)

$(CH_2D)TiCl_3L$ was prepared from the addition of the relevant bidentate ligand to freshly prepared $(CH_2D)TiCl_3$. This was synthesised from $Cp_2Ti(CH_2D)_2$ which was in turn synthesised from Cp_2TiCl_2 as follows:

$$Cp_2TiCl_2 \xrightarrow[\text{ii) } H_2O \text{ iii) pentane}]{\text{i) } (CH_2D)Li,\ Et_2O} Cp_2Ti(CH_2D)_2 \xrightarrow[-Cp_2TiCl_2]{TiCl_4,\ \text{toluene}} (CH_2D)TiCl_3$$

The reaction of Cp_2TiCl_2 and $(CH_2D)Li$, **7.1b**, produced orange needle-shaped crystals of $Cp_2Ti(CH_2D)_2$ as described in the experimental section.[3] Being light and thermally sensitive they needed to be stored at -20°C in the dark, as they decompose readily to a brown then eventually black solid. Bamford and co-workers proposed the following decomposition scheme for the photolysis reaction:[4]

$$Cp_2TiMe_2 \longrightarrow [Cp_2TiMe_2]^* \longrightarrow [Cp(C_5H_4)TiMe] + CH_4 \longrightarrow '(C_5H_4)_2Ti' + CH_4$$

This complex has already been investigated for α-agostic interactions using IPR analysis. The ^1H NMR spectra in $CDCl_3$ at room temperature compares favourably to that obtained by Green et al for $Cp_2Ti(CH_2D)_2$ in C_6D_6.[2] A triplet at –0.108ppm for the CH_2D group and a singlet at –0.059ppm for the CH_3 group gave a small isotope shift of 0.049ppm, therefore showing no evidence for agostic interactions.

The reaction of $Cp_2Ti(CH_2D)_2$ with two equivalents of $TiCl_4$ produces a solution of $(CH_2D)TiCl_3$ and Cp_2TiCl_2.[5] Being volatile the $(CH_2D)TiCl_3$ was isolated using vacuum transfer and collected as a frozen purple suspension in toluene at -196°C, which on warming formed an orange solution, indicating the presence of $(CH_2D)TiCl_3$. As well as being extremely air and moisture sensitive the complex is also light and thermally unstable. Hydrocarbon solutions of $MeTiCl_3$ at room temperature decompose more slowly and therefore it was left as a toluene solution and not isolated as a solid, where it would be even less stable.

There has been much interest as to whether an α-agostic interaction exists in $MeTiCl_3$. Electron diffraction studies suggested that a symmetrical distortion existed, such that the methyl group giving a Ti-C-H angle of ca.101° and an unusually long C-H distance of 1.10Å.[6] A positive value of +11.27Hz has also been observed for the ^2J(H-H) coupling constant,[7] which is unique, with sp^3 C-H systems normally being negative, and positive values normally being associated with sp^2 C-H character. It was therefore proposed that the C-H bond was donating electron density into the empty metal d orbitals. However, these results have recently been disproved with a negative ^2J(H-H) being measured,[8] and new electron diffraction studies showing a normal Ti-C-H angle of 109°.[9] IPR analysis showed a small isotope shift of 0.041ppm at room temperature with little temperature dependence,[2] and it is now thought that the geometry of the CH_3Ti system is more or less tetrahedral.

8.1.3 Preparation of $(CH_2D)TiCl_3$dme, 8.1

$$(CH_2D)TiCl_3 \xrightarrow[\text{ii) pentane}]{\text{i) dme, toluene}} (CH_2D)TiCl_3\text{dme}$$

8.1

Treatment of the toluene solution of $(CH_2D)TiCl_3$ with an excess of dimethoxyethane gave a violet solution that was precipitated with pentane to yield $(CH_2D)TiCl_3$dme, **8.1**, as a violet/pink powder.[10] The six co-ordinate octahedral (figure 8.2) complex was found to be more stable than the parent alkyl and more stable in the solid state than solution. Despite

this the complex still required to be stored in the dark at –20°C, where it was stable for a few weeks.

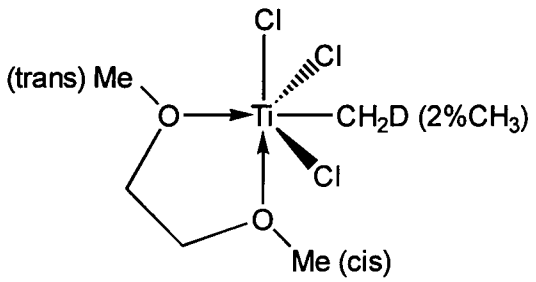

Figure 8.2

NMR Studies

A NMR sample was prepared in $CDCl_3$, the concentration was deliberately kept low to prevent the complex from precipitating out during low temperature analysis, which would lead to poor resolution. The ^1H NMR spectrum at room temperature shows two broad resonances indicating a fluxional dme group. A triplet at 2.66ppm is also observed for the monodeuterated methyl CH_2D-Ti, and as anticipated a small singlet appears at a slightly higher frequency of 2.71ppm, for the protiomethyl CH_3-Ti (figure 8.3). This small amount of protiomethyl complex is caused by the 2% LiH in the 98% LiD purchased from Aldrich for the synthesis of $(CH_2D)Li$.

Variable temperature ^1H NMR analysis was carried out, and highly digitised spectra recorded at 20°C intervals from 20°C down to -60°C ($CDCl_3$ freezes at -64°C, preventing lower temperatures being measured). As the temperature was lowered the broad resonance for the fluxional dimethoxyethane became resolved into four main peaks with an integral ratio of 3:2:2:3. This is due to two inequivalent methyl groups bonded to the oxygen, one that is trans to the CH_2D-Ti and the other that is cis to it (figure 8.4). The two CH_2 groups in O-CH_2-CH_2-O are also inequivalent thereby causing the observed ratio of integrals. The isotope shifts, $\Delta\delta$, were measured along with the coupling constants ^2J(H-D) and ^2J(H-H) where possible, and the results shown in table 8.1

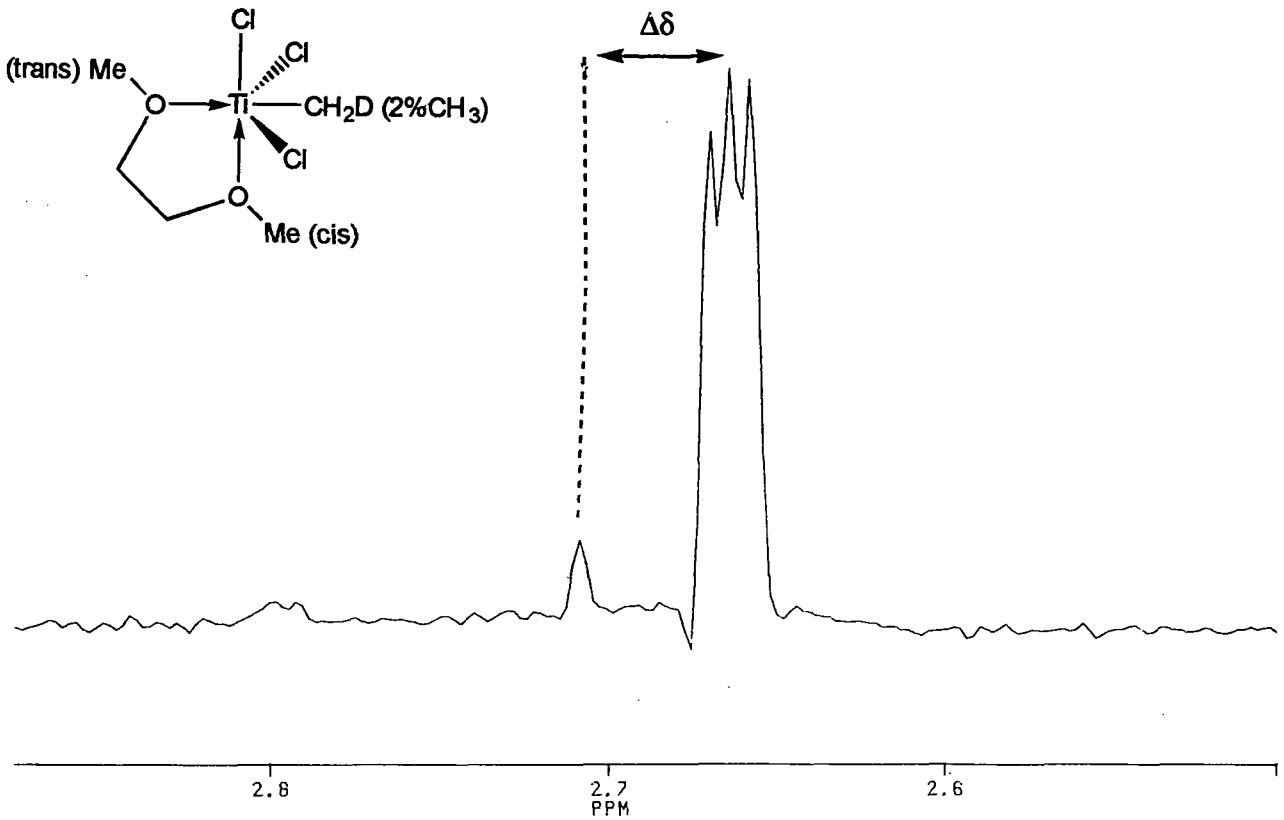

Figure 8.3 Part of the ^{1}H NMR spectrum of **8.1** in $CDCl_3$ at room temperature

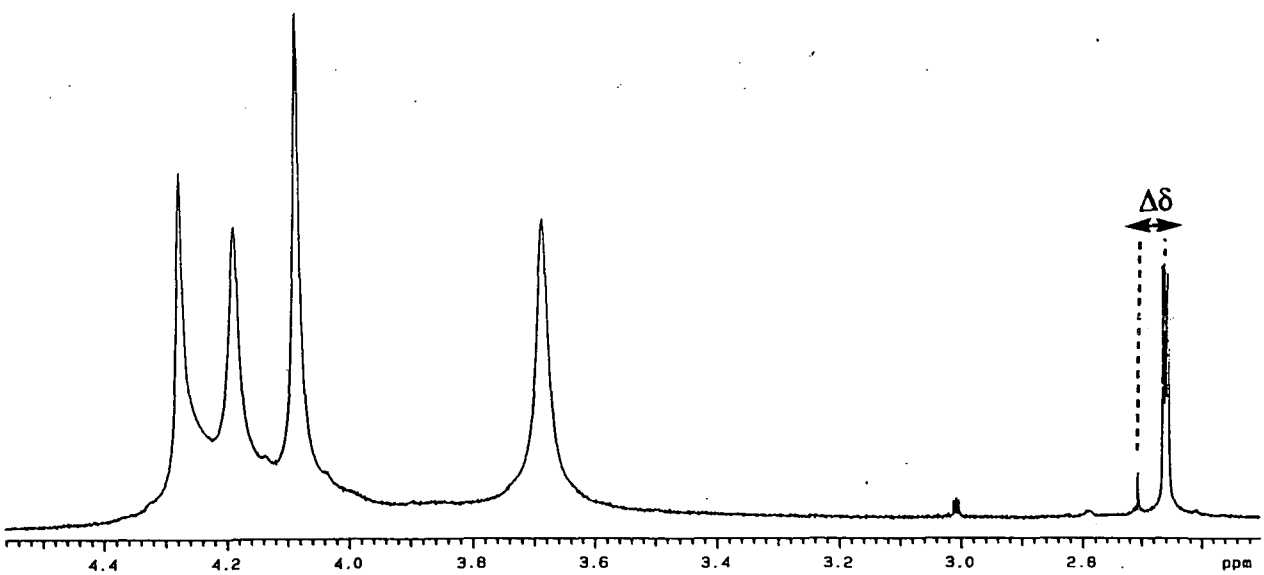

Figure 8.4 Part of the ^{1}H NMR spectrum of **8.1** in $CDCl_3$ at -60°C

Temp. (°C)	^2J(H-D)/Hz	^2J(H-H)/Hz[i]	$\delta(CH_3)$/ppm	$\delta(CH_2D)$/ppm	$\Delta\delta$/ppm[ii]
+20	-	-	2.7084	2.6636	0.0448
0	-1.6	-10.4	2.705	2.659	0.046
-20	-1.6	-10.4	2.718	2.672	0.047
-40	-	-	2.733	2.686	0.047
-60	-	-	-[iii]	2.704	-

i) Coupling constants $^2J(H\text{-}H) = 6.5[^2J(H\text{-}D)]$. Sometimes, particularly at low temperatures the triplet is not observed; ii) $\Delta\delta = \delta(CH_3 - CH_2D)$; iii) Not observed.

Table 8.1

Table 8.1 shows a small but significant isotope shift, $\Delta\delta$, upon deuteration, but very little temperature dependence. For an agostic interaction an isotope shift of at least 0.1ppm with a significant temperature dependence would be expected. As discussed in Chapter 7, the shifts observed are therefore most likely due to second order isotope effects, where redistribution of the vibrational energy levels upon deuteration cause minor changes in the electronic nature of the methyl group, and not from an agostic interaction.

It was hoped that ^{13}C-^1H heteronuclear shift correlation NMR could be carried out so that the relative sign of the geminal coupling constants could be measured and used as a probe into agostic bonding. The sparing solubility in NMR solvents and the sensitivity of the complex meant that this was not possible, however, the $^2J(H\text{-}H)$ value for the complex is assumed to be negative as there are no examples with positive values. The $^2J(H\text{-}H)$ values for the dme complex show no deviation from the range of values (-7.9 to – 12.2Hz) previously observed for 18 electron transition metal methyl complexes, and also no temperature dependence.

No $^1J(C\text{-}H)$ coupling constant was measured and therefore no evidence for an agostic interaction could be taken from it. Often only a value in the region normally observed for simple sp^3 hybridised methyl groups are seen and therefore gives no indication of an agostic interaction.

8.1.4 Preparation of $(CH_2D)TiCl_3$tmeda, 8.2

$$(CH_2D)TiCl_3 \xrightarrow[\text{ii) pentane}]{\text{i) tmeda, toluene}} (CH_2D)TiCl_3\text{tmeda}$$

8.2

Treatment of a toluene solution of $(CH_2D)TiCl_3$ with an excess of a bidentate nitrogen ligand, tetramethylethylenediamine, followed by precipitation with pentane gave $(CH_2D)TiCl_3$tmeda, **8.2**, as a violet powder.[10]

NMR Studies

Like the dme analogue, the ^1H NMR spectrum of the **8.2** in $CDCl_3$ at room temperature (figure 8.5) shows a fluxional tmeda group with one broad resonance at approximately 2.9ppm, with the CH_3-N group being indistinguishable from the CH_2-N group. Next to this resonance a triplet at 2.44ppm and a small singlet at 2.49ppm were assigned to the CH_2D-Ti and CH_3-Ti groups respectively.

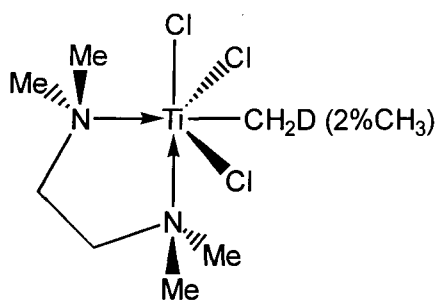

Figure 8.7

During variable temperature ^1H NMR analysis the resonance for tmeda group resolved into two main peaks, one of which obscured the protiomethyl singlet, therefore preventing the isotope shift from being measured. Addition of a small amount of $(CH_3)TiCl_3$tmeda was therefore used to enhance this singlet. The ^1H NMR spectrum at -20°C (figure 8.6) shows a triplet at 2.46ppm for CH_2D-Ti group and a large singlet at 2.51ppm for the CH_3-Ti group. Unlike the signals for dme analogue which resolved into four sharp resonances at low temperature, the tmeda group in **8.2** appears as two main resonances, even at -60°C. A resonance at 2.46ppm appears for the CH_3-N groups, and a resonance at 3.01ppm appears for the CH_2-N groups (figure 8.7).

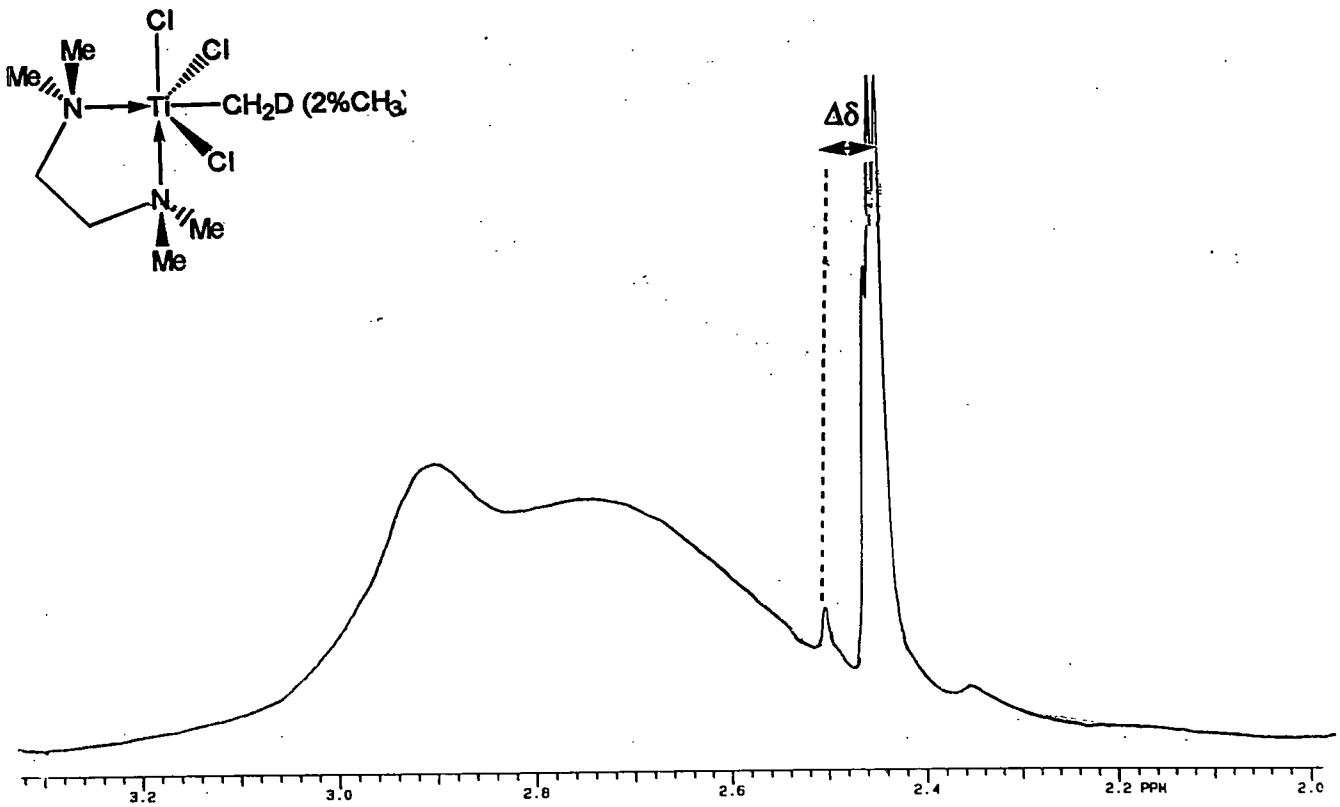

Figure 8.5 Part of the ^{1}H NMR spectrum of **8.2** in $CDCl_3$ at room temperature

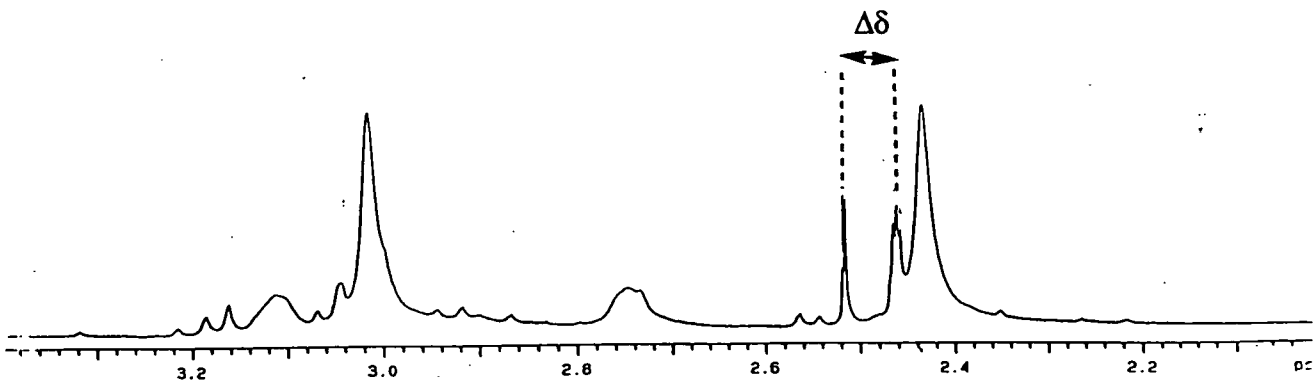

Figure 8.6 Part of the ^{1}H NMR spectrum of **8.2** in $CDCl_3$ at -20°C

Temp. (°C)	^{2}J(H-D)/Hz	^{2}J(H-H)/Hz	δ(CH_3)/ppm	δ(CH_2D)/ppm	Δδ
+20	-	-	2.49376	2.44417	0.0496
0	-1.53	-9.94	2.50255	2.45027	0.0523
-20	-1.45	-9.92	2.51590	2.46020	0.0557
-40	-	-	2.52847	2.47450	0.0540
-60	-	-	2.54223	2.48652	0.0557

Table 8.2

Table 8.2 shows the results from the variable temperature ^{1}H NMR experiments. At room temperature (CH_2D)$TiCl_3$tmeda has an isotope shift of 0.049ppm, similar to that found for the dme complex. However the tmeda complex shows a greater temperature dependence with an isotope shift of 0.056ppm at -60°C whereas the dme complex has a value of only 0.047ppm. Despite this, a significantly greater isotope shift of at least 0.1ppm and with a large temperature dependence is required as evidence for an agostic bond. Again the ^{2}J(H-H) coupling constant shows values that are expected for sp^3 carbons.

8.1.5 Preparation of (CH_2D)$TiCl_3$diphos, 8.3

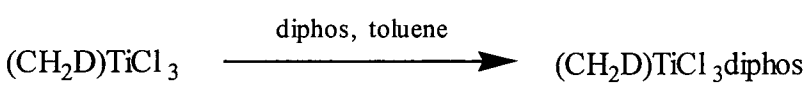

8.3

In an attempt to investigate a complex similar to the agostic $MeTiCl_3$dmpe, (CH_2D)$TiCl_3$diphos, **8.3**, [diphos = 1,2-bis(diphenylphosphino)ethane] was prepared, which also has a bidentate phosphorus ligand. On addition of diphos to (CH_2D)$TiCl_3$ the product began to precipitate from the toluene solution.[10] Unfortunately the product was only sparingly soluble in both $CDCl_3$ and C_6D_6 causing the CH_3-Ti resonance to be obscured by a large broad CH_2D-Ti resonance in the ^{1}H NMR spectra, therefore preventing any isotope shift from being measured.

8.1.6 Conclusions

Both $(CH_2D)TiCl_3$dme, **8.1**, and $(CH_2D)TiCl_3$tmeda, **8.2**, show small temperature independent isotope shifts. However, the absence of IPR effects is not definitive evidence for the absence of an agostic bond, as was shown with $(CH_2D)TiCl_3$dmpe (figure 8.1). The complexes may have an acute Ti-C-H angle indicating an agostic bond but similar bond lengths. Since the IPR method depends on there being a difference between the zero point energies (and hence bond lengths), this could explain the small isotope shifts, which were also found with $MeTiCl_3$. Neutron diffraction studies may provide this evidence but this is an expensive technique and requires suitable crystals.

8.2 Investigation of $[M(N^tBu)_2(CH_2D)_2]_2$ (M = W, Mo), and Mo(N-2,6-$^iPr_2C_6H_3)_2(CH_2D)_2$

8.2.1 Introduction

Recently, examples of metal-imido complexes showing α-agostic interactions have been reported, the first being $[Nb(C_5H_5)(N\text{-}2,6\text{-}^iPr_2C_6H_3)(CH_2CMe_3)_2$ (figure 8.8).[11] The structure determined by X-ray diffraction showed close contact between the α-hydrogen on each neopentyl methylene and the metal centre with a Nb-H distance averaging 2.36Å, and a Nb-C-H_α angle averaging 88°.

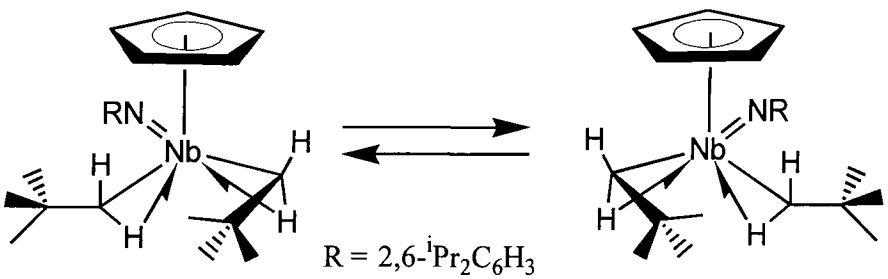

Figure 8.8

^1H NMR studies on the partially deuterated derivative $[Nb(C_5H_5)(N\text{-}2,6\text{-}^iPr_2C_6H_3)(CHDCMe_3)_2]$ showed that on each monodeuterated pair a 0.11ppm upfield shift was observed relative to the per-protio compound. These shifts are consistent with the presence of α-agostic interactions and also show significant temperature dependence. However the complex is formally a 16 electron species and the addition of four more electrons from the two agostic C-H bonds would then form a 20 electron complex. The actual situation is thought to lie somewhere in between the two extremes with the cyclopentadienyl ring competing with the imido group to donate electrons to the metal.

Like the niobium complex, the dimers $[M(N^tBu)_2(CH_3)_2]_2$ (M = W, Mo) (figure 8.9) are 16 electron complexes and therefore have an empty orbital with which to accept electrons. The structure of $[Mo(N^tBu)_2(CH_3)_2]_2$ was determined by X-ray diffraction and shows the first example of an unsymmetrically bridging imido ligand with the three Mo-N bond

lengths corresponding to those expected for triple, double and single bonded nitrogens respectively.[12]

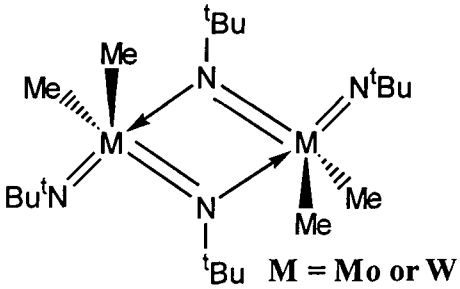

Figure 8.9

Furthermore, the ^1H NMR spectra indicate the possibility of the complexes being monomeric in solution. In both the tungsten and molybdenum complexes only one resonance is observed for the t-butyl groups and only one for the methyl groups. This suggests that the complexes are either fluxional dimers or monomeric in solution. If the latter were to be the case then the possibility of an agostic interaction would be more likely. In monomeric form the imido ligands would be approximately 90° to each other and therefore aligned with the same d orbitals. With each d orbital only able to accept a maximum of two electrons, this would prevent both nitrogens donating their electron lone pairs to the metal in the form of triple bonds. This would make the metal more electron deficient and therefore more likely to accept electrons from the methyl group in the form of an agostic bond.

Recently the complex $[Mo(NAr)_2Me_2]$ (Ar = 2,6- $^iPr_2C_6H_3$) has been synthesised and the structure determined by X-ray diffraction has shown it to be monomeric,[13] presumably due to steric effects caused by the large aryl groups preventing the dimer (where the molybdenum is 5 co-ordinate) from forming (figure 8.10). The hydrogen atoms were not refined and therefore provide no evidence for agostic interactions. However a recent molecular structure of $Mo(NR)(NAr)(CH_2CMe_3)_2$ (R = ^{t}Bu, Ar = 2,6- $^iPr_2C_6H_3$) has shown evidence for agostic interactions (figure 8.11).[14] The metal-hydrogen contacts of 2.35Å ($Mo\cdots H_a$) and 2.44Å ($Mo\cdots H_b$) and Mo-C-H_α angles of 91.1 and 98.0° respectively, are comparable with the multiple agostic interactions found in the niobium complex in figure 8.8.

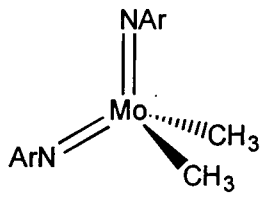

potential α-agostic interactions

Figure 8.10

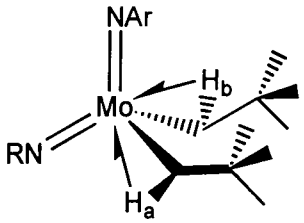

Ar = 2,6-$^{i}Pr_2C_6H_3$ R = ^{t}Bu

Figure 8.11

It was therefore of interest to investigate $[M(N^tBu)_2Me_2]_2$, (M = W, Mo) and $Mo(NAr")_2Me_2$ (Ar" = 2,6-$^{i}Pr_2C_6H_3$) complexes for agostic interactions, by carrying out NMR studies on their monodeuterated methyl analogues, using the IPR technique.

8.2.2 Preparation of $[W(N^tBu)_2(CH_2D)_2]_2$, 8.4

$$W(N^tBu)_2(NH^tBu)_2 \xrightarrow{^tBuOH,\ pentane} W(N^tBu)_2(O^tBu)_2 \xrightarrow[ii)\ pentane]{i)\ Zn(CH_2D)_2,\ Et_2O} [W(N^tBu)_2(CH_2D)_2]_2$$

8.4

The synthesis of $W(N^tBu)_2(NH^tBu)_2$ is described in Chapter 2 and this was converted into $W(N^tBu)_2(O^tBu)_2$ by the reaction with two equivalents of t-butanol in pentane.[15] Fractional distillation of the crude orange/red oil gave pure $W(N^tBu)_2(O^tBu)_2$ as a pale yellow oil, in reasonable yield. $Zn(CH_2D)_2$, synthesised from the reaction of $ZnCl_2$ and two equivalents of CH_2DMgCl, was then reacted with the oil. Red/orange crystals of the dimer $[W(N^tBu)_2(CH_2D)_2]_2$, **8.4**, were formed from pentane at -20°C.

NMR Studies

The ^1H NMR spectrum of **8.4** in $CDCl_3$ at room temperature is consistent with the published data (figure 8.12). Two main resonances are observed, a singlet at 1.04ppm for the t-butyl group and a triplet at 1.386ppm for the CH_2D group. A small singlet accounting for the 2% CH_3 is seen at 1.411ppm, giving a small isotope shift of 0.025ppm. The variable temperature analysis, summarised in table 8.3, shows no observable temperature dependence and therefore no evidence for an agostic interaction.

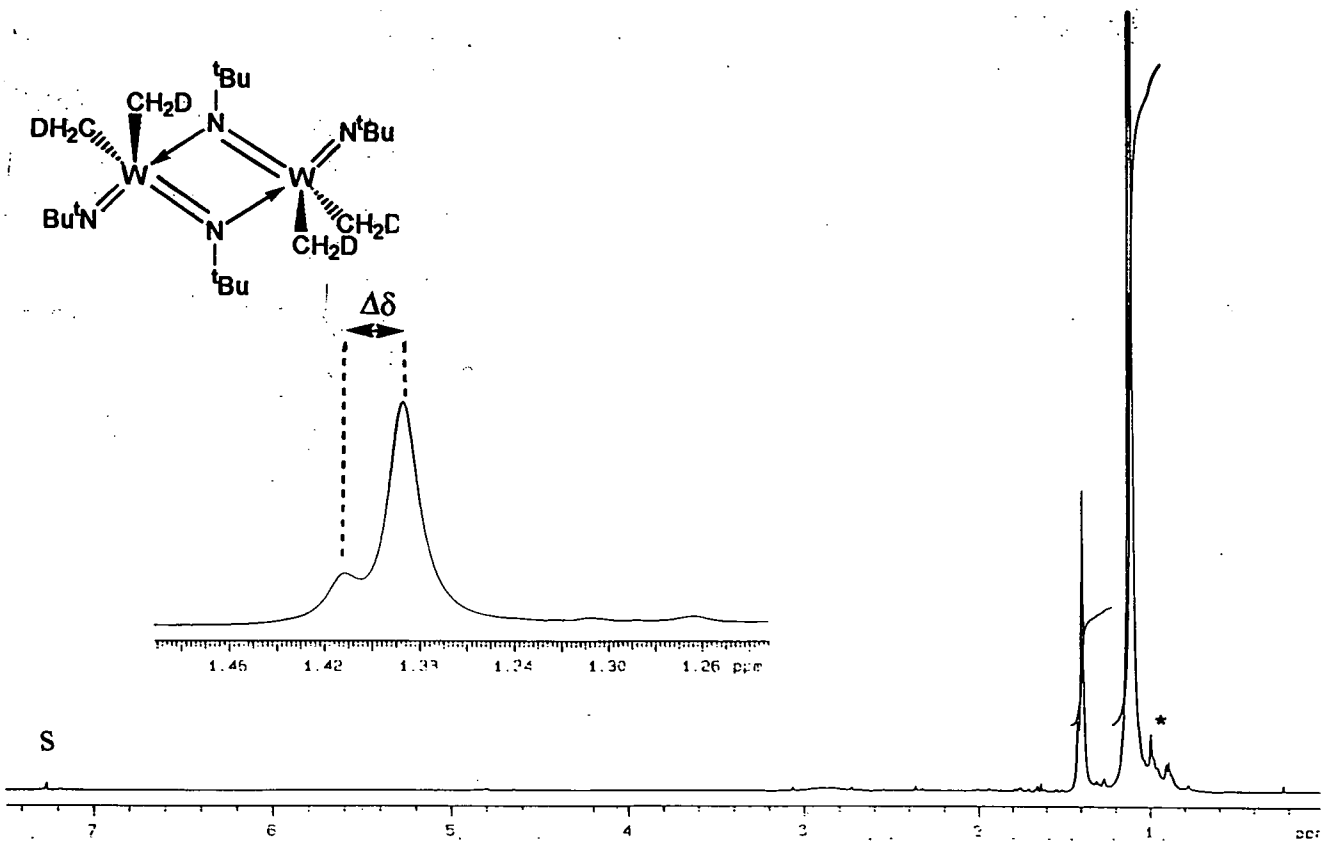

Figure 8.12 ^{1}H NMR spectrum of **8.4** in $CDCl_3$ at room temperature

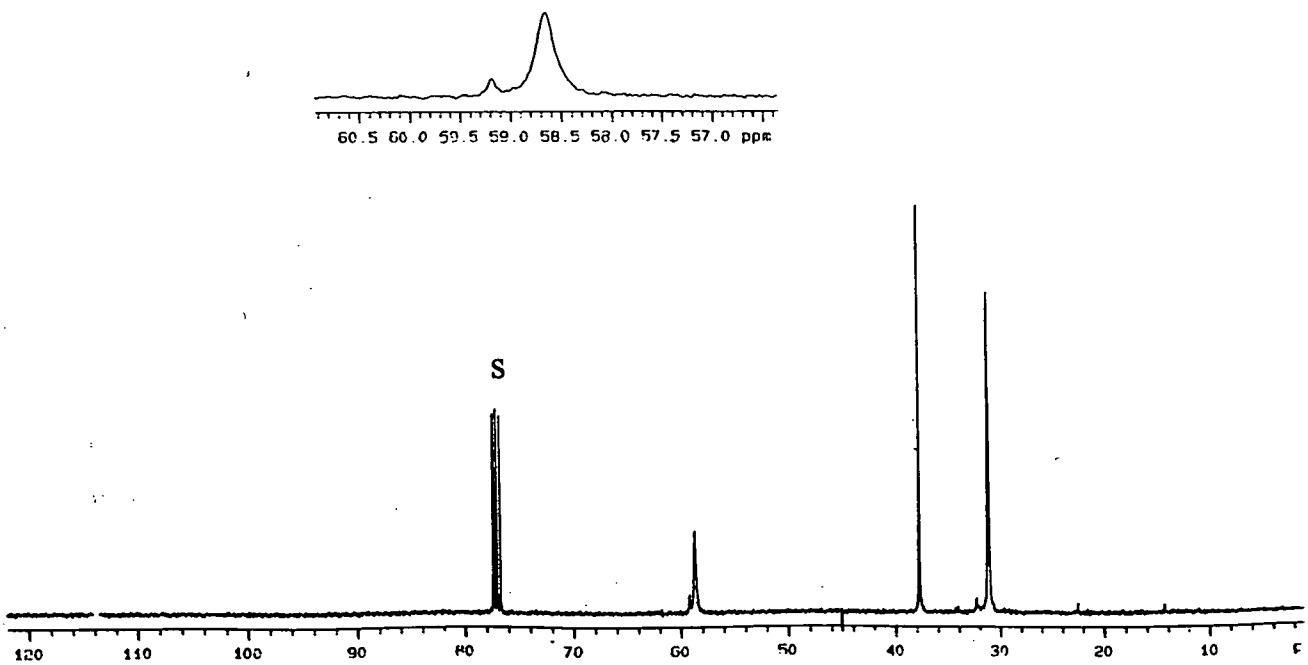

Figure 8.13 $^{13}C\{^{1}H\}$ NMR spectrum of **8.4** in $CDCl_3$ at –40°C

Temp. (°C)	^{2}J(H-D)/Hz	^{2}J(H-H)/Hz	δ(CH_3)/ppm	δ(CH_2D)/ppm	Δδ
+20	-	-	1.411	1.386	0.025
0	-	-	1.412	1.388	0.024
-20	-	-	1.422	1.397	0.025
-40	-	-	1.429	1.403	0.026
-60	-	-	1.435	1.409	0.026

Table 8.3

However, the low temperature $^{13}C\{^1H\}$ NMR studies gave some valuable information regarding the structure of the complex in solution. As the temperature was lowered to 0°C the t-butyl singlet starts to resolve into two peaks and at -40°C two distinct peaks are seen at 37.7ppm and 31.1ppm, indicating that they are in two different environments (figure 8.13). This suggests that **8.4** is a dimer in solution and not the monomer as hoped. The ^1H NMR spectrum must show the terminal and bridging t-butyl groups above coalescence. As discussed earlier, the dimer being more coordinately saturated diminishes the chances of an agostic bond, thereby explaining the very small isotope shift observed.

8.2.3 Preparation of $[Mo(N^tBu)_2Me_2]_2$, 8.5

$$Mo(N^tBu)_2Cl_2dme \xrightarrow[\text{ii) Pentane}]{\text{i) MeMgCl, Et}_2O} [Mo(N^tBu)_2Me_2]_2$$

8.5

The preparation of $Mo(N^tBu)_2Cl_2dme$ is described in Chapter 2 and this complex was used initially to prepare the protiomethyl complex, from the reaction with 2 equivalents of CH_3MgCl in diethyl ether, followed by extraction into pentane.[12] Violet crystals of the dimer $[Mo(N^tBu)_2(CH_3)_2]_2$, **8.5**, formed at -20°C. Low temperature $^{13}C\{^1H\}$ NMR studies of the complex in $CDCl_3$ showed the singlet for the t-butyl resonance to resolve into two peaks, indicating the presence of the dimer in solution, as with the tungsten analogue. Studies with the monodeutero analogues were therefore expected to give similar results and were not carried out.

8.2.4 Preparation of $Mo(NAr")_2(CH_2D)_2$ (Ar" = 2,6-^{i}Pr$_2$C$_6$H$_3$), 8.6

Since the X-ray structure of $Mo(NAr")_2Me_2$ has shown it to be monomeric,[13] it would therefore be more likely to form agostic interactions than the dimers $[M(N^tBu)_2(CH_2D)_2]_2$ M = Mo, W).

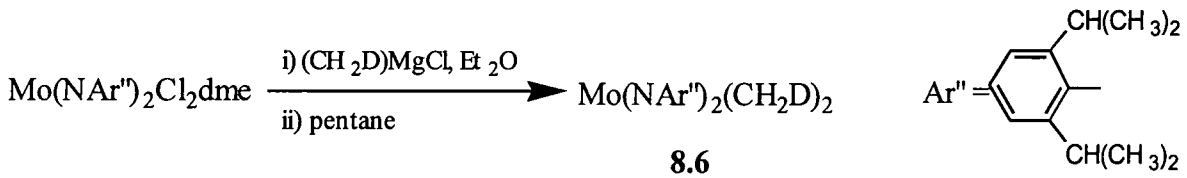

$Mo(NAr")_2Cl_2dme$ was prepared in a similar manner to the analogous t-butyl complex, $Mo(N^tBu)_2Cl_2dme$ and its synthesis is described in Chapter 2 (section 2.5.1). Conversion into the monodeuterated complex, $Mo(NAr")_2(CH_2D)_2$, was achieved by the reaction with two equivalents of $(CH_2D)MgCl$ in diethyl ether, followed by recrystallisation from pentane at -20°C. Pure $Mo(NAr")_2(CH_2D)_2$, **8.6**, formed as dark red crystals.

NMR Studies

The ^{1}H NMR spectrum carried out in C_7D_8 at room temperature (figure 8.14) show the aryl group as a set of resonances for the C_6H_3 group in the aromatic region, a doublet at 1.09ppm and a septet at 3.58ppm, for the C-H group and CH_3 groups respectively in $CH(CH_3)_2$. More importantly the monodeuterated methyl groups are seen as a triplet at 1.300ppm and the 2% CH_3 as a singlet at 1.340ppm giving a small isotope shift of 0.04ppm. Variable temperature NMR studies were carried out at 20°C intervals from 20°C down to -80°C (toluene freezes at -93°C) and the isotope shifts are summarised in table 8.4.

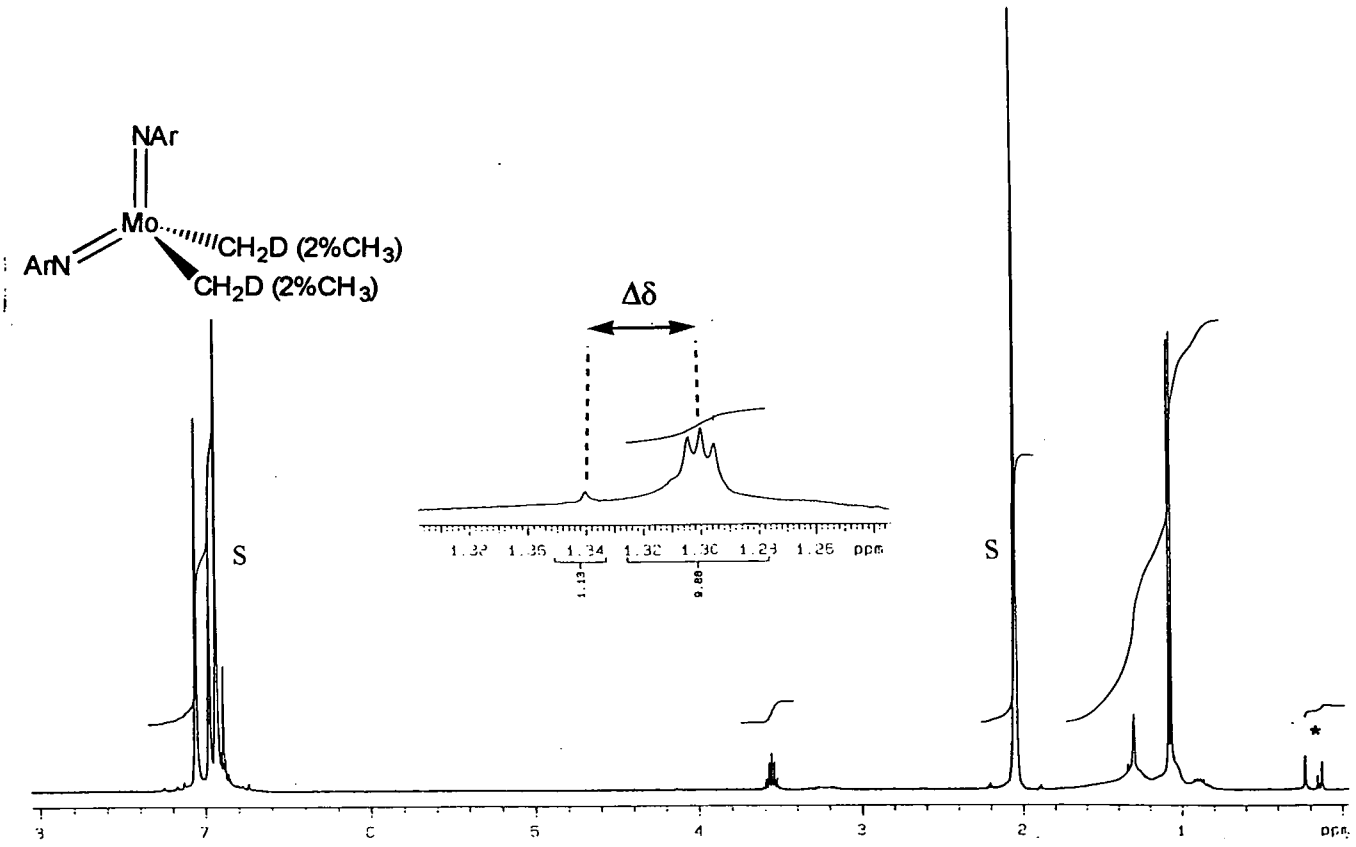

Figure 8.14 ^{1}H NMR spectrum of **8.6** in C_7D_8 at room temperature

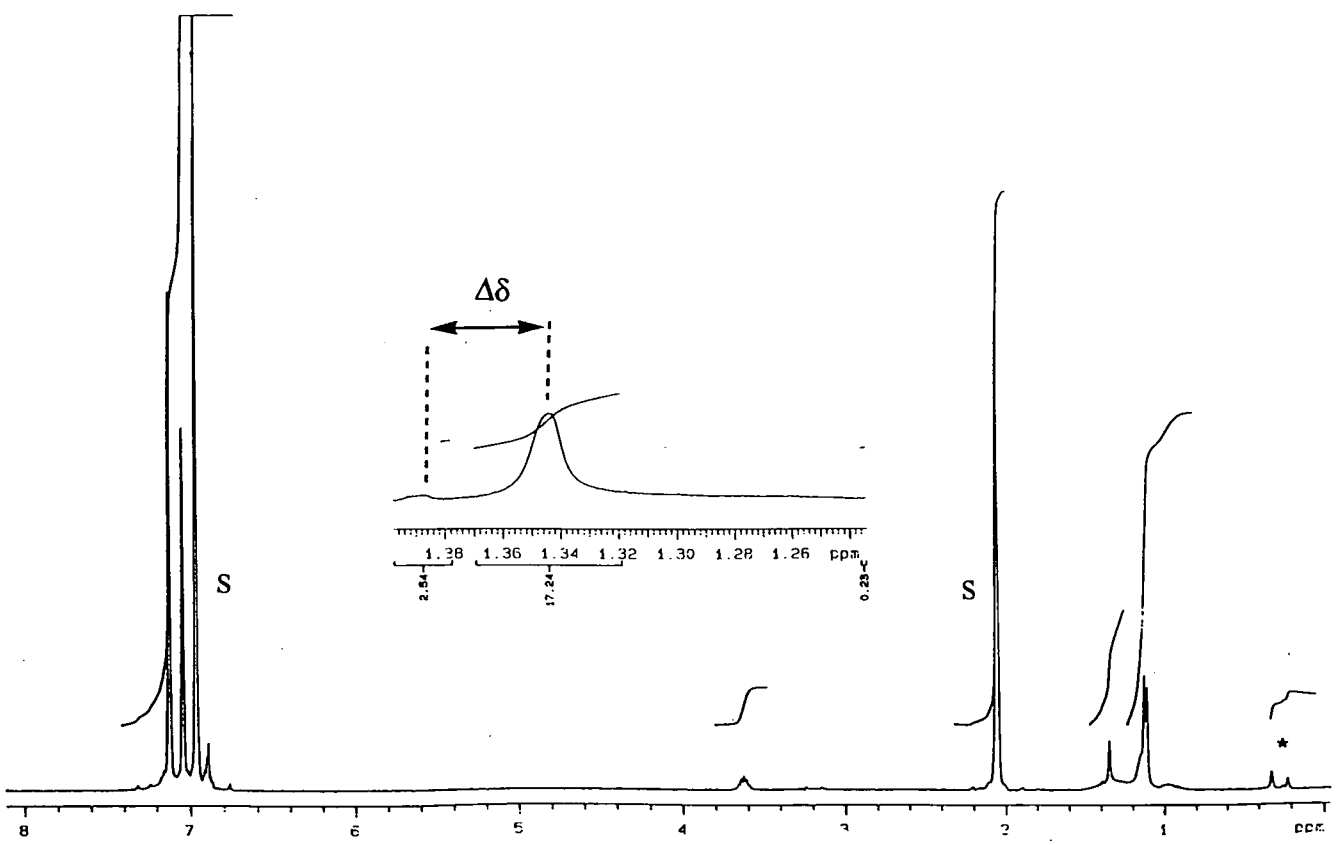

Figure 8.15 ^{1}H NMR spectrum of **8.6** in C_7D_8 at -80°C

Temp. (°C)	^{2}J(H-D)/Hz	^{2}J(H-H)/Hz	δ(CH_3)/ppm	δ(CH_2D)/pp m	Δδ
+20	-1.8	-11.7	1.340	1.300	0.04
0	-1.6	-10.4	1.344	1.305	0.041
-20	-	-	1.357	1.316	0.042
-40	-	-	1.379	1.337	0.042
-60	-	-	1.377	1.334	0.043
-80	-	-	1.387	1.344	0.043

Table 8.4

The ^{1}H NMR spectrum at -80°C (figure 8.15) shows that although the CH_3 and CH_2D resonances have shifted to higher frequency, compared to that at room temperature (figure 8.14), the isotope shift, Δδ, has a similar value of 0.043ppm, therefore showing very little temperature dependence. From the table we can say that no evidence has been gained for agostic interactions in **8.6**.

8.2.5 Conclusions

Being dimers in solution as well as in the solid state and therefore sterically saturated, it is unlikely that $[W(N^tBu)_2Me_2]_2$, **8.4**, or $[Mo(N^tBu)_2Me_2]_2$, **8.5**, will form agostic interactions, and this was confirmed with small isotope shifts, with no temperature dependence, for the tungsten complex. Although small isotope shifts were measured for $Mo(NAr")_2(CH_2D)_2$, **8.6**, and therefore no evidence for α-agostic interactions obtained, we cannot rule out the possibility. X-ray crystallographic studies with refined hydrogen atoms, or preferentially neutron diffraction studies are needed to acquire this evidence.

8.3 Experimental

8.3.1 Preparation of $(CH_2D)TiCl_3dme$, 8.1

$\underline{Cp_2Ti(CH_2D)_2}$

A suspension of Cp_2TiCl_2 (1.0g, 3.25mmol) and diethyl ether (50ml) was wrapped in aluminium foil and cooled to 0°C. A solution of CH_2DLi (14.2ml of a 0.55M solution in diethyl ether, 7.8mmol) was added dropwise. The solution was allowed to warm to room temperature, then stirred in the dark for 2hr. Degassed water was added dropwise to the orange solution, until the evolution of gas had ceased, and the organic layer was separated from the aqueous layer. The solvent was removed from the ether layer under reduced pressure, then the residue was extracted into pentane (20ml) and left to crystallise in the dark at -20°C. $Cp_2Ti(CH_2D)_2$ (yield not determined due to light and thermal sensitivity) was formed as orange needle-shaped crystals and stored in the dark at -20°C, where it was stable for 2 to 3 days.

^1H NMR δ/ppm $CDCl_3$; 4.6 (s, 5H, C_5H_5), -0.037 (s, CH_3), -0.068 (t, 2H, CH_2D)

$\underline{(CH_2D)TiCl_3}$

The preparation was carried out using the double Schlenk apparatus in figure 8.x. One side of the apparatus was quickly (in the dark and at a low temperature as possible) charged with $(CH_2D)_2TiCp_2$ (0.21g, 1.05mmol), and cooled to -78°C. A 10% solution of $TiCl_4$ in toluene (2.3ml of a 0.91M solution, 2.1mmol) was then added dropwise and the mixture was stirred for 30 min. The apparatus was then cooled to -196°C and placed under reduced pressure. The frozen suspension was slowly warmed and the resulting volatiles transferred under reduced pressure into the empty Schlenk at -196°C. A frozen purple suspension of $(CH_2D)TiCl_3$ in toluene was produced which on melting formed $(CH_2D)TiCl_3$ as an orange solution (ca. 2mmol, yield not determined due to light and thermal instability) that was not isolated but used immediately for the addition of the ligand.

$(CH_2D)TiCl_3dme$, 8.1

A 10% solution of dimethoxyethane in toluene (2.2ml of a 0.96M solution, 2.1mmol) was added dropwise to the $(CH_2D)TiCl_3$ (ca. 2mmol) solution at -78°C, in the dark. On warming to room temperature a violet solution formed that was precipitated as a violet powder with pentane (10ml). The solution was filtered and the filtrate was washed with pentane (2 x 10ml) then dried under reduced pressure yielding $(CH_2)TiCl_3dme$, **8.1**, (yield not determined due to light and thermal sensitivity) as a violet/pink powder which was stored in the dark at -20°, where it was stable for a few weeks.

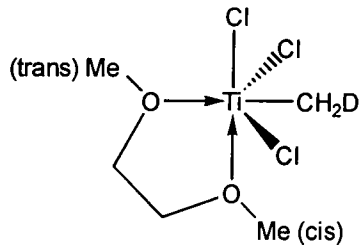

^1H NMR: δ/ppm, 250 MHz, $CDCl_3$, at room temperature

ca.4.1 [br s, 2 x 2H, $(CH_2$-O)]
ca.3.7 [br s, 2 x 3H, $(CH_3$-O)]
2.71 [s, (2% CH_3-Ti)]
2.66 [t, 2H, $^2J_{HD}$=1.6Hz, $(CH_2D$-Ti)]

8.3.2 Preparation of $(CH_2D)TiCl_3$tmeda, 8.2

$(CH_2D)TiCl_3$tmeda was prepared in the same manner as described for the dme complex, with a 10% solution tetramethylethylenediamine in toluene (3.2ml of a 0.66M solution, 2.1mmol) added to the solution of $(CH_2D)TiCl_3$ (ca. 2mmol) in toluene. $(CH_2D)TiCl_3$tmeda, **8.2**, (yield not determined) was isolated as a violet powder and stored at -20°C in the dark.

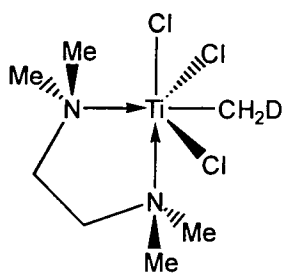

^1H NMR: δ/ppm, 250 MHz, $CDCl_3$, at room temperature

ca.2.9 [br, 4 x 3H, $(CH_3$-N), 2 x 2H, $(CH_2$-N)]
2.49 [s, $(CH_3$-Ti)]
2.44 [t, 2H, $^2J_{HD}$=1.5Hz, $(CH_2D$-Ti)]

8.3.3 Preparation of $(CH_2D)TiCl_3$diphos, 8.3

$(CH_2D)TiCl_3$ in toluene (ca. 2mmol) was transferred under reduced pressure onto 1,2-bis(diphenylphosphino)ethane (0.84g, 2.1mmol) at -196°C. On warming to room temperature a partially insoluble orange/red precipitate formed, which on cooling to -20° fully precipitated. The precipitate was filtered and the remaining toluene was removed under reduced pressure (as reported some of the toluene was entrenched in the product and impossible to remove) leaving $(CH_2D)TiCl_3$diphos, **8.3**, (yield not determined) as an orange powder.

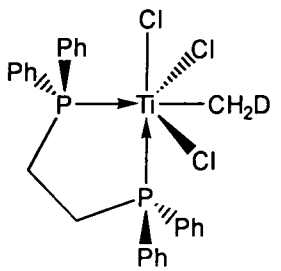

^{1}H NMR: δ/ppm, 250 MHz, C_7D_8, at room temperature

ca.7.4 [br, 4]
(CH_3-Ti obscrurred)
ca.3.0 [br, 2H, (CH_2D-Ti)]

8.3.4 Preparation of $[W(N^tBu)_2(CH_2D)_2]_2$, 8.4

<u>$W(N^tBu)_2(O^tBu)_2$</u>

A solution of $W(N^tBu)_2(NH^tBu)_2$ (7.0g, 14.9mmol) in pentane (20ml) was cooled to 0°C. ^{t}BuOH (2.15g, 29mmol) was added and the mixture was stirred for 1hr. The solvent was removed under reduced pressure and the resultant red/orange solution was purified by fractional distillation. Pure $W(NtBu)_2(O^tBu)_2$ (b.pt. 60-72°C, 10^{-3}mmHg, 3.6g, 7.6mmol, 51% yield) was collected as a pale yellow oil. Higher boiling fractions were contaminated with $W(N^tBu)(O^tBu)_4$.

^{1}H NMR δ/ppm C_6D_6: 1.35 (s, 18H, $NCMe_3$), 1.42 (s, 18H, $OCMe_3$)

$Zn(CH_2D)_2$

Diethyl ether (5ml) was added to $ZnCl_2$ (0.25g, 1.84mmol) and the mixture was cooled to -78°C with stirring. $(CH_2D)MgCl$ (7.5ml of a 0.4M solution, 3.0mmol) was added dropwise over 10min. The solution was warmed to 0°C and stirred for 30min. The $Zn(CH_2D)_2$ produced was not isolated but was transferred under reduced pressure onto the reactants shown below.

$[W(N^tBu)_2(CH_2D)_2]_2$, 8.4

$W(N^tBu)_2(O^tBu)_2$ (0.25g, 0.53mmol) was frozen at -196°C and placed under reduced pressure. $Zn(CH_2D)_2$ (ca. 1.2mmol) in diethyl ether (5ml) was transferred onto the frozen suspension under reduced pressure. The mixture was warmed slowly to room temperature forming a deep orange solution. Pentane (5ml) was added and $[W(N^tBu)_2(CH_2D)_2]_2$, **8.4**, (0.1g, 0.13mmol, 65% yield) was formed as orange/red block-shaped crystals.

^1H NMR: δ/ppm, 400 MHz, $CDCl_3$, at room temperature

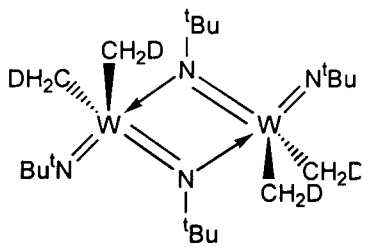

1.411 [s, (2% CH_3-W)]

1.386 [t, 2H, $^2J_{HD}$=1.5Hz, (CH_2D-W)]

1.04 [s, 2 x 9H, ($NCMe_3$)]

8.3.5 Preparation of $[Mo(N^tBu)_2(CH_3)_2]_2$, 8.5

A solution of $Mo(N^tBu)_2Cl_2dme$ (0.25g, 0.63mmol) in diethyl ether (10ml) was cooled to -78°C. CH_3MgBr (0.45ml of 3M solution, 1.35mmol) was added dropwise over 30min and the mixture was allowed to warm to room temperature, then stirred for 2hr. The solvent was removed under reduced pressure, the product was then extracted with pentane (2x10ml) and filtered. The volume of the solution was reduced (10ml) and the solution was then cooled to -20°C. $[Mo(N^tBu)_2(CH_3)_2]_2$, **8.5**, (0.13g, 78% yield) formed as violet crystals.

^{1}H NMR δ/ppm $CDCl_3$; 1.02ppm (s, 12H, CH_3), 1.39 (s, 36H, $NCMe_3$).

8.3.6 Preparation of $Mo(NAr")_2(CH_2D)_2$ (Ar" = 2,6-^{i}Pr$_2$C$_6$H$_3$), 8.6

A solution of $Mo(NAr")_2Cl_2dme$ (0.25g, 0.41mmol from Chapter 2) in diethyl ether (20ml) was cooled to -78°C (dry ice/acetone). $(CH_2D)MgCl$ (0.26ml of a 0.4M solution, 1.05mmol) was added dropwise over 10min and the mixture was allowed to warm to room temperature over 2hr, then stirred for 48hr. The solvent was removed under reduced pressure from the dark red solution and the product was extracted into pentane. The solution was filtered from the $MgCl_2$, and the solvent was removed under reduced pressure, yielding $Mo(NAr")_2(CH_2D)_2$, **8.6**, (pure by NMR, yield not determined) as a dark red solid.

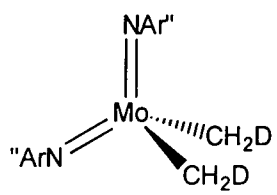

^{1}H NMR: δ/ppm, 250 MHz, C_7D_8, at room temperature

ca.7.0 [m, 2 x 3H, (C_6H_3)]

3.58 [sep, 2 x 1H, (C<u>H</u>Me_2)]

1.340 [s, (2% CH_3-Mo)]

1.300 [t, 2 x 2H, $^2J_{HD}$=1.6Hz, (CH_2D-Ti)]

1.09 [d, 4 x 6H, (CH<u>Me</u>$_2$)]

8.4 References

1 Z. Dawoodi, M.L.H. Green, V.S.B. Mtetwa, K. Prout, A.J. Schultz, J.M. Williams and T.F. Koetzle, *J. Chem. Soc., Dalton Trans.*, 1986, 1629.

2 M.L.H. Green, A.K. Hughes, N.A. Popham, A.H.H. Stephens and L-L. Wong, *J. Chem Soc., Dalton Trans.*, 1992, 3077.

3 J.F. Hanlan, *Can. J. Chem.*, 1972, **50**, 747.

4 C.H. Bamford, R.J. Puddaphat and D.M. Slater, *J. Organomet. Chem.*, 1978, **159**, C31.

5 H. de Vries, *Rec. Trav. Chim.*, 1961, **80**, 866.

6 A. Berry, Z. Dawoodi, A.E. Derome, J.M. Dickenson, A.J. Downs, J.C. Green, M.L.H. Green, P.M. Hare, D.W.H. Ranki and H.E. Robertson, *J. Chem. Soc., Chem. Comm.*, 1986, 520.

7 J.C. Green and M.P. Payne, *Magn. Reson. Chem.*, 1987, **25**, 544

8 M.L.H. Green and A.K. Hughes, *J. Chem. Soc. Chem. Comm.*, 1991, 1231.

9 P. Briant, J.C. Green, A. Haaland, H. Mollendal, K. Rypdal and J. Tremmel, *J. Am. Chem. Soc.*, 1989, **111**, 1920.

10 G.W. Fowles, D.A. Rice and J.D. Wilkins, *J. Chem. Soc.*, 1971, 1920

11 A.D. Poole, D.N. Williams, A.M. Kenwright, V.C. Gibson, W. Clegg, D.C.R. Hockless and D.A. O'Neill, *Organometallics*, 1993, **12**, 2549.

12 W.A. Nugent and R.L. Harlow, *J. Am. Chem. Soc.*, 1980, 159.

13 G. Walker, Ph.D. Thesis, Imperial College, London, 1997.

14 A. Bell, W. Clegg, P.W. Dyer, M.R.J. Elsegood, V.C. Gibson and E.L. Marshall, *J. Chem. Soc., Chem. Comm.*, 1994, 2547.

15 W.A. Nugent, *J. Am. Chem. Soc.*, 1983, 965.

Chapter 9

Investigation of Titanium and Zirconium Neopentyl Chloro Complexes, MNp_xCl_{4-x} (x = 1 – 4), for α-Agostic Interactions

9.1 Introduction

The kinetic and thermal instability of many metal alkyl complexes has made the study and chemistry of such species difficult due to facile decomposition routes. The most important decomposition reaction is β-elimination, converting a metal alkyl into metal hydride and alkene, a reaction which can be prevented by employing alkyl groups which have no β-hydrogens. The simplest alkyl ligands containing no β-hydrogens are methyl and neopentyl (2,2-dimethylpropyl, CH_2CMe_3). The chemistry of $TiMe_xCl_{4-x}$ and its bromide analogues have been extensively studied,[1] and $TiMeX_3$ complexes (X = Cl, NMe_2, OR) are widely employed in organic synthesis.[2] However, the chemistry of the neopentyl complexes, $Ti(CH_2CMe_3)_xCl_{4-x}$ (x = 1-4) and their zirconium analogues have been less widely studied.

The homoleptic tetraneopentyls of all the Group 4 metals have been described along with their thermal stabilities, and comparisons made between MMe_4 and $M(CH_2CCMe_3)_4$.[3] Schrock and coworkers investigated the possibility of preparing alkylidenes by "inducing" α-abstraction from $ZrNp_2X_2L_2$ (figure 9.1).[4]

$$ZrNp_2Cl_2(tmeda) \xrightarrow[50^oC,\ 12hr]{CD_2Cl_2} ZrNpCl_3(tmeda) + CMe_4$$

Figure 9.1

They instead found that $ZrNp_2Cl_2$tmeda decomposes to give one equivalent of neopentane and $ZrNpCl_3$tmeda, suggesting that neopentyl radicals and $ZrNpCl_2$tmeda are the initial decomposition products (figure 9.1). They also found that the reaction of $ZrNp_2Cl_2(Et_2O)_2$ with half an equivalent of $MgNp_2$ gives $ZrNp_3Cl$ and a small amount of $ZrNp_4$, and that the addition of ligands including PMe_3 and tmeda to $ZrNp_3Cl$ causes disproportionation into $ZrNp_4$ and $ZrNp_2Cl_2$ (figure 9.2).

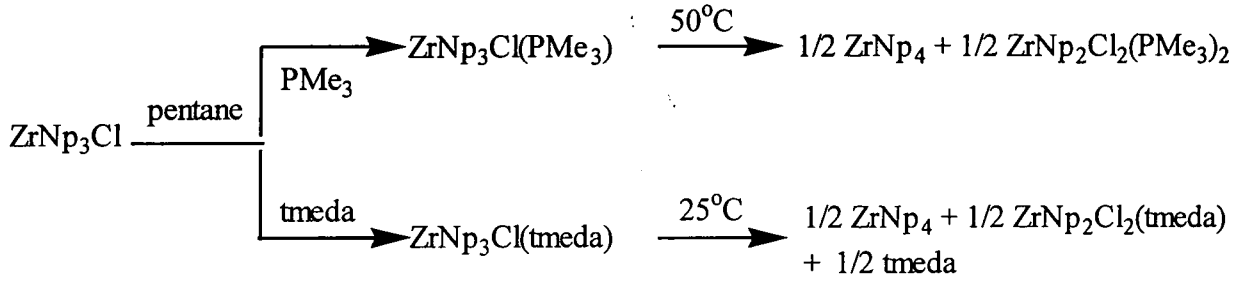

Figure 9.2

Recently, Guzman and coworkers described the synthesis of $TiNpCl_3$, $Ti(CH_2CHMe_2)Cl_3$ and $Ti(CH_2SiMe_3)Cl_3$.[5] In a following publication they then report the crystal structure of $Ti(CH_2SiMe_3)Cl_3$ determined by X-ray diffraction.[6] The complex, like that of $MeTiCl_3$, has the dimeric centrosymmetric structure, $Me_3SiCH_3TiCl_2(\mu\text{-}Cl)_2TiCl_2CH_2SiMe_3$ (figure 9.3).

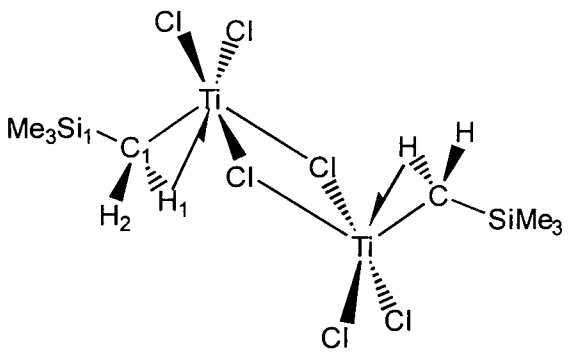

$r(Ti\text{-}H_1)$	2.30(4)Å
$r((Ti\text{-}H_2)$	2.31(4)Å
$r(C_1\text{-}H_1)$	0.94(4)Å
$r(C_1\text{-}H_2)$	0.89(4)Å
$<(Ti\text{-}C_1\text{-}H_1)$	96(3)°
$<(Ti\text{-}C_1\text{-}H_2)$	99(3)°
$<(Ti\text{-}C_1\text{-}Si_1)$	126.9°

Figure 9.3

The $Ti\text{-}C_1$ bond, whose length is 2.003(4)Å, is the shortest of the bonds of the Ti-C(alkyl) type in the series of structurally investigated compounds. According to Ginzburg's data,[7] the Ti-C distance in compounds where the Ti···H-C agostic interaction has been postulated exceeds somewhat that found in $MeTiCl_3$, and varies in the range 2.07-2.52Å. The C_1 atom in the dimer is involved in a distorted tetrahedral coordination. The $Si_1\text{-}C_1\text{-}Ti$ bond angle has increased to 126.9(2)° while the $Ti\text{-}C_1\text{-}H_{1\text{-}2}$ angles have actually diminished to 96(3)° and 99(3)° respectively, compared with the 'ideal' value of 109.5° characteristic of tetrahedral coordination. The 'non-valence' $Ti\text{-}H_{1\text{-}2}$ distances are 2.30(4) and 2.31(4)Å and also fall within the range of values corresponding to the possible agostic interaction.

The geometrical characteristics found for the Ti···H-C fragment in the dimer (distortion of the tetrahedral coordination of the C_1 and the shortening of the Ti-C_1 bond) may be induced by purely steric causes, namely by the bulk of the trimethylsilyl substituent. On the other hand, the characteristic distortion of the C_1 atom does not rule out the possibility of an agostic interaction.

More recently Hoyt and coworkers described the crystal structure of Np_3ZrCl as polymeric chains with a strictly linear symmetric –Cl-$ZrNp_3$-Cl-$ZrNp_3$- repeating unit (figure 9.4).[8] The two adjacent Np_3Zr moieties are arranged in a staggered conformation presumably to reduce steric strain.

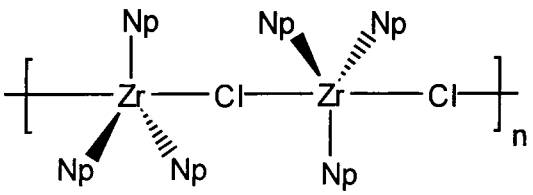

Figure 9.4

Although the two hydrogen atoms in the CH_2 group were not refined, and therefore no evidence for agostic interactions taken from them, the solid-state infra-red spectra of both Np_3ZrCl and $ZrNp_4$ contain features near 2700cm^{-1}, which may indicate possible agostic interactions.

Three general approaches to the synthesis of Np_3ZrCl have been used and these are summarised in equations (i) to (iii). The products can be purified by either sublimation or recrystallisation.

$$ZrCl_4 + 3ZrNp_4 \longrightarrow 4Np_3ZrCl \qquad \text{(i)}$$

$$ZrCl_4 + 3NpLi \longrightarrow Np_3ZrCl + 3LiCl \qquad \text{(ii)}$$

$$ZrNp_4 + HCl \longrightarrow Np_3ZrCl + NpH \qquad \text{(iii)}$$

i) The comproportionation reaction between $ZrNp_4$ and $ZrCl_4$.

ii) The metathetic reaction between $ZrCl_4$ and 3 equivalents of NpLi or NpMgCl.

iii) The reaction of Np_4Zr with 1 equivalent of HCl/Et_2O solution.

The last two reactions do not provide a general synthetic route to all the partially alkylated species, $TiNp_xCl_{4-x}$ and $ZrNp_xCl_{4-x}$ (x = 1-4). The comproportionation reaction between homoleptic neopentyls, MNp_4, and the metal tetrachlorides provide the most satisfactory route to the mixed neopentyl chloro complexes, with suitable control of reaction stoichiometry.

9.1.1 Aims

The above observations led us to investigate whether the comproportionation reaction between the tetraneopentyls and tetrachlorides of titanium and zirconium could be used as a possible route to preparing <u>all</u> the neopentyl chloro complexes. Isotopic perturbation of resonance experiments involving the use of labelled $Me_3CCH\dot{D}$-M (M = Ti, Zr) complexes could then be used to probe for any α-agostic interactions, and their light and thermal stability also assessed.

9.2 Preparation of $MNp_xCl_{(4-x)}$ (M = Zr, Ti; x = 0 – 4)

The deuterium labelled complexes, $M(CHDCMe_3)_4$, $M(Np\text{-}d)_4$ (M = Ti, Zr), were prepared using the labelled Grignard reagent, $Me_3CCHDMgCl$, **7.2**, the preparation of which is described in Chapter 7 using a new improved synthesis of $Me_3CCHDCl$ developed from $Me_3CCHDOH$.

9.2.1 Preparation of $Zr(CH_2CMe_3)_4$ and $Zr(CHDCMe_3)_4$, 9.1

$$ZrCl_4 + 4Np(d)MgCl \xrightarrow{\text{hexane}} ZrNp(d)_4 + 2MgCl_2$$

9.1

Both the protio and labelled $ZrNp_4$ were prepared in a similar manner, according to the literature procedures, by the alkylation of the tetrachloride with 3 equivalents of Me_3CCH_2MgCl or $Me_3CCHDMgCl$ in hexane.[3] Sublimation produced $Zr(CH_2CMe_3)_4$ and $Zr(CHDCMe_3)_4$, **9.1**, respectively, as colourless crystals, in 69% yield. The product was found to decompose slowly at room temperature over a number of weeks.

As discussed in the literature,[3] an NMR sample in $CDCl_3$ always shows small amounts of neopentane in the ^1H NMR spectrum at 0.92 ppm, and over a week at room temperature the sample becomes darker with more neopentane produced. As expected the partially labelled complex $Zr(CHDCMe_3)_4$ contains a small amount of the protio complex $Zr(CH_2CMe_3)(CHDCMe)_3$ from the 2% LiH in the starting material, LiD. A singlet is observed for the CH_3 group with the CHD group appearing as a triplet at 1.207ppm (figure 9.5). The t-butyl group appears as a singlet at 1.08ppm.

9.2.2 Preparation of $Ti(CH_2CMe_3)_4$ and $Ti(CHDCMe_3)_4$, 9.2

$$TiCl_4 + 4Np(d)MgCl \xrightarrow{Et_2O} TiNp(d)_4 + 2MgCl_2$$

9.2

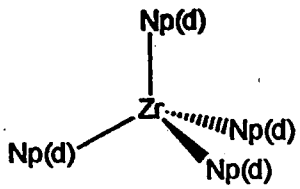

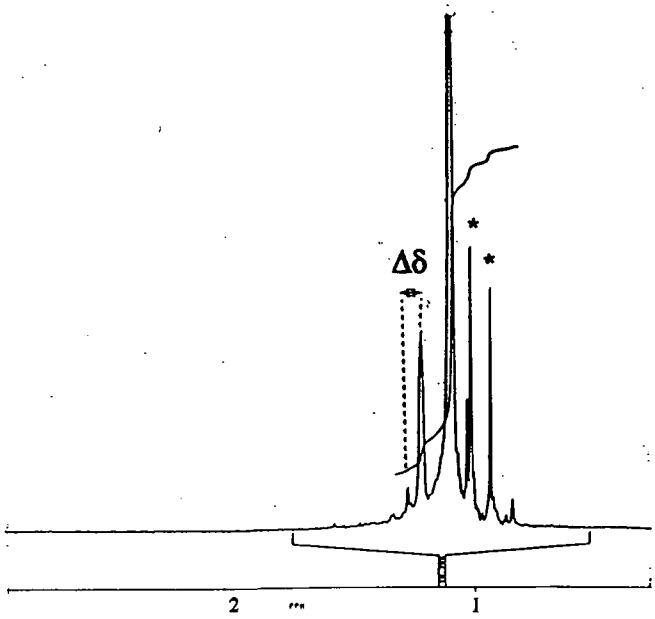

Figure 9.5 ^{1}H NMR spectrum of $Zr(CHDCMe_3)_4$ in $CDCl_3$ at 250MHz

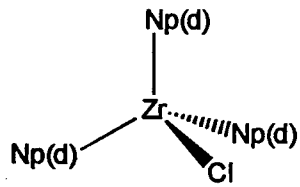

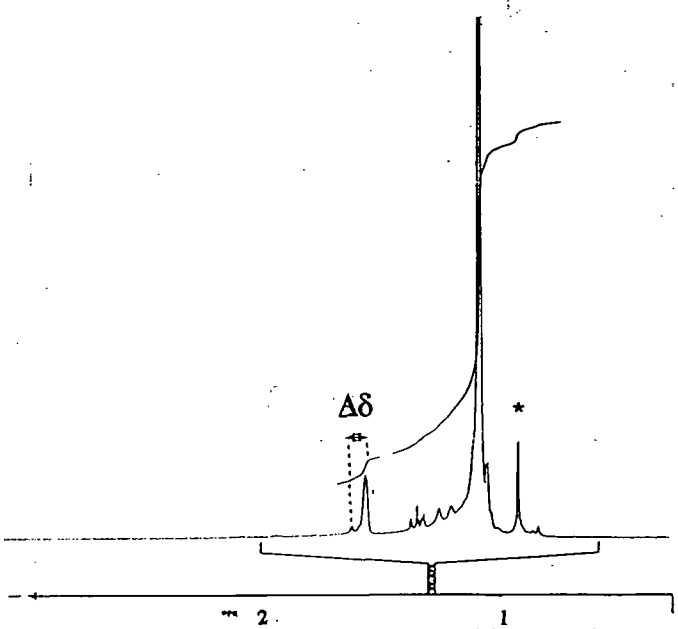

Figure 9.7 ^{1}H NMR spectrum of $(Me_3CCHD)_3ZrCl$ in $CDCl_3$ at 250MHz

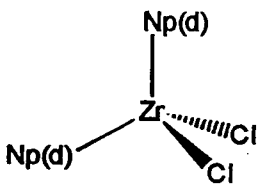

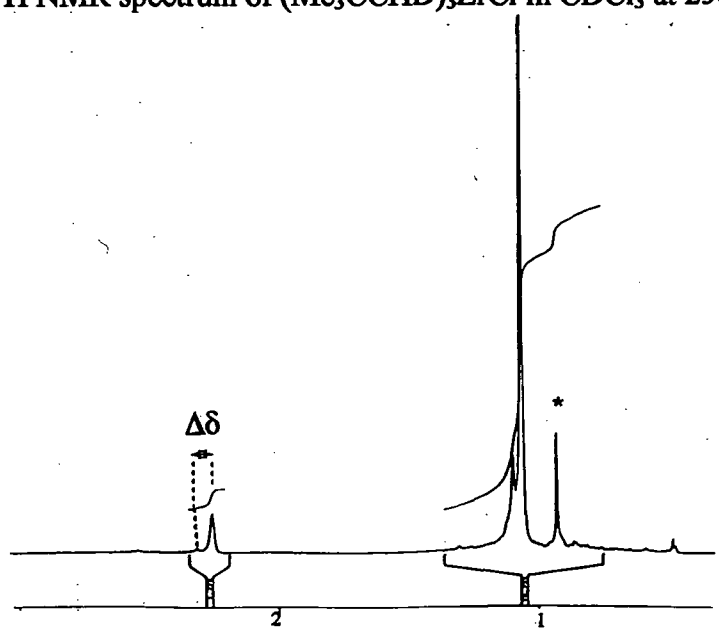

Figure 9.10 ^{1}H NMR spectrum of $(Me_3CCHD)_2ZrCl_2$ in $CDCl_3$ at 250MHz

The stoichiometric reaction of $TiCl_4$ and 4 equivalents of Me_3CCH_2MgCl or $Me_3CCHDMgCl$ in diethyl ether forms a dark solution. Sublimation yields the corresponding $Ti(CH_2CCMe_3)_4$ and $Ti(CHDCMe_3)_4$, **9.2**, in only 20% yield, as pale yellow crystalline solids. $TiNp_4$ is thermally unstable, zirconium being more stable, with the product decomposing to a black insoluble solid after being stored at room temperature for a few days.

The ^1H NMR spectrum of $Ti(CHDCMe_3)_4$ in $CDCl_3$, shows similar chemical shifts for the t-butyl groups to that observed for the zirconium analogue, at 1.09ppm. The CH_2 singlet and CHD triplets were shifted to higher frequencies, appearing at 2.059ppm and 2.000ppm respectively, giving a similar isotope shift of 0.059ppm (figure 9.6).

Both the protio and labelled tetraneopentyl zirconium and titanium complexes were subsequently used in comproportionation reactions with the corresponding tetrachlorides. The reactants were loaded into NMR tubes with deutero chloroform, then sealed and the reaction monitored, using ^1H NMR spectroscopy.

9.2.3 Preparation of $(Me_3CCH_2)_3ZrCl$ and $(Me_3CCHD)_3ZrCl$, 9.3

$$ZrCl_4 + 3NpMgCl \xrightarrow{\text{hexane}} 3Np_3ZrCl + 3MgCl_2$$

The protio complex $(Me_3CCH_2)_3ZrCl$ was synthesised by the reaction of $ZrCl_4$ and NpMgCl, according to the literature synthesis, with Np_3ZrCl being formed as a yellow solid following sublimation.[8]

$$3ZrNp(d)_4 + ZrCl_4 \xrightarrow{CDCl_3} 4Np(d)_3ZrCl$$

9.3

Due to the small quantities of $Zr(CHDCMe_3)_4$ available the labelled complex $(Me_3CCHD)_3ZrCl$ was synthesised by the comproportionation reaction using an NMR tube reaction. The reaction of $ZrCl_4$ with 3 equivalents of $ZrNp(d)_4$ in $CDCl_3$ led to the formation of a yellow solution at room temperature and within 3 hours all the partially

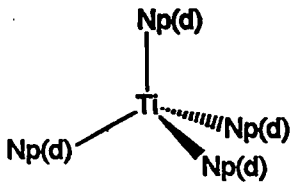

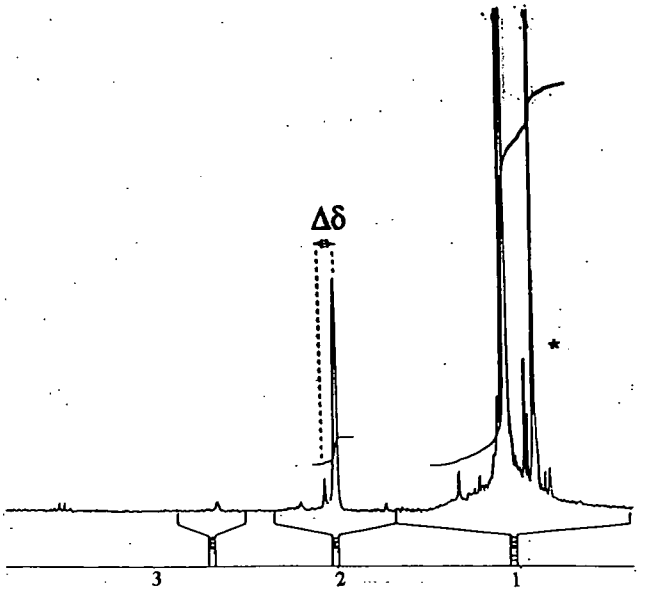

Figure 9.6 ^{1}H NMR spectrum of $Ti(CHDCMe_3)_4$ in $CDCl_3$ at 250MHz

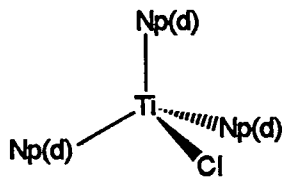

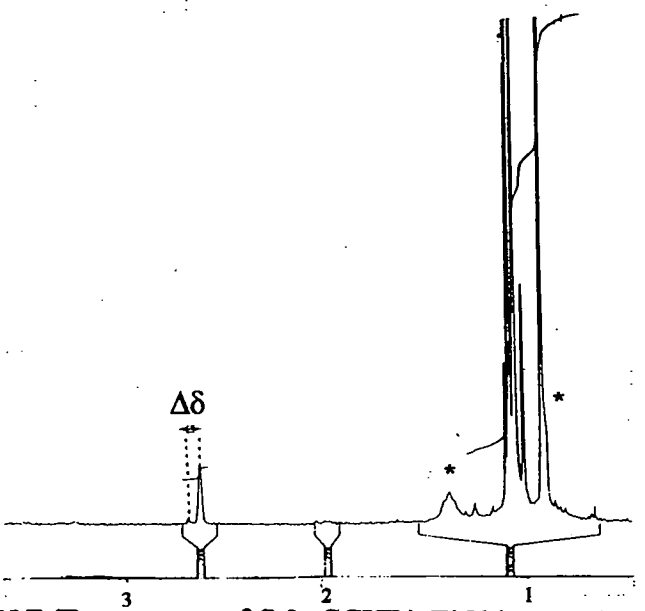

Figure 9.8 ^{1}H NMR spectrum of $(Me_3CCHD)_3TiCl$ in $CDCl_3$ at 250MHz

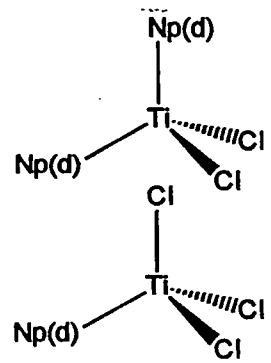

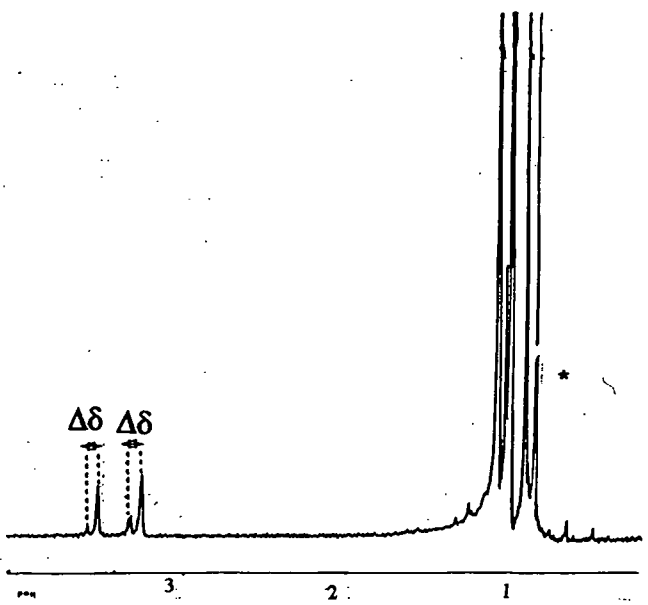

Figure 9.11 ^{1}H NMR spectrum of $(Me_3CCHD)_2TiCl_2$ and $(Me_3CCHD)TiCl_3$ in $CDCl_3$

soluble $ZrCl_4$ had reacted forming a yellow homogeneous solution of $(Me_3CCHD)_3ZrCl$, **9.3**. The sample was more thermally unstable than the tetraneopentyl complex, with the solution darkening over a period of a few days and neopentane being produced as the decomposition product.

The ^1H NMR spectrum of **9.3** shows the t-butyl resonance at a similar chemical shift to that of the tetraneopentyl analogue (figure 9.7). The replacement of one neopentyl group for a chloro derivative means that the CH_2 singlet and CHD triplet are shifted to higher frequencies in comparison, appearing at 1.628 and 1.568ppm respectively.

9.2.4 Preparation of $(Me_3CCH_2)_3TiCl$ and $(Me_3CCHD)_3TiCl$, 9.4

Having not been previously synthesised, attempts were made to prepare the protio complex, $(Me_3CCH_2)_3TiCl$ using the same methods as for $(Me_3CCH_2)_3ZrCl$. The reaction of $TiCl_4$ and 3 equivalents of NpMgCl in diethyl ether gave Np_3TiCl as bright orange solid, following sublimation. This rapidly decomposed to a dark brown solid at room temperature. This led to preparation of $(Me_3CCHD)_3TiCl$ being carried out in an NMR tube with $TiCl_4$ being reacted with 3 equivalents of $TiNp(d)_4$ in $CDCl_3$ as follows:

$$3TiNp(d)_4 + TiCl_4 \xrightarrow{CDCl_3} 4Np(d)_3TiCl$$

9.4

After 20 minutes at room temperature all the tetraneopentyl complex had reacted forming an orange solution of $(Me_3CHD)_3TiCl$, **9.4**. At this stage the product was stored at -196°C. A brown precipitate began to form over a period of a few hours at room temperature with increasing amounts of neopentane being seen in the ^1H NMR spectrum.

The ^1H NMR spectrum (figure 9.8) shows resonances for the CH_2 and CHD groups at 2.631 and 2.692ppm respectively giving an isotope shift of 0.058ppm. These chemical shifts for the CH_2 and CHD groups are to higher frequencies compared to the tetraneopentyl complex due to the replacement of a neopentyl group for a more

electronegative chloride ligand. Since titanium is more electronegative than zirconium these shifts are also to higher frequencies than the corresponding zirconium complex.

9.2.5 Preparation of $(Me_3CCH_2)_2ZrCl_2$ and $(Me_3CCHD)_2ZrCl_2$, 9.5

Wengrovius and Schrock could only isolate $ZrNp_2X_2$ as the adduct $ZrNp_2X_2(Et_2O)_2$ from the reaction of $ZrCl_4$ with 2 equivalents of NpLi in Et_2O.[4] Attempts to promote α-abstraction by the addition of nitrogen or phosphorus ligands gave the corresponding substituted complexes, $ZrNpX_2L_2$ (figure 9.9). These complexes were found to be thermally unstable, decomposing at varying rates in benzene at 25-50°C, yielding approximately two equivalents of neopentane, a trace of 2,2,5,5-tetramethylhexane and a black, insoluble tar.

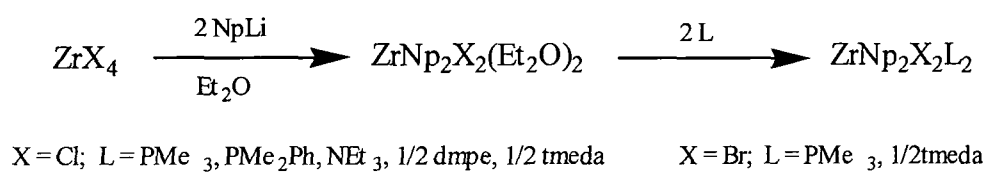

Figure 9.9

A reaction in an NMR tube was therefore used to synthesise both the protio and labelled complexes $(Me_3CCH_2)_2ZrCl_2$ and $(Me_3CCHD)_2ZrCl_2$ according to the stoichiometry:

$$ZrNp(d)_4 + ZrCl_4 \xrightarrow{CDCl_3} 2Np(d)_2ZrCl_2$$

9.5

The reaction of $ZrNp_4$ with 1 equivalent of $ZrCl_4$ in $CDCl_3$ was monitored by ^1H NMR spectroscopy, in the dark, at room temperature. Np_3ZrCl started to form immediately followed by the appearance of Np_2ZrCl_2 after 1 hour. New resonances were observed in the ^1H NMR spectrum (figure 9.10) with a singlet for the CH_2 group at 2.315ppm and a triplet at 2.256ppm for the CHD group giving an isotope shift of 0.059ppm. The t-butyl

groups at 1.07ppm were only slightly shifted, relative to those of the tetra- and tris-neopentyl complexes.

After 2 hours nearly all of the $ZrNp_4$ had been converted to a yellow solution of Np_2ZrCl_2, **9.5**. At this stage the complex was stored at -196°C. After a further 4 hours at room temperature the solution began to darken and at 24 hours a black insoluble precipitate had formed. However even in such decomposed samples neopentane was the only decomposition product observed in the ^1H NMR spectrum and Np_2ZrCl_2 was still the major diamagnetic, soluble, species present.

9.2.6 Preparation of $(Me_3CCH_2)_2TiCl_2$ and $(Me_3CCHD)_2TiCl_2$, 9.6

$$TiNp(d)_4 + TiCl_4 \xrightarrow{CDCl_3} 2Np(d)_2TiCl_2$$

9.6

To our knowledge Np_2TiCl_2 had not been isolated or characterised before and therefore both the protio and labelled complexes were prepared by reactions carried out in an NMR tube. The NMR tube was charged with equimolar quantities of both $TiNp_4$ and $TiCl_4$ with $CDCl_3$ as the solvent, and the tube flame sealed under vacuum. At room temperature a rapid reaction commenced and was monitored by ^1H NMR spectroscopy. After 5 minutes $TiNp_3Cl$ along with two new complexes, $TiNp_2Cl_2$ and $TiNpCl_3$, were produced. After 20 minutes the reaction consisted of mainly $TiNp_2Cl_2$, **9.6**, with the CH_2 group appearing at 3.303ppm and the CHD group at 3.245ppm giving an isotope shift of 0.056ppm (figure 9.11).

The product was found to be thermally sensitive with the formation of a brown precipitate being observed during the reaction. Immediately after completion of the reaction the product was stored at -196°C.

9.2.7 Preparation of $(Me_3CCH_2)TiCl_3$ and $(Me_3CCHD)TiCl_3$, 9.7

Guzman and co-workers described the synthesis of $(Me_3CCH_2)TiCl_3$ along with $(Me_3SiCH_2)TiCl_3$ and $(Me_2CHCH_2)TiCl_3$ by reacting $TiCl_4$ with only 1/2 an equivalent of LiR in Et_2O at low temperature (-50 to -55°C), followed by distillation of the final product.[5] $NpTiCl_3$ was isolated in nearly quantitative yield as a bright red liquid, crystallising at -30°C.

The necessity for an excess of $TiCl_4$ arises because the LiCl formed as a result of the reaction is thought to bind to $TiCl_4$ forming the double salts $TiCl_4{\cdot}(LiCl)_n$. These are insoluble in hydrocarbons and unreactive towards LiR, therefore leading to the removal of $TiCl_4$ from the reaction sphere, decreasing the $TiCl_4$:LiR ratio and leading to the formation of a mixture of organotitanium compounds, as follows:

$$2LiR + 2TiCl_4 \longrightarrow Li_2TiCl_6 + 0.6RTiCl_3 + 0.1R_2TiCl_2 + 0.3TiR_4$$

On this basis it was postulated that the synthesis of $RTiCl_3$ would require a molar ratio of LiR:$TiCl_4$ = 1:2 as follows:

$$LiR + 2TiCl_4 \longrightarrow RTiCl_3 + LiTiCl_5 \downarrow$$

However we have not encountered the corresponding magnesium halide adduct, $TiCl_4{\cdot}(MgCl_2)_n$ in reactions using NpMgCl with $TiCl_4$ or $ZrCl_4$ in ether or chloroform solvents and therefore have continued to use stoichiometric quantities. The low isolated yield of $TiNp_4$ is a consequence of thermal decomposition during sublimation and reduction of $TiCl_4$ by the alkylating agent.

The complexes are described as being stable under the conditions of IR irradiation and at room temperature for a long time in the absence of traces of oxygen, moisture and in the dark. In 1961 De Vries reported the formation of $NpTiCl_3$ from the reaction of $MeTiCl_3$ with 2-methyl propene (isobutylene).[9] With isobutylene being a gas and therefore difficult to handle an attempt was made to carry out a similar reaction with β-pinene as follows:

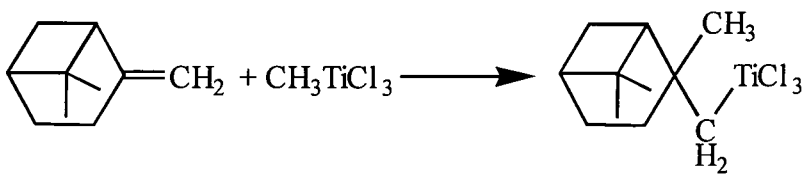

Attempts at this reaction were unsuccessful and therefore the comproportionation reaction was used for the preparation of $NpTiCl_3$ as follows:

$$TiNp(d)_4 + 3TiCl_4 \xrightarrow{CDCl_3} 4Np(d)TiCl_3$$

9.7

The stoichiometric reaction of $TiNp_4$ with 3 equivalents of $TiCl_4$ in $CDCl_3$ in a sealed NMR tube was monitored at room temperature using ^1H NMR spectroscopy. After 5 minutes at room temperature two new products were observed, $Np(d)_3TiCl$ and $Np(d)TiCl_3$ with only a trace of $Np(d)_2TiCl_2$. The resonances assigned to $Np(d)TiCl_3$ grew in intensity and after 20 minutes the sample consisted of mainly $Np(d)TiCl_3$, **9.7**, as an orange solution. Although some decomposition was observed during the reaction, the final product, once formed, seemed relatively thermally stable compared to Np_2TiCl_2.

The ^1H NMR spectrum shows the t-butyl group at 1.08ppm, whereas the CH_2 and CHD are shifted to higher frequencies compared to the others discussed (figure 9.11). The CH_2 singlet appears at 3.563ppm and the CHD triplet is seen at 3.504ppm giving an isotope shift of 0.059ppm.

9.2.8 Preparation of $(Me_3CCH_2)ZrCl_3$ and $(Me_3CCHD)ZrCl_3$, 9.8

Unlike $NpTiCl_3$, $NpZrCl_3$ had not been synthesised previously. Again the comproportionation reaction was used as follows:

$$ZrNp(d)_4 + 3ZrCl_4 \xrightarrow{CDCl_3} 4Np(d)ZrCl_3$$

9.8

Unlike the analogous titanium reaction, the synthesis of $NpZrCl_3$ appeared to require the use of excess $ZrCl_4$ (i.e., more than 3 equivalents). The stoichiometric reaction of $ZrNp_4$ and 3 equivalents of $ZrCl_4$ gave a mixture of Np_2ZrCl_2 and $NpZrCl_3$. The reaction of $ZrNp_4$ and 4.5 equivalents of $ZrCl_4$ in $CDCl_3$ or C_6D_6 initially gave a solution of Np_3ZrCl followed by Np_2ZrCl_2 and finally after one hour resulted in the formation of $NpZrCl_3$. After 4 hours the mixture consisted of mainly $NpZrCl_3$, **9.8**, as a partially soluble yellow solid, unreacted NMR silent $ZrCl_4$ as a white solid and a small amount of Np_2ZrCl_2. The solution darkened slowly over a number of days at room temperature but the yellow solid seemed reasonably stable and could be stored for many weeks at -40°C in the absence of light.

The partial solubility of $(Me_3CCHD)ZrCl_3$ caused a slightly broad ^1H NMR spectrum, causing the small CH_2 resonance to be swamped by the CHD resonance. However comparisons could be made between pure samples of $(Me_3CCH_2)ZrCl_3$ with a CH_2 resonance at approximately 2.65ppm and $(Me_3CCHD)ZrCl_3$ with CHD resonance at approximately 2.6ppm separately, giving a small isotope shift. Again the t-butyl resonance appeared at 1.08ppm.

9.3 Discussion

9.3.1 IPR studies and ^{1}H NMR trends

Low temperature ^{1}H NMR analysis was carried out on the monodeuterated complexes from 20°C down to –60°C, at 20°C intervals. The isotope shifts, Δδ, were measured and the results are shown in table 9.1 for the zirconium complexes and table 9.2 for the titanium complexes.

Compound	$\delta(CH_2)^i$ 20°C	δ(CHD) 20°C	$\Delta\delta^{ii}$ 20°C	$\delta(CH_2)$ -60°C	δ(CHD) -60°C	Δδ -60°C
$ZrNp_4$	1.264	1.207	0.057	~1.26	~1.20	~0.06
$ZrNp_3Cl$	1.628	1.568	0.060	~1.60	~1.54	~0.06
$ZrNp_2Cl_2$	2.315	2.356	0.059	2.336	2.274	0.062
$ZrNpCl_3$	~2.6	~2.65	-[iii]	-	-	-

i) all δ values in ppm

ii) $\Delta\delta = \delta(CH_2 - CHD)$ in ppm

iii) Δδ could not be measured accurately due to partial solubility of complex.

Table 9.1 ^{1}H NMR isotope shifts for $ZrNp(d)_xCl_{(4-x)}$ (x = 1-4)

Compound	$\delta(CH_2)$ 20°C	δ(CHD) 20°	Δδ 20°C	$\delta(CH_2)$ -60°C	δ(CHD) -60°C	Δδ -60°C
$TiNp_4$	2.059	2.000	0.059	1.997	1.937	0.060
$TiNp_3Cl$	2.689	2.631	0.058	2.687	2.627	0.060
$TiNp_2Cl_2$	3.303	3.245	0.056	3.350	3.289	0.061
$TiNpCl_3$	3.563	3.504	0.059	3.588	3.525	0.063

Table 9.2 ^{1}H NMR isotope shifts for $TiNp(d)_xCl_{(4-x)}$ (x = 1-4)

All the complexes were found to have similar $\Delta\delta$ values, ranging from 0.056 to 0.060ppm at room temperature. These values are higher than the complexes discussed in Chapter 8 but show little temperature dependence. Since temperature dependent isotope shifts of greater than 0.1ppm are expected for agostic interactions, it is assumed that these shifts are due to secondary isotope effects (discussed in Chapter 7).

From the tables and the ^{1}H NMR spectra of the complexes (figures 9.5 to 9.11), it can be seen that the t-butyl resonances remain in the same positions whereas the CH_2 and CHD resonances move to higher frequencies in the following order:

$$\mathbf{MNp_4 < Np_3MCl < Np_2MCl_2 < NpMCl_3} \qquad \mathbf{M = Zr < Ti}$$

As each neopentyl ligand is replaced by a more electronegative chloride ligand, the CH_2 and CHD resonances shift to higher frequencies, and titanium being more electropositive than zirconium causes larger shifts for the titanium than zirconium analogues.

9.3.2 $^{13}C\{^1H\}$ NMR trends

Studies of the NMR spectra (^{1}H, ^{13}C, and ^{47,49}Ti) of complete series of methyl titanium complexes, together with carbon, silicon, tin and lead analogues, XMe_nCl_{4-x} (X = C, Si, Sn, Pb, Ti; n = 0-4) have demonstrated that the ^{13}C chemical shifts of titanium complexes are consistently to high frequency of the other compounds.[10] For example for $TiMe_4$ $\delta(^{13}C)$ = 69ppm compared to –9 to 31.4ppm for other XMe_4 compounds, and for $ZrMe_4$, the only methyl zirconium complex studied, δ = 33.2ppm. The unusual ^{13}C NMR shifts of the titanium complexes have been ascribed to the presence of low-lying empty d orbitals, which overlap strongly with the π-component of the Ti-C bond, leading to a large paramagnetic contribution to the ^{13}C chemical shifts.

$ZrNp_xCl_{4-x}$	$\delta(CH_2)$/ppm	$TiNp_xCl_{4-x}$	$\delta(CH_2)$/ppm
$ZrNp_4$	102.5	$TiNp_4$	119.5
$ZrNp_3Cl$	105.0	$TiNp_3Cl$	126.9
$ZrNp_2Cl_2$	113.8	$TiNp_2Cl_2$	142.3
$ZrNpCl_3$	partiallysoluble	$TiNpCl_3$	163.2

Table 9.3: ^{13}C chemical shifts of the CH_2 resonances in MNp_xCl_{4-x} (M = Ti, Zr)

As can be seen in table 9.3 the ^{13}C chemical shifts of the CH_2 resonances of the neopentyl titanium and zirconium complexes show similar trends. Like the ^1H NMR resonances, the ^{13}C NMR CH_2 resonances move to higher frequency in the series MNp_4 < MNp_3Cl <MNp_2Cl_2 < $MNpCl_3$ for both titanium and zirconium. The chemical shifts of these CH_2 resonances are to higher frequency in all the titanium complexes than their zirconium analogues, and given the additional alkyl group, all are to higher frequency than in the analogous titanium methyl complex.

9.3.3 Reaction sequence

Monitoring the reactions of MNp_4 and MCl_4 has allowed us to determine the sequence of reaction steps by which the comproportionation reaction occurs. The room temperature reaction of $TiNp_4$ with 3 equivalents of $TiCl_4$ as a homogeneous solution in $CDCl_3$, was monitored by ^1H NMR spectroscopy and revealed that the initial products of the reaction (5 minutes at 23°C) were $NpTiCl_3$ and Np_3TiCl in a 1:1 molar ratio, with only a trace (< 5 mol%) of Np_2TiCl_2, as determined by integration of the CH_2 resonances. The remainder of the sample was unreacted $TiNp_4$, and NMR silent $TiCl_4$. These observations are consistent with a simple mechanism for neopentyl exchange, namely the bimolecular exchange of one neopentyl and one chloride ligand, as follows;

$$TiNp_4 + TiCl_4 \longrightarrow TiNpCl_3 + TiNp_3Cl$$

Subsequently the CH_2 resonances assigned to $NpTiCl_3$ and Np_2TiCl_2 grew in intensity, and after 20 minutes at 23°C the sample consisted of pure (by NMR) $NpTiCl_3$. In the case of titanium, all the species are very soluble in $CDCl_3$ and the solution remained homogeneous throughout. As indicated above, other ratios of reactants allow the synthesis, after approximately 30 minutes at 23°C of samples containing essentially pure samples (<5% of any other species) of any of the titanium neopentyl chlorides.

In the case of zirconium, qualitative studies of the kinetics of the comproportionation reactions were complicated by the insolubility, in $CDCl_3$ and C_6D_6 of polymeric $ZrCl_4$ and the sparing solubility of $NpZrCl_3$. When 3 equivalents of $ZrNp_4$ were reacted with 1 equivalent of $ZrCl_4$ in $CDCl_3$ the ^1H NMR spectrum after 30 minutes at 23°C showed approximately equimolar quantities of $ZrNp_4$ and Np_3ZrCl. The spectrum did not show signals assigned to either Np_2ZrCl_2 or the sparingly soluble $NpZrCl_3$. The sample did however clearly contain unreacted $ZrCl_4$. After 2 hours at 23°C the sample consisted of pure Np_3ZrCl. These observations are consistent with a mechanism where the rate determining step is attack of $ZrNp_4$ on solid $ZrCl_4$ to give soluble species $NpZrCl_3$ and Np_3ZrCl, which then react rapidly with the excess $ZrNp_4$ in solution giving Np_3ZrCl. At this reaction stoichiometry, the concentration of $NpZrCl_3$ and Np_2ZrCl_2 is always too low to observe by ^1H NMR. Attempts to study the intermediates produced by other reaction stoichiometries are frustrated by solubility difficulties, although we have successfully prepared solutions containing Np_2ZrCl_2 and $NpZrCl_3$ as the final products.

9.3.4 Structure

The related $(Me_3SiCH_2)TiCl_3$ has been shown to be dimeric in the solid state, with two bridging chloride ligands. Since all the titanium neopentyl chloro complexes are highly soluble in chloroform they are presumably either monomeric or dimeric in solution. The same applies to the zirconium neopentyl chloro complexes $ZrNp_4$, Np_3ZrCl and Np_2ZrCl_2 which are all soluble in chloroform and benzene, although the solid state structure of Np_3ZrCl consists of a Zr-Cl-Zr-Cl linear polymer. However the sparing solubility of $NpZrCl_3$ indicates that it presumably has an extended chloride bridged structure.

9.3.5 Thermal stability

$$MNp_4 > Np_3MCl > NpMCl_3 > Np_2MCl_2 \qquad M = Zr > Ti$$

Shown above is the observed order of thermal stability for both the titanium and zirconium neopentyl chloro complexes. The titanium neopentyl complexes were found to be stable in the absence of light at low temperatures (-40°C), but were maintained at -196°C for long term storage. The only product of the thermal decomposition reactions that could be identified by ^1H NMR was neopentane, the dark insoluble metal containing products have not been identified.

All the zirconium complexes were found to be more thermally stable than the corresponding titanium analogues. This is most likely due to Ti(IV) complexes being more prone to reduction to Ti(III) than Zr(IV). The zirconium neopentyl complexes did not show any significant light sensitivity, and were moderately thermally stable. Solutions of Np_2ZrCl_2 or Np_3ZrCl began to darken after standing at room temperature for 1 hour and NMR spectra showed the formation of neopentane. Both compounds were stable for many weeks at -40°C, but were stored at -196°C where they were stable indefinitely.

There are three main decomposition routes for metal–carbon σ-bonds to account for the low stability of metal alkyls.

i) Conversion of a metal alkyl into a metal hydride and alkene via β-hydrogen elimination.
ii) Intra- and inter-molecular α-elimination.
iii) Homolytic photochemical metal-carbon bond cleavage.

The most important decomposition reaction is β-hydrogen elimination (i), but this can be discounted for the neopentyl metal complexes because there are no β-hydrogens. Neopentyl α-elimination (ii) is likely to be the significant mechanism during stage one of the decomposition of the Np_xMCl_{4-x} complexes. However such reactions generally have sufficiently high activation energies that they can be prevented by avoiding elevated temperatures. This would explain the stability of the titanium and zirconium complexes at

low temperature. Many alkyl complexes of early transition metals are also prone to photochemical bond cleavage and require handling in the absence of light. The thermal instability of the unreported complexes meant that they could not be isolated as solids and therefore did not allow other analysis such as infra-red, mass spectroscopy and elemental analysis, to be carried out.

9.3.6 Conclusions

We have demonstrated that all the neopentyl chloro complexes of titanium and zirconium are accessible via the comproportionation reaction, with the complexes Np_3TiCl, Np_2TiCl_2, Np_2ZrCl_2 and $NpZrCl_3$ being reported for the first time. The thermal sensitivity of Np_3TiCl, Np_2TiCl_2 and Np_2ZrCl_2 could explain why they have not been reported. Spectroscopic studies have helped to provide a reaction scheme but did not provide conclusive evidence for agostic interactions in solution.

9.4 Experimental

9.4.1 Preparation of $Zr(CH_2CMe_3)_4$ and $Zr(CHDCMe_3)_4$, 9.1

These two isotopomers were prepared according to the same method. A suspension of $ZrCl_4$ (1.86g, 8mmol) in hexane (20ml) was cooled to 0°C and treated dropwise over 15 min with an Et_2O solution of $Me_3CCHDMgCl$ or Me_3CCH_2MgCl (6mmol, 0.75 x theory). The mixture was then stirred at room temperature for 24hr. The cloudy brown solution was filtered and the solvent was removed under reduced pressure leaving a brown solid. Sublimation under reduced pressure (50°C, 10^{-3}mmHg) gave $Zr(CHDCMe_3)_4$ and $Zr(CH_2CMe_3)_4$, **9.1**, (1.55g, 4.1mmol, 69% yield based on NpMgCl) as colourless crystals.

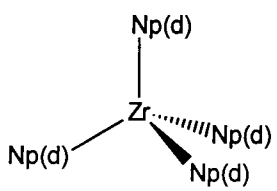

Data characterising $Zr(CH_2CMe_3)_4$

^{1}H NMR: δ/ppm, 250 MHz, $CDCl_3$	**^{13}C {^{1}H} NMR: δ/ppm, 62.5 MHz, $CDCl_3$**
1.267 [s, 8H, (CH_2)]	102.5 [CH_2]
1.08 [s, 36H, (CMe_3)]	35.8 [$\underline{C}Me_3$]
	35.2 [$C\underline{Me_3}$]

Data characterising $Zr(CHDCMe_3)_4$

^{1}H NMR: δ/ppm, 250 MHz, $CDCl_3$	**^{13}C {^{1}H} NMR: δppm, 62.5 MHz, $CDCl_3$**
1.264 [s, 2%CH_2]	102.3 [CHD]
1.207 [t, 4H, $^2J_{HD}$=1.6Hz, (CHD)]	35.2 [$C(\underline{C}H_3)_3$]
1.08 [s, 36H, (CMe_3)]	

9.4.2 Preparation of $Ti(CHDCMe_3)_4$ and $Ti(CH_2CMe_3)_4$, 9.2

These two isotopomers were prepared according to the same method. Neat $TiCl_4$ was added to Et_2O at -78°C precipitating the etherate, $TiCl_4(Et_2O)_2$, and this was treated dropwise over 20 min with an Et_2O solution of $Me_3CCHDMgCl$ or Me_3CH_2MgCl (8mmol). The mixture turned dark during the addition and was stirred for a further 4hr at room temperature shielded from light. The solution was filtered and the solvent was removed under reduced pressure leaving a black oil. Sublimation under reduced pressure (40°C, 10^{-3}mmHg) gave $Ti(CHDCMe_3)_4$ and $Ti(CH_2CMe_3)_4$, **9.2**, (0.53g, 1.6mmol, 20% yield) as pale yellow crystals.

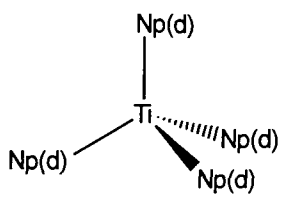

Data characterising $Ti(CH_2CMe_3)_4$

^{1}H NMR: δ/ppm, 250 MHz, $CDCl_3$	**$^{13}C\{^1H\}$ NMR: δ/ppm, 62.5 MHz, $CDCl_3$**
2.060 [s, 8H, (CH_2)]	119.1 [CH_2]
1.09 [s, 36H, (CMe_3)]	37.6 [$\underline{C}Me_3$]
	34.4 [$C\underline{Me_3}$]

Data characterising $Ti(CHDCMe_3)_4$

^{1}H NMR: δ/ppm, 250 MHz, $CDCl_3$	**$^{13}C\{^1H\}$ NMR: δppm, 62.5 MHz, $CDCl_3$**
2.059 [s, 2%CH_2]	118.5 [CHD]
2.000 [t, 4H, $^2J_{HD}$=1.5Hz, (CHD)]	37.5 [$\underline{C}Me_3$]
1.09 [s, 36H, (CMe_3)]	34.4 [$C\underline{Me_3}$]

9.4.3 Preparation of $Zr(CHDCMe_3)_3Cl$ and $Zr(CH_2CMe_3)_3Cl$, 9.3

A 5mm NMR tube was loaded in the glovebox with a mixture of the solids, $ZrNp(d)_4$ (0.05g, 0.133mmol) and $ZrCl_4$ (0.01g, 0.044mmol). The NMR tube was attached to the vacuum line, cooled to -196°C, and $CDCl_3$ (ca. 0.5ml) transferred onto the reactants under reduced pressure. The tube was flame sealed under vacuum and allowed to warm to room temperature forming a yellow solution. The reaction was monitored by ^1H NMR spectroscopy and showed the slow formation of $ZrNp(d)_3Cl$, and after 3hr at room temperature the solution consisted of >95% $ZrNp(d)_3Cl$, **9.3**. Being thermally unstable the complex was stored at -196°C.

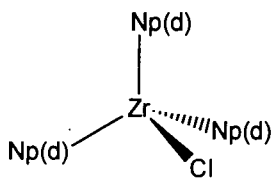

Data characterising $Zr(CH_2CMe_3)_3Cl$

^1H NMR: δ/ppm, 250 MHz, $CDCl_3$	**$^{13}C\{^1H\}$ NMR: δ/ppm, 62.5 MHz, $CDCl_3$**
1.633 [s, 6H, (CH_2)]	105.0 [CH_2]
1.08 [s, 27H, (CMe_3)]	34.9 [$C\underline{Me_3}$]

Data characterising $Zr(CHDCMe_3)_3Cl$

^1H NMR: δ/ppm, 250 MHz, $CDCl_3$	**$^{13}C\{^1H\}$ NMR: δppm, 62.5 MHz, $CDCl_3$**
1.628 [s, 2%CH_2]	104.8 [CHD]
1.568 [t, 3H, $^2J_{HD}$=1.4Hz, (CHD)]	34.9 [$C\underline{Me_3}$]
1.08 [s, 27H, (CMe_3)]	

9.4.4 Preparation of $Ti(CHDCMe_3)_3Cl$ and $Ti(CH_2CMe_3)_3Cl$, 9.4

A 5mm NMR tube was loaded with $TiNp_4$ (0.01g, 0.03mmol) and attached to the Schlenk line. The tube was cooled to -196°C and $CDCl_3$ (ca. 0.5ml) transferred under vacuum. The solution was warmed to room temperature forming a yellow solution, then cooled to -78°C and treated dropwise with a solution of $TiCl_4$ (0.10ml of a 10% solution in $CDCl_3$, 0.01mmol). The solution was frozen at -196°C and the NMR tube was flame-sealed under vacuum. The NMR tube was warmed to room temperature, the solution rapidly turned orange and the reaction was monitored by ^1H NMR, which showed the formation of $TiNp_3Cl$ and disappearance of $TiNp_4$. After approximately 20min at room temperature in the dark the solution consisted of only $TiNp_3Cl$, **9.4**. The product being light and thermally unstable was stored at -196°C.

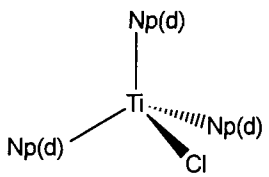

Data characterising $Ti(CH_2CMe_3)_3Cl$

^1H NMR: δ/ppm, 250 MHz, $CDCl_3$		**$^{13}C\{^1H\}$ NMR: δ/ppm, 62.5 MHz, $CDCl_3$**	
2.692	[s, 6H, (CH_2)]	126.9	[CH_2]
1.09	[s, 27H, (CMe_3)]	38.9	[$\underline{C}Me_3$]
		33.8	[$C\underline{Me_3}$]

Data characterising $Ti(CHDCMe_3)_3Cl$

^1H NMR: δ/ppm, 250 MHz, $CDCl_3$

2.689 [s, (2% CH_2)]
2.631 [t, 3H, $^2J_{HD}$=1.5Hz, (CHD)]
1.07 [s, 27H, (CMe_3)]

9.4.5 Preparation of $Zr(CHDCMe_3)_2Cl_2$ and $Zr(CH_2CMe_3)_2Cl_2$, 9.5

In a similar manner as for $Zr(CHDCMe_3)_3Cl$, an NMR tube containing $ZrNp_4$ (0.03g, 0.079mmol) and $ZrCl_4$ (0.018g, 0.079mmol) was cooled to -196°C, and $CDCl_3$ (ca. 0.5ml) was transferred under reduced pressure. The tube was sealed, warmed to room temperature and the reaction was monitored by ^1H NMR spectroscopy. Initially $ZrNp_3Cl$ formed, closely followed by $ZrNp_2Cl_2$, and after approximately 2hr at room temperature a yellow solution containing >95% $ZrNp_2Cl_2$, **9.5**, had formed. At this stage the solution was stored at –196°C as the solution darkened rapidly forming an insoluble black tar after 24hr at room temperature.

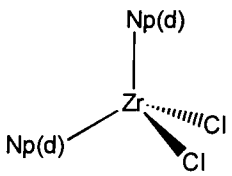

Data characterising $Zr(CH_2CMe_3)_2Cl_2$

^1H NMR: δ/ppm, 250 MHz, $CDCl_3$	**$^{13}C\{^1H\}$ NMR: δ/ppm, 62.5 MHz, $CDCl_3$**
2.310 [s, 4H, (CH_2)]	113.8 [CH_2]
1.09 [s, 18H, (CMe_3)]	37.4 [$\underline{C}Me_3$]
	33.6 [$C\underline{Me_3}$]

Data characterising $Zr(CHDCMe_3)_2Cl_2$

^1H NMR: δ/ppm, 250 MHz, $CDCl_3$	**$^{13}C\{^1H\}$ NMR: δppm, 62.5 MHz, $CDCl_3$**
2.315 [s, 2%CH_2]	114.0 [CHD]
2.256 [t, 2H, $^2J_{HD}$=1.6Hz, (CHD)]	34.2 [$C\underline{Me_3}$]
1.07 [s, 18H (CMe_3)]	

9.4.6 Preparation of $Ti(CHDCMe_3)_2Cl_2$ and $Ti(CH_2CMe_3)_2Cl_2$, 9.6

In the same manner as for $TiNp_3Cl$ a 5mm NMR tube with $TiNp_4$ (0.01g, 0.03mmol) and $CDCl_3$ (ca. 0.3ml) was cooled to -78°C. A solution of $TiCl_4$ (0.30ml of a 10% solution in $CDCl_3$, 0.03mmol) was added dropwise. The solution was frozen at -196°C and the NMR tube was flame-sealed under vacuum. The NMR tube was warmed to room temperature, the solution rapidly turned orange and the reaction was monitored by ^1H NMR spectroscopy. Resonances attributed to $TiNp_4$, $TiNp_3Cl$, $TiNp_2Cl_2$ and also $TiNpCl_3$ were observed during the reaction and after 1hr at room temperature in the dark the solution consisted of only $TiNp_2Cl_2$, **9.6**. Some decomposition occurred during the reaction, with the formation of some brown precipitate and with the product being light and thermally unstable it was stored at -196°C.

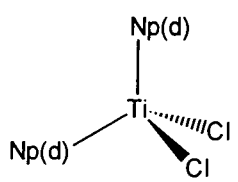

Data characterising $Ti(CH_2CMe_3)_2Cl_2$

^1H NMR: δ/ppm, 250 MHz, $CDCl_3$		**$^{13}C\{^1H\}$ NMR: δ/ppm, 62.5 MHz, $CDCl_3$**	
3.31	[s, 4H, (CH_2)]	142.3	[CH_2]
1.00	[s, 18H, (CMe_3)]	37.1	[$\underline{C}Me_3$]
		32.3	[$C\underline{Me}_3$]

Data characterising $Ti(CHDCMe_3)_2Cl_2$

^1H NMR: δ/ppm, 250 MHz, $CDCl_3$		**$^{13}C\{^1H\}$ NMR: δ/ppm, 62.5 MHz, $CDCl_3$**	
3.303	[s, 2%CH_2]	141.0	[t, CHD]
3.245	[t, 2H, $^2J_{HD}$=1.5Hz, (CHD)]	32.2	[$C\underline{Me}_3$]
1.01	[s, 18H, (CMe_3)]		

9.4.7 Preparation of $Ti(CHDCMe_3)Cl_3$ and $Ti(CH_2CMe_3)TiCl_3$, 9.7

In the same manner as for $TiNp_3Cl$ and $TiNp_2Cl_2$, a 5mm NMR tube charged with $TiNp_4$ (0.01g, 0.03mmol) and $CDCl_3$ (ca. 0.3ml) was cooled to -78°C. A solution of $TiCl_4$ (0.30ml of a 10% solution in $CDCl_3$, 0.03mmol) was added dropwise. The solution was frozen at -196°C and the NMR tube was flame-sealed under vacuum. The NMR tube was warmed to room temperature, the solution rapidly turned orange and the reaction was monitored by ^1H NMR spectroscopy. Resonances attributed to $TiNp_3Cl$ and $TiNpCl_3$ were observed during the reaction and after 2hr at room temperature in the dark the solution consisted of only $TiNpCl_3$, **9.7**. Some decomposition occurred during the reaction, with the formation of some brown precipitate and with the product being light and thermally unstable it was stored at -196°C.

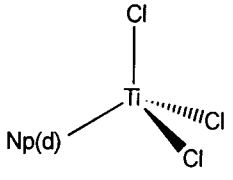

Data characterising $Ti(CH_2CMe_3)Cl_3$

^1H NMR: δ/ppm, 250 MHz, $CDCl_3$	**$^{13}C\{^1H\}$ NMR: δ/ppm, 62.5 MHz, $CDCl_3$**
3.574 [s, 2H, (CH_2)]	163.2 [CH_2]
1.08 [s, 9H, (CMe_3)]	33.0 [$C\underline{Me}_3$]

Data characterising $Ti(CHDCMe_3)Cl_3$

^1H NMR: δ/ppm, 250 MHz, $CDCl_3$

3.563 [s, 2%CH_2]
3.504 [t, 1H, $^2J_{HD}$=1.4Hz, CHD]
1.09 [s, 9H, CMe_3]

9.4.8 Preparation of $Zr(CHDCMe_3)Cl_3$ and $Zr(CH_2CMe_3)Cl_3$, 9.8

In the same manner as for $ZrNp_2Cl_2$ an NMR tube containing $ZrNp_4$ (0.01g, 0.026mmol) and $ZrCl_4$ (0.027g, 0.118mmol, 1.5 x theory) was cooled to -196°C, and $CDCl_3$ (ca.5ml) was transferred onto the reactants under reduced pressure. The tube was sealed, warmed to room temperature and the reaction was monitored by ^1H NMR spectroscopy. Initially $ZrNp_3Cl$ formed, followed by $ZrNp_2Cl_2$, then $ZrNpCl_3$ as a partially soluble yellow precipitate. After 4hr at room temperature a sizeable amount of $ZrNpCl_3$ was produced as a yellow precipitate with the solution containing >70% $ZrNpCl_3$, **9.8**, the remainder being $ZrNp_2Cl_2$, with no further reaction observed. Although the solution darkened rapidly the precipitate was fairly stable, in comparison to $ZrNp_2Cl_2$.

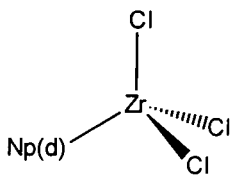

Data characterising $Zr(CH_2CMe_3)Cl_3$

^1H NMR: δ/ppm, 250 MHz, $CDCl_3$	**$^{13}C\{^1H\}$ NMR: δ/ppm, 62.5 MHz, $CDCl_3$**
ca.2.6 [br s, 2H, (CH_2)]	sample insufficiently soluble
1.08 [s, 9H, (CMe_3)]	

Data characterising $Zr(CHDCMe_3)Cl_3$

^1H NMR: δ/ppm, 250 MHz, $CDCl_3$	**$^{13}C\{^1H\}$ NMR: δppm, 250MHz, $CDCl_3$**
ca.2.6 [br s, 1H, (CHD)]	sample insufficiently soluble
1.10 [s, 9H (CMe_3)]	

9.5 References

1 M. Bottrill, P.D. Gavens, J.W. Kelland and J. McMeeking in G. Wilkinson, F.G.A. Stone and E.W. Abel (eds.) *Comprehensive Organometallic Chemistry*, Pergamon, Oxford, 1982, Volume 3, Chapter 22.4; M. Bochmann in G. Wilkinson, F.G.A. Stone and E.W. Abel (eds.) *Comprehensive Chemistry II – A review of the literature 1982-1994*, Elsevier Science Ltd., Oxford, 1995, Volume 4, Chapter 5, pp. 280-288.

2 M. T. Reetz, *Titanium Organic Synthesis* in M. Schlosser (ed.) *Organometallics in Synthesis-A Manual,* Wiley, Chichester, 1994.

3 (a) P.J. Davidson, M.F. Lappert and R. Pearce, *J. Organomet. Chem.,* 1973, **57**, 269; (b) W. Mowat and G. Wilkinson, *J. Chem. Soc., Dalton Trans., 1973, 1120.*

4 J. H. Wengrovious and R.H. Schrock, *J. Organomet. Chem.,* 1981, **205**, 310.

5 I. Sh Guzman, O.I. Adrov, G.N. Bonderenko, E.I. Tinyakova and B.A. Dologoplosk, *Organomet. Chem. in the U.S.S.R.*., 1990, **3** , 694.

6 M.Y. Antipin, Y.T. Struchkov, I.S. Guzman and O.I. Adrov, *Organomet. Chem. in the U.S.S.R.,* 1990, **3**, 967.

7 A.G. Ginzburg, *Usp. Khim.,*1988, **57**(12), 2046, [English translation in *Russ. Chem. Rev.,* 1988(12)].

8 L.K. Hoyt, J.L. Pollitte and Z. Xue, *Inorg. Chem.,* 1994, **33**, 2497.

9 H. De Vries, *Recueil trav. Chim.* 1961, **80**, 866.

10 S. Berger, W. Bock, G. Frenking, V. Jonas and F. Müller, *J. Am. Chem. Soc.,*1995, **117**, 3820.

Appendices

Appendix A - Experimental Techniques

All manipulations of air and/or moisture sensitive compounds were performed under an atmosphere of dry nitrogen (BOC) using standard Schlenk-line and glove-box (Braun Labstar 50) techniques.

Solvents were dried by storing over 3Å molecular sieves (Lancaster) followed by prolonged reflux under nitrogen over the appropriate drying agent. The solvents were collected and stored in Young's ampoules and degassed using the freeze-thaw technique. The drying agents used were as follows (solvent in parentheses): sodium (toluene), potassium (hexane, tetrahydrofuran), lithium aluminium hydride (diethyl ether) and calcium hydride (dichloromethane).

NMR solvents (C_6D_6, $CDCl_3$ and C_7D_8) were stored in Young's ampoules over 3Å molecular sieves and degassed using the freeze thaw technique. Manipulations were carried out using vacuum distillation.

NMR spectra were run in C_6D_6, $CDCl_3$ and C_7D_8, and recorded on the following machines (nuclei and frequencies in parenthesis): Brüker AC-250 (^1H at 250.13 MHz; ^{13}C at 62.9 MHz; ^{19}F at 235.36 MHz and ^{31}P at 101.2 MHz); Varian VXR-400 (^1H at 400 MHz and ^{13}C at 100 MHz); Varian XL-200 (^1H at 200 MHz). Chemical shifts are quoted as δ in ppm with respect to the following unless otherwise stated: ^1H (C_6D_6, 7.16ppm; $CDCl_3$, 7.27; C_7D_8, 6.98ppm); ^{13}C (C_6D_6, 128.7ppm; $CDCl_3$, 77.7ppm; C_7D_8, 125.2ppm).

Infra-red spectra were recorded on a Perkin-Elmer FTIR spectrometer. Elemental analysis and mass spectra were performed by the microanalytical services of this department.

Starting materials were used as received, except where otherwise stated. Grignard reagents, where necessary, were standardised by titration against n-propanol using 1,10-phenanthroline as an indicator, to determine the exact concentration.

Appendix B - Crystal Data

B.1 Crystal data for $Mo(N^tBu)_2Cl_2dme$

Table 1 – Summary data

$C_{12}H_{28}MoN_2O_2$	399.20	
Temperature	293(2) K	
Wavelength	0.71703 Å	
Crystal system	Orthorhombic	
Space group	Pbca	
Unit cell dimensions	a = 9.864(2) Å	$\alpha = 90.0°$
	b = 12.495(3) Å	$\beta = 90.0°$
	c = 29.853(6) Å	$\gamma = 90.0°$
Volume	3679.4(13) $Å^3$	
Z	8	
Density	1.441 g/cm^{-1}	
Absorption coefficient	1.004 mm^{-1}	
F(000)	1648	
θ range	2.47 – 26.15°	
Index ranges	$-11 \leq h \leq 12, -15 \leq k \leq 15, -36 \leq 1 \leq 19$	
Reflections collected	14709	
Independent reflections	3340 [R(int) = 0.0673]	
Refinement method	Full-matrix-least-squares on F^2	
Data / restraints / parameters	3340 / 0/ 257	
Goodness of fit on F^2	1.211	
Final R indices [$I > 2\sigma(I)$]	$R_1 = 0.0453$, $wR_2 = 0.1091$	
R indices (all data)	$R_1 = 0.0508$, $wR_2 = 0.1132$	
Extinction coefficient	0.0022(2)	
Largest diff. peak and hole	0.510 and –0.509 $e.A^{-3}$	

Table 2. Atomic coordinates (x 10^4) and equivalent isotropic displacement parameters (A^2 x 10^3) for 1. U(eq) is defined as one third of the trace of the orthogonalized Uij tensor.

	x	y	z	U(eq)
Mo(1)	-53(1)	890(1)	3570(1)	27(1)
Cl(1)	944(1)	-807(1)	3766(1)	40(1)
Cl(2)	-736(1)	2395(1)	3109(1)	36(1)
O(1)	-451(3)	-103(2)	2896(1)	31(1)
O(2)	1834(3)	1012(2)	3076(1)	33(1)
N(1)	-1683(3)	668(3)	3759(1)	32(1)
N(2)	793(3)	1573(3)	3986(1)	33(1)
C(1)	-1223(5)	-1088(3)	2922(2)	38(1)
C(3)	729(5)	-250(4)	2618(2)	39(1)
C(4)	1503(5)	779(4)	2617(1)	37(1)
C(6)	2717(5)	1921(4)	3118(2)	42(1)
C(01)	-2967(4)	766(3)	3996(1)	32(1)
C(11)	-2928(5)	42(4)	4406(2)	42(1)
C(12)	-3163(5)	1934(4)	4129(2)	42(1)
C(13)	-4116(5)	408(5)	3681(2)	47(1)
C(02)	1232(4)	1971(3)	4425(1)	31(1)
C(21)	2747(5)	1720(5)	4472(2)	47(1)
C(22)	990(6)	3167(4)	4434(2)	46(1)
C(23)	423(5)	1395(4)	4786(2)	43(1)

Table 3 Bond lengths [A] and angles [deg] for 1.

Mo(1)-N(2)	1.722(3)
Mo(1)-N(1)	1.726(3)
Mo(1)-O(2)	2.380(3)
Mo(1)-O(1)	2.397(3)
Mo(1)-Cl(1)	2.4095(11)
Mo(1)-Cl(2)	2.4267(10)
O(1)-C(3)	1.441(5)
O(1)-C(1)	1.450(5)
O(2)-C(6)	1.437(5)
O(2)-C(4)	1.438(5)
N(1)-C(01)	1.455(5)
N(2)-C(02)	1.467(5)
C(3)-C(4)	1.495(6)
C(01)-C(11)	1.522(6)
C(01)-C(12)	1.526(6)
C(01)-C(13)	1.539(6)
C(02)-C(22)	1.513(6)
C(02)-C(23)	1.523(6)
C(02)-C(21)	1.534(6)
N(2)-Mo(1)-N(1)	107.1(2)
N(2)-Mo(1)-O(2)	92.06(13)
N(1)-Mo(1)-O(2)	160.29(13)
N(2)-Mo(1)-O(1)	160.26(13)
N(1)-Mo(1)-O(1)	92.26(13)
O(2)-Mo(1)-O(1)	68.94(9)
N(2)-Mo(1)-Cl(1)	93.64(11)
N(1)-Mo(1)-Cl(1)	99.19(11)
O(2)-Mo(1)-Cl(1)	83.56(7)
O(1)-Mo(1)-Cl(1)	79.38(7)
N(2)-Mo(1)-Cl(2)	99.16(11)
N(1)-Mo(1)-Cl(2)	92.94(11)
O(2)-Mo(1)-Cl(2)	79.38(7)
O(1)-Mo(1)-Cl(2)	83.04(7)
Cl(1)-Mo(1)-Cl(2)	158.96(4)
C(3)-O(1)-C(1)	110.3(3)
C(3)-O(1)-Mo(1)	114.7(2)
C(1)-O(1)-Mo(1)	118.7(2)
C(6)-O(2)-C(4)	112.3(3)
C(6)-O(2)-Mo(1)	118.1(3)
C(4)-O(2)-Mo(1)	113.6(2)
C(01)-N(1)-Mo(1)	162.9(3)
C(02)-N(2)-Mo(1)	162.8(3)
O(1)-C(3)-C(4)	107.7(3)
O(2)-C(4)-C(3)	106.8(3)
N(1)-C(01)-C(11)	108.6(3)
N(1)-C(01)-C(12)	108.5(3)
C(11)-C(01)-C(12)	111.2(4)
N(1)-C(01)-C(13)	108.7(3)
C(11)-C(01)-C(13)	109.7(4)
C(12)-C(01)-C(13)	110.1(4)
N(2)-C(02)-C(22)	107.7(3)
N(2)-C(02)-C(23)	108.5(3)
C(22)-C(02)-C(23)	111.8(4)
N(2)-C(02)-C(21)	107.5(3)
C(22)-C(02)-C(21)	110.8(4)

C(23)-C(02)-C(21)	110.4(4)

Symmetry transformations used to generate equivalent atoms:

Table 4 Anisotropic displacement parameters (A^2 x 10^3) for 1. The anisotropic displacement factor exponent takes the form: -2 pi^2 [h^2 a*^2 U11 + ... + 2 h k a* b* U12]

	U11	U22	U33	U23	U13	U12
Mo(1)	28(1)	28(1)	26(1)	0(1)	1(1)	1(1)
Cl(1)	43(1)	34(1)	44(1)	6(1)	-5(1)	8(1)
Cl(2)	42(1)	31(1)	36(1)	4(1)	-2(1)	5(1)
O(1)	34(2)	32(2)	28(1)	-6(1)	4(1)	-4(1)
O(2)	34(2)	34(2)	31(1)	1(1)	6(1)	-3(1)
N(1)	32(2)	29(2)	35(2)	2(1)	3(1)	1(1)
N(2)	39(2)	28(2)	31(2)	1(1)	-3(1)	0(2)
C(1)	43(3)	29(2)	41(2)	-7(2)	-2(2)	-6(2)
C(3)	47(3)	35(2)	34(2)	-8(2)	15(2)	-3(2)
C(4)	39(3)	43(2)	29(2)	-1(2)	9(2)	0(2)
C(6)	40(3)	46(3)	39(2)	0(2)	4(2)	-10(2)
C(01)	25(2)	40(2)	30(2)	-1(2)	4(2)	0(2)
C(11)	41(3)	42(3)	41(3)	6(2)	3(2)	-9(2)
C(12)	41(3)	40(2)	44(3)	-3(2)	7(2)	6(2)
C(13)	34(3)	64(3)	42(3)	-10(2)	-2(2)	-1(2)
C(02)	32(2)	36(2)	23(2)	-1(2)	-6(2)	-4(2)
C(21)	37(3)	60(3)	42(3)	-2(2)	-9(2)	3(2)
C(22)	53(3)	38(3)	45(3)	-9(2)	0(2)	-4(2)
C(23)	48(3)	54(3)	28(2)	1(2)	-2(2)	-7(2)

Table 5 Hydrogen coordinates (x 10^4) and isotropic displacement parameters (A^2 x 10^3) for 1.

	x	y	z	U(eq)
H(1A)	-666(49)	-1665(38)	3058(15)	45
H(1B)	-1468(47)	-1298(36)	2619(16)	45
H(1C)	-1947(50)	-920(35)	3123(16)	45
H(3A)	1227(50)	-851(36)	2739(16)	47
H(3B)	481(50)	-439(38)	2305(17)	47
H(4A)	2313(50)	705(37)	2456(14)	44
H(4B)	975(48)	1357(37)	2475(15)	44
H(6A)	3002(49)	1963(39)	3414(18)	50
H(6B)	2269(50)	2556(41)	3037(16)	50
H(6C)	3401(52)	1876(38)	2901(16)	50
H(11A)	-2753(50)	-699(42)	4332(16)	50
H(11B)	-2239(52)	261(38)	4610(16)	50
H(11C)	-3787(53)	68(37)	4575(16)	50
H(12A)	-2391(52)	2172(39)	4313(16)	50
H(12B)	-3208(50)	2277(39)	3869(17)	50
H(12C)	-3995(53)	2024(39)	4280(16)	50
H(13A)	-3997(55)	-343(46)	3601(16)	56
H(13B)	-5038(50)	523(45)	3843(19)	56
H(13C)	-4110(52)	846(39)	3400(18)	56
H(21A)	3334(52)	2109(40)	4231(17)	56
H(21B)	3093(50)	1877(39)	4781(18)	56
H(21C)	2893(52)	939(43)	4427(17)	56
H(22A)	1472(53)	3516(41)	4202(17)	55
H(22B)	1261(51)	3451(41)	4700(18)	55
H(22C)	10(52)	3384(43)	4400(18)	55
H(23A)	734(50)	1597(40)	5082(17)	52
H(23B)	507(50)	580(42)	4755(17)	52
H(23C)	-568(53)	1589(39)	4754(16)	52

B.2 Crystal data for $Ti[\eta^5:\eta^1\text{-}C_5H_4(CH_2)_3N(H)Me](\eta^5\text{-}C_5H_5)Cl$

Table 1 – Summary data

$C_{14}H_{19}ClNTi$	284.65	
Temperature	293(2) K	
Wavelength	0.7073 Å	
Crystal system	Monoclinic	
Space group	P2(1)/n	
Unit cell dimensions	a = 7.901(3) Å	α = 90.0°
	b = 13.424(2) Å	β = 101.2340(10)°
	c = 12.568(2) Å	γ = 90.0°
Volume	1307.34(5) $Å^3$	
Z	4	
Density	1.446 g/cm^{-1}	
Absorption coefficient	0.835 mm^{-1}	
F(000)	596	
θ range	2.24 – 27.50°	
Index ranges	$-6 \leq h \leq 10, -17 \leq k \leq 16, -16 \leq l \leq 14$	
Reflections collected	6294	
Independent reflections	2887 [R(int) = 0.0797]	
Refinement method	Full-matrix-least-squares on F^2	
Data / restraints / parameters	2883 / 0/ 158	
Goodness of fit on F^2	1.088	
Final R indices [$I > 2\sigma(I)$]	$R_1 = 0.0632$, $wR_2 = 0.1225$	
R indices (all data)	$R_1 = 0.1284$, $wR_2 = 0.1607$	
Largest diff. peak and hole	0.488 and –0.626 $e.A^{-3}$	

Table 2. Atomic coordinates (x 10^4) and equivalent isotropic displacement parameters (A^2 x 10^3) for 1. U(eq) is defined as one third of the trace of the orthogonalized Uij tensor.

	x	y	z	U(eq)
Ti(1)	802(1)	7825(1)	4176(1)	19(1)
N(23)	-1074(5)	9022(3)	3304(3)	20(1)
C(2)	-1363(7)	6724(4)	3180(4)	28(1)
C(3)	2764(6)	9156(4)	4126(4)	23(1)
C(4)	2063(6)	8916(4)	2014(4)	27(1)
C(5)	-2884(6)	8957(4)	3474(4)	27(1)
C(6)	-1573(6)	6761(3)	4261(4)	26(1)
C(7)	-1136(6)	9205(4)	2127(4)	24(1)
C(8)	263(7)	6292(3)	3161(4)	28(1)
C(9)	2684(6)	8582(4)	3154(4)	22(1)
C(10)	527(7)	9633(4)	1871(4)	28(1)
C(11)	3527(6)	8563(4)	5005(4)	31(1)
C(12)	3382(6)	7636(4)	3480(4)	27(1)
C(13)	-102(7)	6334(3)	4917(4)	28(1)
C(14)	1041(7)	6046(3)	4238(4)	28(1)
C(15)	3894(6)	7622(4)	4624(4)	29(1)
Cl(1)	2(2)	8583(1)	5833(1)	25(1)

Table 3. Bond lengths [A] and angles [deg] for 1.

Ti(1)-N(23)	2.312(4)
Ti(1)-C(3)	2.374(5)
Ti(1)-C(9)	2.374(5)
Ti(1)-C(13)	2.376(5)
Ti(1)-C(6)	2.377(5)
Ti(1)-C(12)	2.383(5)
Ti(1)-C(14)	2.396(5)
Ti(1)-C(15)	2.413(5)
Ti(1)-C(11)	2.414(5)
Ti(1)-C(8)	2.415(5)
Ti(1)-C(2)	2.418(5)
Ti(1)-Cl(1)	2.5064(14)
N(23)-C(5)	1.488(6)
N(23)-C(7)	1.491(6)
C(2)-C(6)	1.401(7)
C(2)-C(8)	1.414(7)
C(3)-C(11)	1.399(7)
C(3)-C(9)	1.435(6)
C(4)-C(9)	1.490(7)
C(4)-C(10)	1.532(7)
C(6)-C(13)	1.409(7)
C(7)-C(10)	1.524(7)
C(8)-C(14)	1.413(7)
C(9)-C(12)	1.413(7)
C(11)-C(15)	1.401(7)
C(12)-C(15)	1.416(7)
C(13)-C(14)	1.412(7)

N(23)-Ti(1)-C(3)	80.0(2)
N(23)-Ti(1)-C(9)	81.8(2)
C(3)-Ti(1)-C(9)	35.2(2)
N(23)-Ti(1)-C(13)	123.9(2)
C(3)-Ti(1)-C(13)	153.2(2)
C(9)-Ti(1)-C(13)	147.2(2)
N(23)-Ti(1)-C(6)	90.0(2)
C(3)-Ti(1)-C(6)	168.1(2)
C(9)-Ti(1)-C(6)	149.8(2)
C(13)-Ti(1)-C(6)	34.5(2)
N(23)-Ti(1)-C(12)	114.5(2)
C(3)-Ti(1)-C(12)	57.4(2)
C(9)-Ti(1)-C(12)	34.6(2)
C(13)-Ti(1)-C(12)	113.5(2)
C(6)-Ti(1)-C(12)	133.7(2)
N(23)-Ti(1)-C(14)	138.3(2)
C(3)-Ti(1)-C(14)	134.7(2)
C(9)-Ti(1)-C(14)	113.0(2)
C(13)-Ti(1)-C(14)	34.4(2)
C(6)-Ti(1)-C(14)	57.1(2)
C(12)-Ti(1)-C(14)	80.7(2)
N(23)-Ti(1)-C(15)	135.7(2)
C(3)-Ti(1)-C(15)	56.9(2)
C(9)-Ti(1)-C(15)	57.5(2)
C(13)-Ti(1)-C(15)	100.5(2)
C(6)-Ti(1)-C(15)	133.9(2)
C(12)-Ti(1)-C(15)	34.3(2)
C(14)-Ti(1)-C(15)	79.1(2)
N(23)-Ti(1)-C(11)	110.8(2)
C(3)-Ti(1)-C(11)	34.0(2)
C(9)-Ti(1)-C(11)	57.2(2)
C(13)-Ti(1)-C(11)	119.2(2)
C(6)-Ti(1)-C(11)	150.8(2)
C(12)-Ti(1)-C(11)	56.5(2)
C(14)-Ti(1)-C(11)	109.7(2)
C(15)-Ti(1)-C(11)	33.7(2)
N(23)-Ti(1)-C(8)	108.1(2)
C(3)-Ti(1)-C(8)	132.5(2)
C(9)-Ti(1)-C(8)	98.2(2)

C(13)-Ti(1)-C(8)	56.9(2)
C(6)-Ti(1)-C(8)	56.8(2)
C(12)-Ti(1)-C(8)	77.9(2)
C(14)-Ti(1)-C(8)	34.1(2)
C(15)-Ti(1)-C(8)	95.4(2)
C(11)-Ti(1)-C(8)	128.9(2)
N(23)-Ti(1)-C(2)	81.7(2)
C(3)-Ti(1)-C(2)	147.8(2)
C(9)-Ti(1)-C(2)	115.8(2)
C(13)-Ti(1)-C(2)	56.7(2)
C(6)-Ti(1)-C(2)	34.0(2)
C(12)-Ti(1)-C(2)	108.3(2)
C(14)-Ti(1)-C(2)	56.7(2)
C(15)-Ti(1)-C(2)	129.3(2)
C(11)-Ti(1)-C(2)	162.9(2)
C(8)-Ti(1)-C(2)	34.0(2)
N(23)-Ti(1)-Cl(1)	82.50(11)
C(3)-Ti(1)-Cl(1)	89.34(12)
C(9)-Ti(1)-Cl(1)	124.17(12)
C(13)-Ti(1)-Cl(1)	82.68(13)
C(6)-Ti(1)-Cl(1)	82.98(13)
C(12)-Ti(1)-Cl(1)	136.10(13)
C(14)-Ti(1)-Cl(1)	114.11(13)
C(15)-Ti(1)-Cl(1)	105.05(13)
C(11)-Ti(1)-Cl(1)	79.81(13)
C(8)-Ti(1)-Cl(1)	137.53(13)
C(2)-Ti(1)-Cl(1)	114.26(14)
C(5)-N(23)-C(7)	107.8(4)
C(5)-N(23)-Ti(1)	115.9(3)
C(7)-N(23)-Ti(1)	118.6(3)
C(6)-C(2)-C(8)	108.1(4)
C(6)-C(2)-Ti(1)	71.4(3)
C(8)-C(2)-Ti(1)	72.9(3)
C(11)-C(3)-C(9)	107.9(4)
C(11)-C(3)-Ti(1)	74.6(3)
C(9)-C(3)-Ti(1)	72.4(3)
C(9)-C(4)-C(10)	114.0(4)
C(2)-C(6)-C(13)	108.3(5)
C(2)-C(6)-Ti(1)	74.6(3)
C(13)-C(6)-Ti(1)	72.7(3)
N(23)-C(7)-C(10)	114.1(4)
C(14)-C(8)-C(2)	107.9(5)
C(14)-C(8)-Ti(1)	72.2(3)
C(2)-C(8)-Ti(1)	73.1(3)
C(12)-C(9)-C(3)	106.6(4)
C(12)-C(9)-C(4)	125.9(5)
C(3)-C(9)-C(4)	127.4(4)
C(12)-C(9)-Ti(1)	73.0(3)
C(3)-C(9)-Ti(1)	72.4(3)
C(4)-C(9)-Ti(1)	121.7(3)
C(7)-C(10)-C(4)	115.7(4)
C(3)-C(11)-C(15)	109.2(5)
C(3)-C(11)-Ti(1)	71.4(3)
C(15)-C(11)-Ti(1)	73.1(3)
C(9)-C(12)-C(15)	108.9(4)
C(9)-C(12)-Ti(1)	72.4(3)
C(15)-C(12)-Ti(1)	74.0(3)
C(6)-C(13)-C(14)	108.0(4)
C(6)-C(13)-Ti(1)	72.8(3)
C(14)-C(13)-Ti(1)	73.6(3)
C(13)-C(14)-C(8)	107.8(5)
C(13)-C(14)-Ti(1)	72.0(3)
C(8)-C(14)-Ti(1)	73.7(3)
C(11)-C(15)-C(12)	107.4(4)
C(11)-C(15)-Ti(1)	73.2(3)
C(12)-C(15)-Ti(1)	71.7(3)

Symmetry transformations used to generate equivalent atoms:

B.3 Crystal data for $Ta(NMe_2)_5$

Table 1 – Summary data

$C_{10}H_{30}N_5Ta$	402.34	
Temperature	150.0(2) K	
Wavelength	0.71073Å	
Crystal system	Orthorhombic	
Space group	Ccmm	
Unit cell dimensions	a = 7.9003(2) Å	$\alpha = 90.0°$
	b = 13.8450(3) Å	$\beta = 90.0°$
	c = 14.5442(3) Å	$\gamma = 90.0°$
Volume	1590.84(6) $Å^3$	
Z	4	
Density	1.676 g/cm^{-1}	
Absorption coefficient	6.897 mm^{-1}	
F(000)	792	
θ range	2.80 – 27.44°	
Index ranges	$-8 \leq h \leq 10, -17 \leq k \leq 15, -18 \leq 1 \leq 17$	
Reflections collected	5620	
Independent reflections	988 [R(int) = 0.0520]	
Refinement method	Full-matrix-least-squares on F^2	
Data / restraints / parameters	983 / 0/ 75	
Goodness of fit on F^2	1.232	
Final R indices [$I > 2\sigma(I)$]	$R_1 = 0.0283$, $wR_2 = 0.0687$	
R indices (all data)	$R_1 = 0.0880$, $wR_2 = 0.2183$	
Extinction coefficient	0.0000(4)	
Largest diff. peak and hole	2.517 and –0.701 $e.A^{-3}$	

Table 2. Atomic coordinates (x 10^4) and equivalent isotropic displacement parameters (A^2 x 10^3) for 1. U(eq) is defined as one third of the trace of the orthogonalized Uij tensor.

	x	y	z	U(eq)
Ta	1715(1)	0	7500	33(1)
N(1)	-781(6)	0	7500	39(1)
C(1)	-1868(9)	0	6694(7)	87(4)
N(2)	2209(12)	872(6)	6401(6)	37(2)
C(2)	3536(11)	811(8)	5702(7)	49(2)
C(3)	1377(13)	1820(7)	6354(7)	51(2)
N(3)	2548(12)	1090(6)	6692(6)	44(2)
C(4)	1883(12)	1262(8)	5760(7)	57(2)
C(5)	3972(11)	1752(6)	6862(7)	59(2)

Table 3. Bond lengths [A] for 1.

Ta-N(1)	1.971(5)
Ta-N(3)	2.023(9)
Ta-N(3)#1	2.023(9)
Ta-N(3)#2	2.023(9)
Ta-N(3)#3	2.023(9)
Ta-N(2)	2.041(8)
Ta-N(2)#1	2.041(8)
Ta-N(2)#2	2.041(8)
Ta-N(2)#3	2.041(8)
N(1)-C(1)	1.453(9)
N(1)-C(1)#1	1.453(9)
N(2)-C(2)	1.463(12)
N(2)-C(3)	1.469(12)
N(3)-C(5)	1.472(12)
N(3)-C(4)	1.473(13)

Symmetry transformations used to generate equivalent atoms:
#1 x,y,-z+3/2 #2 x,-y,-z+3/2 #3 x,-y,z

Table 4. Bond angles [deg] for 1.

N(1)-Ta-N(3)	109.0(3)
N(1)-Ta-N(3)#1	109.0(3)
N(3)-Ta-N(3)#1	71.0(5)
N(1)-Ta-N(3)#2	109.0(3)
N(3)-Ta-N(3)#2	142.0(5)
N(3)#1-Ta-N(3)#2	96.5(5)
N(1)-Ta-N(3)#3	109.0(3)
N(3)-Ta-N(3)#3	96.5(5)
N(3)#1-Ta-N(3)#3	142.0(5)
N(3)#2-Ta-N(3)#3	71.0(5)
N(1)-Ta-N(2)	101.0(3)
N(1)-Ta-N(2)#1	101.0(3)
N(2)-Ta-N(2)#1	103.1(5)
N(1)-Ta-N(2)#2	101.0(3)
N(2)-Ta-N(2)#2	157.9(5)
N(2)#1-Ta-N(2)#2	72.5(5)
N(1)-Ta-N(2)#3	101.0(3)
N(2)-Ta-N(2)#3	72.5(5)
N(2)#1-Ta-N(2)#3	157.9(5)
N(2)#2-Ta-N(2)#3	103.1(5)
C(1)-N(1)-C(1)#1	107.6(8)
C(1)-N(1)-Ta	126.2(4)
C(1)#1-N(1)-Ta	126.2(4)
C(2)-N(2)-C(3)	109.9(8)
C(2)-N(2)-Ta	130.3(6)
C(3)-N(2)-Ta	118.6(6)
C(5)-N(3)-C(4)	109.1(8)
C(5)-N(3)-Ta	128.0(6)
C(4)-N(3)-Ta	122.6(7)

Symmetry transformations used to generate equivalent atoms:
#1 x,y,-z+3/2 #2 x,-y,-z+3/2 #3 x,-y,z

Table 5. Anisotropic displacement parameters (A^2 x 10^3) for 1. The anisotropic displacement factor exponent takes the form: -2 pi^2 [h^2 a*^2 U11 + ... + 2 h k a* b* U12]

	U11	U22	U33	U23	U13	U12
Ta	35(1)	37(1)	28(1)	0	0	0
I(1)	28(2)	60(3)	29(2)	0	0	0
C(1)	49(3)	159(12)	52(5)	0	-8(3)	0
I(2)	38(4)	41(5)	31(4)	3(3)	4(3)	1(3)
C(2)	55(4)	53(5)	38(4)	3(4)	10(3)	-3(3)
C(3)	66(4)	40(4)	46(4)	7(3)	7(4)	8(4)
I(3)	51(5)	41(4)	41(5)	3(3)	-3(3)	-8(3)
C(4)	79(6)	52(5)	41(5)	4(4)	-1(3)	3(4)
C(5)	59(5)	51(4)	66(5)	7(4)	1(4)	-13(4)

Table 6. Hydrogen coordinates (x 10^4) and isotropic displacement parameters (A^2 x 10^3) for 1.

	x	y	z	U(eq)
H(1A)	-1201(27)	175(64)	6151(12)	104
H(1B)	-2782(67)	470(47)	6779(27)	104
H(1C)	-2353(90)	-645(17)	6609(36)	104
H(2A)	3024(13)	845(49)	5089(7)	58
H(2B)	4145(56)	198(22)	5768(29)	58
H(2C)	4329(48)	1350(28)	5781(29)	58
H(3A)	805(71)	1888(20)	5760(19)	61
H(3B)	2227(17)	2330(7)	6421(47)	61
H(3C)	544(61)	1873(20)	6851(28)	61
H(4A)	2812(19)	1228(54)	5314(9)	69
H(4B)	1358(85)	1902(23)	5733(16)	69
H(4C)	1036(69)	768(33)	5612(21)	69
H(5A)	4868(37)	1632(34)	6410(29)	70
H(5B)	4417(56)	1643(34)	7483(18)	70
H(5C)	3580(22)	2421(6)	6807(47)	70

Appendix C - Colloquia and Lectures Organised by the Department of Chemistry During the period 1994 - 95

October 5 Prof. N.L. Owen, Brigham Young University, Utah, USA
"Determining Molecular Structure – the INADEQUATE NMR way"

October 19 Prof. N. Bartlett, University of Califonia
"Some Aspects of Ag(II) and Ag(III) Chemistry"

November 2 Dr P.G. Edwards, University of Wales, Cardiff
"The Manipulation of Electronic and structural Diversity in Metal Complexes – New ligands"

November 3 Prof. B.F.G. Johnson, Edinburgh University
"Arene-metal Clusters"

November 9 Dr G. Hogarth, University College London
"New Vistas in Metal-imido Chemistry"

November 10 Dr M. Block, Zeneca Phamaceuticals, Macclesfield
"Large-scale Manufacture of ZD 1542, a Thromboxane Antagonist Synthase Inhibitor"

February 8 Dr D. O'Hare, Oxford University
"Synthesis and Solid-state Properties of Poly-, Oligo- and Multidecker Metallocenes"

March 1 Dr M. Rosseinsky, Oxford University
"Fullerene Intercalation Chemistry"

March 22 Dr M. Taylor, University of Auckland, New Zealand
"Structural Methods in Main-group Chemistry"

April 26 Dr M. Schroder, University of Edinburgh
"Redox-active Macrocyclic Complexes : Rings, Stacks and Liquid Crystals"

During the period 1995 – 1996

November 15 Dr A. Sella, UCL, London
"Chemistry of Lanthanides with Polypyrazoylborate Ligands"

November 29 Prof. D. Tuck, University of Windsor, Ontario, Canada
"New Indium Coordination Chemisry'

February 12 Dr P. Pringle, University of Bristol
"Catalytic Self-replication of Phospines on Platinum(0)"

February 21 Dr C.R. Pulham, University of Edinburgh
"Heavy Metal Hydrides – an Exploration of the Chemistry of Stannanes and Plumbanes"

February 28 Prof. E.W. Randall, Queen Mary & Westfield College
"New Perspectives in NMR Imaging"

March 6 Dr R. Whitby, University of Southampton
"New Approaches to Chiral Catalysts : Induction of Planar and Metal Centred Assymetry"

March 7 Dr D.S. Wright, University of Cambridge
"Synthetic Applications of Me_2N-p-Block Metal Reagents"

March 13 Prof. D. Garner, Manchester University
"Mushrooming in Chemistry"

During the period 1996 – 1997

October 9 Prof. G. Bowmaker, University of Aukland, New Zealand
"Coordination and Materials Chemistry of the Group 11 and Group 12 Metals"

October 22 Prof. L. Gade, University of Wurtzberg, Germany
"Organic Transformations with Early-Late Heterobimetallics Synergism and Selectivity"

November 2 Dr P. Mountford, Nottingham University
"Recent Developments in Group IV Imido Chemistry"

November 18 Prof. G.A. Olah, University of Southern California, USA
"Crossing Conventional Lines in my Chemistry of the Elements"

November 19 Prof. R.E. Grigg, University of Leeds
"Assembly of Complex Molecules by Palladium-Catalysed Queueing Processes"

December 3 Prof. K. Muller-Dethlefs, York University
"Chemical Applications of Very High Resolution ZEKE Photoelectron Spectroscopy"

January 15 Dr. V.K. Aggarwal, University of Sheffield
"Sulphur Mediated Assymetric Synthesis"

January 16 Dr. S. Brooker, University of Otago, New Zealand
Macrocycles: Exciting yet Controlled Thiolate Coordination Chemistry"

February 4 Dr. A.J. Bannister, University of Durham
"From Runways to Non-metallic Metals - A New Chemistry Based on Sulphur"

Appendix D - Conferences and Symposia Attended

1. "Anglo/German Inorganic Chemistry Meeting"
   University of Marburg, September 1997.

2. "1st Anglo Dutch Symposium on Organometallic Chemistry and Catalysis"
   University of Sheffield, September 1996.

3. "North East Graduate Symposium"
   University of Sunderland, April 1996.

4. "North East Graduate Symposium"
   University of Durham, April 1995.